HPV RESEARCH GROUP
INSTITUTE OF CANCER & GENETICS
SCHOOL OF MEDICINE
CARDIFF UNIVERSITY

Nucleoside Analogue Drugs and Human Papillomavirus Associated Neoplasia

By Áine Sinéad Flynn
2013

Thesis submitted in partial fulfilment of the requirements for the degree of Doctor of Philosophy

Acknowledgements

I dedicate this thesis to my other half, Matthew, and to my parents, Mary and Martin, for their unconditional support throughout. I also extend my gratitude to my sister, brother and all my close friends for their endless encouragement.

I would like to thank my supervisory team, Dr Ned Powell, Dr Amanda Tristram and Prof Chris McGuigan, for their assistance and guidance through all aspects of the PhD project. I would like to extend my gratitude to Dr Samantha Hibbitts for the professional and cordial advice she offered throughout the project. I am also grateful to my department head, Prof Alison Fiander, and to my other colleagues and dear friends within the HPV research group: Rachel H, Rachel R, Sadie, Dean, Evelyne and in particular to Tiffany, who kindly provided the cell lines to undertake my work; their contribution, friendship and empathy was invaluable.

Thank you to Dr Amanda Tonks and to Dr Alex Tonks for their more than helpful professional mentoring and advice, and thanks to the staff of their respective research groups, Medical Microbiology and Haematology, for their kind technical assistance.

I am deeply indebted to Fabrizio Pertusati, Davide Carta and Karen Hinsinger, who during their time at the Welsh School of Pharmacy synthesized the analogue compounds for the project and for their ceaseless help in trying to teach a biologist Chemistry.

I would like to acknowledge the administrative staff of the Institute of Cancer and Genetics and the Postgraduate Research Degrees Office, as well as Dr Claudia Consoli and all my other colleagues at Cardiff University who have contributed in one way or another to the submission of this thesis.

Finally, I would like to thank Cardiff University for the President's Research Scholarship to undertake this work as well as the Institute of Cancer and Genetics in the Cardiff School of Medicine.

Summary

The anti-viral acyclic nucleoside monophosphate compound Cidofovir has shown efficacy in treatment of Human Papillomavirus (HPV) associated genital intraepithelial neoplasia; however, the mechanism of action of Cidofovir in this setting has not been determined. This investigation focused on modifying nucleoside analogue compounds to increase their efficacy in HPV positive cell models of disease, in addition to determining the molecular mechanism of action of Cidofovir in premalignant HPV associated intraepithelial neoplasia.

ProTide modification increases the efficacy of nucleoside analogue compounds by increasing their cellular permeability. Cidofovir was not amenable to ProTide manipulation; however, ProTide derivatives of its sister compounds, Adefovir and Tenofovir, were synthesized. Parent Adefovir and Tenofovir and a range of their respective ProTide modified daughter compounds were examined for inhibition of cell growth and effect on cell size and morphology in HPV positive and negative transformed cell lines. The most effective compounds were further examined for dose response in normal HPV negative untransformed Human Epidermal Keratinocytes (HEKs) and naturally HPV immortalized short term (NHIST) cell lines cloned from vulval and vaginal intraepithelial neoplasia biopsies. ProTide analogues displayed striking increased efficacy in comparison to their parent compounds; however, they did not show specificity to transformed or HPV positive cell lines.

Cidofovir did not show specificity to HPV positive cells when examined for growth inhibitory effect in HPV positive and negative cell models. A variety of molecular processes were examined to determine the mechanism by which Cidofovir inhibits cell growth in validated NHIST cell lines and HEK cells. At the concentrations investigated, Cidofovir did not cause apoptosis in HPV positive or negative cells and its growth inhibitory effect appeared likely to be associated with cell cycle arrest or senescence. The effects of radiation on the molecular response induced by Cidofovir were also evaluated as previous studies suggested Cidofovir can function as a radiosensitizer. Cidofovir combined with gamma radiation did not result in apoptosis but was associated with an augmented molecular response in NHIST cell lines. On the contrary, Cidofovir combined with gamma radiation caused a major apoptotic response in HPV negative HEKs, suggesting such a combination could result in disadvantageous effects on healthy tissue if it were used *in vivo.*

Abbreviations

Abbreviation	Definition
5-FU	5-fluorouracil
7-AAD	7-aminoactinomycin D
ABCTP	ATP-binding Cassette Transporter Protein
AIN	Anal intraepithelial neoplasia
ALA	Aminolaevulinic acid
ALT	Alternative Lengthening of Telomeres
AMC	7-amino-4-methylcoumarin
ANP	Acyclic nucleoside phosphonate
AP endonuclease	Apurinic/apyrimidinic endonuclease
APOT	Amplification of papillomavirus oncogene transcripts
ATCC	American Type Culture Collection
ATM	Ataxia-telangiectasia mutated
ATP	Adenosine-triphosphate
ATR	Ataxia telangiectasia and rad3 related
BCA	Bicinchoninic acid
BER	Base excision repair
BLAST	Basic local alignment search tool
BP	Base pairs
BSA	Bovine serum albumin
BVDU	(E)-5-(2-Bromovinyl)-2'-deoxyuridine
CAM	Cell adhesion molecule
CDA	Cytidine deaminase
CDK	Cyclin dependant kinase
cDNA	Complementary DNA
CDV-pp	Cidofovir diphosphate
CIN	Cervical intraepithelial neoplasia
CMV	Cytomegalovirus
CPD	Cyclobutane pyrimidine dimers
CR	Conserved region
CR	Complete response
CRPV	Cottontail rabbit papillomavirus
Ct	Crossing threshold
dATP	Deoxyadenosine triphosphate
dCK	Deoxycytidine kinase
DCMC	Dicyclohexyl-4-morpholinecarboxamidine

Abbreviation	Definition
dCTP	Deoxycytidine triphosphate
DDC	Dicyclohexylcarbodiimide
DEVD	Asp-Glu-Val-Asp
dGMP	Deoxyguanosine monophosphate
DIPS	Detection of integrated papillomavirus sequences
dlg	Discs large
DMEM	Dulbecco's Modified Eagle's Medium
DMSO	Dimethyl sulfoxide
DNA PKcs	DNA-dependent protein kinase, catalytic subunit
DSB	Double strand break
DT	Population doubling time
DTT	Dithiothreito
E6TP1	E6-targeted protein 1
ECL	Enhanced Chemiluminescence
EDTA	Ethylenediaminetetraacetic acid
EGF	Epidermal growth factor
EGTA	ethyleneglycolaminoethyltetraacetic acid
ET3N	Triethylamine
EV	Epidermodysplasia verruciformis
FDA	Food and Drug Administration
FdUrd	5-fluoro-2'-deoxyuridine
FGF	Fibroblast growth factor
FS (mix)	FastStart (mix)
GAP	GTPase-activating proteins
gDNA	Genomic DNA
GGR	Global genomic repair
GMEM	Glasgow Minimal Essential Medium
H&E	Hematoxylin and eosin (stain)
HBV	Hepatitis B virus
HCl	Hydrochloric acid
hCNT	Human Concentrating Nucleoside Transporters
HCV	Hepatitis C virus
HEKs	Human Epidermal Keratinocytes
hENT	Human Equilibrium Nucleoside Transporters
HGVS	Human Genome Variation Society
HHV	Human herpes virus

Abbreviation	Definition
HKGs	Housekeeping genes
HIV	Human immunodeficiency virus
HNSCC	Head and neck squamous cell carcinoma
HPMPC	(S)-1-(3-Hydroxy-2-phosphonylmethoxypropyl)cytosine
HPV	Human papillomavirus
HR	Homologous recombination
HR-HPV	High Risk-HPV
HSIL	High-grade squamous intraepithelial lesion
HSV	Herpes simplex virus
IARC	International Agency for Research on Cancer
IC50	Inhibitory concentration 50
ISSVD	International Society for the Study of Vulvar Diseases
LDS	Lithium dodecyl sulfate
LR-HPV	Low Risk-HPV
LSIL	Low grade squamous intraepithelial lesion
MAF	Minor Allele Frequency
MDR-1	Multidrug resistance protein 1
MgCl2	Magnesium chloride
MHRA	Medicines and Healthcare Products Regulatory Agency
MMEJ	Microhomology-mediated end joining
MMR	Mismatch repair
MOA	Mechanism of action
MOPS	3-(N-morpholino)propanesulfonic acid
MRP-1	Multidrug resistance- associated protein 1
MTS	3-(4,5-dimethylthiazol-2-yl)-5-(3-carboxymethoxyphenyl)-2-(4-sulfophenyl)-2H-tetrazolium)
NA	Nucleic acid
NaCl	Sodium chloride
NaOH	Sodium hydroxide
NCBI	National Center for Biotechnology Information
NER	Nucleotide excision repair
NHEJ	Non-homologous end joining
NHIST	Naturally HPV immortalized short term (cell lines)
NMR	Nuclear magnetic resonance
NMSC	Non-melanoma skin cancer
NT	Nucleoside transporter

Abbreviation	Definition
OAT	Organic Anionic Transporter
OCT	Organic Cationic Transporter
ORECNI	Office for Research Ethics Committees Northern Ireland
ORF	Open reading frame
PARP	Poly ADP ribose polymerase
PBS	Phosphate buffered saline
PCNA	Proliferating cell nuclear antigen
PCR	Polymerase chain reaction
PD	Population doublings
PD	Progressive Disease
PDGF	Platelet-derived growth factor
PDT	Photodynamic therapy
PDZ	PSD-95/disc large/ZO-1
PH3P	Triphenylphosphine
PIN	Penile intraepithelial neoplasia
PMEA	9-(2-phosphonomethoxyethyl) adenine)
PML	Promyelocytic leukemia
PMPA	(R)-9-(2-phosphonylmethoxypropyl) adenine
PMS	Phenazine methosulfate
PMSF	Phenylmethylsulfonyl Fluoride
PR	Partial Response
pRb	Retinoblastoma protein
RECIST	Response Evaluation Criteria in Solid Tumours
RFU	Relative Fluorescence Units
RPA	Replication protein A
RQ	Relative quantification
RSV	Rous sarcoma virus
RT	Reverse transcription/transcriptase
RT-qPCR	Real time-quantitative PCR
SCC	Squamous Cell Carcinoma
SD	Stable disease
SDS	Sodium dodecyl sulphate
SEM	Standard error of the mean
sFRP	secreted Frizzled-related proteins
SI	Selectivity index
SNP	Single-nucleotide polymorphism

Abbreviation	Definition
SNV	Single Nucleotide Variant
TBE	Tris-Borate-EDTA
TBST	Tris-buffered saline tween
TDF	Tenofovir disoproxil fumarate
TFT	Trifluorothymidine
TK	Thymidine kinase
TM	Melting temperature
TMSBr	Bromotrimethylsilane
TSG	Tumor suppressor gene
URR	Upstream regulatory region
UTR	Untranslated region
UV	Ultraviolet
VaIN	Vaginal intraepithelial neoplasia
VEGF	Vascular endothelial growth factor
VIN	Vulval intraepithelial neoplasia
VLP	Virus like particle
VZV	Varicella zoster virus
XP	Xeroderma pigmentosum
β-ME	β-Mercaptoethanol

Contents

List of Figures

List of Tables

List of Equations

1. Introduction

1.1. The Cell Cycle, DNA Repair and Cancer

1.1.1. The Cell Cycle

Neoplasia, meaning new growth, is a consequence of uncontrolled cell division/abnormal cell proliferation. Normal cell proliferation involves the reproduction of one cell to form two daughter cells. The sequence of stages through which a cell passes between one division and the next is known as the cell cycle. This cycle is made up of four stages; G_1, S, G_2 and M phase (Weinberg, 2013). G_1, S and G_2 make up interphase, where the cycling cell spends most its time and performs the majority of its pre-divisional functions including growth and replication of cellular organelles and DNA. M phase involves the partitioning of the cell to produce two new daughter cells and includes mitosis and cytokinesis. G_1 and G_2 are gap phases preceding the S and M phases respectively, in which the cell verifies that the cellular processes that occurred in previous phases were completed accurately (Weinberg, 2013).

Most eukaryotic cells are quiescent and exist in an inactive state called G_0, a phase outside the cell cycle (Gray et al., 2004). Mitogens or growth factors can induce cells in G_0 to re-enter the cell cycle and pass the G_1 restriction point (Foijer and Te Riele, 2006). Before they pass this restriction point, cell division is dependent on mitogens, however, afterwards they are committed to progress through the cell cycle without the need for growth factors (Pardee, 1989, Foijer and Te Riele, 2006).

Cyclins and cyclin dependent kinases (CDKs) coordinate passage of the cell through the different stages of the cell cycle (Weinberg, 2013). Cyclins are the regulatory subunits of highly specific CDKs and upon binding the cyclin induces a conformational change in the catalytic subunit of the CDK revealing its active site. Different cyclin-CDK complexes are present at specific points in the cell cycle. D-type cyclins and CDK4/6 drive cell cycle progression through G_1. E-type cyclins and CDK2 are involved in G_1 to S phase transition via phosphorylation of certain substrates. A-type cyclins and CDK2 complexes are important for S phase progression. A-type cyclins followed by B-type cyclins associate with

CDK1 and direct cell cycle progression through G_2. Finally, B-type cyclins and CDK1 trigger many of the events involved in mitosis (Weinberg, 2013).

A second form of cell cycle regulation is checkpoint control, which is a more supervisory form of regulation in comparison to regulation via the cyclin kinase family (Collins et al., 1997). Cell cycle checkpoints are a series of biochemical signalling pathways that sense and induce a cellular response to DNA damage and are important for maintaining the integrity of the genome. The G_1 checkpoint occurs at the end of the G_1 phase and can lead to the arrest of the cell cycle in response to DNA damage (Murray, 1994). The G_2 checkpoint occurs at the end of the G_2 phase and can lead to the arrest of the cell cycle in response to damaged or unreplicated DNA to ensure proper completion of S phase (Murray, 1994). The M checkpoint or mitotic spindle assembly checkpoint can lead to the arrest of chromosomal segregation in response to misalignment on the mitotic spindle during metaphase of mitosis (Murray, 1994). Disruption of these checkpoints can lead to mutations that may induce carcinogenesis (Pecorino, 2012). The phases of the cell cycle including checkpoints, cyclin-CDK complexes and CDK inhibitors are outlined in Figure 1.1.

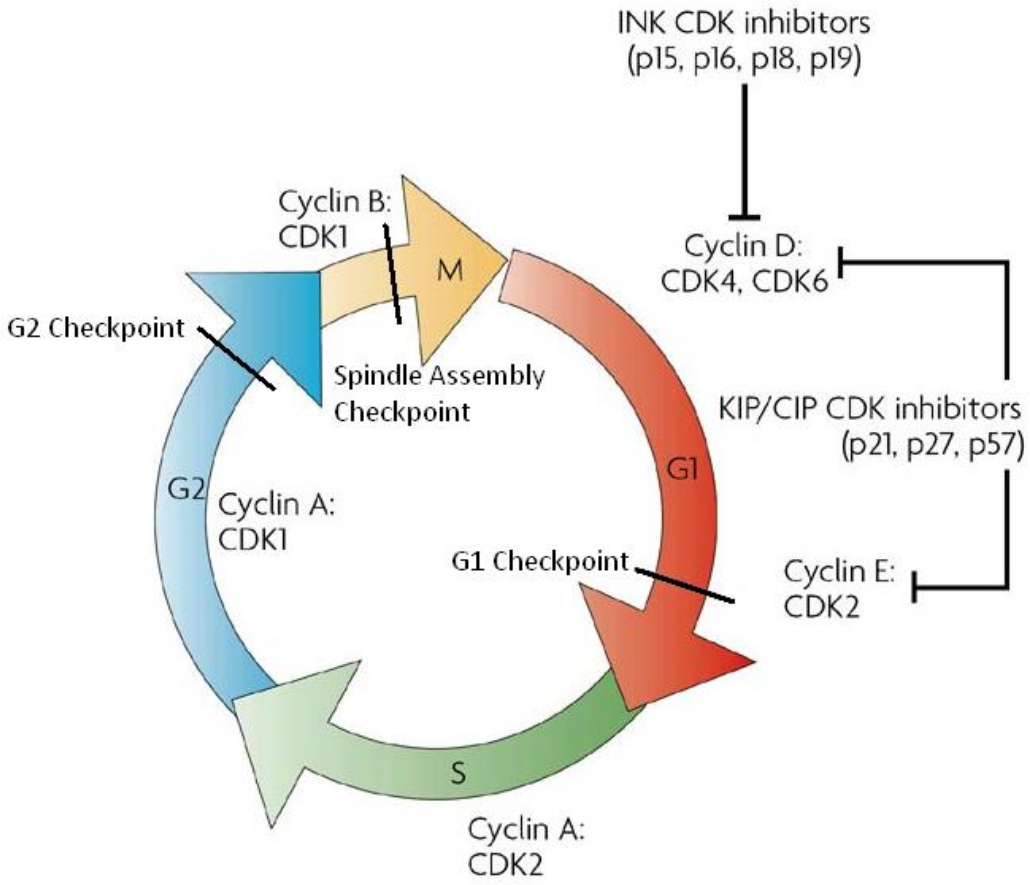

Adapted from Dehay et al. 2007

Figure 1.1. The Mammalian Cell Cycle

The mammalian cell cycle is composed of four individual phases: G_1, S, G_2 and M. The G_1 and G_2 phases precede S phase (during which DNA is replicated) and M phase (mitosis) respectively. The G_1 checkpoint occurs at the end of G_1 phase and functions to inhibit cell cycle progression in response to unfavorable environmental conditions and DNA damage. The G_2 checkpoint occurs at the end of the G_2 phase and inhibits progression of the cell cycle in response to damaged or incorrectly replicated DNA. The spindle assembly checkpoint occurs during M phase and blocks anaphase if chromatids are not correctly assembled on the mitotic spindle. Specific cyclin and CDK complexes drive progression through the various phases of the cell cycle. CDK inhibitors block the actions of CDKs at various points of the cell cycle. The four INK4 proteins (p16, p15, p18 and p19) inhibit the cyclin D-CDK4/6 complexes that are active in early and mid G_1 phase. The three KIP/CIP CDK inhibitors (p21, p27 and p57) can inhibit the remaining cyclin-CDK complexes and are active throughout the cell cycle.

1.1.2. DNA Repair

To maintain the integrity of the genome and avoid deleterious mutations cells possess several different mechanisms of DNA damage repair:

Nucleoside excision repair (NER) is a DNA damage repair pathway involved in the excision of major UV-induced photoproducts caused by sunlight such as cyclobutane pyrimidine dimers (CPDs) and the (6-4) pyrimidine–pyrimidone photoproducts (6-4PPs) (de Laat et al., 1999).

Base excision repair (BER) occurs in response to smaller DNA damage lesions caused by simple alkylating agents, free radicals and hydrolysis at both a spontaneous and continuous level (Seeberg et al., 1995, Offer et al., 1999). DNA glycosylases are the main enzymes involved in BER and act by removing damaged or modified bases through cleavage of the N-glycosylic bond between the defective base and the deoxyribose moieties of the nucleotide residues (Seeberg et al., 1995).

Mismatch repair (MMR) corrects DNA base-base mismatches and insertion/deletion mispairs generated during DNA replication and recombination (Li, 2008). As well as genome-wide instability, defects in MMR are linked to predisposition to particular types of cancer including hereditary non-polyposis colorectal cancer, resistance to chemotherapeutic agents, and aberrations in meiosis and sterility (Li, 2008).

Homologous recombination (HR) repairs a variety of DNA lesions, including single-strand DNA gaps, interstrand crosslinks and DNA double strand breaks (DSBs) (Krejci et al., 2012). DNA DSBs can be created by a number of different processes, including treatment with genotoxic chemicals, ionizing radiation, collapse of replication forks and endogenous DNA breaks (Krejci et al., 2012). HR uses extensive regions of DNA homology to accurately repair DSBs using the genetic code on the undamaged sister chromatid or homologous chromosome (Kanaar et al., 1998). HR repairs damaged DNA during S phase of the cell cycle (Saleh-Gohari and Helleday, 2004).

Non-homologous end-joining (NHEJ) repairs DNA DSBs using no or very limited sequence homology to re-join juxtaposed ends directly, in a manner that is not necessarily error free

(Kanaar et al., 1998, Moore and Haber, 1996). NHEJ can repair DNA DSBs at any point during the cell cycle (Rothkamm et al., 2003). As NHEJ is typically an imprecise process it can be useful for immune diversification in lymphocytes; however, it may also contribute to some of the genetic changes associated with cancer and ageing (Lieber et al., 2003).

Microhomology-mediated end joining (MMEJ) is a third less characterized DSB repair mechanism. In MMEJ DNA DSBs are repaired via the use of microhomologous sequences of approximately 5 to 25 nucleotides (McVey and Lee, 2008). However, this form of repair always results in deletions (McVey and Lee, 2008). It is thought that MMEJ contributes to oncogenic chromosome rearrangements and genetic variation in humans (McVey and Lee, 2008).

1.1.3. The Hallmarks of Cancer

The connection between deregulation of the cell cycle, defects in DNA repair pathways and unchecked proliferation resulting in neoplasia is evident. Defects in the synthesis, regulation, or recognition of growth factors/mitogens and related proteins that modulate the cell cycle can all result in tumour formation and cancer progression (Pecorino, 2008).

It has been proposed that the majority of cancer genotypes are a manifestation of eight crucial transformations in cell physiology, termed hallmarks of cancer, which together with two transformation enabling characteristics dictate malignant cell and tissue growth (Hanahan and Weinberg, 2000, Hanahan and Weinberg, 2011). The eight hallmarks of cancer include:

1.1.3.1. Self-Sufficiency in Growth Signals

Normal cells cannot divide and proliferate without the aid of mitogenic signals. However, oncogenes have evolved, which encode proteins that mimic mitogens and trick the cell into proliferation (Hanahan and Weinberg, 2000). Tumours often show autocrine cell growth, and are rarely dependent upon exogenous growth stimulation. Three characteristic molecular approaches for achieving autonomy are observed and involve alteration of;

- extracellular growth signals
- transcellular transducers of those signals
- intracellular circuits that translate those signals into action (Hanahan and Weinberg, 2000)

Cell surface receptors that relay positive growth signals to the cell interior can be targets of deregulation during tumorigenesis (Hanahan and Weinberg, 2000). Over expression of growth promoting receptors may induce cancer cells to become hyper-sensitive to normal levels of growth factor that would not ordinarily initiate proliferation (Hanahan and Weinberg, 2000). Additionally, cancer cells can alternate the types of extracellular matrix receptors they express, supporting ones that transmit positive proliferative signals (Lukashev and Werb, 1998). Alterations in intracellular signalling molecules, for example the SOS-Ras-Raf-MAPK cascade, which receive and process signals emitted by ligand-activated growth factor receptors and integrins, are the most complex autonomic features of cancer cells. An estimated 25% of human tumours bear structurally abnormal Ras, which allows for the release of mitogenic signals into cells in the absence of activation by their usual upstream regulators (Medema and Bos, 1993).

1.1.3.2. Insensitivity to Growth Inhibitory Signals

Cancer cells exist by evading cell cycle inhibitory signals. For example, disruption of the key antiproliferative pRb pathway liberates E2F which stimulates cell proliferation leaving cells insensitive to anti-growth factors. Aside from direct mutation, pRb activity, which is associated with TGFβ control (Franch et al., 1995), can be disrupted in several different ways in various types of human tumours (Hanahan and Weinberg, 2000). Some tumours lose sensitivity to TBFβ through dysfunctional/mutated cell surface receptors (Markowitz et al., 1995). Another study found that under particular cellular growth conditions pRb removal transforms TGFβ growth-inhibitory effects into growth-stimulatory effects (Herrera et al., 1996).

1.1.3.3. Evasion of Programmed Cell Death

It is now accepted that acquired resistance to apoptosis is a fundamental hallmark of the majority of cancers. This has been demonstrated in transgenic mice, where inactivation of

pRb in the choroid plexus resulted in the formation of slow growing microscopic tumours with high apoptotic rates. The accompanying inactivation of p53 led to fast growing tumours with low numbers of apoptotic cells (Symonds et al., 1994).

1.1.3.4. Limitless Replicative Potential

Immortalized cells are cells that have gained an infinite growth capacity allowing them to replicate indefinitely (Adolphe and Thenet, 1990, Hayflick, 1997). The majority of tumour cells that are grown in cell culture appear to be immortalized, suggesting that at some stage during tumorigenesis advancing premalignant cell populations lose their ability to limit mitosis, overcome senescence and acquire unlimited replicative potential (Hanahan and Weinberg, 2000).

Telomere conservation is apparent in nearly all types of malignant cells (Shay and Bacchetti, 1997). Most cells accomplish telomere conservation via up-regulation of telomerase, which functions as a reverse transcriptase enzyme using intrinsic RNA as a template to elongate the guanine-rich strand of telomere DNA (Bryan and Cech, 1999). Other cells preserve telomere length by activating a mechanism termed Alternative Lengthening of Telomeres (ALT), which is thought to maintain telomere length through homologous recombination-mediated DNA replication (Cesare and Reddel, 2010). In order to prohibit normal human cells from unlimited replicative potential, both mechanisms are heavily suppressed under normal physiological conditions (Bryan and Cech, 1999).

1.1.3.5. Sustained Angiogenesis

In the initial stages of cancer progression, proliferating neoplastic cells lack the ability to form new blood vessels from pre-existing vessels, a process termed angiogenesis. This restricts their capacity for expansion. In order to advance to a larger tumour mass, neoplastic cells must develop angiogenic ability (Hanahan and Folkman, 1996). Negative and positive signals can promote or inhibit angiogenesis.

Tumours appear to activate angiogenesis by altering the balance of angiogenic inducers and inhibitors which is promoted by altered gene expression (Hanahan and Folkman, 1996). Numerous tumours show increased expression of vascular endothelial growth

factor (VEGF) and/or fibroblast growth factor (FGF), or decreased expression of endogenous inhibitors such as interferon-β (Singh et al., 1995).

1.1.3.6. Tissue Invasion and Metastasis

The ability of cancer cells to invade and metastasize enables them to escape the primary tumour mass and colonize new areas in the body, where nutrients and space are not limited (Hanahan and Weinberg, 2000). Tissue invasion and metastasis use similar strategies which involve changes in the physical coupling of cells to their microenvironment and activation of extracellular proteases. Various classes of proteins such as cell to cell adhesion molecules (CAMs) and integrins, which are involved in cell adhesion and attachment, are altered in cells possessing invasive or metastatic characteristics (Hanahan and Weinberg, 2000). In cancer, the most observed change in cell-environment interactions involves E-cadherin, a calcium dependent cell-cell adhesion molecule, which is universally expressed on epithelial cells. The coupling of adjacent cells by E-cadherin allows for the relay of anti-proliferative signals by cytoplasmic contacts with β-catenin, a protein that helps coordinate transcription and cell to cell adhesion, to intracellular signalling cascades (Christofori and Semb, 1999). Normal E-cadherin function can be lost in many epithelial cancers due to inactivation of E-cadherin or β-catenin genes by mutation, transcriptional repression or proteolysis of the extracellular cadherin domain (Christofori and Semb, 1999).

1.1.3.7. Reprogramming of Energy Metabolism

Reprogramming of energy metabolism is described as an emerging hallmark of cancer (Hanahan and Weinberg, 2011). Unlike normal cells, in the presence of oxygen, cancer cells alter their glucose metabolism by limiting their energy metabolism mostly to glycolysis, which leads to a process called “aerobic glycolysis” (Vander Heiden et al., 2009). As this process is counterproductive, in that 18 fold less ATP can be produced by this method compared to normal aerobic respiration (Nelson and Cox, 2005), cancer cells compensate for this by increasing the importation of glucose into the cytoplasm by up-regulating glucose transporters, such as GLUT1 (Krzeslak et al., 2012). It has been suggested that cancer cells use aerobic respiration to facilitate the uptake and incorporation of glycolytic intermediates into biomolecule synthesis, such as nucleosides,

amino acids and lipids, all of which are required for the formation of new cancer cells (Vander Heiden et al., 2009).

1.1.3.8. Immunoevasion

Evading immune destruction is described as another emerging hallmark of cancer (Hanahan and Weinberg, 2011). It is thought that cancer cells evade immune elimination by disabling elements of the immune system that have been targeted to eradicate them. (Hanahan and Weinberg, 2011). A murine study found that melanoma tumour expression of CCL21, a chemo-attractant for a range of leukocytes and lymphoid tissue inducer cells, was associated with immunotolerance (Shields et al., 2010). However, immunoevasion as a core hallmark of cancer is yet to be further developed (Hanahan and Weinberg, 2011).

1.1.4. Transformation Enabling Characteristics

In addition to the previously outlined hallmarks of cancer, Hanahan and Weinberg, 2011 , also described two transformation enabling characteristics of cancer cells: tumour promotion of inflammation and genome instability and mutation. To complement the work outlined in this thesis the latter is discussed in more detail than the former.

1.1.4.1. Tumour Promotion of Inflammation

Tumour promotion of inflammation can contribute to several of the hallmarks of cancer by delivering bioactive chemokines to the tumour microenvironment, which in turn can promote tumour growth, angiogenesis, invasion and metastasis (Karnoub and Weinberg, 2006, Hanahan and Weinberg, 2011).

1.1.4.2. Genome Instability and Mutation

Genome instability and mutation enable cell transformation by providing selective growth advantage to subclonal populations of cells. This results in outgrowth of the mutant cells in a local tissue environment and subsequent dominance of the defective genotype (Hanahan and Weinberg, 2011). Genome instability can occur via a range of different processes, which can be classified according to the category of event stimulated. Chromosomal instability caused by failure in mitotic chromosome transmission or failure of the spindle mitotic checkpoint results in changes in chromosome number (Aguilera and Gomez-Gonzalez, 2008, Draviam et al., 2004). Micro- and mini-satellite instability results

in repetitive-DNA expansions or contractions caused by replication slippage (Aguilera and Gomez-Gonzalez, 2008). Genome instability generating mutations including micro-insertions, micro-deletions and base substitutions result from replication errors, impairment of BER or MMR (Aguilera and Gomez-Gonzalez, 2008). Genome instability resulting in DNA rearrangements such as translocations, duplications, inversions and deletions involve changes in the genetic linkage of two DNA fragments, which ultimately occur via DNA DSBs (Aguilera and Gomez-Gonzalez, 2008).

1.1.5. Gain of Function Mutations

There are several different classifications of mutation. Based on effect on gene product function mutations can be classified as gain of function or loss of function. Gain of function mutations are mutations that change the product of a gene resulting in a new and abnormal function. Oncogene activation is an example of gain of function mutation (Osborne et al., 2004). Oncogenes were originally identified in tumour causing viruses and were later found to be analogous to or derived from genes in animal host cells that encode growth regulatory proteins, namely, proto-oncogenes (Nelson and Cox, 2005).

On occasion during a viral infection, the DNA sequence of a host proto-oncogene can be copied by the virus and incorporated into its genome. Subsequently during the viral replication cycle this gene may become defective due to mutation. When the defective gene is expressed in the host cell the resulting abnormal protein product interferes with correct regulation of cell growth, which occasionally results in tumour formation (Nelson and Cox, 2005). An example of this process can be seen with Rous sarcoma virus (RSV). The RSV retrovirus was the first oncogenic virus to be identified (Rous, 1911). The gene that enables RSV to transform cells is *v-src* (Martin, 1970), which encodes a tyrosine kinase enzyme. *v-src* is derived from a proto-oncogene termed *c-src* found in normal vertebrate cellular DNA (Stehelin et al., 1976).

Proto-oncogenes can also become efficient oncogenes without a viral intermediate. Chromosomal rearrangements, chemical agents and radiation are among the factors that contribute to oncogenic mutations. The mutations that activate oncogenes are genetically dominant and the oncogenic defect can be in any of the proteins involved in intra-cellular

signalling. For example, oncogenes can encode: secreted proteins (secreted Frizzled-related proteins (sFRP)), growth factors (platelet-derived growth factor (PDGF)), transmembrane protein receptors (ErbB), cytoplasmic signalling proteins (Ras) and several transcription factors (Jun and Fos) (Nelson and Cox, 2005).

1.1.6. Loss of Function Mutations

Loss of function mutations involve mutations in tumour suppressor genes (TSGs). These genes have protein products whose function is to inhibit cell division if DNA damage/mutation occurs, therefore, they negatively modulate cell cycle progression (Collins et al., 1997). Examples of tumour suppressor gene products are pRb and p53. Inactivation of both copies of a tumour suppressor gene is usually required for loss of function. In contrast to gain of function oncogenes, loss of function mutations can be carried in the gene pool with no direct deleterious consequence. Mutations in pRb and p53 are examples of loss of function mutations (Nelson and Cox, 2005).

1.1.7. p53 Tumour Suppressor Protein

p53, also termed the "Guardian of the Genome", is a sequence-specific transcription factor that modulates most of its downstream effects via activation or repression of target genes. It is a central element of several stress response pathways that prevent growth and survival of possible malignant cells; however, it is also one of the most frequently mutated tumour suppressor genes found in cancer (Levine and Oren, 2009).

When the cell is not exposed to stress or DNA damaging agents, levels of p53 are tightly controlled predominantly by Mdm2, its negative regulator, through the ubiquitin-proteasome degradation pathway in order to maintain normal homeostatic levels of cell growth (Haupt et al., 1997). Activation via phosphorylation of p53 in response to stresses such as DNA damage, hypoxia and/or oncogene activation disrupts the binding of Mdm2 to p53 (Shieh et al., 1997), allowing p53 to proceed to regulate a number of downstream responses such as DNA repair, apoptosis, cell-cycle arrest, senescence or regulation of autophagy (Hofseth et al., 2004, Tasdemir et al., 2008). In addition, p53 is also involved in cell survival (Singh et al., 2002), chromosomal segregation, DNA recombination, gene amplification, development and differentiation (Hofseth et al., 2004). The p53 induced

response is influenced by several different factors, including the action and availability of p53 co-activators as well as the type of cellular stress and characteristics of the assaulted cell (Haupt et al., 1997).

1.1.7.1. p53 Function

p53 induces DNA repair via a range of different mechanisms. In the first instance p53 regulates the transcription of several genes involved in NER including the global genomic repair (GGR)-specific damage recognition genes DDB2 and XPC (Adimoolam and Ford, 2003). Additionally, p53 has been shown to be directly involved in BER. Activation of BER by p53 in response to DNA damage is associated with its capability to interact with DNA polymerase β and AP endonuclease. Moreover, p53 can stabilize the interaction of DNA polymerase β with abasic DNA (Zhou et al., 2001). p53 has also been shown to be involved in DNA DSB repair. It has been found that p53 is directly involved in re-joining of DSBs with short complementary ends of single-stranded DNA in gamma-irradiated mouse embryonic fibroblasts (Tang et al., 1999). Additionally, it has been suggested that p53 plays a role in restraining DNA exchange between inadequate homologous sequences, therefore inhibiting tumorigenic genome rearrangements (Akyuz et al., 2002).

p53 can induce apoptosis at a number of different levels. It can stimulate the extrinsic apoptotic pathway via the transcription of genes encoding the transmembrane proteins, PERP, Fas and DR5 (Hofseth et al., 2004, Vousden and Lu, 2002). It also plays a role in the intrinsic apoptotic pathway by regulating the transcription of a subset of the Bcl-2 family including Bid, Bax, Noxa, and PUMA, which function by promoting cytochrome C release from the mitochondria (Hofseth et al., 2004). The release of cytochrome C as well as APAF-1, whose transcription is also regulated by p53 (Kannan et al., 2001), from mitochondria and their subsequent interaction with pro-caspase-9 is required for the formation of the apoptosome (Adams and Cory, 2002).

p53 can delay the transition through G_1, G_2 and the mitotic spindle checkpoints. p53 induces the expression of several cell cycle regulatory genes including *CDKN1A/CIP1/WAF1*, which encodes a G_1 CDK inhibitor, p21. p21 binds to and inhibits the CDK4/cyclin D and CDK2/cyclin E complexes and prevents them from phosphorylating

downstream target proteins responsible for cell cycle progression (He et al., 2005). Gadd45, another p53-regulated protein, has been found to contribute to G_2 arrest (Jin et al., 2000). With regards to the mitotic spindle checkpoint, it has been shown that the presence of spindle inhibitors impede the passage of cells through mitosis, but p53 null mouse embryo fibroblasts will go through numerous rounds of DNA synthesis with incomplete chromosome segregation, which results in the formation of tetraploid and octaploid cells (Cross et al., 1995).

Cellular senescence, the process in which cells permanently lose their ability to divide or replicate, is linked to p53 control. The expression of *CDKN1A* increases at an early stage in senescent cells, indicating that p53 plays a role in inducing senescence at an initial stage in the process (Itahana et al., 2001, Stein et al., 1999).

p53 has been shown to possess a dual role in the regulation of autophagy, a catabolic process that involves the degradation of unnecessary or dysfunctional cellular components to recycle valuable biomolecules through lysosomal machinery. Cytoplasmic p53 has been found to repress autophagy (Tasdemir et al., 2008), whereas nuclear p53 has been found to induce autophagy (Crighton et al., 2006).

1.1.8. Retinoblastoma Tumour Suppressor Protein (pRb)

The retinoblastoma gene was the first tumour suppressor gene to be discovered (Friend et al., 1986). Its protein product, pRb, is a nuclear phosphoprotein that functions to suppress progress through the G_1 phase of the cell cycle by restricting the transcription of genes required for G_1-to-S-phase progression (Harbour and Dean, 2000). Active hypo-phosphorylated pRb sequesters transcription factors such as E2F, which are required to activate the transcription of S phase genes, therefore preventing the passage of cells across the G_1 checkpoint in normal cells. However, during the middle to late stage of the G_1 phase, complexes of cyclin D/CDK4 and/or CDK6 elicit the phosphorylation of pRb, which causes its dissociated from E2F and inhibits its growth suppressive function. The CDK inhibitor 2 (*CDKN2*) gene encodes p16INK4 protein, which binds to, and inhibits the CDK4- and CDK6- phosphorylation and inactivation of pRb (Pande et al., 1998, Lukas et al., 1995, Harbour and Dean, 2000). Tumour suppression via pRb requires the central 'pocket'

domain of the protein, which is disrupted by the majority of naturally arising tumour-promoting genetic alterations and mutations, and is targeted by viral oncoproteins that disrupt pRb function (Harbour and Dean, 2000).

1.2. Human Papillomavirus

1.2.1. Definition and Classification

It is now accepted that Human Papillomaviruses (HPV) are the primary causative agents of clinically abnormal gynaecological and anogenital epithelial lesions (van de Nieuwenhof et al., 2008). Infection with HPV is also known to lead to the development of respiratory tract papillomas and other hyper-proliferative epithelial lesions of the head and neck region such as the conjunctiva, ear canals, nasal sinuses and tonsils (Chow et al., 2010).

HPV is a member of the family Papillomaviridae. More than 150 different genotypes of HPV have been isolated to date (Tommasino, 2013), each having a specific tropism to a particular epithelium type/site (Doorbar, 2006). Each genotype is characterized as being more than 10% different from all other HPV genotypes in their *L1* genetic sequence (Bernard, 2005). Furthermore, these viruses can be divided into five genetically distinct genera: Alpha, Beta, Gamma, Mu and Nu. Distinct genera share no more than 60% nucleotide sequence identity in the *L1* Open Reading Frame (ORF) (IARC, 2007). Subgroups within each genus are termed species, where species within a particular genus share between 60 and 70% nucleotide sequence identity (IARC, 2007).

Gamma, Mu and Nu papillomaviruses make up the minority of currently classified HPVs and normally cause benign cutaneous papillomas such as superficial warts and verrucas (Doorbar, 2006). The two primary HPV genera are the Alpha and Beta papillomavirus genera, with an estimated 90% of known HPV types falling within one of these two genera (Doorbar, 2006). The largest genus is the Alpha papillomavirus group, whose members infect genital mucosa. Greater than 30 different types of the Alpha virus genus infect cervical epithelium, with a subgroup of these being associated with premalignant lesions and invasive cancer development and progression (Doorbar, 2006). Such cancer associated HPVs are classified into High- and Low-Risk HPVs (HR-HPV and LR-HPV respectively) depending on the incidence with which they are identified in cancers. HR-HPVs are most frequently found in cancers, with HPV16 being the most prevalent type in the general population and the known causative agent in approximately 61% of all cervical cancers (de Sanjose et al., 2010). In addition to HPV16, Alpha HPV types 18, 31, 33, 35, 39,

45, 51, 52, 56, 58, 59 and 66 are classified as group one carcinogens by the International Agency for Research on Cancer (IARC) (IARC, 2012). HPV6 and 11 are low risk Alpha papillomaviruses, which are rarely associated with gynaecological cancer but are commonly found in genital warts. Alpha HPVs also include several cutaneous viruses, for example HPV2, but are rarely linked to cancers. Beta papillomaviruses have been related to unapparent or latent cutaneous infections in the general population. Beta papillomaviruses become problematic in immuno-suppressed patients and in individuals who have inherited disorders such as Xeroderma pigmentosum (XP), where infection can spread rapidly and become associated with non-melanoma skin cancer (NMSC) (Harwood and Proby, 2002). A summary of the different virus types and species within each specific HPV genus is outlined Table 1.1.

Table 1.1. HPV Genera, Species and Types

Genus	Species	IARC Group 1 Carcinogenic HPV Types	Other HPV Types Within Species	Species Characteristics
Alpha	1		32, 42	Low risk, oral/genital mucosa
	2		3, 10, 28, 29, 78, 94	Low risk, cutaneous lesions
	3		61, 62(cand), 72, 81, 83, 84, 86(cand), 87(cand), 89(cand)	Low risk, mucosal lesions
	4		2, 27, 57	Common skin warts, benign genital lesions in children
	5	**51**	26, 69, 82	High risk, mucosal lesions
	6	**56, 66**	30, 53	High risk, mucosal lesions
	7	**18, 39, 45, 59**	68, 70, 85, 97	High risk, mucosal lesions
	8		7, 40, 43, 91(cand)	Low risk, mucosal/cutaneous
	9	**16, 31, 33, 35, 52, 58**	67	High risk, mucosal lesions
	10		6, 11, 13, 44, 74	Low risk, mucosal lesions
	11		34, 73	High risk, mucosal lesions
	13		54	Low risk, mucosal lesions
	14		90	Low risk, mucosal lesions
	15		71	Low risk, mucosal lesions
Beta	1		5, 8, 12, 14, 19, 20, 21, 25, 36, 47, 93	Benign cutaneous, also reported in malignant lesions
	2		9, 15, 17, 22, 23, 37, 38, 80	Benign cutaneous, also reported in malignant lesions
	3		49, 75, 76	Benign cutaneous lesions
	4		92(cand)	Pre-/malignant cutaneous lesions
	5		96(cand)	Pre-/ malignant cutaneous lesions
Gamma	1		4, 65, 95	Cutaneous lesions
	2		48	Cutaneous lesions
	3		50	Cutaneous lesions
	4		60	Cutaneous lesions
	5		88	Cutaneous lesions
Mu	1		1	Heterogeneous lesions with intracytoplasmic inclusion bodies
	2		63	Heterogeneous lesions with intracytoplasmic inclusion bodies
Nu	1		41	Several larger uncharacterized ORFs in viral genome

From de Villiers et al. 2004

The table shows division of Papillomaviridae (human) into genera and species. Specific HPV types are outlined for each species with emphasis on the IARC group 1 carcinogenic types (highlighted in yellow). Species characteristics such as tissue tropism and pathological properties are also outlined. (cand) = candidate HPV.

1.2.2. HPV Genomic Structure

The HPV genome consists of double-stranded circular DNA of approximately 8000 base pairs (bp) (Narisawa-Saito and Kiyono, 2007). The genome has an upstream regulatory region (URR) spanning 400 – 700 base pairs (bp), six early (*E1, E2, E4, E5, E6* and *E7*) region ORFs and two late (*L1* and *L2*) region ORFs (Chow et al., 2010). The origin of replication is located in the URR, as well as core transcription factor binding sites, early promoters and several enhancer and repressor regulatory proteins (Chow et al., 2010). The virus replicates as multi-copy episomal plasmids in the nucleus of infected dividing basal and parabasal keratinocytes. Amplification in the copy number can be seen as the keratinocytes differentiate up through the various layers of epithelium reaching the mid to upper spinous cell layer (Chow et al., 2010). HPV genome structure is depicted in Figure 1.2.

1.2.3. Physical Structure of HPV; L1 and L2 Capsid Proteins

A non-enveloped icosahedral capsid of estimated 55 nm in diameter encloses the HPV genome. The capsid is composed of two structural capsid proteins, one major and one minor, L1 and L2 respectively (Roden and Viscidi, 2006). The L1 capsid protein forms 72 pentameric capsomeres that constitute the major portion of the icosahedral virion. One copy of the L2 protein is embedded into each of the 72 pentamers, which promotes shape and stability (Buck et al., 2008). HPV virions do not have a membrane envelope and are stable to environmental extremes due to cross-linking of L1 capsid proteins by disulphide bonds (Chow et al., 2010). An atomic model of the surface of a HPV virion is outlined in Figure 1.3.

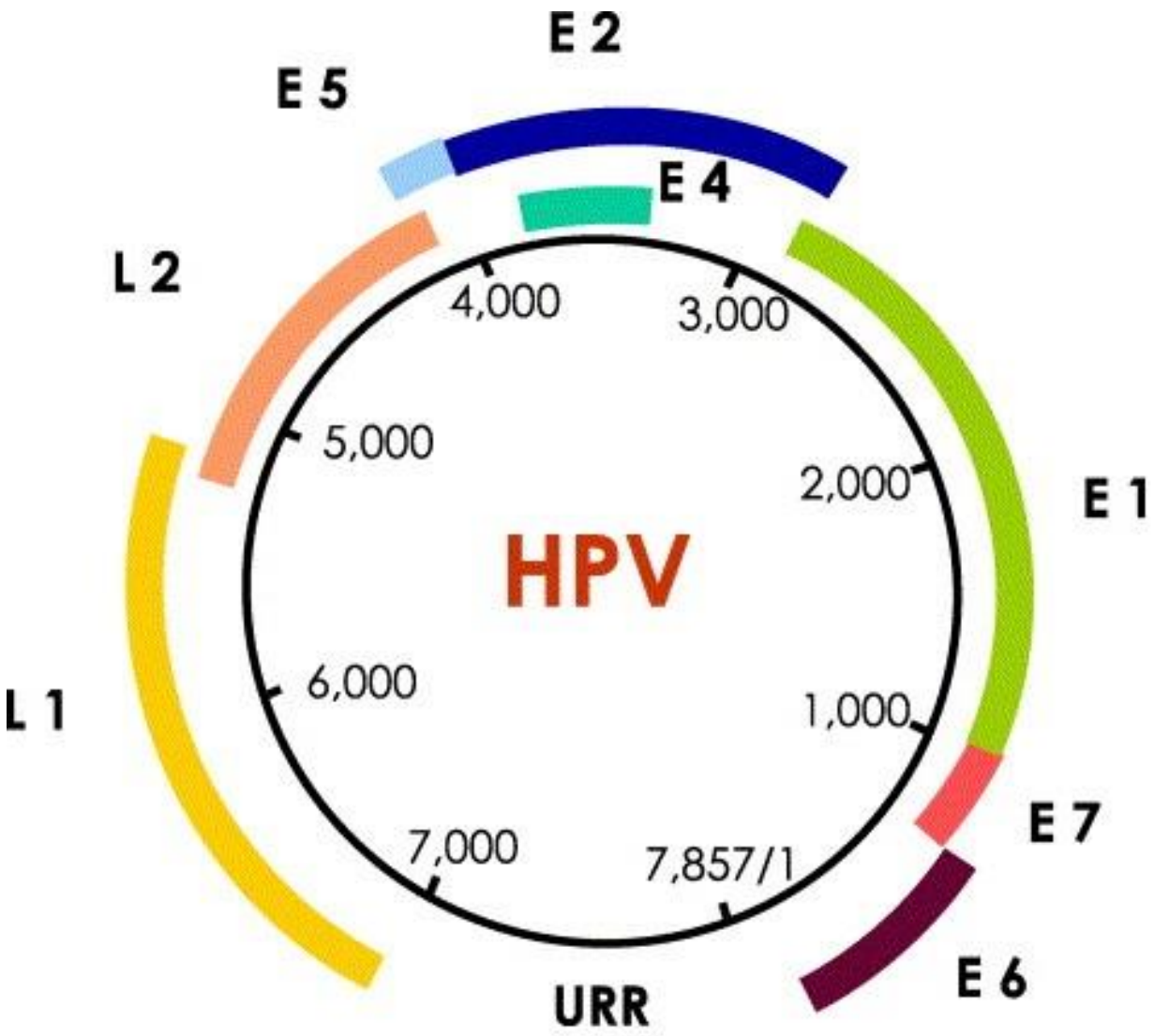

Adapted from Muñoz et al. 2006

Figure 1.2. HPV Genomic Structure

Schematic presentation of the circular HPV DNA genome based on HPV16. The figure shows the arrangement of the early ORFs (E1, E2, E4, E5, E6 and E7) and the late capsid ORFs (L1 and L2). Both sets of early and late ORFs are separated by a non-coding upstream regulatory region (URR) of about 1000 bp, which contains cis-elements required for regulation of gene expression, replication of the genome, and its packaging into virus particles.

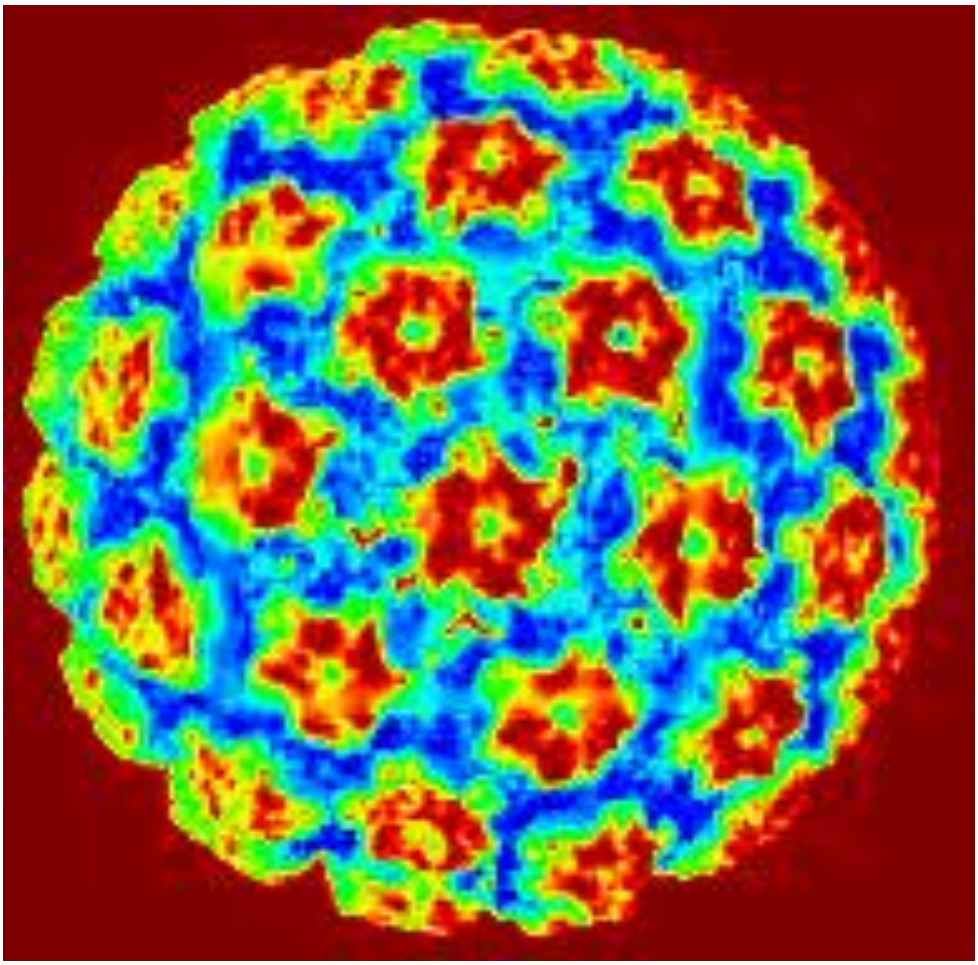

Adapted from Modis et al. 2002

Figure 1.3. Molecular Surface of a HPV Virion

Heat map of the molecular surface of the atomic model of a HPV virion. The model was generated using combined image reconstructions from electron cryomicroscopy of bovine papillomavirus with coordinates from the crystal structure of small virus-like particles of the human papillomavirus type 16 L1 protein.

1.2.4. HPV Infection and Virus Life Cycle

1.2.4.1. Initiation of HPV Infection

HPV is transmitted from one individual to another via direct dermal/mucosal contact with an infected person. The virus requires entry to the basal epithelial layer and access to the immature dividing basal cells to initiate infection (Doorbar, 2006). It is speculated that heparin sulphate proteoglycans play a role in the initial binding/virus uptake event and that α6 integrin molecules act as secondary receptors for efficient infection (Shafti-Keramat et al., 2003, McMillan et al., 1999). The viral particles are taken into the host epithelial cells very slowly after binding, the mode of entry differing between genotypes. For example, HPV16 is taken into the cell via clatherin coated endocytosis (Day et al., 2003), whereas, HPV31 is thought to enter via caveolae (Bousarghin et al., 2003).

It is presumed that the reducing environment of the host cell disrupts the disulphide cross-links of the L1 protein, and the acidic conditions in endosomes disassembles the capsid, releasing the viral genome into the cytoplasm, where it is transported to the nucleus with the aid of the minor capsid protein L2 (Chow et al., 2010).

1.2.4.1.1. E1 and E2 Viral DNA Replication Proteins

Early in HPV infection the viral genome exists as a stable episome. It is thought this process requires the expression of E1 and E2, the viral replication proteins (Doorbar, 2006). The E1 and E2 mRNAs are derived from the same primary transcripts but spliced differently (Chow et al., 2010). E1 is a DNA helicase and the only enzyme encoded by HPV, rendering it problematic to obtain selective inhibitors of HPV replication (Chow et al., 2010). The E2 protein initiates viral DNA replication and genome segregation in replicative cells (Chiang et al., 1992). It is a DNA-binding protein that identifies and binds to a particular palindromic motif in the non-coding region of the viral genome (Dell et al., 2003). E2 binding in this region is required to recruit the E1 helicase to the viral origin, which in turn binds to host cell proteins needed for DNA replication such as replication protein A (RPA) and DNA polymerase *α* primase (Conger et al., 1999, Loo and Melendy, 2004). The E2 protein then separates from the viral origin in an ATP dependent process, allowing the assembly of E1 into a double hexameric ring (Sanders and Stenlund, 1998, Sedman and Stenlund, 1998).

Besides functioning in the initiation of replication, the E2 protein also has other functions. For example, HPV DNA replicates concurrently with the host cell DNA during S-phase and the E2 protein is responsible for anchoring viral episomes to mitotic chromosomes to ensure equal partitioning and segregation during the mitotic division (You et al., 2004). Furthermore, E2 acts as a repressor of the transcription of viral oncogenes, *E6* and *E7*, at high levels by displacing a transcriptional activator from a site adjacent to the early promoter, whereas, at low levels it allows for transcription activation (Doorbar, 2006).

This early stage of HPV infection is termed as a latent or clinically unapparent infection since the host is HPV DNA positive, but no lesions can be detected (Wright, 2006).

1.2.4.2. Promotion of Cell Proliferation

The HPV oncoproteins, E5, E6 and E7, are required along with E1 and E2, for viral episome replication above the basal layer of the epithelium (Doorbar, 2006). The HPV oncoproteins condition the infected differentiating host cell to support viral DNA amplification by interfering with signal transduction pathways and inactivating major tumour suppressor proteins. They are the means by which HR-HPV types promote cell transformation and immortalization (Munger et al., 1989).

1.2.4.2.1. E7 Oncoprotein

The E7 oncoprotein is approximately 100 amino acids long and contains two highly conserved regions (CRs), the amino-terminal CR1 and CR2 domains (Wang et al., 2010). The mature E7 protein binds, sequesters and directs pRb to its ubiquitin-mediated proteolysis (Huh et al., 2007). This results in the liberation of E2F, which leads to the expression of proteins needed for cell cycle progression and entry into S phase, bypassing cell cycle arrest and cellular senescence. In addition to the degradation of pRb, E7 also destabilizes p130, a pRb related protein, which is responsible for regulating homeostasis in differentiated cells by preventing them from re-entering the S phase. Thus, disruption of p130 by E7 promotes S-phase re-entry in differentiated cells (Genovese et al., 2008).

In addition to its association with pocket proteins such as pRb and p130, E7 can also interact with histone deacetylases to maintain HPV episomal DNA and extend the life span of infected keratinocytes (Longworth and Laimins, 2004).

E7 can interact with AP1 transcription factors such as c-Jun, JunB, JunD and c-Fos. It can trans-activate c-Jun-induced transcription from a Jun responsive promoter (Antinore et al., 1996). c-Jun is a proto-oncogene that has several cell proliferation promoting attributes such as repression of p53 transcription through binding to a variant AP-1 site in the p53 promoter (Schreiber et al., 1999). In addition, c-Jun also induces the transcription of cyclin D1 (Schwabe et al., 2003), where cyclin D1 phosphorylates pRb resulting in the liberation of E2F and cell cycle progression.

HR-HPV E7 also prevents p21 from inhibiting CDK2/cyclin E activity and proliferating cell nuclear antigen (PCNA)-dependent DNA replication through interaction with sequences that modulate anti-proliferative activity in the carboxy-terminal end of the p21 protein (Funk et al., 1997).

1.2.4.2.2. E6 Oncoprotein

The main function of E7 is to stimulate unscheduled S-phase entry and cell cycle progression. However, the increase in liberated E2F, which occurs as a result of E7 activity, can induce and stabilize p53 levels (Seavey et al., 1999, Wu and Levine, 1994, Nip et al., 2001) in an effort to control unchecked cell proliferation by causing apoptosis. The second major HPV oncoprotein, E6, complements the role of E7 by inhibiting p53 induced apoptosis in response to unscheduled S-phase entry.

E6 is small highly basic 158 amino acid protein that contains two zinc-binding domains (Ristriani et al., 2000). E6 uses the ubiquitin-ligase E6-AP to induce p53 degradation. An E6/E6-AP complex forms before the formation of the stable ternary complex that includes p53 (Scheffner et al., 1993), this complex in turn is recognized by the ubiquitin-dependent proteolysis system and causes the degradation of p53 via this pathway (Scheffner et al., 1993). Thus, by preventing the accumulation of cellular p53, HPV has the ability to overcome p53 growth arrest and apoptosis-inducing functions.

The E6 oncoprotein has many other p53-independent functions that may augment the anti-apoptotic and oncogenic potential of HPV. E6 is thought to be involved in the reduction of apoptosis induced by Bak. E6 associates with pro-apoptotic Bak and decreases its function by increasing the level of Bak degradation. Similar to its effect on

p53, degradation presumably occurs via ubiquitination by the E6-AP protein. Bak may represent a normal cellular target of E6-AP when HPV is not infecting the host (Thomas and Banks, 1998).

Additionally, the E6 protein can increase transcription of the *hTERT* gene, which codes for the catalytic subunit of the telomerase holoenzyme. Telomerase synthesizes telomere repeat sequences (TTAGGG) which prevent loss of DNA from chromosomal ends during genome replication, thus, avoiding cell senescence (Klingelhutz et al., 1996). The enzyme uses an RNA template, namely TERC, to add telomere repeats to chromosome ends. The TERT subunit of the enzyme is the restricting component in telomerase activity and over-expression of the *hTERT* gene alone is enough to generate elevated levels of telomerase activity in cells (McMurray and McCance, 2004). Further to its enzymatic activity, telomerase has demonstrated direct association with double-strand break-sensing proteins (human homologues of the yeast Ku protein, Ku70 and Ku80), which suppress the potential DNA damage responses at telomere ends (McMurray and McCance, 2004). The exact molecular mechanism of E6 up-regulation of *hTERT* transcription is yet to be fully determined. One study found that E6 increased *hTERT* transcription correspondingly with E6-induced telomerase activity in transduced primary human foreskin keratinocytes. Furthermore, E6 induced a 6.5-fold increase in the activity of a 5' promoter region in the *hTERT* gene in the same cells (Veldman et al., 2001). A different study suggested that E6 interferes with a repressive complex present on the proximal E box in the *hTERT* promoter as HPV16 E6 activated the *hTERT* promoter principally through this region in transfected primary human foreskin keratinocytes (McMurray and McCance, 2003). The E box site is specific for the Myc/Mad/Max transcription factors in addition to USF1 and USF2 and upon addition of exogenous USF1 or USF2, the authors found repression of E6 activation of the *hTER*T promoter, Moreover, they found that siRNA against USF1 or USF2 resulted in greater activation of the *hTERT* promoter by E6 and that loss of c-Myc function reduced such activation. Through chromatin immunoprecipitations the authors found that there was a reduction in binding of USF1 and USF2 at the *hTERT* promoter proximal E box, and an accompanying increase in c-Myc bound to the same site in the presence of E6. It was suggested that a repressive complex containing USF1 and USF2 is present in normal cells

with minimal telomerase activity and that such a repressive complex is replaced by c-Myc in E6 transfected keratinocytes, which coincides with higher levels of *hTERT* transcription and telomerase activity (McMurray and McCance, 2003).

Another p53 independent mechanism whereby E6 augments the oncogenic potential of HPV is through its PDZ domain binding function. The PDZ binding activity of E6 results in atypical cellular morphology and disruption of intercellular junction formation (Watson et al., 2003). PDZ (PSD-95/disc large/ZO-1) domains are 80 - 90 amino acid protein-interaction domains frequently found in multi-domain scaffolding proteins, which bind to short peptide motifs of other proteins (Ponting and Phillips, 1995, Kim, 1997). A number of PDZ domain containing proteins have been identified as binding partners of HR-HPV E6. One such protein is the human homologue of the Drosophila tumour suppressor protein, discs large (Dlg) (Gardiol et al., 1999). Dlg is expressed in several different cell types including epithelial cells, where it is located in areas of cell-cell contact (Lue et al., 1994). Disruption of Dlg results in loss of polarity in epithelial cells and neoplastic progression (Woods et al., 1996). E6 interacts with Dlg through a highly conserved region in its C-terminal domain (Kiyono et al., 1997). Once bound to Dlg, E6 mediates the proteasomal degradation of this protein and abolishes its tumour suppressor function (Gardiol et al., 1999), further contributing to oncogenesis by HPV.

E6 has also been shown to regulate G protein signalling by degrading GTPase-activating proteins (GAPs). One study found that E6TP1 (E6-targeted protein 1), a protein to which E6 binds and targets for ubiquitin-mediated degradation, has high homology to GAP domains of Rap GAPs. The study confirmed human E6TP1 displays GAP activity for Rap1 and Rap2. Expression of E6 promoted the degradation of E6TP1 and enhanced the GTP loading of Rap, which leads to continuous activation of the Rap small-G-protein pathway (Singh et al., 2003).

1.2.4.2.3. E5 Oncoprotein

HPV E5 is the third and least well characterized HPV oncoprotein. It is a transmembrane protein found mainly in the cellular endoplasmic reticulum, which can promote retardation of endosomal acidification through association with the vacuolar proton

ATPase. It is assumed this influences growth factor receptor recycling, which results in an increase in epidermal growth factor receptor regulated signalling and the conservation of a replication efficient environment in the upper epithelial layers (Crusius et al., 2000).

1.2.4.3. Progeny Virus Assembly and Release

If infectious progeny virions are to be produced, HPV must eventually amplify and package its genome. Late events in the infection process are thought to depend on the variations in the cellular environment as the HPV infected cell passes towards the upper epithelial surface (Bodily and Meyers, 2005). This depends largely upon up-regulation of the differentiation dependent promoter, which for the majority of HPV types is positioned within the *E7* ORF (Bodily and Meyers, 2005). Activation of this promoter depends on host cell signalling and results in an increase in the level of viral replication proteins (Bodily and Meyers, 2005).

The end stage in the HPV productive infection cycle involves the packaging of the amplified viral DNA into newly formed infectious particles. L1 and L2 viral capsid proteins appear after the commencement of genome amplification (Florin et al., 2002). It is thought that the events that link genome amplification to capsid protein synthesis are dependent on adjustments in mRNA splicing and on the production of transcripts that finish in the late polyadenylation site (Doorbar, 2006).

In addition to L1 and L2, it has been suggested that E2 may promote the competency of genome encapsulation during natural infection (Zhao et al., 2000). By means of nuclear localization signals located at its N- and C-termini, L2 localizes to the nucleus and associates with promyelocytic leukaemia (PML) bodies. In contrast, L1 clusters into capsomeres in the cytoplasm prior to transportation to the nucleus. Once it has been transported to the nucleus it is incorporated into PML bodies once L2 has bound and dislodged the PML component SP100 (Florin et al., 2002).

The L2 capsid protein then links to L1 via a hydrophobic region near its C terminus, which is believed to embed into a central hole in the L1 capsomeres (Finnen et al., 2003). Disulphide cross-linking of the capsomeres gives rise to virus maturation and stabilization as the infected host cells near the surface of the epithelium (Buck et al., 2008). The

delayed expression of HPV antigens is thought to restrict the ability of the immune system to identify infection up until the infected cell reaches the superficial epithelial surface (Tindle, 2002).

1.2.4.3.1. E4 Protein

Productive HPV infection is associated with significant expression of E4 protein, where E4 is thought to have several different functions at different stages of the HPV lifecycle. Several HPV types encode E4 proteins that promote cell cycle arrest in G_2 and counteract E7 directed cellular proliferation which can complement HPV genome amplification (Nakahara et al., 2002, Knight et al., 2011). It has been hypothesized that HPV1 E4 inhibits competing host cell DNA synthesis by suppressing licensing of cellular origins of replication, which liberates host cell DNA replication machinery favouring HPV genome amplification (Roberts et al., 2008).

HR-HPV E4 is thought to be involved in late gene expression (Wilson et al., 2007), as well as assisting in progeny virus escape at the cornified envelope at the cell surface. E4 can interrupt the keratin network of the epithelium and can affect the structural stability of the cornified envelope (Doorbar et al., 1991, Roberts et al., 1993).

1.2.5. HPV Infection Outcome; Regression or Progression to Cancer

In most people immunity will develop to HPV after a period of months or years and productive infection terminates. These people ultimately become HPV DNA negative (Wright, 2006). However, in the absence of lesion regression with persistent HPV infection, progression to cancer may occur. Expression of the HPV oncogenes, whilst necessary for productive HPV infection to drive host cell proliferation in order to increase episomal replication, may become deregulated resulting in increased cell proliferation in the lower epithelial layers. This leads to abortive HPV infection, where the virus is primarily confined to its proliferative phase and cannot effectively complete its productive life cycle (Doorbar, 2005). The increased rate of cell proliferation along with failure to repair secondary mutations can result in genome instability, which further promotes an oncogenic phenotype.

1.2.5.1. HPV Genome Integration

The genomic instability that results from abortive HPV infection and uncontrolled cellular proliferation can lead to the incorporation of viral genetic material into the host genome, a process termed viral integration. During productive infection, the HPV genome replicates as circular episomal DNA, however, as infection progresses to pre-malignant and malignant lesions, HPV DNA is found increasingly integrated into cellular DNA and there is much evidence that integration contributes to the carcinogenic process (Kalantari et al., 2010). HPV integration usually occurs at common fragile sites within chromosomes and appears to be randomly distributed throughout the genome (Yu et al., 2005). Integration of HPV DNA commonly results in the loss of the viral *E2* repressor, remodelling of the *E6/E7* promoter and because the *E6* and *E7* ORFs are nearly always retained, continued expression of E6 and E7 oncoproteins results (Yu et al., 2005).

1.2.5.2. Co-factors for HPV Associated Cancer Progression

The HPV viral oncoproteins are fundamental components in the initiation and maintenance of a malignant phenotype; however, alone they are not sufficient for cancer development (zur Hausen, 1999). Most sexually active women encounter HPV infection at some point in their lives (Bosch and de Sanjose, 2003); however, as only a minority of such cases progress to invasive cancer additional co-factors are required to promote this transformation (Kalantari et al., 2010). Several co-factors responsible for the progression of HPV related cancer have been identified. These include:

- Smoking (Hildesheim et al., 2001, Wang et al., 2009)
- Multiparity in cervical cancer (Hildesheim et al., 2001)
- Long term oral contraceptive use in cervical cancer (Hildesheim et al., 2001)
- Prior or co-infection with other non-HPV sexually transmitted viruses such as Herpes simplex virus (HSV) (Smith et al., 2002)
- Genetic variation, for example p53 polymorphism (Storey et al., 1998)

An illustration of HPV infection progression in epithelial cells is outlined in Figure 1.4.

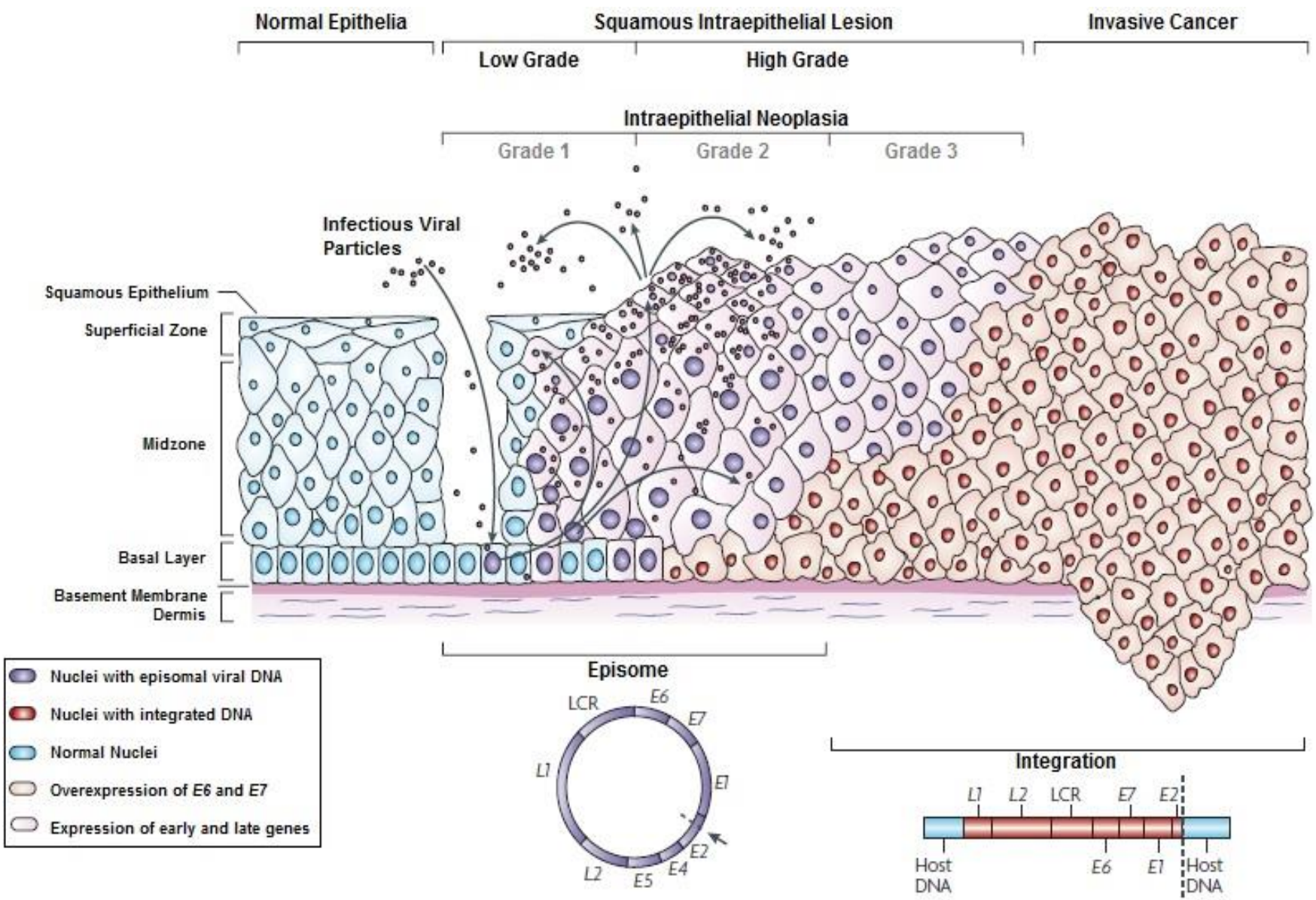

Adapted from Woodman et al. 2007

Figure 1.4. HPV-Mediated Progression to Invasive Carcinoma

Basal epithelial cells rest on the basement membrane, which is supported by the dermis. HPV gains access to the basal cells through micro-abrasions in the upper epithelial layers. Following infection, the early HPV genes are expressed and viral DNA replicates from episomal DNA (purple nuclei). In the upper epithelial layers viral genome replication is amplified, and E4 and the late HPV genes, L1 and L2, are expressed. L1 and L2 encapsulate newly synthesized viral genomes to form progeny virions in the nucleus. Shedding of the virus can then initiate new infection. A minority of HR-HPV infections progress to high-grade intraepithelial neoplasia. The malignant progression of untreated lesions is associated with integration of the HPV genome into host chromosomes (red nuclei). This event usually results in loss or disruption of the E2 ORF, and subsequent up-regulation of E6 and E7. LCR, long control region.

1.2.6. HPV and Cervical Cancer

1.2.6.1. Prevalence

Nearly every case of cervical cancer results from HPV infection, giving a HPV prevalence rate of >99% for this type of neoplasia (Walboomers et al., 1999). Cervical cancer is the third most common cancer in women (GLOBOCAN, 2008). Over half a million new cases of cervical cancer were estimated for 2008 worldwide, responsible for 274,000 deaths (GLOBOCAN, 2008). In 2008 incidence was nearly ten times greater in developing countries compared with Europe (GLOBOCAN, 2008). A recent worldwide HPV genotype distribution study found HPV16 and HPV18 in 71% of 8977 cases of invasive cervical cancer (de Sanjose et al., 2010). The study also found HPV types 16, 18, and 45 in 94% of 470 cervical adenocarcinoma cases. Additionally, patients with invasive cervical cancers associated with HPV types 16, 18, or 45 presented at a younger mean age than patients with other HPV types. HPV types 6, 30, 61, 67, 69, 82, and 91 were found in 1% of the 8977 cases of invasive cervical cancer (de Sanjose et al., 2010).

1.2.6.2. Cervical Intraepithelial Neoplasia

Cervical intraepithelial neoplasia (CIN), the precursor of cervical cancer, usually manifests within the cervical transformation zone, where the endocervical columnar cells merge with the stratified squamous epithelial cells of the ectocervix (Jordan and Singer, 1976). A unique layer of squamocolumnar junctional cells with distinct cuboidal morphology and gene-expression profile have been identified at this site (Herfs et al., 2012). Biomarkers that exclusively present on squamocolumnar junctional cells are conserved in squamous cell carcinomas and adenocarcinomas that originate from this region (Herfs et al., 2012). The processes by which viral-host cell interactions lead to neoplasia at this particular site remain to be elucidated, although it is thought that HR-HPV types such as HPV16 cannot correctly regulate their productive cycle at this junctional site, and that changes in both the timing and level of viral protein expression may influence neoplastic development in this region (Doorbar, 2006). Figure 1.5 shows the location and histology of cells in the squamocolumnar junction.

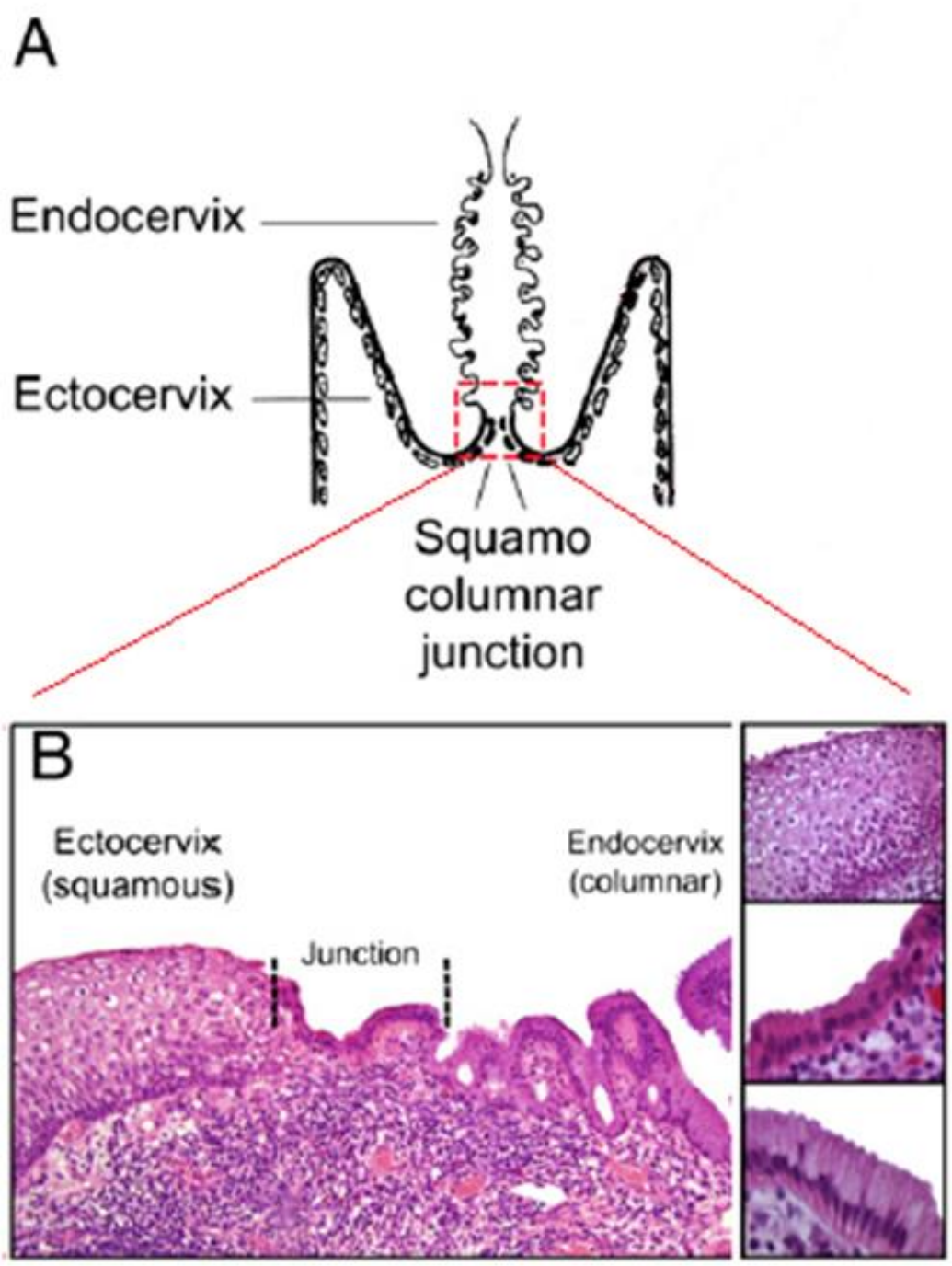

Adapted from Herfs et al. 2012

Figure 1.5. Site and Histology of the Squamocolumnar Junction

(A) Schematic diagram of the human cervix with the squamocolumnar junction separating the endocervix from the ectocervix. (B) Histology of the adult cervix, with squamous cells (Top right), junctional cells (Middle right), and columnar cells (Bottom right).

The progression of high-grade pre-cancerous cervical neoplasia occurs in patients who cannot clear their HPV infection and who hold active HPV infection for years to decades post initial virus exposure. On the basis of viral gene expression, Low grade squamous intraepithelial lesions (LSIL) or CIN1, caused by both HR- and LR-HPV types, are comparable to productive HPV infections. In addition to this, viral coat proteins are often detected in cells at the epithelial surface in LSIL (Middleton et al., 2003). However, the productive phase of the virus life cycle is inadequately supported in High grade squamous intraepithelial lesions (HSIL) or CIN2/3; therefore, this grade of cervical lesion has a greater proliferative phase (Doorbar, 2006). Overall, the risk of progression from CIN1 through to cervical cancer is 1% per year (Holowaty et al., 1999).

1.2.6.3. Cervical Screening

Cervical cytology, which involves the staining and microscopic examination of exfoliated cervical cells, is the current screening tool for premalignant and malignant cervical lesions (Kalantari et al., 2010). Eighty percent of cervical cancers are preventable in developed countries by routine screening with cervical smear tests (Kalantari et al., 2010). However, implementation of such programs can prove challenging in developing countries. Additionally, cervical cytology can be associated with poor reproducibility and high rates of false negative results (Stoler et al., 2001). Several factors can contribute to false negative results, including:

- *Specimen preparation*; clumping of cells when they are not spread evenly and uniformly on the microscope slide. Additionally, cervical cells can become distorted If exposed to air for too long prior to fixation (Burd, 2003)
- *Sample contamination*: other components of the cervical specimen such as blood, bacteria, or yeast may contaminate the sample and inhibit the identification of abnormal cells (Burd, 2003)
- *Human error*: as the average cervical cytology slide contains 50,000 to 300,000 cells, a sample that contains only a few abnormal cells within a crowded background of normal cells may be diagnosed as a false negative result if the abnormal cells were missed, particularly by overburdened cytologists with a large workload (Burd, 2003)

1.2.7. Other HPV Associated Cancers

In addition to vulval neoplasias (discussed in detail in the following section) and cervical neoplasias, HPV transformation can also be implicated in a range of other precancerous and malignant lesions.

HPV DNA and/or HPV antibodies have been found in *in situ* and invasive vaginal neoplasia (Daling et al., 2002). A recent meta-analysis identified HPV DNA in 100% of 107 vaginal intraepithelial neoplasia grade 1 (VaIN1) cases, 90.1% of 191 VaIN2/3 cases and 69.9% of 136 vaginal cancer cases (De Vuyst et al., 2009).

HPV has also been associated with penile cancer; however, there is a wide variation in HPV prevalence from study to study. A recent meta-analysis of 1,266 penile squamous cell carcinoma (SCC) cases indicate a HPV prevalence of 47.9%, with the most prevalent type being HPV16, followed HPV6 and HPV18 (Backes et al., 2009).

The majority of anal cancer and anal cancer precursors are HPV positive. One study found HPV DNA in 38 of 47 cases of anal carcinoma, which gave a HPV prevalence of 80.9%, with HPV16 being the most common type detected. In the same study HPV had a prevalence of 87.9% in 33 cases of anal intraepithelial neoplasia (AIN) (Varnai et al., 2006). In a larger meta-analysis HPV positivity was found in 91.5% of 671 AIN1 cases, 93.9% of 609 AIN2/3 cases and 84.3% of 955 anal carcinoma cases (De Vuyst et al., 2009).

With regards to HPV associated head and neck squamous cell carcinoma (HNSCC) cases, HPV DNA was detected in 25.9% of 5,046 HNSCC cancer specimens in a systemic review of 60 different studies (Kreimer et al., 2005).

HPV has also been implicated in the development on non-melanoma skin cancer in immunocompromised patients and in people who have Epidermodysplasia Verruciformis (EV) (Harwood and Proby, 2002). Additionally HPV DNA has been detected in lung cancer (Fei et al., 2006), breast cancer (Akil et al., 2008), prostate cancer (Leiros et al., 2005) and cancer of the bladder and urethra (Moonen et al., 2007).

1.2.8. HPV Prevention: Vaccination

At present, two prophylactic HPV vaccines are available. The first is a quadrivalent vaccine, Gardasil® (Merck & Co. Inc., Whitehouse Station, New Jersey, USA; Sanofi Pasteur MSD, Lyon, France), which contains virus-like particles (VLPs) composed of L1 proteins from HPV types 6, 11, 16 and 18 (Monsonego et al., 2010). The other is a bivalent vaccine, Cervarix® (GlaxoSmithKline, Rixensart, Belgium), and is comprised of VLPs for HPV types 16 and 18 (Monsonego et al., 2010). Many developed countries, including the UK, have HPV vaccination programs for girls aged between 12 - 14 years as the main target population.

Gardasil® protects against cervical, vulvar, vaginal, and anal cancer caused by HPV types 16 and 18, as well as genital warts caused by HPV types 6 and 11. Additionally, Gardasil® can be used to prevent precancerous or dysplastic lesions caused by HPV types 6, 11, 16, and 18 including CIN, VIN, VaIN and AIN. Gardasil® can also be used in boys to prevent HPV associated neoplasia of the anus and genital warts (Merck, 2011). Cervarix®, on the other hand, is approved for females only for the prevention of cervical cancer and CIN (GlaxoSmithKline, 2012).

As HPV is spread via contact with infected individuals, inhibition of transmission by vaccinated individuals could indirectly protect disadvantaged communities that are frequently difficult to reach through screening programs. Lack of knowledge regarding the risks of sexual behaviour and the cause of cervical neoplasia has been highlighted a barrier for the efficient implementation of routine gynaecological screening and HPV vaccination (Henderson et al., 2011, Monsonego et al., 2010).

1.3. Vulval Intraepithelial Neoplasia

1.3.1. Vulval Intraepithelial Neoplasia Pathology

Vulvar intraepithelial neoplasia (VIN) is a premalignant lesion affecting the skin and mucosal tissue of the vulva (van de Nieuwenhof et al., 2008). Histologically, VIN manifests as inadequately to undifferentiated basal cells and/or extremely atypical squamous epithelial cells involving the complete thickness of the epithelium, with or without a warty, hyperkeratotic surface (Bruchim et al., 2007). There are two distinct types of VIN: Classic/Usual VIN or differentiated VIN (McCluggage, 2009). The latter is diagnosed less commonly and is also known as simplex VIN. Differentiated VIN is described as a neoplastic lesion with hyperplasia and hyperkeratosis/parakeratosis of the squamous epithelium along with elongation of the rete ridges, which are the epidermal thickenings that extend downward between dermal papillae. Differentiated VIN is not graded and is not caused by HPV infection, but arises from vulval dystrophy, often lichen sclerosis (McCluggage, 2009).

Classic VIN, on the other hand, is associated with HR-HPV infection, with types 16 and 18 being the most common (McCluggage, 2009). Such HPV associated VIN lesions tend to be multifocal, pigmented, white, red, or a combination of these colour tones (Bruchim et al., 2007). Like its HPV-related counterpart CIN, classic VIN is divided into three grades, namely VIN1, 2 and 3 (McCluggage, 2009). The three-grade system of VIN is defined according to the degree of cellular dysplasia in each layer of affected epithelium. The International Society for the Study of Vulvar Diseases (ISSVD) has recommended an adjustment in the classification of classic VIN, with the VIN1 category being abandoned and lesions currently diagnosed as VIN1 being referred to as flat condyloma or HPV effect. In this classification, classic VIN2 and 3 are combined into a single category, termed classic VIN (McCluggage, 2009). Classic VIN lesions comprise the molecular variations in epithelial cell differentiation, which occur as a consequence of HPV infection. When the dysplastic cells of VIN lesions penetrate the epithelial basement membrane the lesion becomes malignant and is referred to as invasive carcinoma (van de Nieuwenhof et al., 2008). Figure 1.6 shows haematoxylin and eosin (H&E) staining of normal vulval epithelia and VIN3 epithelia.

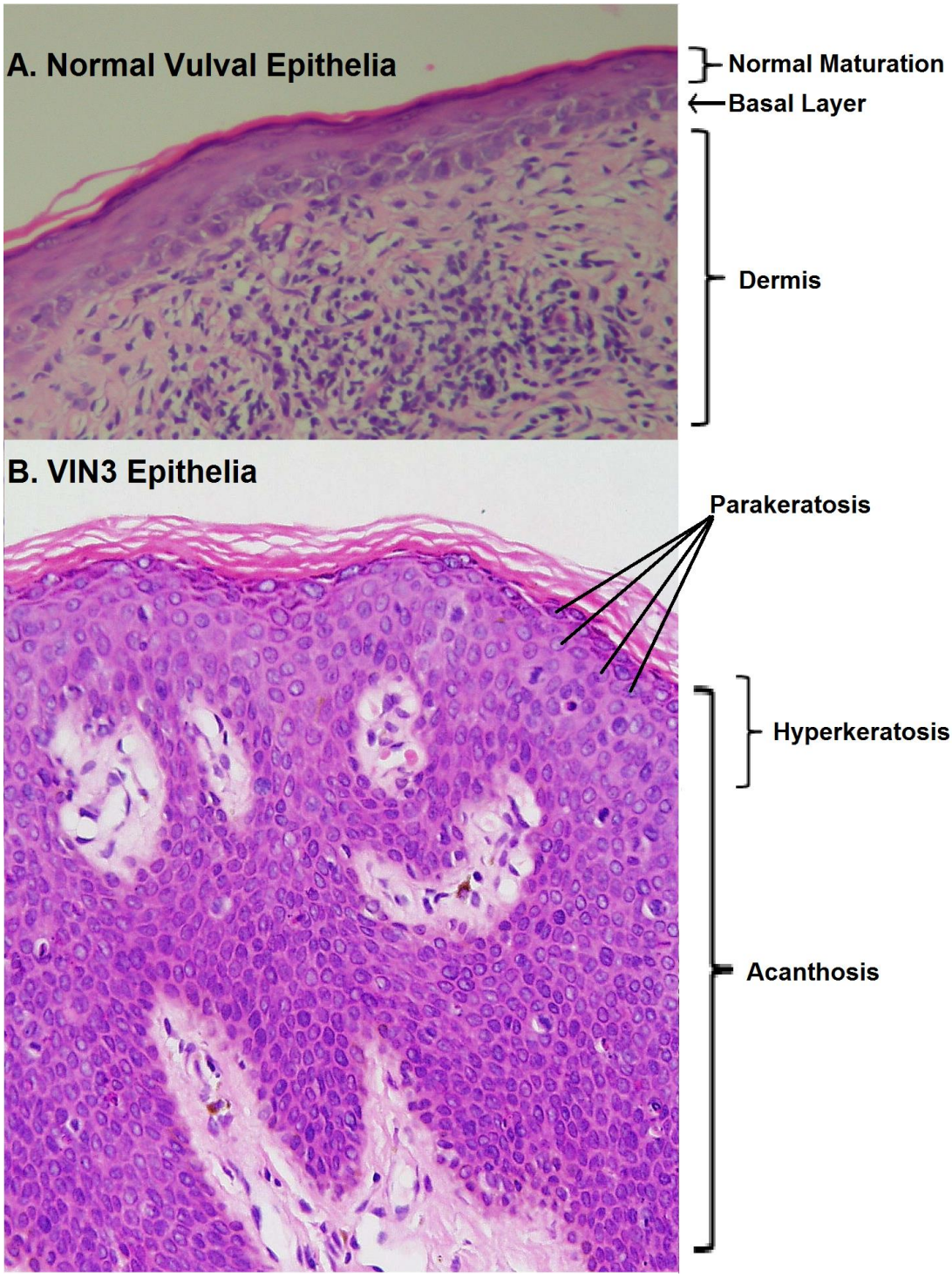

Images kindly provided by Dr Amanda Tristram, Cardiff University

Figure 1.6. Haematoxylin and Eosin Staining of Vulval Epithelia

(A) Normal vulval epithelia with a clear cut basal layer and normal maturation. (B) VIN3 epithelia with acanthosis (diffuse epidermal hyperplasia/thickening of the skin), hyperkeratosis (thickening of the stratum corneum/uppermost keratinous layer), parakeratosis (retention of nuclei in the stratum corneum) and abnormal mitotic figures involving the entire thickness of the epidermis.

Risk factors (van de Nieuwenhof et al., 2008) for VIN include:

- *Age*; HPV associated VIN is more common in younger women, often in their 4th to 5th decade
- *Tobacco use*; Cigarette smoking is reported in about 60 - 80% of VIN cases
- *Genital warts*; A history of genital herpes and Human Immunodeficiency Virus (HIV) infection are common in young women with usual VIN
- *Immunosuppression*; Immunosuppressants, used to prevent rejection after transplantation or to treat a chronic autoimmune disease, increase the risk of developing HPV associated VIN
- *Number of sexual partners*; The greater the number of sexual partners a person has, the more likely they are to contract genital HPV infection

1.3.2. Prevalence of HPV in VIN and Vulval Cancer

A recent study examined HPV prevalence in 2296 archived paraffin embedded vulva specimens from 39 different counties using a PCR based DNA enzyme immunoassay. HPV DNA was found in 86.7% of 587 VIN cases, where 535 cases were classified as usual VIN, 48 cases were classified as differentiated VIN and 4 cases had histological features of both usual and differentiated VIN. Differentiated VIN had lower HPV prevalence (48.9%) compared to usual VIN (90.3%). In the same study HPV DNA was found in 28.6% of 1709 invasive vulvar cancer cases (de Sanjose et al., 2013). Overall prevalence of HPV DNA in VIN and invasive vulvar cancer cases was highest in younger women, where HPV positivity was found in 93% of 115 VIN patients younger than 37 years of age at diagnosis, and 48.1% of 312 invasive vulvar cancer patients younger than 56 years of age at diagnosis. HPV16 was found to be the most common type (72.5%) followed by HPV33 (6.5%) and HPV18 (4.6%) (de Sanjose et al., 2013).

A different meta-analysis calculated HPV prevalence in VIN and invasive vulvar cancer from 63 separate studies across Asia, Europe, North America and Latin America, all of which used PCR based assays for detection. HPV DNA was present in 67.8% of 90 VIN1 cases, 85.3% of 1061 VIN2/3 cases and 40.4% of 1873 vulval cancer cases (De Vuyst et al., 2009). HPV6 (22.4%), 16 (9.8%) and 11 (9.0%) were the most prevalent HPV types found in the VIN1 samples. Whereas, HPV16 (71.9%), 33 (8%) and 18 (5%) were the most frequent

HPV types observed in the VIN2/3 cases. Similarly, HPV 16 (32.2%), 33 (4.5%) and 18 (4.4%) were the most common types observed in vulval cancers. The incidence of infection with multiple HPV types decreased from 13.4% in VIN1 to 2.8% in vulvar carcinoma (De Vuyst et al., 2009).

In an earlier study a total of 13,176 *in situ* and invasive vulvar carcinomas were identified over a 28 year period (1973 to 2000) (Judson et al., 2006). Of these, 57% of the patients were diagnosed with carcinoma *in situ* and 44% with invasive disease. It was estimated that vulvar carcinoma *in situ* increased 411% and that invasive vulvar cancer increased 20% during the period examined. They found carcinoma *in situ* incidence increased up to the age of 40 – 49 years and then decreased, whereas, invasive vulvar cancer risk increased as women age, increasing rapidly after the sixth decade (Judson et al., 2006).

The increase in HPV associated VIN without similar increase in invasive vulvar carcinoma may be explained by several different factors. One explanation is the increased application of vulval biopsy, a diagnostic method that contributes to earlier and more effective discovery of VIN lesions, which may have been missed previously (Kaufman, 1995). Earlier diagnosis and treatment of VIN may avert the eventual development of invasive SCC (Kaufman, 1995). Additionally, it has been hypothesised that the malignant progression of VIN is slow, suggesting that a limited number of these lesions progress to invasive vulvar SCC (Kaufman, 1995).

1.3.3. Diagnosis of HPV Associated VIN

Vulval biopsy is the method employed to attain an accurate diagnosis of a suspicious vulval lesion (van de Nieuwenhof et al., 2008). A punch biopsy with a minimal size of 4 mm, which penetrates the entire thickness of the epithelium is obtained from the edge of the lesion along with a small segment of unaffected tissue (van de Nieuwenhof et al., 2008). If invasive disease is suspected, the biopsy is taken from the most suspicious area of the lesion (van de Nieuwenhof et al., 2008). To aid VIN diagnosis a vulvoscopy can also be performed. This procedure examines the vulval area using a colposcope with optional use of a 5% acetic acid solution to highlight abnormal vascular patterns (van de Nieuwenhof et al., 2008). Advantages of vulvoscopy include the possible visualisation of

formerly unidentified, subclinical lesions, as well as the ability to better ascertain the distribution of an already clinically evident disease (van de Nieuwenhof et al., 2008). However, disadvantages of vulvoscopy include low sensitivity of aceto-white staining as a predictor of HPV positivity, as well as the fact that acetic acid can be very painful on ulcerative or de-epithelised lesions (van de Nieuwenhof et al., 2008).

1.3.4. Treatment of HPV Associated VIN

Although HPV associated VIN is recognised as an uncommon chronic skin disorder, a considerable range of treatment options are available (van de Nieuwenhof et al., 2008).

1.3.4.1. Surgical Excision

Surgical excision protocols encompass skinning vulvectomy, radical vulvectomy, and wide local excision of the area (Campion and Singer, 1987, van de Nieuwenhof et al., 2008, Bruchim et al., 2007). This may be done using "cold-knife", diathermy or laser excision. Although this is the historical standard of treatment, surgery can be mutilating due to the recurrent nature of the lesion, where many patients require repeated treatment over a prolonged follow-up period. This can lead to patient distress on physical, emotional, mental and psychosexual levels (van de Nieuwenhof et al., 2008).

1.3.4.2. Photodynamic Therapy

Photodynamic therapy (PDT) uses a topical photosensitizer and light to initiate the formation of highly reactive singlet oxygen and other free radicals (Lai and Mercurio, 2010). Cell death in the area treated is attributed to apoptosis, necrosis, immunologic effects, and the destruction of vascular endothelium (Lai and Mercurio, 2010). Topical 5-aminolaevulinic acid (ALA) is the compound of choice generally used in PDT (Lai and Mercurio, 2010). ALA is preferentially absorbed and induces protoporphyrin IX accumulation in rapidly proliferating cells, which has the advantage of minimising incidental damage to surrounding healthy tissues (Bedwell et al., 1992). Absence of ulceration/scar formation and shorter healing times in comparison with other treatment options are examples of PDT advantages. However, hyperkeratotic and pigmented lesions do not respond effectively to PDT (Lai and Mercurio, 2010).

1.3.4.3. Imiquimod

Imiquimod (Aldara®, 3M Pharmaceuticals, St Paul, MN) is an imidazoquinoline amine, which has the ability to induce innate and cell-mediated immunity as well as having anti-viral activity (Lai and Mercurio, 2010). It is extremely efficient in terms of clearance of lesions, especially genital warts, and has a low rate of recurrence post treatment (van de Nieuwenhof et al., 2008). Moreover, Imiquimod can be used by itself or potentially in amalgamation with other treatment options to augment the shrinking of lesions before performing ablative procedures (Lai and Mercurio, 2010). A small-scale study using topical applications of Imiquimod produced encouraging results, where Imiquimod reduced VIN lesion size by 25% after 16 weeks of treatment in 81% of 26 patients treated with the compound (van Seters et al., 2008). The chemical structure of Imiquimod can be seen in Figure 1.7 (A).

1.3.4.4. 5-Fluorouracil

5-fluorouracil (5-FU) is a topical chemotherapeutic agent that functions by arresting DNA synthesis (Lai and Mercurio, 2010). However, many patients do not respond to treatment with 5-FU and pain and burning frequently limit the duration of treatment (van de Nieuwenhof et al., 2008). The chemical structure of 5-FU is shown in Figure 1.7 (B).

1.3.4.5. Interferon

Alpha Interferons, which are components of the innate immune response that are rapidly induced during viral infection, have been used in the treatment of genitourinary neoplastic lesions and show variation in their therapeutic effects (Spirtos et al., 1990, Ikic et al., 1981, Yliskoski et al., 1990). However, as these molecules are an extremely expensive treatment substitute and due to their limited therapeutic effects, they are not used as standard in the treatment of VIN (van de Nieuwenhof et al., 2008).

1.3.4.6. Cidofovir

Cidofovir, a deoxycytidine monophosphate analogue, has shown potential in the topical treatment of HPV associated VIN (Tristram and Fiander, 2005). Cidofovir is an acyclic nucleoside phosphonate (ANP) compound and is discussed in detail in the following section. The chemical structure of Cidofovir is shown in Figure 1.7 (C).

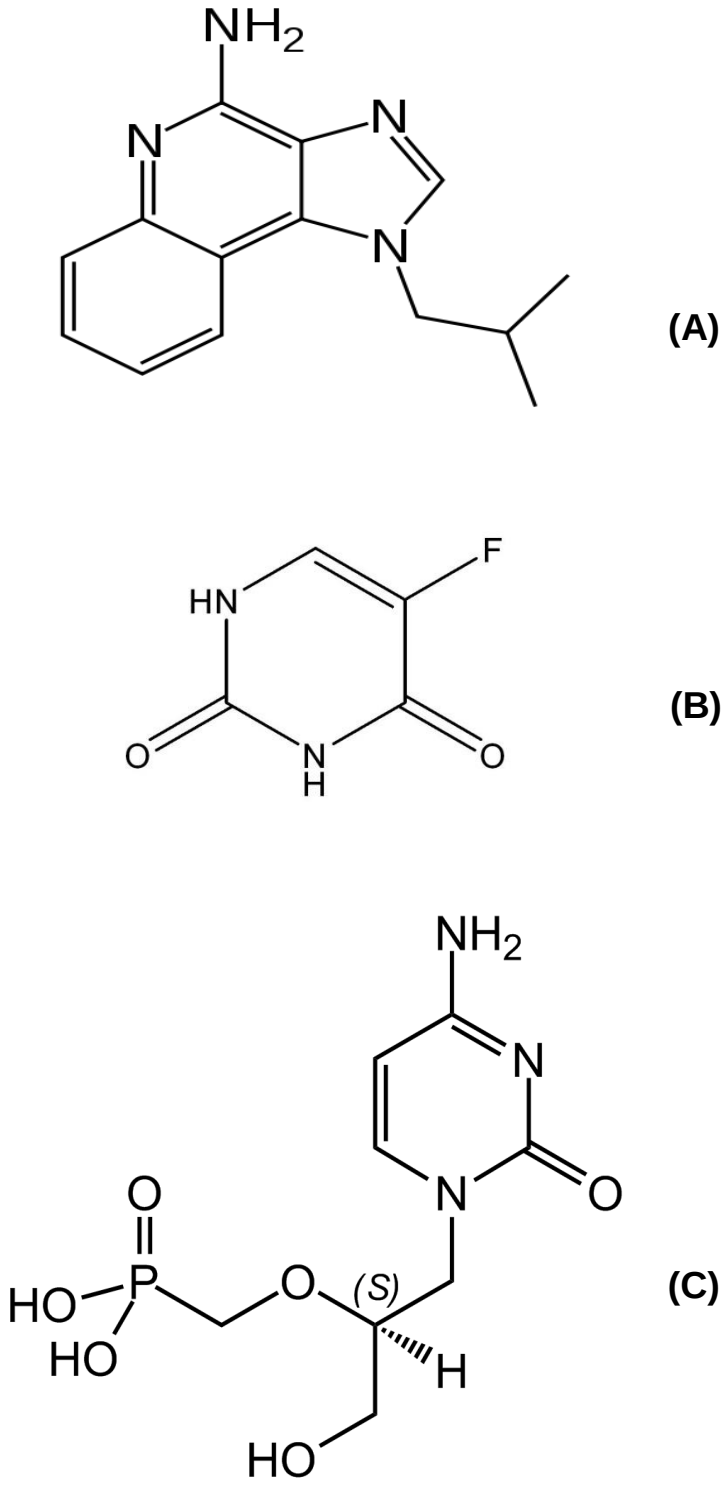

Figure 1.7. Chemical Structure of (A) Imiquimod, (B) 5-fluorouracil and (C) Cidofovir

Imiquimod (trade name Aldara), an immune response modifier; 5-fluorouracil (trade name Efudex), an irreversible inhibitor of thymidylate synthase; and Cidofovir (trade name Vistide), a selective inhibitor of viral DNA polymerase, have all shown varying degrees of efficacy in topical treatment of VIN.

1.4. Acyclic Nucleoside Phosphonates

Preservation of healthy tissue in areas affected by VIN would be a great advantage as opposed to other invasive and sometimes mutilating treatment options such as excisional surgery, laser therapy, etc. A topical treatment option that specifically targets the cause of the disease, that being HPV in usual VIN, is highly desirable. Acyclic nucleoside phosphonates (ANPs) are a category of nucleotide analogues, which have a phosphonate group chemically attached to the alkyl side chain of purine or pyrimidine molecules (Ballatore et al., 2001). ANPs display broad-spectrum anti-viral activity against a range of DNA and RNA viruses as well as displaying anti-neoplastic activity (De Clercq, 2011a). Currently there are three ANPs approved for clinical use; Adefovir for the treatment of chronic hepatitis B virus (HBV) infections, Tenofovir for the treatment of HIV and HBV infections and Cidofovir for the treatment of cytomegalovirus (CMV) retinitis in AIDS patients (De Clercq, 2011a).

Comparable to naturally occurring DNA bases, ANP compounds are most active in their triphosphate form, which interacts with their target enzyme, either viral DNA polymerase or reverse transcriptase, and exerts therapeutic effect by causing chain termination and inhibition of genome replication (Xiong et al., 1997). Unlike earlier nucleoside analogue compounds such as: acyclovir, penciclovir, and ganciclovir, ANP compounds already contain the first (mono)phosphate group needed before the addition of two further phosphate groups render them to their active triphosphate form. In terms of anti-viral treatment, the addition of the initial phosphate group in earlier nucleoside analogues was via specific virus encoded kinases and this constituted a rate limiting step. Due to viral resistance through mutation or absence of viral kinases, the therapeutic effects of these nucleoside analogues may be limited in some viruses (Field and Biron, 1994). ANP compounds are active against a wider range of viruses as they circumvent the first kinase step and rely on host cellular enzymes only.

1.4.1. Nucleoside Analogue Metabolism

Metabolism of nucleoside analogue compounds begins with cellular uptake via transport across the plasma membrane. Nucleoside transporters (NTs) are membrane transport

proteins that mediate the uptake of naturally occurring physiological nucleosides as well as anti-neoplastic and anti-viral nucleoside analogue drugs (Baldwin et al., 1999). Several different classes of NT proteins exist, including: Equilibrium Nucleoside Transporters (hENT in humans), which mediate the transport of purine and pyrimidine nucleosides down their concentration gradients (Young et al., 2008); Concentrating Nucleoside Transporters (hCNT in humans), which transport nucleoside analogues against a concentration gradient (Pastor-Anglada et al., 2008); Organic Cationic Transporters and Organic Anionic Transporters (OCTs and OATs respectively), which use facilitated transport to mediate the uptake of nucleoside analogue compounds into target cells (Roth et al., 2012); and ATP-binding Cassette (ABC) Transporter Proteins, which mediate ATP-dependent transport of nucleosides in and out of cells (Goldman, 2002)

With regards to intracellular uptake of pyrimidine nucleoside analogues currently used in cancer chemotherapy, the deoxycytidine analogue Cytarabine relies upon plasma concentrations of the drug and enters cells mainly by hENT mediated processes. Gemcitabine, another analogue of deoxycytidine, requires both hENT and hCNT NTs for its intracellular uptake. Capecitabine, a pyrimidine nucleoside compound developed to overcome the low oral bioavailability of 5-FU, is metabolized to 5'-deoxy-5-fluorocytidine after oral administration and transported into cells via hENT NTs (all reviewed in Damaraju et al., 2003).

Once nucleoside analogue compounds have entered their target cells they are metabolized to their active tri-phosphate derivatives by the action of cytosolic enzymes such as nucleoside kinases and nucleoside diphosphate kinases (De Clercq and Holy, 2005). Cytarabine is phosphorylated to its triphosphate form by deoxycytidine kinase (dCK) and other nucleotide kinases. Similarly, gemcitabine is phosphorylated to its monophosphate derivative by dCK and to its active triphosphate by pyrimidine nucleotide kinases (all reviewed in Damaraju et al., 2003).

1.4.1.1. Nucleoside Analogue Resistance

Nucleoside analogues exert therapeutic effect when fully metabolized to their tri-phosphate derivatives. However, some cancer cells can over-express certain NT proteins in order to eject therapeutic nucleoside analogues from within the cell, resulting in drug resistance and cancer cell survival (Wijnholds et al., 2000). Multidrug resistance 1 (MDR1) P-glycoprotein and multidrug resistance protein 1 (MRP1), members of the ABC transporter superfamily, are examples of NT proteins that can induce a multi-drug resistant phenotype when over-expressed in cancer cells (Wijnholds et al., 2000). In addition to over-expression of nucleoside efflux proteins, cancer cells can also incur drug resistance by reducing expression of NT proteins that promote intracellular uptake of therapeutic nucleoside analogues, such as hENT in trifluorothymidine resistance (Temmink et al., 2010). Additionally, cancer cells can reduce the expression of nucleoside phosphorylating enzymes, such as thymidine kinase (TK) in trifluorothymidine resistance (Temmink et al., 2010). Furthermore, nucleoside resistance can occur in cancer cells due to increased deaminase activity, such as cytidine deaminase (CDA) in Cytarabine resistance (Ohta et al., 2004).

1.4.2. Cidofovir

Cidofovir ((S)-1-(3-hydroxy-2-phosphonylmethoxypropyl) cytosine; HPMPC, Vistide), the primary drug of interest in this project, is a nucleoside analogue of deoxycytidine monophosphate, which has anti-viral activity against a wide range of DNA viruses such as HPV, Herpes simplex virus type 1 (HSV-1) and type 2 (HSV-2), human herpes virus type 6 (HHV-6), varicella-zoster virus (VZV), CMV, Epstein-Barr virus (EBV), etc. (De Clercq, 1996). Cidofovir is currently approved for CMV infection, but is also potentially an effective treatment option for benign and premalignant vulvar and extra-genital HPV lesions including VIN (Snoeck et al., 2001b, Tristram and Fiander, 2005).

1.4.2.1. Cidofovir Pharmacology

The mechanism of action of Cidofovir in CMV infections is well documented (Xiong et al., 1997). Cidofovir is a hydrophilic polar molecule that enters cells through interaction with the NT hOAT1 (Cihlar et al., 1999). Once inside the host cell, it undergoes two stages of

phosphorylation, via pyrimidine nucleoside monophosphate kinase and then pyruvate kinase to form the active metabolite, Cidofovir diphosphate (CDVpp) (Cihlar and Chen, 1996). As CDVpp embodies structural similarity to naturally occurring host nucleotides it acts as a competitive inhibitor and an alternative substrate for CMV DNA polymerase (Xiong et al., 1997). CDVpp, which is incorporated into a growing strand of DNA complimentary to deoxyguanosine monophosphate (dGMP), is not excised by the exonuclease activity of human-CMV DNA polymerase causing a decline in the rate of DNA elongation (Xiong et al., 1997). The incorporation of a second CDVpp molecule is required to further inhibit DNA elongation (Xiong et al., 1997).

The diphosphate form of Cidofovir has a half-life of 17 hours. However, its choline derivative, which is formed following the uptake and metabolism of Cidofovir (Johnson and Gangemi, 1999), has a half-life of greater than 48 hours resulting in the need for infrequent dosing . However, in spite of its long-half-life, the cellular uptake of Cidofovir is slow due to its negatively charged phosphate group (De Clercq, 2003).

1.4.2.2. Cidofovir and HPV

Unlike its role in CMV infection, the mechanism of action of Cidofovir in HPV positive cells is not clearly defined. ANPs have higher affinities for viral DNA polymerases compared to cellular DNA polymerases (Kramata et al., 1996 and references therein), but as HPV utilizes host cell DNA polymerase instead of a virally encoded polymerase it is unclear how Cidofovir induces its therapeutic effect in HPV positive cells.

Previous studies examining the effect of Cidofovir in HPV positive cells show varied results. For example, it has been suggested that Cidofovir promotes an antiproliferative effect in HPV positive cell lines via inhibition of E6 and E7 oncoproteins (Amine et al., 2009, Sirianni et al., 2005), re-accumulation of p53 and pRb (Snoeck et al., 2001a), induction of apoptosis (Andrei et al., 2001, Snoeck et al., 2001a, Donne et al., 2007), cell cycle arrest (Abdulkarim et al., 2002) or generation of double stranded breaks (Deberne et al., 2013, De Schutter et al., 2013). In some studies the radiosensitizing ability of Cidofovir in HPV positive cells has also been reported (Abdulkarim et al., 2002, Sirianni et al., 2005). Due to the potential use of Cidofovir in the topical treatment of HPV associated VIN, these varied

and sometimes contradictory results, require further work to elucidate the exact mechanism of action of the compound in this setting.

1.4.2.3. Cidofovir and VIN

Although Cidofovir is licensed for CMV infection it has shown promise in the treatment of VIN, as well as specificity to HPV positive cell lines and lesions (De Schutter et al., 2013, Amine et al., 2009, Abdulkarim et al., 2002, Tristram and Fiander, 2005). In a pilot study (Tristram and Fiander, 2005), Cidofovir treatment caused ulceration of diseased tissue in nearly every case (N=12), with no effect seen on the peripheral healthy skin when applied as a 1% topical formulation on alternative days for 16 weeks. Four out of 12 women completely cleared the disease, with resolution of long standing symptoms and histological and viral clearance; three of the 12 woman showed a partial response to the treatment; two women did not respond to Cidofovir treatment and one woman appeared to have resolved the disease but tested positive for invasive disease at the final biopsy (Tristram and Fiander, 2005). Images from this pilot study, showing clearance of VIN3 with Cidofovir treatment, are shown in Figure 1.8.

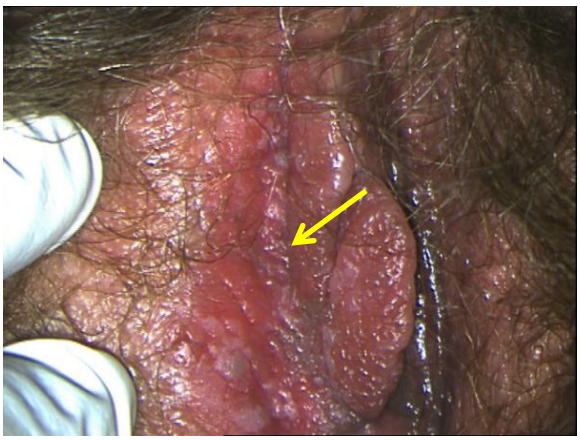

(A)

(B)

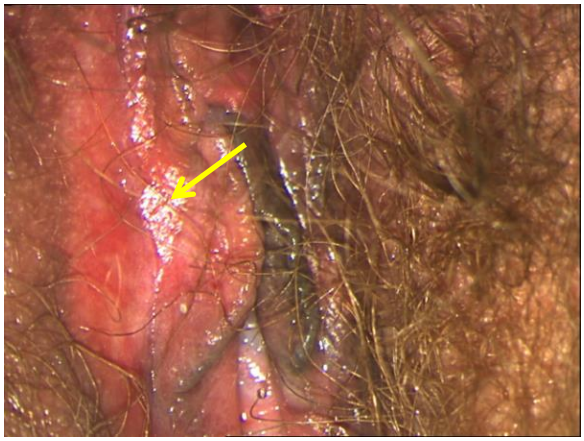

(C)

Images kindly provided by Dr Amanda Tristram, Cardiff University

Figure 1.8. Clearance of VIN3 with Topical Cidofovir Treatment

(A) A VIN3 lesion on the right anterior vulva of a patient before Cidofovir treatment; (B) Ulceration of the same lesion during Cidofovir treatment; (C) Clearance of the lesion post Cidofovir treatment.

1.4.3. Adefovir and Tenofovir

A recent review (Huttunen et al., 2011) described prodrug compounds as "inactive, bioreversible derivatives of active drug molecules that must undergo an enzymatic and/or chemical transformation *in vivo* to release the active parent drug, which can then elicit its desired pharmacological effect in the body". Adefovir (PMEA) [9-(2-phosphonylmethoxyethyl) adenine] and Tenofovir (PMPA) [(R)-9-(2-phosphonylmethoxypropyl) adenine] are adenine derivative ANPs and sister compounds of Cidofovir. Due to their poor oral bioavailability they have been converted to their oral prodrug forms, Adefovir dipivoxil or bis(pivaloyloxymethyl)-PMEA [bis(POM)-PMEA] and Tenofovir disoproxil or bis(isopropyloxycarbonyloxymethyl)-PMPA [bis(POC)-PMPA] (Figure 1.9) (De Clercq, 2003). Adefovir dipivoxil is approved for the treatment of HBV infections and Tenofovir disoproxil fumarate for the treatment of both HIV and HBV infections (De Clercq, 2011b). Similar to Cidofovir, Adefovir and Tenofovir, in their diphosphate forms, have a higher affinity to viral DNA polymerase and reverse transcriptase enzymes such as HSV-1 DNA polymerase and HIV-1 reverse transcriptase when compared with their cellular counterparts and act as competitive inhibitors or alternate substrates of deoxyadenosine triphosphate (dATP) for these enzymes (Kramata et al., 1996 and references therein).

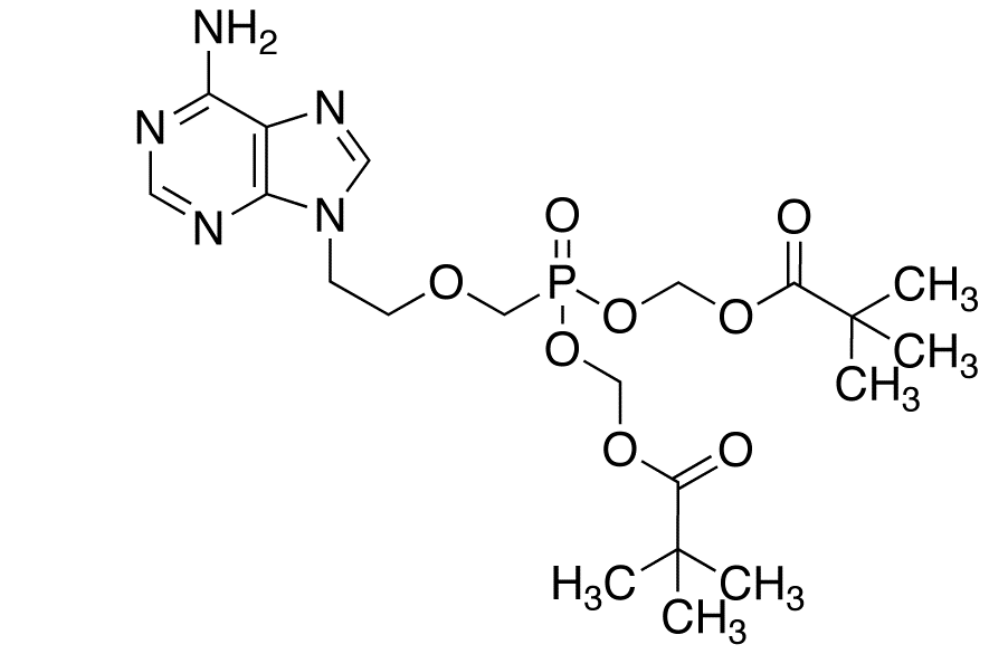

(A)

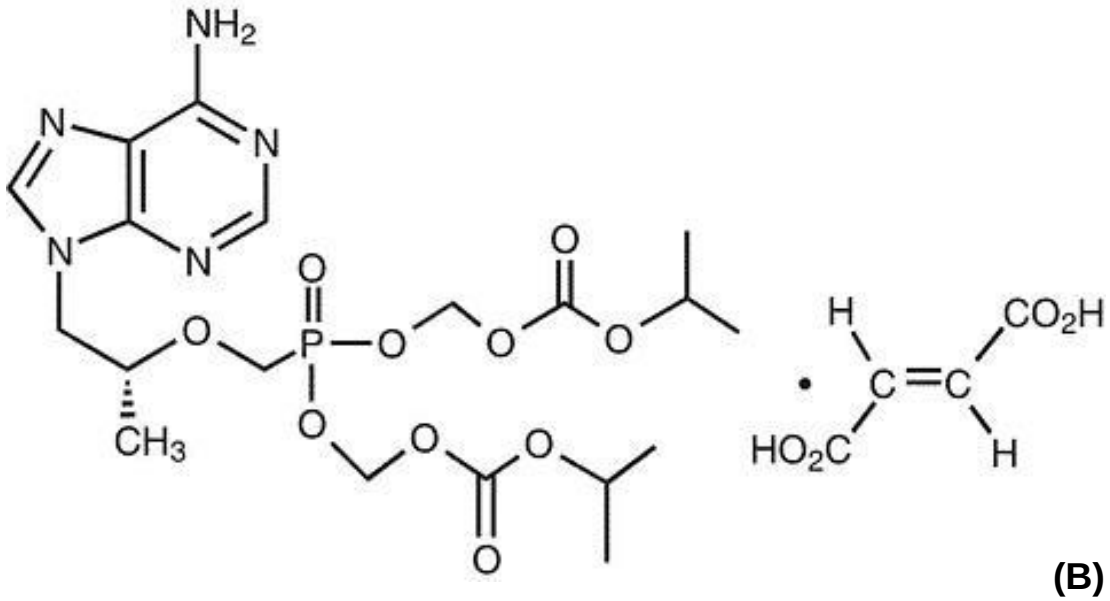

(B)

Figure 1.9. Chemical Structure of (A) Adefovir dipivoxil and (B) Tenofovir disoproxil

Adefovir dipivoxil and Tenofovir disoproxil are the respective oral prodrug derivatives of the acyclic nucleoside phosphonates Adefovir and Tenofovir, both of which are derived from an adenine nucleobase.

1.4.4. ProTide Technology

ANP compounds are effective against a wide range of viruses as they include the first monophosphate group needed to eventually become a triphosphate molecule. However, the negative charge on the phosphate group results in low cell membrane permeability and can be subject to dephosphorylation, hence some form of chemical manipulation is desirable to avert these potential problems (Mehellou et al., 2009). Pronucleotides or ProTides are nucleoside monophosphate prodrugs designed to efficiently permeate target cells, avoiding the first rate-limiting nucleoside phosphorylation step (Serpi et al., 2013). ProTide drugs are usually nucleosides and more recently sugars, which by means of chemical manipulation have the charge on their phosphate groups masked by an amino acid ester promoiety linked by a P-N bond to allow efficient passive cell-membrane penetration (Mehellou et al., 2009, Serpi et al., 2013, Wagner et al., 2000). For efficient cell membrane permeability the ProTide phosphate masking groups should be: lipophilic so they can pass through the cell via passive diffusion; stable in human plasma; have the ability to hydrolyze in cells; and non-cytotoxic. Once the compound has entered the cell, the masking groups are enzymatically cleaved to liberate the phosphorylated biomolecule (Mehellou et al., 2009).

ProTide technology has resulted in improved anti-viral and anti-cancer therapy, where nucleoside resistance may have occurred via down regulation of nucleoside metabolising enzymes such as dCK and other monophosphate kinases. Additionally, as ProTide modification can increase lipophilicity of certain nucleoside analogues it can lead to more efficient passive diffusion of the compound into cells and independence from nucleoside transporters. It has also been suggested that ProTide modification promotes a degree of deaminase resistance in certain nucleoside analogues (McGuigan et al., 2009). A schematic representation of the ProTide concept is outlined in Figure 1.10.

The development of aryloxy phosphoramidate triesters as an efficient ProTide model for the intracellular transfer of charged bio-active anti-viral nucleoside monophosphates using intracellular enzymatic activation of the prodrug to liberate the nucleoside monophosphate has been previously outlined (Cahard et al., 2004). The aryloxy phosphoramidate triesters block the charge on the phosphate group to increase the

efficacy of anti-viral drugs. Via structure-activity relationships it was found that alpha amino acids, such as alanine, were essential for the approach. Furthermore, it was found that the ester and aryl moieties could be alternated, provided the ester can be cleaved by esterase, and the aryl is a reasonable leaving group. Finally, it was established that a P-N bond within the molecule is vital for efficient activity (Cahard et al., 2004). Another study suggested that the activation of aryloxy phosphoramidates to release monophosphate species progressed in four steps, which are outlined schematically in Figure 1.11 (Mehellou et al., 2009).

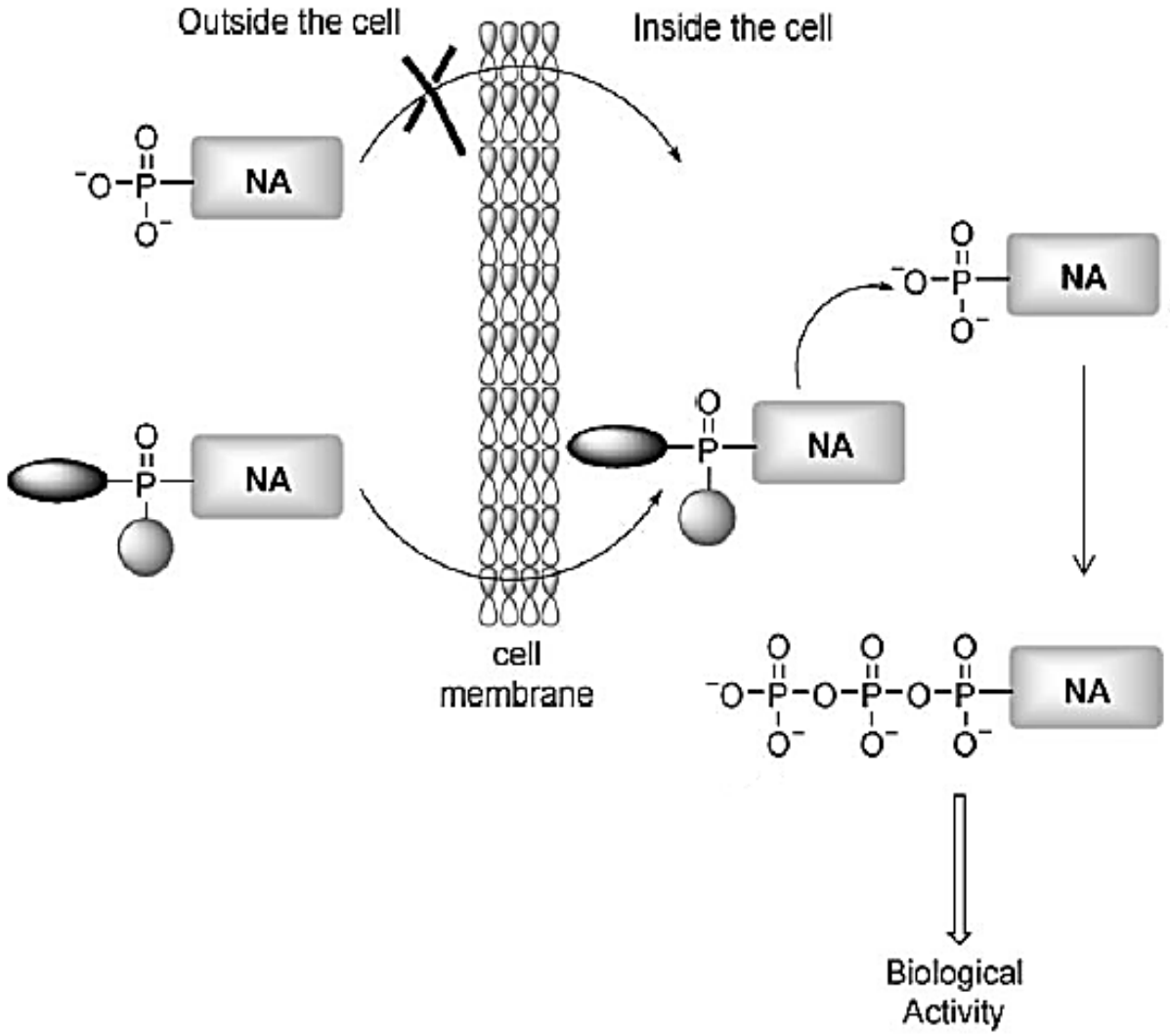

Adapted from Mehellou et al. 2009

Figure 1.10. Schematic Representation of the ProTide Concept

Masking of the negative charge on the phosphate group of a monophosphate nucleic acid (NA) allows for more efficient cell membrane permeability. Once inside the host cell masking groups are cleaved releasing the monophosphate NA. Subsequent phosphorylations render the NA to its most active tri-phosphate form.

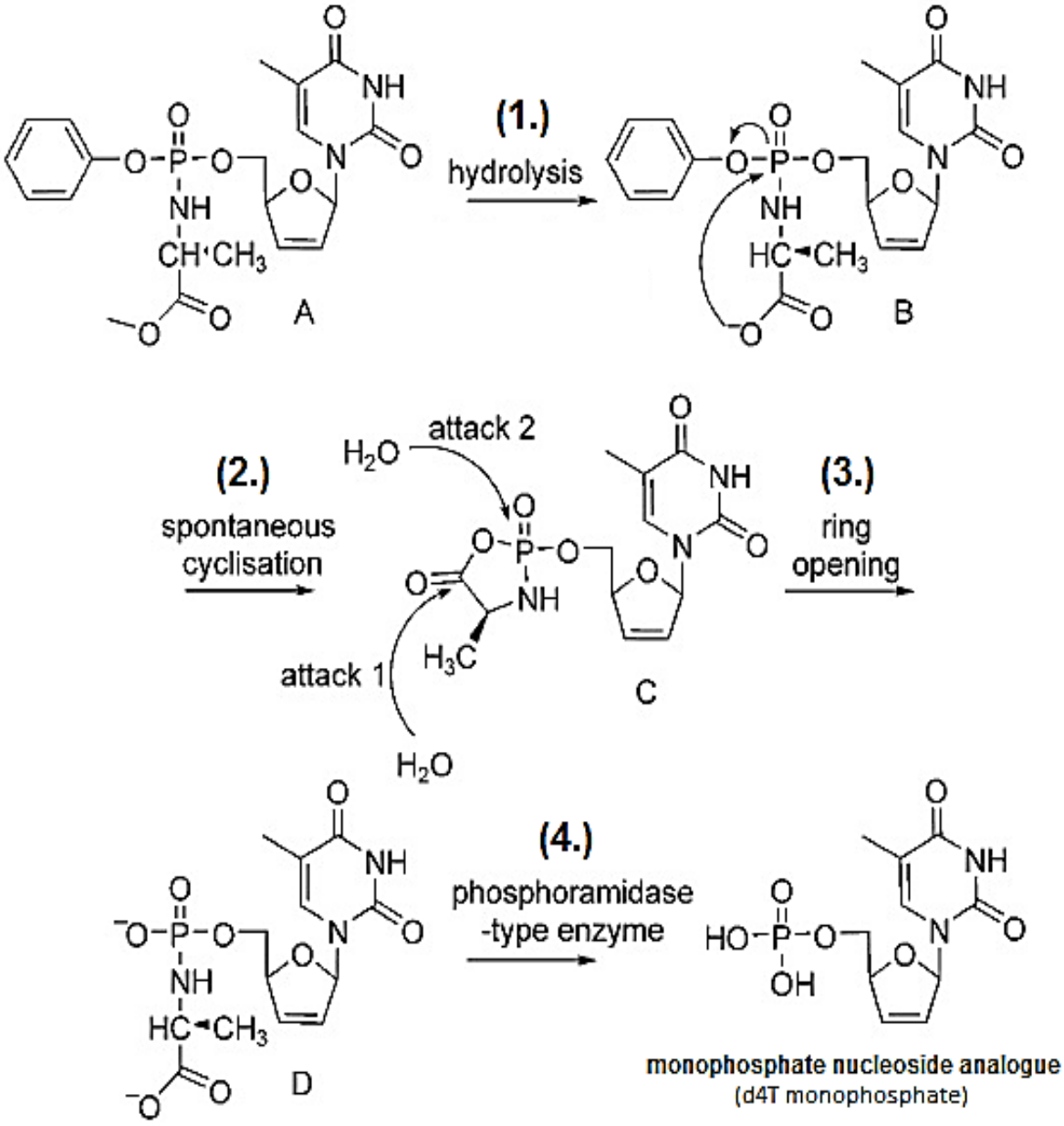

Adapted from Mehellou et al. 2009

Figure 1.11. Hypothesized Mechanism of Phosphoramidate Activation

(1) *Activation of aryloxy phosphoramidates begins with cleavage of the ester moiety (A) by an esterase such as cathepsin A.* ***(2)*** *Intracellular displacement of the phenoxy group by the carboxylate anion (B) results in the formation of a five-membered ring mixed anhydride (C) by spontaneous cyclisation.* ***(3)*** *The cyclic anhydride intermediate undergoes hydrolysis and opens up to give phosphoalaninate (D) (this step is not enzyme assisted).* ***(4)*** *Cleavage of the P-N bond of the phosphoalanine intermediate by a phosphoramidase-type enzyme generates the monophosphate nucleoside analogue (d4T monophosphate in this example).*

1.4.4.1. ProTide Derivatives of Acyclic Nucleoside Phosphonates

The ProTide approach is also applied to increase the anti-viral and anti-neoplastic activity of acyclic nucleoside analogues that lack the first monophosphate group. For example, phosphoramidates of 4'-Azidouridine, which is inactive against hepatitis C virus (HCV) in its primary form, showed a great improvement in anti-HCV activity with non-toxic effects in replicon assays (Perrone et al., 2007).

The Food and Drug Administration (FDA) approved anti-HIV compound 2',3'-Didehydro-2',3'-dideoxythymidine (d4T) also shows low efficiency in phosphorylation to its monophosphate form (Balzarini et al., 1989), therefore, a series of d4T phosphoramidates were prepared and examined for their degree of anti-HIV activity (Siddiqui et al., 1999). Several of the derivative compounds displayed greater than 10-fold selectivity index (SI) compared with the parent d4T (Siddiqui et al., 1999). This again highlights the increased efficacy of the phosphoramidate analogues.

Phosphoramidate analogues were also derived from (E)-5-(2-Bromovinyl)-2'-deoxyuridine (BVDU), a uridine analogue, which exhibits powerful anti-HSV-1 and anti-VZV activity in cell culture. The phosphoramidate analogues were less effective than their parent compound against VZV, HSV-1 and HSV-2 (Harris et al., 2001). However, when other BVDU phosphoramidates were examined as anti-neoplastic compounds they showed increased antiproliferative activity against cancer cell lines, where some of the analogues were more efficient at inhibiting certain cancer cell lines and not others (McGuigan et al., 2005).

1.5. RT3VIN

In spite of obvious advantages such as ease of use/self-administration and fewer hospital visits, there is currently no licensed topical treatment option for VIN (Shylasree et al., 2008). RT3VIN was a randomized phase II UK multi-centre treatment trial of topical Imiquimod and Cidofovir in women with usual and differentiated high grade VIN . Patients were recruited to the trial from October 2009 to January 2013. Women were eligible if they met the following criteria:

- They were older than 16 years of age at trial commencement
- They agreed to using efficient contraception for the duration of the trial
- They had a VIN3 biopsy taken no longer than 3 months previous to entering the trial, which was ≥ 20 mm in diameter
- Patients with perianal disease could be included but the disease must not have extended into the anal canal
- Patients had to give a three way written informed consent (for screening, trial and cross-over)

Exclusion criteria of the trial included:

- Patients with current invasive vulval or anogenital carcinoma
- Pregnancy, breastfeeding or patients trying to conceive
- Patients who were unresponsive to previous treatment with Cidofovir or Imiquimod
- Patients with impaired renal function
- Patients who were unable to comply with protocol treatment
- Patients who were undergoing treatment or had treatment in the previous 4 weeks

A total of 180 patients were recruited and randomized on a 1:1 basis to either Cidofovir or Imiquimod using a Fleming single stage design. Both topical treatment options were applied three times a week for up to 24 weeks. A thin layer of Cidofovir gel or Imiquimod cream was spread over the affected area at night and the area was washed using aqueous cream and water the following day.

For the duration of the trial, clinical assessment in addition to the application of Response Evaluation Criteria in Solid Tumours (RECIST) (Eisenhauer et al., 2009), a set of published rules that define when patients respond, stabilize, or progress during treatments, was used to monitor progress. After 30 weeks a biopsy was taken from each patient to examine the histology of the lesion and to determine HPV status of the tissue.

At the end of the trial, patients were assigned to one of four categories determined by their response to the treatment. The categories were:

1. Complete Response (CR) – all treated lesions disappeared within the 24 weeks
2. Partial Response (PR) – at least a 30% decrease was seen in the pathological severity of the lesion
3. Progressive Disease (PD) – at least a 20% increase in the pathological severity of the lesion was seen
4. Stable Disease (SD) – No positive or negative change was seen in the disease state

At the time of submission of this thesis the clinical results of the RT3VIN clinical trial were under analysis.

1.6. Naturally HPV16 Immortalized Short Term Cell Lines; an *in vitro* Model of Neoplastic Disease

Transformed cell lines have many advantages related to ease of use, but they are a poor model for *in vivo* cellular behaviour. *In vivo* tumours are far more diverse than the limited number of clonal lines available. Additionally, transformed cell lines are often derived from more aggressive and metastatic tumours rather than from primary lesions, and therefore represent only a subset of tumours. They are a particularly poor model of early stage neoplastic conditions like VIN. Studies of premalignant conditions in particular should ideally utilise more biologically relevant models. This has led to increasing interest in the use of primary cultures to investigate tumour behaviour (Burdall et al., 2003). This is particularly important when assessing the effects of potential therapeutic agents, as many established cell lines and even late passage primary cultures, have developed resistance to such agents over time (Johnson and Gangemi, 1999).

To address these issues, naturally HPV16 Immortalized Short Term (NHIST) monoclonal cell lines were derived from VIN3 and VaIN3 biopsies by Tiffany Onions in the HPV Research Group at Cardiff University. For ease of reference for the remainder of this thesis the VIN NHIST cell line will be termed M08 and the corresponding VaIN NHIST cell line will be termed A09 or NHIST cell lines collectively. Prior to use these cell lines were validated in terms of baseline oncogene expression levels, HPV integration status, telomere dynamics and telomerase activity and DNA methylation state (data in preparation for publication at the time of submission of this thesis). The notable difference between M08 and A09 was that *E2* expression was absent in the M08 cell line indicating that the HPV16 DNA may have integrated. Amplification of Papillomavirus Oncogene Transcripts (APOT) and Detection of Integrated Papillomavirus Sequence (DIPS) results also indicated that the HPV16 DNA was likely to have integrated in the M08 cell line; however, at the time of submission of this thesis southern blotting had not been performed to confirm this result. *E2* expression was not disrupted in the A09 cell line and APOT and DIPS were negative indicating that HPV DNA in the A09 cell line was likely to be episomal. In addition to *E2; E4* and *E5* transcription was also absent in the M08 cell line. A09 cells expressed all HPV genes.

The M08 and A09 cell lines were used to assess the growth inhibitory effects of nucleoside analogue compounds and to investigate the molecular mechanism of action of Cidofovir in HPV associated premalignant disease. The previous studies that aimed to determine the mechanism of action of Cidofovir in HPV positive cells mainly utilized transformed cell lines such as SiHa, HeLa, CaSki, SCC90, Hep2 and Me180 (Abdulkarim et al., 2002, Amine et al., 2009, De Schutter et al., 2013, Donne et al., 2007, Sirianni et al., 2005); all derived from malignant tumours. Such transformed cell lines would not be an accurate model of premalignant vulval or vaginal intraepithelial neoplastic disease.

1.7. HPV Radiosensitivity and DNA Double Strand Breaks

Radiosensitivity can be defined as the relative susceptibility of cells, tissues, organs, organisms, and other substances to the injurious action of ionising radiation. The purpose of radiosensitizing compounds in cancer treatment is to selectively modify tumour cells and/or normal tissues so that therapeutic gain is achieved using conventional radiation (Coleman and Turrisi, 1990). DSBs are the foremost cytotoxic lesions produced by radiation (Jackson, 2002). The first cellular response to DSBs involves the recruitment of large protein complexes which begin the DSB repair cascade (Brandsma and Gent, 2012). Examples of foci that occur in response to ionizing radiation may include: locally phosphorylated histone H2AX as well as 53BP1, RPA and RAD51 (Brandsma and Gent, 2012). Phosphorylation of histone H2AX occurs primarily via the Ataxia-telangiectasia mutated (ATM) kinase (Burma et al., 2001), which is attracted to the DSB foci by the Mre11-Rad50-Nbs1 Complex (Lee and Paull, 2005). Other proteins such as ATR and DNA-dependent protein kinase catalytic subunit (DNA-PKcs) (Falck et al., 2005) are also recruited to the site of the DSB and help trigger a DNA damage response. Of note, ATM phosphorylates and activates p53 protein (Banin et al., 1998), which is also attracted to the DSB site. Activated p53 then proceeds to initiate its cellular response to DNA damage, which can include DNA repair, apoptosis, cell cycle arrest, senescence etc.

With regards to HPV and radiosensitivity, HPV positive invasive disease of oropharyngeal regions appears to be more responsive to radiotherapy compared with HPV negative solid tumours of the same areas (Vu et al., 2010). In a review (Vu et al., 2010) of several different HNSCC studies (Gillison et al., 2000, Lindel et al., 2001, Reimers et al., 2007, Weinberger et al., 2006), which examined patient survival in terms of HPV status, a 60-80% reduction in the risk of mortality owing to their disease, compared to their HPV-negative counterparts, was observed in HPV positive patients.

A recent study examined the radiation response of five HPV/p16INK4a positive and five HPV negative HNSCC cell lines (Rieckmann et al., 2013). The authors found that on average the HPV positive cell lines displayed greater radiosensitivity compared to the HPV negative cell lines. The radiosensitivity result correlated with elevated levels of residual DSBs in the HPV positive cell lines, indicating that HPV positive cells are more susceptible to radiation

induced DSBs. To complement these data, a different study (Kimple et al., 2013) also found increased radiosensitivity in HPV positive cell lines when compared to HPV negative cell lines and a genome-wide microarray analysis found that multiple p53 pathway genes were up-regulated in the HPV positive cells following irradiation. It was therefore concluded that in spite of E6 ubiquitination of p53, low levels of wild-type p53 in HPV positive HNSCC cell lines could be activated by radiation.

As HPV associated neoplasia responds better to radiotherapy, further research into the exact molecular processes resulting in this finding is needed to better develop therapeutic strategies involving radiation and possible combination treatment options.

1.8. Hypotheses

The main aim of this project was the evaluation of ANP compounds, particularly Cidofovir, in NHIST cell lines. Compounds of interest were evaluated in terms of specificity, inhibition of cell growth and mechanism of action in HPV positive cell lines to establish an agreement with or to challenge previously published and occasionally inconsistent literature. The mechanism of action of Cidofovir in the cell lines was compared to that occurring *in vivo* using clinical material from the RT3VIN clinical trial. The approaches used to investigate the following hypotheses are outlined in detail in the introductory sections of each results chapter.

Hypothesis A

i. *Cidofovir displays anti-growth activity in NHIST cell lines*
ii. *IC50 values obtained for Cidofovir in NHIST cell lines are similar to those outlined in previously published literature*

This hypothesis aimed to investigate the validity of the experimental dosing system using the NHIST cell lines as they had never been subjected to Cidofovir treatment prior to this study. Previous studies describe Cidofovir IC50 values and indicate possible specificity of the compound to HPV positive transformed ME180, HEP2, HeLa, CK-1, CaSki and HeLa cell lines (Andrei et al., 1998, Abdulkarim et al., 2002).

Hypothesis B

Cyclic ProTide analogues of Cidofovir have increased anti-growth activity compared with acyclic parent Cidofovir in NHIST cell lines

This hypothesis was derived from the ProTide technology principle. As the negative charge on Cidofovir hinders and delays its cellular entry, ProTide analogues of cyclic Cidofovir were developed to mask its negative charge and increase cellular permeability.

Hypothesis C

ProTide analogues of Adefovir and Tenofovir are more efficient at inhibiting cell growth of HPV positive immortalized cell lines in comparison to the parent compounds from which they were derived

The Cidofovir sister compounds, Adefovir and Tenofovir, are derived from an adenine nucleobase rather than a cytosine nucleobase. Few studies have examined the effects of Adefovir and Tenofovir in the treatment of HPV, but owing to the huge increases in

efficacy described for ProTide analogues (Mehellou et al., 2009) it was hypothesised that ProTide versions of Adefovir and Tenofovir may display an anti-growth effect in HPV positive cells.

Hypothesis D

The NHIST cell lines, M08 and A09, are TP53 wild-type

As the HPV E6 oncoprotein causes degradation of p53 there is minimal selective pressure for p53 mutation in HPV positive cells. However given the potential importance of p53 activity in mediating the response to Cidofovir, it was important to confirm p53 mutation status in the NHIST cell lines.

Hypothesis E

i. *Growth inhibition of Cidofovir treated NHIST cell lines is due to re-accumulation of total and phosphorylated-p53*
ii. *Cidofovir treatment combined with radiation can augment a p53 protein response in NHIST cell lines*

As HPV causes increased cellular proliferation by ubiquitination of the tumour suppressor proteins p53 and pRb via its E6 and E7 oncoproteins, an inhibition of HPV positive cell proliferation produced by Cidofovir may occur by reversal of this process. A re-accumulation of total p53 and activation by phosphorylation could result in apoptosis, cell cycle arrest, senescence, DNA repair or in some cases autophagy. Additionally, previous studies demonstrated a radiosensitizing ability of Cidofovir in HPV positive cell lines (Abdulkarim et al., 2002, Sirianni et al., 2005). It is known that radiation on its own can induce a p53 response (Fei and El-Deiry, 2003). If Cidofovir treatment results in a re-accumulation of total and phosphorylated-p53, further irradiation could augment such a response.

Hypothesis F

i. *Cidofovir inhibits growth of NHIST cell lines by induction of apoptosis*
ii. *Cidofovir can be used as a radiosensitizer and augment an apoptotic response in NHIST cell lines*

This hypothesis is an extension of hypothesis E. As previous published literature suggested Cidofovir inhibits HPV positive cell lines by induction of apoptosis (Andrei et al., 2001), it

was hypothesized that if a p53 response was reactivated by Cidofovir treatment in the NHIST cell lines, it may result in cell death by apoptosis.

Hypothesis G

The increases in total and phosphorylated-p53 levels in Cidofovir and Cidofovir combined with radiation treated NHIST cell lines are due to decreases in E6 expression

This hypothesis is also an extension of hypothesis E. As the E6 oncoprotein causes degradation of p53, the re-accumulation of total and phosphorylated-p53 in Cidofovir and Cidofovir combined with radiation treated NHIST cell lines could be due to an inhibition or decrease in *E6* expression.

Hypothesis H

Increases in total and phosphorylated-p53 levels in Cidofovir and Cidofovir combined with radiation treated NHIST cell lines result in increased p21/CDKN1A transcription

If Cidofovir and Cidofovir combined with radiation induce a total and phosphorylated-p53 response, then phosphorylated-p53 is free to act as a transcription factor for its many target genes, including the cell cycle arrest protein p21. In theory activation of p21 would result in cell cycle arrest and inhibition of cellular proliferation.

Hypothesis I

Differential expression of genes involved in apoptosis is evident in VIN tissue from patients who underwent topical Cidofovir treatment in the RT3VIN clinical trial

This hypothesis was derived from cell line results, which showed differential expression patterns in certain apoptosis related genes after Cidofovir treatment, where a specific effect was seen in HPV positive cell lines. As it was previously demonstrated that Cidofovir produced a specific effect *in vivo* (Tristram and Fiander, 2005), this hypothesis was applied to investigate correlation between *in vitro* cell line work and the *in vivo* RT3VIN clinical trial.

2. Methods

2.1. Cell Culture

2.1.1. Materials

All plasticware for cell culture was obtained from Fisher Scientific UK Ltd, Loughborough, UK. Cell lines used are outlined in Table 2.1; cell culture reagents used are outlined in Table 2.2. Table 2.3 outlines how the cell culture media was formulated. All cell culture was carried out in a class II safety cabinet with stringent aseptic technique.

Table 2.1. Cell Lines, Description and Source

Cell Line	Description	HPV Status	Source
SiHa	Transformed adherent human epithelial cell line derived from a cervical squamous cell carcinoma.	Integrated HPV16	American Type Culture Collection, Manassas, VA
HeLa	Transformed adherent human epithelial cell line derived from a cervical adenocarcinoma.	Integrated HPV18	
C33A	Transformed adherent human epithelial cell line derived from a cervical carcinoma.	HPV negative	
3T3 Mouse feeder cells	Immortalized mouse fibroblastic cell line used for supplementing growth of NHIST cell lines.	HPV negative	Prof Nick Coleman, University of Cambridge
Human Epidermal Keratinocytes, neonatal (HEKn)	Primary human epidermal keratinocytes isolated from neonatal foreskin capable of 30 - 34 population doublings.	HPV negative	Life Technologies Ltd, Paisley, UK
NHIST M08 Vulval Keratinocytes	Homogenous monoclonal adherent human epithelial short term cell line derived from a VIN3 biopsy. Taken from liquid nitrogen storage at passage 5/6, cultured and used in dosing and mechanism of action studies from passage 7 to 10.	HPV16 positive Hypothesized integrated	Onions and Powell et al., unpublished.
NHIST A09 Vaginal Keratinocytes	Homogenous monoclonal adherent human epithelial short term cell line derived from a VaIN3 biopsy. Taken from liquid nitrogen storage at passage 5/6, cultured and used in dosing and mechanism of action studies from passage 7 to 10.	HPV16 positive Hypothesized episomal	

Table 2.2. List and Source of Reagents used for Cell Culture

Reagent	Source
Dulbecco's modified Eagle's Medium Glasgow Minimum Essential Medium Penicillin Streptomycin Epidermal Growth Factor (EGF) Hydrocortisone Cholera Toxin Glutamine Trypsin EDTA 1X solution Phosphate Buffered Saline pH 7.4 Dimethyl sulfoxide (DMSO)	Sigma-Aldrich, Dorset, UK
EpiLife culture medium with Calcium Human Keratinocyte Growth Supplement	Life Technologies Ltd, Paisley, UK
Foetal bovine serum	Autogen Bioclear, Wiltshire, UK

Table 2.3. Formulation of Cell Culture Media

SiHa, HeLa, C33A and 3T3 Feeder Cells		M08 and A09 Keratinocytes	
Component	**Volume**	**Component**	**Volume**
Dulbecco's Modified Eagle's Medium (DMEM)	500 mL	Glasgow Minimal Essential Medium (GMEM)	500 mL
Penicillin/Streptomycin (100X)	5 mL	Penicillin/Streptomycin (100X)	5 mL
		Foetal Calf Serum	50 mL
Foetal Calf Serum	50 mL	Hydrocortisone (50 µg/mL)	250 µL
		Cholera toxin (100 nM)	500 µL
		L-Glutamine (200 nM)	5 mL
		Epidermal growth factor (EGF) (1 µg/mL) (GMEM was formulated with and without EGF)	1 mL per 100 mL media

2.1.2. Culture of SiHa, HeLa, C33A and Mouse 3T3 Feeder Cells

One hundred and seventy five centimetre squared tissue culture flasks were inoculated with 2 x 10^6 cells and 25 mL of Dulbecco's modified Eagle's Medium (supplemented according to Table 2.3). Flasks were incubated at 37°C in 5% CO_2 until cells were ~80% confluent. Flasks were washed with 7 mL phosphate buffered saline before the addition of 5 mL of trypsin/EDTA to each flask. After an incubation period of 3 minutes at 37°C the flasks were tapped by hand to detach the cells from the culture surface. The trypsin was neutralized with the addition of 5 mL media and cells were transferred to a universal

container and centrifuged at 161 g for 5 minutes. Supernatant was discarded and cells were re-suspended in fresh media and counted in a haemocytometer.

2.1.3. Irradiation of Mouse 3T3 Feeder Cells

After the 3T3 feeder cells were stripped from culture flasks and counted they were subjected to 60 Gray (Gy) gamma radiation in a Gammacell 1000 Elite irradiator (MDS Nordion, Ottawa, Canada) and stored at 4°C for further use.

2.1.4. Culture of Human Epidermal Keratinocytes

Human Epidermal Keratinocytes were diluted to 1.25 x 10^4 cells/mL in pre-warmed EpiLife culture medium supplemented with Human Keratinocyte Growth Supplement and added to 6 cm^2 tissue culture dishes. Cells were incubated at 37°C in 5% CO_2 until they became ~80% confluent. Cells were then washed with 2.5 mL of trypsin/EDTA before the addition of 1 mL of fresh 1X trypsin/EDTA solution. Dishes were incubated at 37°C for 10 minutes after which time they were gently tapped before neutralization of trypsin with 1 mL media. The cell suspension was then transferred to a universal container and centrifuged at 181 g for 7 minutes. The supernatant was discarded and cells were counted on a haemocytometer. Cells for subculture were re-inoculated at 2.5 x 10^3 cells/cm^2.

2.1.5. Culture of M08 and A09 Vulval and Vaginal Keratinocytes

M08 vulval and A09 vaginal keratinocytes were inoculated at 8 x 10^5 cells per 10 cm dish with 2 x 10^6 irradiated 3T3 fibroblasts in pre-warmed Glasgow Modified Eagles Medium (supplemented according to Table 2.3) at 37°C in 5% CO_2. After 48 hours the media was changed to EGF positive media. Thereafter, the media was changed every 48 – 72 hours until 80% confluence was reached. After this time, cells were vigorously rinsed with pre-warmed phosphate buffered saline to remove 3T3 cells and 2 mL pre-warmed trypsin was added to each dish. The dishes were incubated at 37°C for 10 – 20 minutes and then gently tapped to detach cells from the culture surface. The trypsin was neutralised with 2 mL media and cells were transferred to a universal container and centrifuged at 161 g for 5 minutes. The supernatant was discarded and cells were re-suspended in fresh media and counted in a haemocytometer.

2.1.6. Storage of Cells

Cells to be stored post stripping and counting were re-suspended in foetal bovine serum with 10% DMSO and aliquoted into 1 mL cryovials. They were then placed in a Mr Frosty freezing container for > 24hours at -80°C, after which time they were transferred into a liquid nitrogen storage facility.

2.1.7. Mycoplasma Detection

Venor®GeM Mycoplasma PCR detection kit (Minerva Biolabs, Berlin, Germany) was used to detect Mycoplasma contamination of cell lines. The primer set is specific to the highly conserved 16S rRNA coding region, allowing for the detection of a range of mycoplasma species. The contents of the Venor®GeM Mycoplasma PCR detection kit are outlined in Table 2.4.

Table 2.4. Components of Venor®*GeM* Mycoplasma Detection PCR Kit

Component	µL of water added for reconstitution
Primer/Nucleotide Mix	65
PCR 10x Reaction Buffer	-
Positive Control DNA	300
Internal Control	300
PCR grade Water	-

2.1.7.1. Template Preparation

Templates for PCR analysis were prepared by transferring 100 µL of supernatant from the test cultures (which had reached 90 – 100% confluence) to sterile micro centrifuge tubes and heating to 95°C for 5 minutes. The samples were then briefly centrifuged (15700 g for 5 seconds) to pellet cellular debris before addition to the PCR mixture.

2.1.7.2. Component Rehydration

The controls and primer/nucleotide mix were rehydrated by centrifuging the tubes with lyophilized components for 5 seconds at 15700 g before the addition of water (volumes outlined in Table 2.4.). The components were then incubated for 5 minutes at room temperature before vortexing and re-centrifugation.

2.1.7.3. Preparation of PCR Mastermix

The PCR reaction mixture was prepared according to Table 2.5.

Table 2.5. Formulation of Mycoplasma Detection PCR Reaction Mixture

Component	µL per 1 PCR reaction
PCR grade Water	15.3
10x Reaction Buffer	2.5
Primer/Nucleotide Mix	2.5
Internal Control	2.5
Hotstar taq (Qiagen, Hilden, Germany)	0.2
Sample DNA/positive control/negative control	2
Total	**25**

2.1.7.4. Thermal Cycle Process

The samples were placed into a Techne TC-512 (Bibby Scientific Limited, Staffordshire, UK) and the thermal cycle conditions outlined in Table 2.6 were used;

Table 2.6. Thermal Cycle for Mycoplasma Detection PCR

Process	Temperature °C	Duration	Number of cycles
Hot start activation	94	15 minutes	-
Denaturation	94	30 seconds	39
Annealing	55	30 seconds	
Elongation	72	30 seconds	
Final extension	72	10 minutes	-

2.1.7.5. Agarose Gel Electrophoresis

A 1.5% agarose gel was made using the formulation outlined in Table 2.7.

Table 2.7. Agarose Gel Formulation for Mycoplasma Detection PCR Products

Component	Quantity	Source
Agarose	1.5 g	Geneflow, Staffordshire, UK
Tris-Borate-EDTA (TBE) buffer (1X)	100 mL	Sigma-Aldrich, Dorset, UK
Ethidium bromide (10 mg/mL)	3 µL	Sigma-Aldrich, Dorset, UK

The agarose powder was dissolved in TBE buffer by heating in a microwave for 3 – 4 minutes until the solution became clear. The solution was cooled to about 65°C before adding the appropriate volume of ethidium bromide. The solution was then poured into a gel mould with comb inserted.

When set, the gel was placed into an electrophoresis tank filled with 1X TBE-buffer. The gel comb was removed and 5 µL of PCR product per reaction was mixed with 5 µL bromophenol blue loading buffer and added to single wells on the gel. For use as a DNA

standard 10 µL of Geneflow 100 bp PCR ranger (Geneflow, Staffordshire, UK) was also added to a peripheral well. Voltage was applied (94 mV/86 mA) and the PCR products were allowed to migrate within the gel according to their size for 20 – 30 minutes.

After electrophoresis, the gel was transferred to a transilluminator and imaged using a GelDock-It TS UVP Imaging System (Ultra-Violet Products Ltd, Cambridge, UK). When examining the gel, the internal control appeared at 191 bp per sample, indicating the PCR preformed successfully. If mycoplasma was detected a second band was visible at 270 bp.

2.2. DNA and RNA extraction

Total DNA and RNA were extracted simultaneously from cell culture experiments using an AllPrep DNA/RNA Mini Kit obtained from Qiagen, Hilden, Germany.

2.2.1. Reagent Preparation

Buffer RPE, Buffer AW1, and Buffer AW2 were each supplied as concentrate. The appropriate volume of ethanol (96 – 100%) was added to obtain a working solution before starting extraction for the first time. Before use, 10 µL β-mercaptoethanol (β-ME) (Sigma-Aldrich, Dorset, UK) was added to 1 mL Buffer RLT Plus in a fume hood wearing appropriate protective clothing.

2.2.2. Cell Lysis and Homogenisation

For each sample to be extracted culture medium was aspirated off the monolayer of cells and the culture surface was rinsed with PBS. Either 350 µL (culture dish < 6 cm diameter) or 600 µL (culture dish 6 – 10 cm diameter) of Buffer RLT Plus was added to each culture surface. The lysates were rinsed over the culture surface, then transferred into separate microcentrifuge tubes and passed through a 20-gauge needle (0.9 mm diameter) fitted to an RNase-free syringe at least 5 times. The homogenized lysates were then transferred to AllPrep DNA spin columns placed in 2 mL collection tubes and centrifuged for 30 seconds at 15700 g. The AllPrep DNA spin columns were then placed into new 2 mL collection tubes and stored at room temperature or at 4°C for later DNA purification. The flow-through from each sample was used for RNA purification.

2.2.3. RNA Purification

Six hundred microlitres of 70% ethanol were added to the flow-through of each sample and mixed well by pipetting. The flow-through/ethanol mixtures were transferred to RNeasy spin columns placed in 2 mL collection tubes and centrifuged for 15 seconds at 15700 g. The flow-through was discarded and 700 µL Buffer RW1 was added to each RNeasy spin column and centrifuged for 15 seconds at 15700 g to wash the spin column membranes. The flow through was again discarded and 500 µL Buffer RPE was added to each RNeasy spin column and centrifuged for a further 15 seconds at 15700 g – this step was carried out twice but on the second occasion the RNeasy spin columns were centrifuged for 2 minutes at 15700 g to wash and dry the spin column membranes, ensuring that no ethanol was carried over during RNA elution. Each RNeasy spin column was then placed in a fresh 1.5 mL collection tube and 30–50 µL RNase-free water was added directly to the spin column membranes and centrifuged for 1 min at 15700 g to elute the RNA.

2.2.4. Genomic DNA Purification

For genomic DNA purification 500 µL Buffer AW1 was added to each initial AllPrep DNA spin column and centrifuged for 15 seconds at 15700 g to wash the spin column membranes. The flow-through was discarded and 500 µL Buffer AW2 was added to each AllPrep DNA spin column and centrifuged for 2 min at 15700 g. Each AllPrep DNA spin column was placed into a new 1.5 mL collection tube and 100 µL Buffer EB was added directly to the spin column membranes and incubated at room temperature for 1 min. The columns were then centrifuged for 1 min at 15700 g to elute the DNA.

2.2.5. Purified DNA and RNA Quantification and Storage

Purified DNA and RNA were quantified by Nanodrop spectrophotometry (Fisher Scientific UK Ltd, Loughborough, UK). Purified DNA was stored at -20°C and purified RNA was stored at -80°C for downstream application.

2.3. Protein Extraction

PathScan® Sandwich ELISA Lysis buffer (Cell Signalling, Massachusetts, USA) was used to extract and preserve total protein from cell culture experiments. Components of the PathScan® Sandwich ELISA Lysis buffer are outlined in Table 2.8.

Table 2.8. Components of 1X PathScan® Sandwich ELISA Lysis Buffer

Component	Concentration
β-glycerophosphate	1 mM
EDTA disodium salt	1 mM
EGTA	1 mM
Leupeptin	1 µg/mL
Sodium chloride	150 mM
Sodium Pyrophosphate	20 mM
Sodium Fluoride	25 mM
Sodium Orthovanadate	1 mM
Tris-Cl	20 mM
Triton X-100	-

One millimolar Phenylmethylsulfonyl Fluoride (PMSF) (Fisher Scientific UK Ltd, Loughborough, UK) was added to 1X lysis buffer chilled on ice immediately before use.

Cells were rinsed with ice-cold PBS and 500 µL/10 cm plate of lysis buffer was added to each culture surface. Plates were left on ice for 5 minutes before scraping off the cell lysate mixture and transferring it to an appropriate tube. The lysates were then sonicated on ice for 30 seconds. Sonicated lysates were centrifuged for 10 minutes at 4°C at 15700 g and resulting supernatants were transferred into fresh tubes. Cell lysates were stored at −80°C in single-use aliquots for downstream application.

2.3.1. Protein Quantification

Total protein from cell lysates was quantified using a Thermo Scientific Pierce® BCA Protein Assay Kit (Fisher Scientific UK Ltd, Loughborough, UK). The Thermo Scientific Pierce BCA Protein Assay was used instead of the conventional Bradford Assay as it is a detergent-compatible formulation based on bicinchoninic acid (BCA) for the colourimetric detection and quantification of total protein. It combines the biuret reaction (the reduction of Cu^{+2} to Cu^{+1} by protein in an alkaline medium) with the highly sensitive and selective colorimetric detection of the cuprous cation (Cu^{+1}) using a unique reagent

containing bicinchoninic acid. The chelation of two molecules of BCA with one cuprous ion forms a purple-colour reaction product, which exhibits a strong absorbance at 562 nm that has an almost linear relationship with increasing protein concentrations over a broad working range. Protein concentrations were determined using standards of bovine serum albumin (BSA). A dilution series of known concentrations was prepared from the protein standard and assayed alongside the unknown samples before the concentration of each unknown was determined using a standard curve.

2.3.1.1. Preparation of Standards and Working Reagent

The components of the Thermo Scientific Pierce® BCA Protein Assay Kit are outlined in Table 2.9.

Table 2.9. Thermo Scientific Pierce® BCA Protein Assay Kit Contents

Component	Quantity/Volume
BCA Reagent A	500 mL
BCA Reagent B	25 mL
Albumin Standard Ampules (2 mg/mL)	10 x 1 mL

The contents of one Albumin Standard (BSA) ampule were diluted into several clean vials using the same diluent (lyses buffer) as the samples. Each 1 mL ampule of 2mg/mL Albumin Standard was sufficient to prepare a set of diluted standards for the working range in triplicate. The formulation of the standards is outlined in Table 2.10.

Table 2.10. Formulation of BSA Standards for Protein Quantification

Vial	Volume of diluent (µL)	Volume and Source of BSA (µL)	Final BSA Concentration (µg/mL)
A	0	300 of Stock	2000
B	125	375 of Stock	1500
C	325	325 of Stock	1000
D	175	175 of vial B dilution	750
E	325	325 of vial C dilution	500
F	325	325 of vial E dilution	250
G	325	325 of vial F dilution	125
H	400	100 of vial G dilution	25
I	400	0	0 = Blank

Two hundred microlitres of working reagent (WR) reagent were required for each sample and were prepared by mixing 50 parts of BCA Reagent A with 1 part of BCA Reagent B.

2.3.1.2. Procedure

Twenty-five microlitres of each standard or unknown sample were aliquoted into separate wells on a 96 well plate. Two hundred microlitres of the WR were then added to each well. The plate was mixed thoroughly on a plate shaker for 30 seconds. The plate was then covered and incubated at 37°C for 2 hours. After the incubation period the plate was allowed to cool to room temperature and the absorbance was measured at 590 nm on a Biochrom Asys Expert Plus microplate reader (Biochrom Ltd., Cambridge, UK).

2.3.1.3. Data Analysis

The average 590 nm absorbance of the measurement of the blank standard replicates was subtracted from the 590 nm measurements of all other individual standard and unknown samples. A standard curve was constructed using GraphPad Prism 4 software (GraphPad Software, Inc., CA, US) by plotting the average Blank-corrected 590 nm measurement for each BSA standard against its concentration in µg/mL. The standard curve was then used to determine the protein concentration of each unknown sample.

2.4. *TP53* Mutation Status

The *TP53* mutation status of short term vulval cell line, M08, and short term vaginal cell line, A09, was determined by direct sequencing using the IARC 2010 protocol (IARC, 2010 Update) for detection of *TP53* mutations.

2.4.1. Primer Sets

Thirteen primer sets designed to amplify exons 2 – 11 of the human *TP53* gene were obtained from Sigma-Aldrich (Dorset, UK). Primer sequence and product size are displayed in Table 2.11.

Table 2.11. Primers, Direction, Region Amplified, Product Length and Thermo Cycle Program for *TP53* Mutation Detection PCR

IARC code	Primer pairs (5' → 3')	Direction	Region Amplified	Product Length	PCR Program
P-559 P-E3Ri	tctcatgctggatccccact agtcagaggaccaggtcctc	F R	Exons 2-3	344 bp	B
P-329 P-330	tgctcttttcacccatctac atacggccaggcattgaagt	F R	Exon 4	353 bp	B
P-326 P-327	tgaggacctggtcctctgac agaggaatcccaaagttcca	F R	Exon 4	413 bp	B
P-312 P-271	ttcaactctgtctccttcct cagccctgtcgtctctccag	F R	Exon 5	248 bp	B
P-239 P-240	gcctctgattcctcactgat ttaacccctcctcccagaga	F R	Exon 6	181 bp	B
P-236 P-240	tgttcacttgtgccctgact ttaacccctcctcccagaga	F R	Exons 5 - 6	467 bp	B
P-333 P-313	cttgccacaggtctccccaa aggggtcagaggcaagcaga	F R	Exon 7	237 bp	C
P-237 P-238	aggcgcactggcctcatctt tgtgcagggtggcaagtggc	F R	Exon 7	177 bp	B
P-316 P-319	ttccttactgcctcttgctt aggcataactgcacccttgg	F R	Exon 8	231 bp	B
P-314 P-315	ttgggagtagatggagcct agtgttagactggaaacttt	F R	Exons 8 - 9	445 bp	B
9F 9R	gacaagaagcggtggag cggcattttgagtgttagac	F R	Exon 9	215bp	E
P-E10Li P-562	caattgtaacttgaaccatc ggatgagaatggaatcctat	F R	Exon 10	260 bp	D
P-E11Le P-E11Re	agaccctctcactcatgtga tgacgcacacctattgcaag	F R	Exon 11	245 bp	B

2.4.2. PCR Reaction Components

Template DNA was extracted from M08 and A09 cells and the PCR reaction mixture for each primer set was formulated according to Table 2.12.

Table 2.12. *TP53* Mutation Detection PCR Reaction Formulation

Component	Source	µL / Reaction	Final Conc.
10X PCR buffer containing 15 mM MgCl2	Qiagen, Hilden, Germany	2	1X
5X Q-Solution	Qiagen, Hilden, Germany	4	1X
dNTP mix (2 mM each)	Life Technologies Ltd, Paisley, UK	2	0.2 mM
Primer, forward 10 µM	Sigma-Aldrich, Dorset, UK	0.8	0.4 µM
Primer, reverse 10 µM	Sigma-Aldrich, Dorset, UK	0.8	0.4 µM
HotStarTaq DNA polymerase (5 U/µl)	Qiagen, Hilden, Germany	0.1	0.5 U
Template DNA	-	1	50 ng
Water, molecuLar biology grade	Sigma-Aldrich, Dorset, UK	9.3	-
TOTAL		20	-

2.4.3. Thermal Cycle Process

The PCR reactions along with a negative control for each condition were run on one of the following four thermal cycle programs (Tables 2.13 – 2.16) on either a Techne TC-512 (Bibby Scientific Limited, Staffordshire, UK) or a GeneAmp PCR System 9700 (Life Technologies Ltd, Paisley, UK).

Table 2.13. *TP53* Mutation Detection PCR Thermo Cycle B Conditions

Process	Temperature °C	Duration	Notes	Number of Cycles
Hot start activation	94	15 minutes		-
Denaturation	94	30 seconds		20
Primers anneal	63	45 seconds	-0.5°C every 3 cycles	
Elongation	72	1 minute		
Denaturation	94	30 seconds		30
Primers anneal	60	45 seconds		
Elongation	72	1 minute		
Final extension	72	10 minutes		-

Table 2.14. *TP53* Mutation Detection PCR Thermo Cycle C Conditions

Process	Temperature °C	Duration	Number of Cycles
Hot start activation	95	15 minutes	-
Denaturation	94	30 seconds	50
Primers anneal	60	30 seconds	
Elongation	72	30 seconds	
Final extension	72	10 minutes	-

Table 2.15. *TP53* Mutation Detection PCR Thermo Cycle D Conditions

Process	Temperature °C	Duration	Notes	Number of Cycles
Hot star activation	94	15 minutes		-
Denaturation	94	30 seconds		20
Primers anneal	58.5	45 seconds	-0.5°C every 3 cycles	
Elongation	72	1 minute		
Denaturation	94	30 seconds		30
Primers anneal	55	45 seconds		
Elongation	72	1 minute		
Final extension	72	10 minutes		-

Table 2.16. *TP53* Mutation Detection PCR Thermo Cycle E Conditions

Process	Temperature °C	Duration	Number of Cycles
Hot star activation	95	15 minutes	-
Denaturation	94	30 seconds	50
Primers anneal	57	30 seconds	
Elongation	72	30 seconds	
Final extension	72	10 minutes	-

PCR products were electrophoresed on a 2% agarose gel with 5X Orange G loading dye (Sigma-Aldrich, Dorset, UK) and visualised under UV light.

2.4.4. Gel Extraction

An illustra GFX PCR DNA and Gel Band Purification Kit (GE Healthcare Life Sciences, Buckinghamshire, UK) was used to purify DNA post agarose gel electrophoresis. The illustra GFX PCR DNA and Gel Band Purification Kit contents are outlined in Table 2.17. Prior to first use, 100 mL absolute ethanol was added to the Wash buffer type 1.

Table 2.17. illustra GFX PCR DNA and Gel Band Purification Kit Contents

Capture buffer
Wash buffer
Elution buffer type 3 (Tris HCL)
Elution buffer type 6 (Sterile H_2O)
illustra™GFX™MicroSpin™Columns
Collection tubes

The agarose gel was placed on a 365 nm benchtop ultraviolet transilluminator (Ultra-Violet Products Ltd, Cambridge, UK) with minimal exposure time. Using a clean scalpel, the agarose band containing the DNA of interest was cut out and placed into a DNase-free 1.5 mL microcentrifuge tube. Three hundred microlitres of Capture buffer type 3 were added

to each excised band of gel and mixed by inversion. Samples were then incubated at 60°C for 15 – 30 minutes, mixing by inversion every 5 minutes to dissolve the agarose. Once the agarose had completely dissolved the colour of the mixture was examined. If the colour of the binding mixture was a dark pink or red, 10 µL of 3 M sodium acetate pH 5.0 (Fisher Scientific UK Ltd, Loughborough, UK) was added and mixed to adjust the pH of the mixture. The capture buffer type 3-sample mixtures were then centrifuged briefly to collect the liquid at the bottom of the tubes and transferred to assembled GFX MicroSpin column and collection tubes. After an incubation period of 1 minute the assembled columns were centrifuged at 15700 g for 30 seconds. The flow-through was discarded and the MicroSpin columns were placed back inside the collection tubes. Five hundred microlitres of Wash buffer type 1 were added to the GFX MicroSpin columns and the columns were centrifuged at 15700 g for 30 seconds. The collection tubes were discarded and the GFX MicroSpin columns were transferred to fresh DNase-free 1.5 mL microcentrifuge tubes. For each sample, 25 µL Elution buffer type 6 was added to the centre of the membrane in the assembled GFX MicroSpin column and incubated for 1 minute at room temperature. Finally, the assembled column and sample collection tubes were centrifuged at 15700 g for 1 minute to recover the purified DNA.

Five microlitres of each purified PCR product were loaded with 5 µL orange G to a 2% agarose gel and the purified products were electrophoresed to ensure there was only one correctly sized DNA band present post gel extraction. This was also carried out to estimate the concentration of purified product post purification by comparing the sample band intensity to the intensity of the standards on the of Geneflow 100 bp PCR ranger.

2.4.5. Sequencing

Primers for sequencing were diluted to 3.2 pmol/µL in fresh 1.5 mL tubes. Twenty microlitres of purified PCR product were aliquoted into appropriately labelled DNase free tubes. Sequencing was performed by Source Bioscience (Source BioScience UK Ltd., Nottingham, UK) who require 1 ng/µL per 100 bp of fragment.

2.4.6. Sequence Analysis

The chromatograms of the Sanger Sequencing reactions were manually analysed using BioEdit software (Ibis Biosciences, Ca, USA) before the generation of fasta files for each sequence. In the nucleotide section of the BLAST® website (NCBI), the *TP53* mRNA reference sequence NM_000546.4 was aligned with the sequences of interest. Where there was an identity between the reference and test sequences of 99% or less, the chromatograms were manually re-examined to rule out false mismatches. If the mismatches appeared to be real the nucleotide location and difference was recorded. The test sequences were then re-aligned with the genomic DNA (gDNA) reference sequence, NC_000017.9, and true mismatches were examined and recorded as per above. The true mismatches common to both mRNA and gDNA reference sequence alignments were searched for in the IARC *TP53* Mutation Database (IARC, November 2012) using the cDNA (mRNA) sequence position.

2.5. Cidofovir and ANP Analogue Dosing

2.5.1. ProTide Synthesis

The compounds outlined in Table 2.18 were used in the dosing studies;

Table 2.18. Compounds used in Dosing Studies

Compound	Source
Cidofovir	Shanghai Sun-Sail Pharmaceutical Science & Technology Co., Ltd., Shanghai, China
Tenofovir	Ningbo Haishu Hobid Imp & Exp Co., Ltd, Ningbo, China
Adefovir	Hubei Maxsource Chemical Co., Ltd, Wuhan, China

Davide Carta, Fabrizio Pertusati and Karen Hinsinger of the McGuigan Group in the Welsh School of Pharmacy confirmed the identity and purity of the compounds by nuclear magnetic resonance (NMR) using a Bruker spectrometer (Bruker, Billerica, MA, USA) and synthesised the prodrug compounds.

An amidate derivative of cyclic Cidofovir was synthesized according to the procedure outlined in the literature (Kern et al., 2002). In brief, Cidofovir was treated with *N,N*-dicyclohexyl-4-morpholinecarboxamidine (DCMC) and 1,3-dicyclohexylcarbodiimide (DCC), which generated dicyclohexyl morpholinocarboxamidine salt. The reaction of cyclic Cidofovir with an excess of L-alanine benzyl ester in the presence of 2,2'-dithiopyridine

and triphenylphosphine in anhydrous pyridine at 60 °C resulted in a mixture of two diastereomers.

The Adefovir and Tenofovir prodrugs were synthesised by addition of bromotrimethylsilane (TMSBr) to a solution of the acyclic nucleoside in dry acetonitrile (ACN) under argon and the reaction was stirred at room temperature overnight. The solvents were then removed under reduced pressure without any contact with air and the residue was dissolved in anhydrous triethylamine (Et_3N) and pyridine, and amino acid ester was added. Aldrithiol-2 and triphenylphosphine (Ph_3P) were dissolved in anhydrous pyridine in a separate flask and immediately added to the reaction. The mixture was stirred for 3 – 5 hours at 50°C before solvent evaporation. The residue was then purified by flash chromatography on silica gel eluted with dichloromethane/methanol.

2.5.2. Compound Formulation

The materials used and volumes for compound formulation are outlined in Table 2.19 and Table 2.20 respectively.

Table 2.19. Materials used for Compound Formulation

Material	Source
Dimethyl sulfoxide (DMSO)	Fisher Scientific, Loughborough, UK
Phosphate buffered saline (PBS) pH 7.4	Sigma-Aldrich, Dorset, UK
Sodium Hydroxide (NaOH) 5M	Sigma-Aldrich, Dorset, UK

Table 2.20. Formulation of Compounds

Compound	ID number /CAS	MW g	Grams g	PBS mL	DMSO mL	DMSO %	mM
Cidofovir	149394-66-1	315.22	15.862	65.000†	40.000	37.92	30.8
cCDV amidate	cf 3293	422.3722	0.0029	6.866	0.166	2.36	1.0
cCDV Salt	cf 3362	554.6193	0.0020	3.607	0.047	1.29	1.0
Tenofovir parent	147127-20-6	287.21	0.0057	20.000	0.200	0.99	1.0
Tenofovir prodrug 1	cf 3472	569.6	0.0103	18.083	0.183	1.00	1.0
Tenofovir prodrug 2	cf 3473	554.58	0.0122	22.000	0.200	0.90	1.0
Tenofovir prodrug 3	cf 3474	554.58	0.0093	16.770	0.170	1.00	1.0
Adefovir parent	106941-25-7	273.19	0.0055	20.000	0.200	0.99	1.0
Adefovir prodrug 1	cf 3475	540.55	0.0048	8.880	0.110	1.22	1.0
Adefovir prodrug 2	cf 3476	555.61	0.0069	12.420	0.200	1.58	1.0

† With the addition of 0.5 mL 5M NaOH

2.5.3. Optimum Cell Number Titration

As each cell line used in the dosing studies had different population doubling times it was necessary to establish the appropriate initial inoculum so the culture would not reach confluence during the experimental period. It was also important to determine the initial cell inoculums for the short term vulval and vaginal cells lines as these cells require contact with other cells to proliferate effectively.

M08 cells were seeded at 5 x 10^3, 7.5 x 10^3 and 1 x 10^4 cells per well in triplicate in a 96 well plate with the appropriate culture medium. After an adherence period of 24 hours, concentrations of 0, 1, 10 and 100 µM Cidofovir were added to the appropriate wells for each initial inocula series. The plates were incubated at 37°C in 5% CO_2 for a further 6 days, where cells were evaluated daily for efficient proliferation and degree of confluence. Viability readings using Trypan blue staining were taken 3 and 6 days post Cidofovir dosing. The optimum initial cell inoculum determined from the study was adjusted per culture surface area when working with different sized culture dishes.

The transformed cell lines, SiHa, HeLa and C33A, were seeded from 1 x 10^2 – 7 x 10^3 cells per well in a 96 well plate and incubated at 37°C in 5% CO_2. After 24 hours, 20 µL of CellTiter 96® AQueous One MTS Solution Reagent (Promega, Southampton, UK) was added to each well and absorbance values were read from 1 – 4 hours at 490 nm to determine the optimum initial cell inoculum as well as optimum time for incubation with the CellTiter 96® AQueous One MTS Solution Reagent.

2.5.4. Dosing Method

In all cases, cells to be used in the dosing experiments were taken from culture and aliquoted at specified cell numbers into 96 well plates, 24 well plates or 6 cm tissue culture dishes without compound. The plates were incubated at 37°C with 5% CO_2 for 24 hours to allow cells to adhere. The compound negative media was then aspirated and fresh media with the desired concentration of compound was added. Cells in all experiments apart from the Prodrug Screen were subjected to just one dose of compound. Cells in the Prodrug Screen were subjected to a second dose of compound 72

hours (3 days) after the initial dose. Untreated/compound negative cells were also cultured alongside treated cells to serve as a negative control.

2.5.5. Radiation and Cidofovir Combined Treatment

Cells in the radiosensitivity assay were pre-treated with their IC50 concentrations of Cidofovir for 6 days. After this time they were stripped from their culture dishes and reseeded into fresh 6 cm culture dishes in the presence of Cidofovir. After an attachment period of 24 hours the 6 cm culture dishes were placed into a Gammacell 1000 Elite irradiator and subjected to either 2 or 20 Gy gamma radiation.

2.6. Assessment of Cell Viability

Viability of cells treated with compounds was assessed at various time points post treatment:

2.6.1. Microscopic Examination and Photomicrographs

Treated cells were examined using bright field microscopically at specific time points for evidence of viability using X100 and X320 magnification on a Zeiss Axiovert 35M inverted microscope.

2.6.2. MTS Viability Protocol

The CellTiter 96® AQ_{ueous} One Solution Cell Proliferation Assay (Promega, Southampton, UK) was the first method employed to quantify cell viability in response to treatment. The colorimetric assay is composed of solutions of a tetrazolium compound (3-(4,5-dimethylthiazol-2-yl)-5-(3-carboxymethoxyphenyl)-2-(4-suLfophenyl)-2H-tetrazolium, inner salt; MTS) and the electron coupling reagent phenazine methosulfate (PMS). MTS is reduced by dehydrogenase enzymes in metabolically active cells into a formazan product. At 490 nm the absorbance of the formazan can be measured directly from a 96-well plate, and absorbance is taken as proportional to the number of living cells.

When cell viability was to be examined, the CellTiter 96® AQueous One MTS Solution Reagent was allowed to thaw at room temperature for approximately 2 hours. Twenty microlitres of CellTiter 96® AQueous One Solution Reagent were then added to each well of a 96-well assay plate containing the cells to be analysed in 100 µL of culture medium.

The plate was then incubated for 3.5 hours at 37°C in 5% CO_2. After this incubation period absorbance was recorded at 490 nm using a Multiskan FC Microplate Photometer (Fisher Scientific UK Ltd, Loughborough, UK). Background interference was controlled for by using 100 µL of culture media without cells and 20 µL of CellTiter 96® AQueous One Solution Reagent. The absorbance of this "blank" solution was then subtracted from the absorbance of the test wells for the final absorbance value, which was proportional to cell viability.

2.6.3. Trypan Blue Dye Exclusion

The Trypan Blue Dye Exclusion assay was also used to determine cell viability post treatment. Live cells have intact cell membranes that exclude Trypan Blue, whereas, dead cells do not and Trypan Blue can enter. Therefore, non-viable/dead cells stained with Trypan Blue appear to have a blue cytoplasm when visualised under a microscope, while cells with a clear cytoplasm are viable. Cells were trypsinized and brought into suspension. Twenty microlitres of cell suspension were removed and an equal volume of 0.4% Trypan Blue (Sigma-Aldrich, Dorset, UK) was added to the cell suspension and mixed by gentle pipetting. Both chambers of a Neubauer haemocytometer (Marienfeld, Lauda-Königshofen, Germany) were filled with approximately 10 µL of the stained cell suspension each and viewed under a Zeiss Axiovert 35M inverted microscope at X200 magnification. Both the number of viable (clear) and non-viable (blue) cells were counted and number of viable cells per mL was calculated by multiplying the number of viable cells counted in one chamber x 10,000.

2.6.4. Flow Cytometry

Flow cytometry using 7-amino actinomycin D (7-AAD) was the third method used to assess viability of treated cells. In a flow cytometry analyser, a laser beam of a particular wavelength is passed through a hydro-dynamically focused stream of cells in suspension, such that only one cell passes through the laser beam at a time. As a cell passes through the laser beam light is deflected and is registered and quantified by a number of detectors strategically positioned around the laser beam. The forward scatter detector is directly in line with the laser beam and detects light scattered in a forward manner, which is proportional to cell size. Side scatter and fluorescence detectors are positioned

perpendicular to the laser beam. The side scatter detectors measure the amount of light scattered to the side of the cell as it passes through the laser beam, which is an indication of cellular granularity. If a cell labelled with a particular fluorochrome passes through a laser beam, the fluorochrome will emit light at a specific wavelength which can be detected by the fluorescence detectors; the fluorescence is quantified and is used to estimate the proportion of cells in the sample that have the particular characteristic that binds the fluorochrome. For example, 7-AAD like Trypan Blue is a membrane impermeant dye that is generally excluded from living cells. However, unlike Trypan Blue it has the ability to intercalate between base pairs in Guanine - Cytosine rich regions in double stranded DNA (Cowden and Curtis, 1981). 7-AAD is excited at 488 nm with an argon laser and emits at 647 nm. Therefore, if a cell suspension incubated with 7-AAD is analysed using an argon laser the florescence emitted will be proportional to the number of dead/non-viable cells in the sample.

Cells to be analysed were striped from culture dishes with trypsin, washed in PBS by centrifugation (232 g/3 minutes) and re-suspended in 100 µL BD FACSFlow Sheath Fluid (BD Biosciences, Oxford, UK) with a final working concentration of 1 µg/mL 7-AAD (Sigma-Aldrich, Dorset, UK). Each sample was analysed on a BD Accuri C6 flow cytometer (BD Biosciences, Oxford, UK) using the blue laser with excitation of 488 nm at a high flow rate until an average of 10,000 events were recorded or until the entire 100 µL of sample was analysed. 7-AAD fluorescence was registered on the FL3 detector through a 670 nm filter. Using FCS express V4 software (De Novo Software, CA, USA) to analyse the data, background fluorescence was gated out by plotting FL1 against FL2 and FL3 against FL4. Fluorescence in terms of signal height was plotted on a log scale against the forward scatter height (FSC-H) parameter and a viable population of cells was identified and gated upon (gate 1). The number of viable cells/mL was calculated using the total number of events counted in the viable population and the volume of cell suspension analysed. To illustrate the effect of compound dosing on cell size the median forward scatter value obtained for the viable population of cells (gate 1) was plotted on a histogram relevant to cell count.

2.6.5. IC50 Value Calculation

Percentage viability of treated cells was calculated by converting the viable count of cells treated with a particular concentration of compound to a percentage of the viable cell count in the corresponding untreated control samples. Percentage viability values were subtracted from 100% to give percentage inhibition values. The concentration that produced 50% inhibition of cell proliferation was the IC50 value.

2.7. Storage of Compounds and Related Reagents

Cidofovir parent compound was stored at room temperature when it was being used frequently and stored at -20°C for long term storage. Cidofovir analogues, Adefovir parent compound, Adefovir analogues, Tenofovir parent compound and Tenofovir analogues were all stored at 4°C for short term use and -20°C for long term use. DMSO, PBS, NaOh, Trypan Blue and BD FACSFlow Sheath Fluid were stored at room temperature. The CellTiter 96® AQueous One MTS Solution Reagent and 1 mg/mL stock 7-AAD were stored at -20°C. For short term use 100 µg/mL 7-AAD was stored at 4°C.

2.8. Assessment of Mechanism of Action of Cidofovir

2.8.1. Cleaved Caspase-3 Activity Assay

Caspase-3 is an executioner of apoptosis and is either partially or totally responsible for the proteolytic cleavage of many key proteins involved in apoptosis. Activation of caspase-3, via both intrinsic and extrinsic pathways, requires proteolytic cleavage of its inactive proenzyme into activated p17 and p12 fragments (Cohen, 1997). Cleaved caspase-3 activity of M08, A09 and HEK cell lines was assessed initially with a Caspase-3 Activity Assay Kit (Cell Signalling, Massachusetts, USA). This is a fluorescent based assay that detects caspase-3 activity in cell lysates. During the assay, activated caspase-3 cleaves a fluorogenic substrate (N-Acetyl-Asp-Glu-Val-Asp-7-amino-4-methylcoumarin or Ac-DEVD-AMC) between DEVD and AMC, yielding highly fluorescent AMC that can be quantified using a fluorescence reader with excitation at 380 nm and emission between 420 - 460 nm. The amount of AMC produced is proportional to the number of apoptotic cells in the sample as cleavage only occurs in lysates of apoptotic cells. The caspase-3 activity assay kit contents are outlined in Table 2.21.

Table 2.21. Caspase-3 Activity Assay Kit Contents

Component	Quantity/Volume
Ac- DEVD-AMC	1 mg
AMC (7-amino-4-methylcoumarin)	250 µL
PathScan Sandwich ELISA Lysis Buffer 1X	30 mL
Caspase Assay Buffer 2X	30 mL
1 M DTT (Dithiothreitol)	200 µL

DTT and Ac-DEVD-AMC were thawed at 37°C just before the experiment. Ac-DEVD-AMC was reconstituted in 1 mL DMSO. One part Assay buffer (2X) was mixed with one part dH_2O, and DTT was added (final concentration of 5 mM) to make 1X assay buffer A. Ac-DEVD-AMC was diluted 1:40 in 1X assay buffer A to make substrate solution B.

Protein lysates were diluted to 2 mg/mL in 1X assay buffer and 25 µL of each lysate to be analysed was aliquoted into separate wells on a black 96 well flat bottomed plate. Two hundred microlitres of substrate solution B were added to the cell lysates and to 25 µL of 1X assay buffer (which served as a negative control). Twenty-five microlitres of positive control AMC (supplied with kit) were added to 200 µL 1X assay buffer A as a positive control. Relative Fluorescence Units (RFU), with excitation at 380 nm and emission at 470 nm, were recorded immediately at 0 hours on a FLUOstar OPTIMA fluorescence plate reader (BMG LABTECH Ltd., Buckinghamshire, UK). The plates were incubated at 37°C in the dark and RFU were further recorded at 1 and 2 hours.

2.8.2. Western Blotting

2.8.2.1. Materials

The materials used for western blotting are outlined in Table 2.22.

Table 2.22. Materials used for Western blotting

Material	Source
NuPAGE® lithium dodecyl sulfate (LDS) Sample Buffer (4x)	Life Technologies Ltd, Paisley, UK
NuPAGE® Sample Reducing Agent (10x)	
NuPAGE® Novex® 4-12% Bis-Tris Gel 1.0 mm, 12 Well	
NuPAGE® MOPS (3-(N-morpholino)propanesulfonic acid) SDS (sodium dodecyl sulphate) Running Buffer (20X)	
NuPAGE® Antioxidant	
MagicMark™ XP Western Protein Standard (20-220 kDa)	
NitrocelluLose membranes, 0.45 µm Pore Size, with filter paper	
NuPAGE® Transfer Buffer (20x)	
5% ECL advance blocking solution	GE Healthcare Life Sciences, Buckinghamshire, UK
Amersham ECL (Enhanced Chemiluminescence) Prime Western Blotting Detection Reagent	
β-Actin (13E5) antibody (rabbit) #4970	Cell Signalling, Massachusetts, USA
P53 antibody (rabbit) #9282	
Phospho-P53 (Ser 15) antibody (rabbit) #9284	
Cleaved Caspase-3 (Asp 175) (5A1E) antibody Rabbit #9664	
p21 Waf1/Cip1 (12D1) Rabbit mAb #2947	
Goat polyclonal Secondary Antibody to Rabbit IgG - H&L (HRP), pre-adsorbed (ab97080)	Abcam, Cambridge, UK
Sterile H_2O	

2.8.2.2. Sample Preparation

M08 and A09 protein lysates were prepared to give a final loading concentration of 14.2 µg protein in 20 µL. HEK lysates were prepared to give a final loading concentration of 8.75 µg protein in 20 µL. The appropriate volumes of LDS sample buffer and reducing agent were added to a fresh 2 mL tube per lysate to each give a final concentration of 1X. The final protein concentrations were made up by adding the required volumes of water and lysate. Samples were mixed thoroughly by vortexing and placed in water bath for 10 minutes at 70^{o}C. After this incubation period the samples were centrifuged for 1 minute at 15700 g. Samples were then stored on ice for immediate use or at -80^{o}C**.**

2.8.2.3. Electrophoresis

The gel cassette was removed from the gel pouch and packaging buffer was drained away and the gel cassette was rinsed with tap water. The white tape covering the slot on the back of the gel cassette was peeled away and the comb was gently removed from the cassette exposing the gel loading wells. The cassette wells were gently washed with 1X running buffer three times and finally the wells were filled with fresh running buffer. The

gel cassette was inserted and secured in the lower buffer chamber of an XCell SureLock™ Mini-Cell Electrophoresis System (Life Technologies Ltd, Paisley, UK). If two gels were to be run, one cassette was placed behind the core and one cassette in front of the core with the well side of the cassettes facing the buffer core.

Five hundred microlitres of antioxidant were added to 200 mL running buffer. The Upper Buffer Chamber/cathode, formed between the two gel cassettes (or one cassette and the buffer dam) on each side of the buffer core, was filled with enough running buffer/antioxidant solution to completely cover the sample wells. The samples were loaded carefully. The lower buffer chamber/anode was filled with 600 mL of running buffer. The lid was aligned to the buffer core and voltage of 200 V was applied for 50 minutes. The expected current for 1 gel was 100 - 125 mA at the beginning and 60-80 mA at the end of electrophoresis.

2.8.2.4. Western Blotting

During electrophoresis the transfer buffer was prepared according to Table 2.23.

Table 2.23. Formulation of Transfer Buffer for Western blot

Component	Volume (mL)
Transfer Buffer (20X)	50
NuPAGE® Antioxidant	1
Methanol	100
Deionised Water	849
Total Volume	1000

The blotting pads were soaked in sufficient transfer buffer until saturated. Soaked blotting pads were placed into the cathode core of the blot module. The nitrocellulose membrane was then soaked in transfer buffer for several minutes. The filter paper was briefly soaked in transfer buffer immediately before use.

Following electrophoresis the gel was removed from the cassette by carefully pulling apart either side of the cassette with a gel knife. The wells were removed from the gel with the gel knife and the pre-soaked transfer membrane was placed onto the gel. Pre-soaked filter paper was placed on top of the transfer membrane and on the other side of the gel. The gel membrane assembly was placed on the blotting pads so that the gel was closest to the

cathode plate as shown in Figure 2.1. Pre-soaked blotting pads were placed on top of the gel membrane assembly and the anode core was placed on top of the pads. The blot module was placed into the lower buffer chamber of the XCell SureLock™ Mini-Cell Electrophoresis System. The blot module was filled with transfer buffer and the outer buffer chamber was filled with deionised water to dissipate heat produced during the run. A voltage of 25 V was applied for one hour. The expected start current for one membrane was 170 mA and the expected end current was 110 mA.

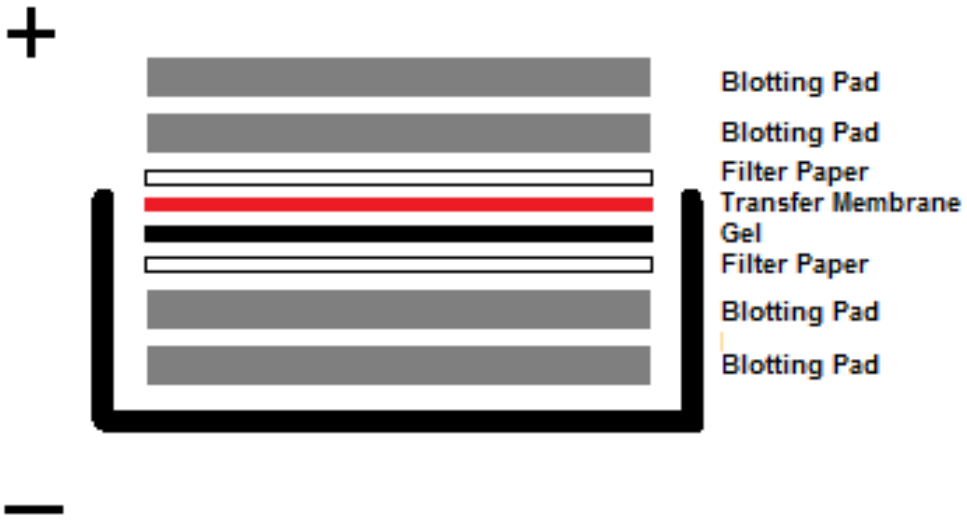

Figure 2.1. Outline of Gel-Membrane Sandwich in Blotting Module

Assembly of blotting pads, filter paper, gel and transfer membrane in the blotting module for protein transfer. The gel-membrane sandwich was assembled so that the gel was closest to the cathode core plate.

2.8.2.5. Blocking and Antibody Staining

TBS-Tween (TBST) was formulated according to Table 2.24.

Table 2.24. Formulation of TBS-Tween for Western blot

Component	Volume (mL)	Final Concentration	Source
2.5 M Tris HCL	20	5 mM	Fisher Scientific UK Ltd, Loughborough, UK.
5 M NaCl	27.7	150 mM	
Tween 20	1	-	
Sterile Water	951.3	-	-
Total Volume	1000	-	-

A 5% blocking solution was prepared by dissolving 0.5 g ECL blocking powder in 10 mL TBST for one membrane. The top left corner of the membrane was cut with a scissors to indicate orientation and the membrane was washed twice for 5 minutes with 20 mL of pure water in a plastic container on a rotary shaker set at 1 revolution per second. Water was poured off and 10 mL of the 5% blocking solution was added. The membrane was incubated for 1 hour on the rotary shaker. During the blocking process the antibody dilution was prepared in 5% blocking solution.

P53, Phospho-p53 and Cleaved Caspase-3 antibodies were diluted 1:1000, whereas, β-Actin and p21 Waf1/Cip1 antibodies were diluted 1:5000 in 10 mL of blocking solution per membrane. After the blocking incubation the solution was decanted, the membrane was rinsed twice with TBST. The membrane was then washed twice in TBST on the shaker for 15 minutes, followed by 3 x 5 minute washes. The membrane was then incubated in the primary antibody diluent overnight in a cold room on a rotary shaker.

The next day the membrane was rinsed in TBST twice, and then washed with TBST on a shaker for 15 minutes, followed by 3 x 5 minute washes. The secondary antibody solution was prepared by diluting the goat polyclonal secondary antibody 1:5000 in 2% ECL blocking solution. The membrane was incubated in 10 mL of secondary antibody per 1 membrane for 60 minutes. After this incubation period the secondary antibody solution was decanted and the membrane was rinsed twice with TBST. The membrane was washed in TBST on a shaker for 15 minutes, followed by 3 x 5 minute washes.

2.8.2.6. Chemiluminescence

The ECL Prime chemiluminescent substrate solutions were prepared by mixing 2 mL of solution A with 2 mL of solution B for one full size blot. The excess liquid was drained from the membrane and it was placed protein side up on a thin transparent plastic sheet. The chemiluminescent substrate was evenly applied to the membrane surface and the reaction was allowed to develop in the dark for 5 minutes. After this time the excess chemiluminescent substrate solution was blotted from the membrane surface with filter paper and the membrane was covered with another clean transparent plastic sheet. The membrane was then subjected to image capture with an LAS-3000 imager (Fujifilm, Tokyo, Japan) using an initial exposure of 10 - 30 seconds to capture any fleeting weak signals, after which time the exposure was adjusted to capture more robust signals (5 - 30 minutes).

2.8.3. RT-qPCR

2.8.3.1. Agilent

Before reverse transcription (RT) and Quantitative Real Time Reverse Transcriptase PCR (RT-qPCR), the quality and integrity of the RNA was examined using an Agilent RNA 6000 Nano Kit and Agilent 2100 bioanalyzer (both Agilent Technologies, Santa Clara, CA, USA). The Agilent RNA kits encompass chips and reagents designed for analysis of RNA fragments. The RNA chips contain interconnected sets of micro channels that are used for separation of nucleic acid fragments based on their size.

Five hundred and fifty microlitres of RNA 6000 Nano gel matrix were aliquoted into a spin filter and centrifuged at 1500 g for 10 minutes at room temperature. Sixty-five microlitres of filtered gel were then dispensed into 0.5 mL RNase-free microfuge tubes.

The RNA 6000 Nano dye concentrate was allowed to equilibrate to room temperature for 30 minutes. After vortexing for 10 seconds and a brief centrifugation, 1 µL of dye was added to the 65 µL aliquots of filtered gel. The solutions were vortexed and centrifuged at 13000 g for 10 min at room temperature.

Nine microlitres of gel-dye mix were pipetted into the well-marked for gel on the RNA 6000 Nano chip which was placed on the priming station. The chip priming station was

closed and the plunger was pressed until it was held by the clip. After 30 seconds the clip was released and the plunger was pulled back to the 1 mL position. The chip priming station was opened and 9 µL of gel-dye mix was pipetted into two of the wells marked. Five microlitres of RNA 6000 Nano marker were then aliquoted in to all 12 sample wells and in the well-marked with the ladder symbol.

One microlitre of ladder was aliquoted into the appropriately marked well. One microlitre of RNA sample was aliquoted into each of the 12 sample wells. The chip was vortexed for 1 minute at 2400 rpm in an IKA vortexer with Agilent chip adaptor and analysed on the Agilent 2100 bioanalyzer within 5 minutes.

2.8.3.2. Reverse Transcription

Reverse transcription of RNA into complementary DNA (cDNA) was carried out using a RT² First Strand Kit (Qiagen, Hilden, Germany). The contents of this kit are outlined in Table 2.25.

Table 2.25. RT² First Strand Kit Contents

GE: 5X genomic DNA (gDNA) Elimination Buffer
BC3: 5X Reverse Transcription Buffer 3
H2O: RNase-free H_2O
P2: Primer and External Control Mix
RE3: RT Enzyme Mix 3

All reagents were briefly centrifuged for 15 seconds at 15700 g. The genomic DNA elimination mixture was prepared for each RNA sample in a sterile PCR tube according to Table 2.26.

Table 2.26. Formulation of Genomic DNA Elimination Mixture for Reverse Transcription

Component	**Quantity**
Total RNA	5 µg
GE (5X gDNA Elimination Buffer)	2 µL
H_2O to a final volume of	10 µL

The contents of each reaction were gently mixed by pipetting followed by brief centrifugation of 15700 g for 30 seconds. Each reaction was incubated at 42°C for 5 min,

then immediately chilled on ice for one minute. The RT cocktail was prepared according to Table 2.27.

Table 2.27. Formulation of Reverse Transcription Cocktail

RT Cocktail	µL Per reaction
BC3 (5X RT Buffer 3)	4
P2 (Primer and External Control Mix)	1
RE3 (RT Enzyme Mix 3)	2
H_2O	3
Final Volume	10

Ten microlitres of RT Cocktail were added to each 10 µl Genomic DNA Elimination Mixture and mixed well by pipetting. The mixtures were incubated at 42°C for 15 minutes and then immediately at 95°C for 5 minutes to stop the reaction. cDNA was diluted 1:5 to 1:10 and stored at -20°C for downstream application.

2.8.3.3. RT-qPCR Apoptosis Arrays

The Human Apoptosis RT² Profiler PCR Arrays examine the expression of 84 key genes involved in apoptosis. The array is a collection of optimized qPCR primer assays in a 96-well plate format for apoptosis pathway focused genes. As well as the 84 genes involved in apoptosis, the array also contained primer sets for 5 housekeeping genes to normalize the array data. It contained a control for genomic DNA contamination by using a primer set that specifically detects non-transcribed genomic DNA with a high level of sensitivity. It contains 3 reverse transcription control wells to test the efficiency of the RT² First Strand Kit reaction with a primer set designed to detect template synthesized from the kit's built-in external RNA control. It contains 3 positive PCR controls to evaluate the efficiency of the PCR itself using an artificial DNA sequence and the primer set that detects it. The functional gene groups include:

A. **Genes involved in the induction of apoptosis:**

Death Domain Receptors: *CRADD, FADD, TNF, TNFRSF10B (DR5).*

DNA Damage: *ABL1, CIDEA, CIDEB, TP53, TP73.*

Extracellular Signals: *CFLAR (CASPER), DAPK1, TNFRSF25 (DR3).*

Other: *BAD, BAK1, BAX, BCL10, BCL2L11, BID, BIK, BNIP3, BNIP3L, CASP1 (ICE), CASP10 (MCH4), CASP14, CASP2, CASP3, CASP4, CASP6, CASP8, CD27 (TNFRSF7), CD70 (TNFSF7), CYCS, DFFA, DIABLO (SMAC), FAS (TNFRSF6), FASLG (TNFSF6), GADD45A, HRK, LTA (TNFB), NOD1 (CARD4), PYCARD (TMS1/ASC), TNFRSF10A, TNFRSF9, TNFSF10 (TRAIL), TNFSF8, TP53BP2, TRADD, TRAF3.*

B. **Anti-apoptosis genes**

AKT1, BAG1, BAG3, BAX, BCL2, BCL2A1 (Bfl-1/A1), BCL2L1 (BCL-X), BCL2L10, BCL2L2, BFAR, BIRC3 (c-IAP1), BIRC5, BIRC6, BNIP2, BNIP3, BNIP3L, BRAF, CD27 (TNFRSF7), CD40LG (TNFSF5), CFLAR (CASPER), DAPK1, FAS (TNFRSF6), HRK, IGF1R, IL10, MCL1, NAIP (BIRC1), NFKB1, NOL3, RIPK2, TNF, XIAP (BIRC4)

C. **Genes involved in the regulation of apoptosis**

Negative Regulation: *BAG1, BAG3, BCL10, BCL2, BCL2A1 (Bfl-1/A1), BCL2L1 (BCL-X), BCL2L10, BCL2L2, BFAR, BIRC2 (c-IAP2), BIRC3 (c-IAP1), BIRC6, BNIP2, BNIP3, BNIP3L, BRAF, CASP3, CD27 (TNFRSF7), CD40LG (TNFSF5), CFLAR (CASPER), CIDEA, DAPK1, DFFA, FAS (TNFRSF6), IGF1R, MCL1, NAIP (BIRC1), NOL3, TP53, TP73, XIAP (BIRC4).*

Positive Regulation: *ABL1, AKT1, BAD, BAK1, BAX, BCL2L11, BID, BIK, BNIP3, BNIP3L, CASP1 (ICE), CASP10 (MCH4), CASP14, CASP2, CASP4, CASP6, CASP8, CD40 (TNFRSF5), CD70 (TNFSF7), CIDEB, CRADD, FADD, FASLG (TNFSF6), HRK, LTA (TNFB), LTBR, NOD1 (CARD4), PYCARD (TMS1/ASC), RIPK2, TNF, TNFRSF10A, TNFRSF10B (DR5), TNFRSF25 (DR3), TNFRSF9, TNFSF10 (TRAIL), TNFSF8, TP53, TP53BP2, TRADD, TRAF2, TRAF3*

D. **DEATH Domain Proteins**

CRADD, DAPK1, FADD, TNFRSF10A, TNFRSF10B (DR5), TNFRSF11B, TNFRSF1A, TNFRSF1B, TNFRSF21, TNFRSF25 (DR3), TRADD

E. **Caspases and Regulators**

Caspases: *CASP1 (ICE), CASP10 (MCH4), CASP14, CASP2, CASP3, CASP4, CASP5, CASP6, CASP7, CASP8, CASP9, CFLAR (CASPER), CRADD, PYCARD (TMS1/ASC).*

Caspase Activators: *AIFM1 (PDCD8), APAF1, BAX, BCL2L10, CASP1 (ICE), CASP9, NOD1 (CARD4), PYCARD (TMS1/ASC), TNFRSF10A, TNFRSF10B (DR5), TP53.*

Caspase inhibitors: *CD27 (TNFRSF7), XIAP (BIRC4)*

The Human Apoptosis RT² Profiler PCR Arrays and RT^2 SYBR Green Mastermix were both obtained from Qiagen, Hilden, Germany.

For one RT-qPCR array the RT^2 SYBR Green Mastermix was briefly centrifuged for 10 - 15 seconds to bring the contents to the bottom of the tube. The PCR components were prepared in a 5 mL tube before transferring to a loading reservoir as described in Table 2.28.

Table 2.28. RT-qPCR Apoptosis Array Master Mix Formulation

Component	µL
2x RT^2 SYBR Green Mastermix	1350
cDNA synthesis reaction	102
RNase-free water	1248
Total volume	2700

Using a 12 channel pipette, 25 µL of the PCR component mix was dispensed into each well in the RT^2 Profiler PCR Array. The array was sealed with an optical adhesive film and centrifuged for 1 min at 1000 g at room temperature to remove air bubbles and placed in an ABI 7900HT RT-PCR System (Life Technologies Ltd, Paisley, UK).

2.8.3.4. RT-qPCR Apoptosis Assays

Genes that were substantially up or down regulated (> two fold) at 12 and 36 hours post dosing were examined further using separate RT² qPCR Assays which contained the same primers as the wells of the genes of interest of the Human Apoptosis RT² Profiler PCR Array. These assays were also performed on the clinical material. RT² qPCR Primer Assays for *TP53, BCL2A1, BCL2L10, BIRC3, HRK, CDKN1A* and housekeeping genes *GAPDH* and *HPRT1* were obtained along with RT² SYBR Green ROX qPCR Mastermix form Qiagen, Hilden, Germany.

The RT^2 SYBR Green Mastermix, RT^2 qPCR Primer Assay, and cDNA synthesis reaction were briefly centrifuged for 10 - 15 seconds to bring the contents to the bottom of the tubes. The PCR components mix was prepared in a 2 mL tube according to Table 2.29.

Table 2.29. RT-qPCR Individual Primer Assay Master Mix Formulation

Component	µL per one reaction
RT2 SYBR Green Mastermix	12.5
RT2 qPCR Primer Assay (10 µM stock)	1
RNase-free water	10.5
Total volume	24

The PCR Mastermix was aliquoted into wells on a 96 well plate and 1 µL cDNA was also added to the appropriate wells. The plate was centrifuged for 1 minute at 1000 g to remove bubbles and placed into an ABI 7900HT RT-PCR System.

2.8.3.5. Instrument set up for Human Apoptosis RT² Profiler PCR Arrays and RT² qPCR Primer Assays

The ABI 7900HT RT-PCR System was programmed for absolute quantification using the thermo cycle outlined in Table 2.30.

Table 2.30. Thermo Cycle Conditions for RT² Apoptosis Array and Individual Primer Assay RT-qPCR

Process	Temperature	Duration	Cycles
HotStart Taq activation	95°C	10 minutes	-
Fluorescence data collection	95°C 60°C	15 seconds 1 minute	50

2.8.3.6. RT-qPCR for E6 and E7

RT-qPCR for the HPV genes, *E6* and *E7*, was performed on a LightCycler carousel-based qPCR system using LightCycler DNA Master SYBR Green I reagent kits and LightCycler reaction capillary tubes (all Roche Applied Science, Mannheim, Germany). Ten microlitres of LightCycler® FastStart Enzyme were added to a full vial of defrosted LightCycler® FastStart Reaction Mix HybProbe to make the FastStart (FS) mix. *E6, E7, HPRT* and *TBP2* forward and reverse primers were obtained from Sigma-Aldrich, Dorset, UK. The FS mix was kept at 4 °C and the qPCR master mix was prepared on a cooling block according to Table 2.31.

Table 2.31. HPV Gene RT-qPCR Master Mix Formulation

	E6 primer pair	E7 primer pair	HPRT primer pair	TBP2 primer pair
Component	µL per 1 reaction			
Forward primer (5 µM)	2	2	2	2
Reverse primer (5 µM)	2	2	2	2
FS mix	2	2	2	2
$MgCl_2$ (25 mM)	1.6	2	1.6	2.4
Water	10.4	10	10.4	9.6
cDNA	2	2	2	2
Total	20	20	20	20

After the qPCR master mix and cDNA were aliquoted into the appropriate capillary tube, they were centrifuged at 1000 g for 5 seconds to bring the mix to the bottom. Water was used as a negative control and all runs included 1:100 CaSki cDNA (frozen communal stock, HPV research group, Cardiff University) in triplicate to serve as a positive control. RT negative control samples for each RT positive sample were also analysed to correct for undigested genomic DNA. The carousel was loaded and the LightCycler was programmed to the thermo cycle outlined in Table

Table 2.32. Thermo Cycle Conditions for HPV Gene RT-qPCR

Process	Temperature °C	Duration	Number of Cycles
Initial Denaturation	95	10 minutes	-
Denaturation	95	10 seconds	60
Primers anneal	60 for E6, HPRT and TBP 62 for E7	5 seconds	
Elongation	72	5 seconds	

2.8.3.7. Human Apoptosis RT² Profiler PCR Arrays, Individual RT² qPCR Primer Assays and HPV Gene RT-qPCR Data Analysis

For the RT² Profiler PCR Arrays and RT² qPCR Primer Assays the baseline for Ct values was defined by choosing the automated baseline option as the ABI 7900HT RT-PCR System SDS 2.4 software used had an adaptive baseline function. The threshold value was manually defined to 0.2, which lay above the background signal but within the lower one-third to lower one-half of the linear phase using the log view of the amplification plots. The CT values for all wells were exported to a blank Excel® spreadsheet for use with the SABiosciences PCR Array Data Analysis Web-based software. Dissociation curve analysis

was performed to verify PCR specificity by checking to see that only a single peak was found in each reaction.

The individual RT^2 qPCR Primer Assay data was analysed manually to obtain standard error of the mean (SEM) values for the replicate values. The delta delta CT (ΔΔCT) method was used to convert the absolute quantification to relative quantification (RQ) by normalizing to the housekeeping/reference genes. The method is outlined as follows;

a) The arithmetic mean of the housekeeping gene CT values was subtracted from the CT values of the treated and untreated target genes, giving a ΔCT value for each target (Equation 2.1);

$$\Delta CT = CT\,Target - CT\,reference$$

Equation 2.1. Delta Ct

b) The ΔCT values of the untreated samples were then subtracted from the ΔCT values of the corresponding treated samples giving a ΔΔCT value (Equation 2.2);

$$\Delta\Delta CT = \Delta CT\,treated - \Delta CT\,control$$

Equation 2.2. Delta Delta Ct

c) The ratio of gene expression change between the treated and untreated samples (relative expression) was derived by calculating the negative value of ΔΔCT as an exponent of 2. The value of 2 is used under the assumption that the product doubled in each cycle (Equation 2.3):

$$R = 2\text{^}(-\Delta\Delta CT)$$

Equation 2.3. Relative Quantification

The Human Apoptosis RT² Profiler PCR Array data was analysed using the SABioscience/Qiagen RT² Profiler PCR Array data analysis version 3.5 web-based software. This software used a derivative of the ΔΔCT method to calculate gene expression ratios. It first calculated the average ΔCT value by subtracting the average CT value of the housekeeping genes from the CT value of the gene of interest and then calculated the ratio of gene expression by calculating the negative value of the average ΔCT as an exponent of 2 (Equations 2.4 and 2.5).

$$Average\ \Delta CT\ =\ (\Delta CT\ (gene\ of\ interest)\ -\ Average\ CT\ (housekeeping\ genes))$$

Equation 2.4. SABioscience Average Delta Ct

$$R\ =\ 2\text{^}(-Average\ (\Delta CT))$$

Equation 2.5. SABioscience Ratio of Gene Expression

Relative expression of the HPV genes was calculated using qBase+ software (Biogazelle, Gent, Belgium). This software utilized the Vandesompele equation (Vandesompele et al., 2002) to correct for differences in PCR efficiencies between the genes examined. The Vandesompele equation is shown in Equation 2.6 below.

$$RQ = \frac{(E_{target})^{\Delta Ct_{target}\,(control-sample)}}{\sqrt[n]{\prod_{\emptyset}^{n}(E_{reference_{\emptyset}})^{\Delta Ct_{reference_{\emptyset}}\,(control-sample)}}}$$

Equation 2.6. Vandesompele Equation (Hellemans et al., 2007, Vandesompele et al., 2002)

E refers to the PCR efficiency, target refers to the target gene (E6 or E7), reference refers to housekeeping genes (TBP2 and HPRT), sample refers to sample of interest, control refers to CaSki, Ct refers to the crossing point, n is the number of reference genes.

The Vandesompele equation is a derivative of the Pfaffl equation (Pfaffl, 2001), where Pfaffl adjusted the ΔΔCT equation to correct for differences in PCR efficiency between a target gene and one housekeeping gene (Pfaffl, 2001, Hellemans et al., 2007). The Vandesompele equation allows for the correction of PCR efficiency differences between a target gene and more than one reference gene (Hellemans et al., 2007).

For each method used to calculate relative quantification, fold change values less than 1.0 were converted into their negative reciprocal values in order to demonstrate down-regulation of gene expression in a biological meaningful way on a histogram. This was termed fold regulation. If the fold change value was 1.0 or more the fold regulation value was the same as the fold change value.

2.8.4. RT-qPCR of RT3VIN Clinical Samples

RT3VIN, a multicentre phase II randomized Cancer Research UK clinical trial (trial number CRUK/06/024), aimed to assess the activity, safety and feasibility of topical formulations of Imiquimod and Cidofovir in 180 women with VIN3.

2.8.4.1. Ethics and Regulatory Approval

Ethical approval for the trial was obtained from the Office for Research Ethics Committees Northern Ireland (ORECNI) (08/NIR03/82). Regulatory approval was obtained from the Medicines and Healthcare Products Regulatory Agency (MHRA) under the Medicines for Human Use Regulations 2004 S.I 2004/1031 (reference number 21323/0020/001-0001). Approval was also obtained from the Research and Development offices at each of the 32 participating hospitals.

2.8.4.2. Study Population and Treatment Regime

Biopsies were collected from women with VIN3 prior to treatment, 6 weeks into treatment and approximately 6 weeks post treatment. Treatment lasted for a maximum of 24 weeks with patients self-applying either a 1% Cidofovir or a 5% Imiquimod cream three times a week.

2.8.4.3. HPV Testing

HPV testing of the RT3VIN samples was carried out by Sadie Jones of the HPV research group at Cardiff University, using HPV type 16 specific PCR, which targeted the *E6* region of the HPV genome. The samples were further examined for the presence of additional HPV types using a PapilloCheck detection kit from Greiner Bio-One, Frickenhausen, Germany.

3. Validation of Experimental Models and Method Development

The results presented in this chapter were obtained from experiments performed to validate and develop experimental models used for compound dosing and mechanism of action (MOA) studies.

3.1. Characterization of Clonal NHIST Cell Lines

For use in the dosing and MOA studies, the novel NHIST cell lines were evaluated in terms of phenotypic and molecular characteristics. The results in this subsection were derived and supplied by Tiffany Onions of the HPV Research Group at Cardiff University.

3.1.1. Initial Heterogeneous Cell Lines; PC08 and PC09

In a pilot study, two heterogeneous cell lines, PC08 and PC09, were derived from VIN3 and VaIN3 tissue biopsies respectively, by Dr Ned Powell of the HPV Research Group at Cardiff University. PC08 was cultured for 19 passages and PC09 was cultured for 21 passages. Early passage heterogeneous PC08 and PC09 cell lines were fastidious in culture, where initial cultures of passage 2 cell lines were highly contaminated with dermal fibroblasts that originated from the original biopsy tissue (Figure 3.1). As fibroblasts overpopulated both cultures quickly, restricting keratinocyte establishment and growth, they were discouraged by culture with irradiated 3T3 feeder cells and were removed by vigorous rinsing with PBS. Both cell lines grew efficiently when supplemented with irradiated 3T3 feeder cells. Photomicrographs of early passage PC09 cells can be seen in Figure 3.2. Keratinocyte colonies were generally round in shape and contained a population of tessellated polygonal keratinocytes as shown in Figure 3.3. Keratinocyte colonies grew outwards due to peripheral cell division, resulting in displacement of surrounding 3T3 feeder cells, forming a ridge on the outer edge of expanding keratinocyte colonies. This was also noticeable when expanding keratinocyte colonies in close proximity converged, which can be seen in Figure 3.4. Early passage (passage 2) heterogeneous PC08 and PC09 cell cultures contained two types of colony variants; type 1 colonies contained laterally growing keratinocyte cells forming ‘flat’ colonies; and type 2 colonies contained differentiating keratinocyte cells forming colonies that appeared to resemble ‘peaks’, as seen in Figure 3.5.

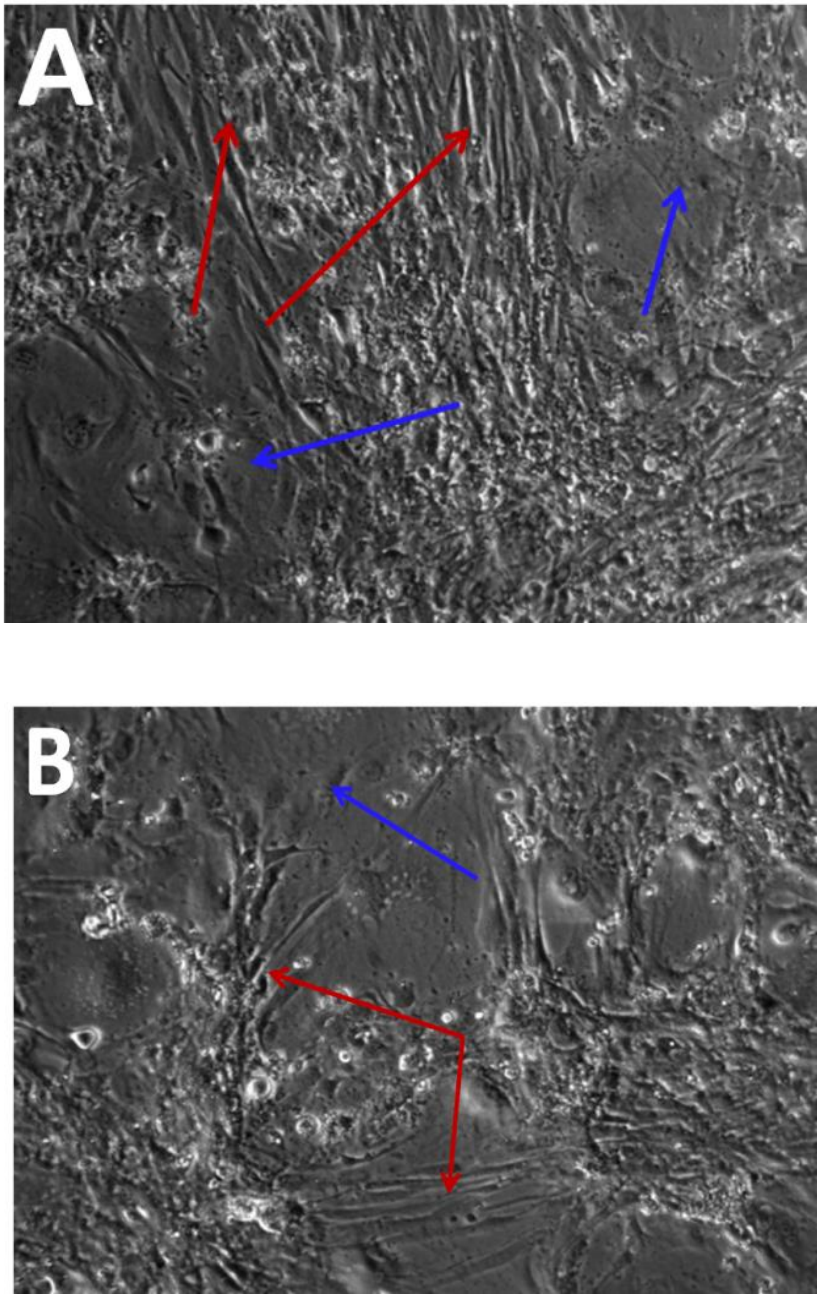

Images kindly provided by Tiffany Onions of the HPV Research Group, Cardiff University

Figure 3.1. Dermal Fibroblast Contamination of Passage 2 PC08 and PC09 Heterogeneous Cell Cultures

(A) Passage 2 PC09 cell culture in 6 cm tissue culture dish. (B) Passage 2 PC08 cell culture in 6 cm tissue culture dish. Both images were taken at 100X magnification. The cultures were comprised of 3T3 feeder cells (blue arrow), which had no characteristic cell shape, and fibroblasts (red arrow) which demonstrated elongated morphology.

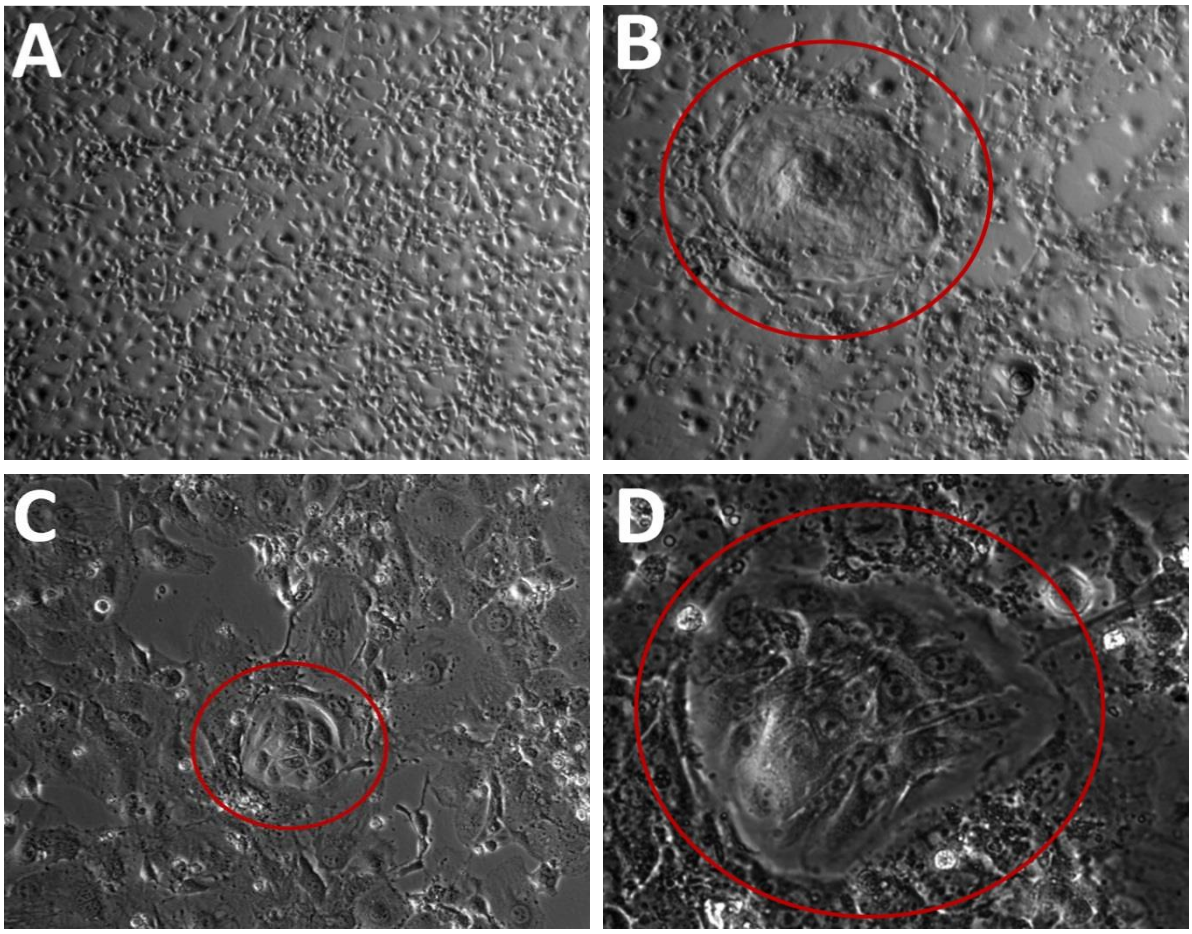

Images kindly provided by Tiffany Onions of the HPV Research Group, Cardiff University

Figure 3.2. Morphological Characteristics of Passage 2 PC09 and 3T3 Feeder Cells in Culture

(A) Irradiated 3T3 feeder cells were used to supplement keratinocyte cell cultures in a 6 cm tissue culture dish (50X magnification). (B) A roughly circular keratinocyte colony (red circle) surrounded by 3T3 feeder cells in a 6 cm tissue culture dish (50X magnification). (C) A keratinocyte colony (red circle) consisting of approximately 10 dividing keratinocyte cells with surrounding 3T3 feeder cells in a 6 cm tissue culture dish (100X magnification). (D) A keratinocyte colony (red circle) consisting of approximately 20 dividing keratinocytes with surrounding 3T3 feeder cells in 6 cm tissue culture dish (320X magnification).

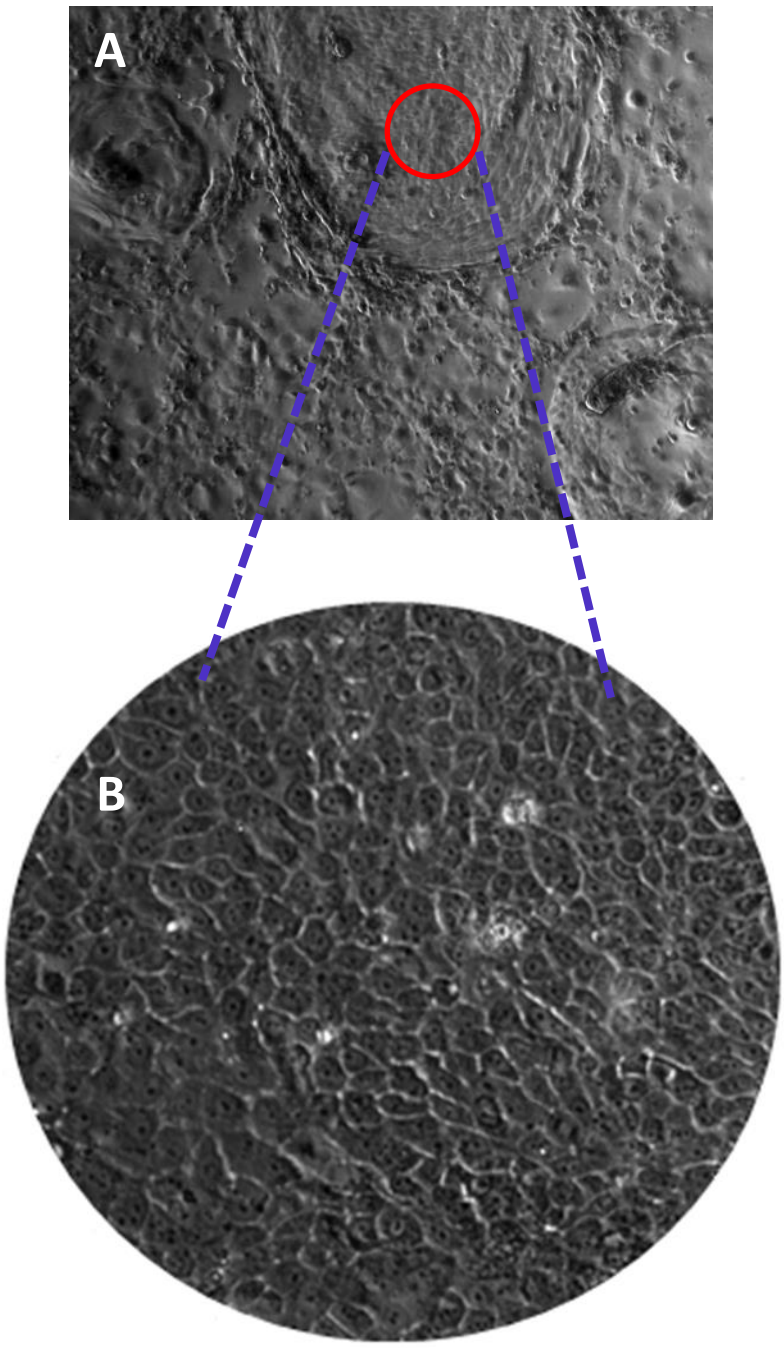

Images kindly provided by Tiffany Onions of the HPV Research Group, Cardiff University

Figure 3.3. Characteristic Morphology of Passage 2 PC09 Keratinocyte Cells

(A) Round keratinocyte colonies surrounded by 3T3 feeder cells in 6 cm tissue culture dish (50X magnification). The red circle highlights an area of laterally growing keratinocytes within a colony which has been magnified as shown in B. (B) Characteristic polygonal morphology and tessellating pattern of keratinocytes within a colony (100X magnification).

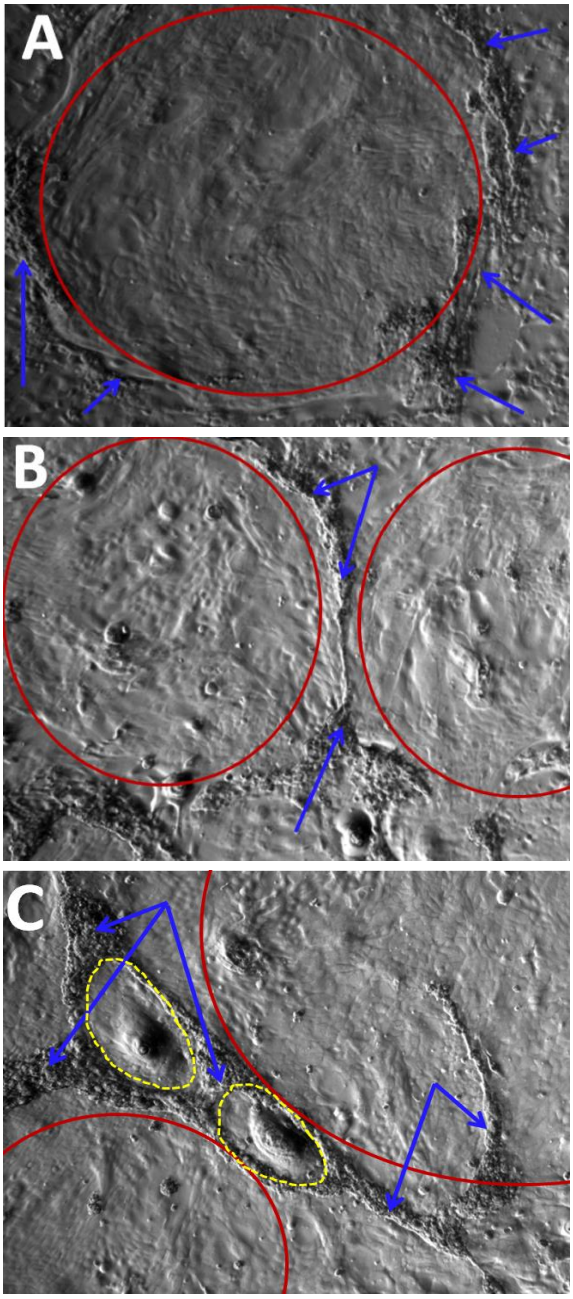

Images kindly provided by Tiffany Onions of the HPV Research Group, Cardiff University

Figure 3.4. Characteristics of 3T3 Feeder Cells Surrounding Expanding Keratinocyte Colonies in Passage 2 PC09 Cultures

(A) A keratinocyte colony containing lateral keratinocytes (red circle) (50X magnification). 3T3 feeder cells form a ridge (blue arrows) on the periphery of expanding keratinocyte colonies. (B) Convergence of two lateral keratinocyte colonies (red circles) forming a ridge of 3T3 feeder cells (blue arrows) (50X magnification). (C) Multiple converging keratinocyte colonies; two larger containing lateral keratinocytes (red circles); and two smaller containing differentiating keratinocytes resembling peaks (yellow circles) (50X magnification).

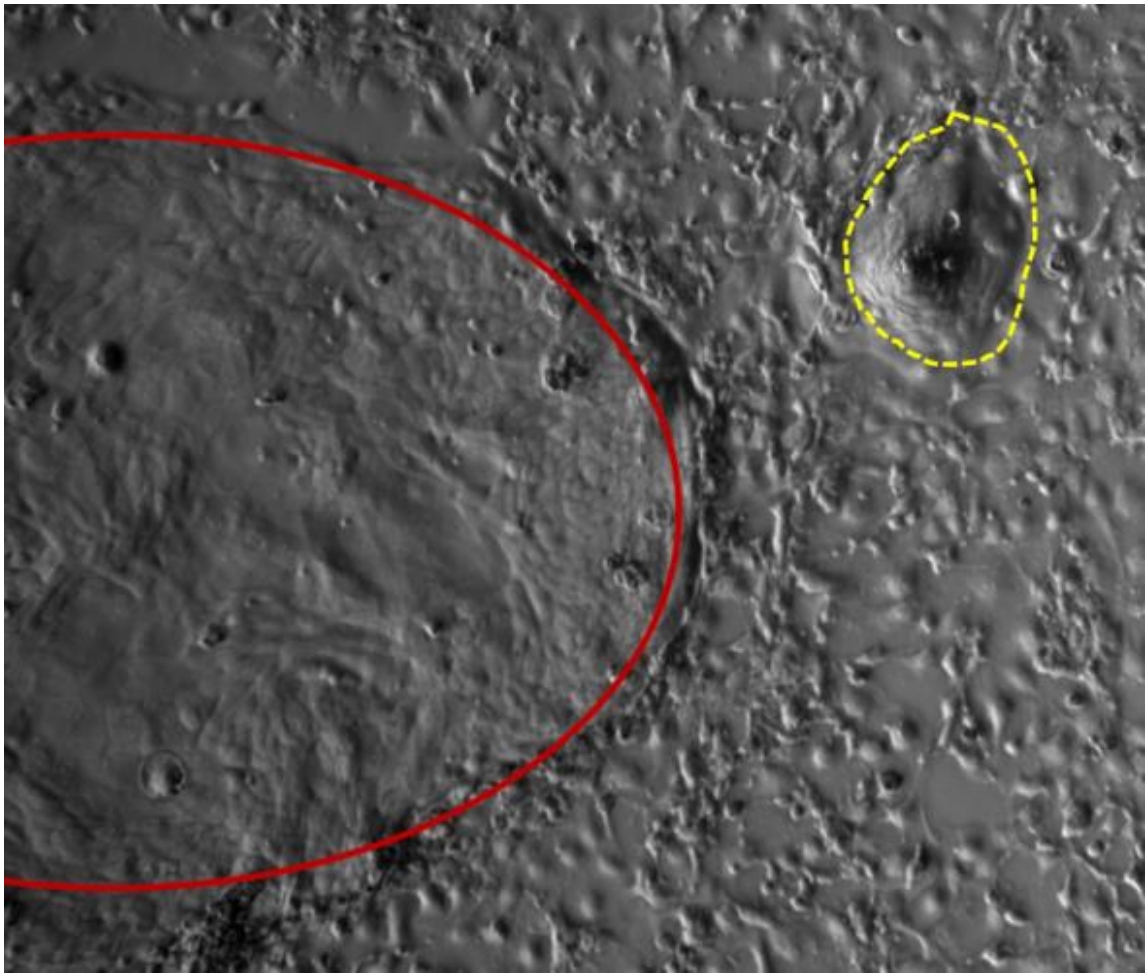

Image kindly provided by Tiffany Onions of the HPV Research Group, Cardiff University

Figure 3.5. Variation in Keratinocyte Colony Morphology in Passage 2 PC08 Cell Cultures

An example of type 1 (red circle) and type 2 (yellow circle) colonies identified in PC08 cultures in 6 cm tissue culture dishes. Type 1 colonies contained lateral keratinocytes that appeared 'flat' and were significantly larger than 'type 2' colonies, which contained differentiating keratinocytes, resembling peaks (50X magnification).

3.1.2. Monoclonal Cell Line Isolation

To produce monoclonal cell cultures, cryopreserved passage 1 PC08 and PC09 polyclonal cell lines were thawed and used to seed 6 cm tissue culture dishes supplemented with irradiated 3T3 feeder cells. To isolate clonal cells, passage 2 PC08 and PC09 cells were allowed to reach approximately 80% confluence before trypsinization and use in dilution cloning in 9 cm tissue culture dishes (in triplicate). Well dispersed keratinocyte colonies emanated on tissue culture dishes seeded with 103 cells (passage 3) and were chosen for ring cloning. Cells isolated within each ring were trypsinized and transferred to individual 6 cm tissue culture dishes resulting in individual clonal cell populations at passage 4. Twelve clonal cell lines were derived from both PC08 and PC09, where each clonal cell line was given a letter of identification and each letter was linked with the parental heterogeneous cell line. The clonal cell lines were referred to as A09 to L09 and M08 to X08. Ten clonal cell lines from PC09 and 3 clonal cell lines from PC08 survived primary isolation and were maintained in culture.

For this project one clone was selected from each parental heterogeneous cell line for use in the compound dosing and mechanism of action studies. M08 was chosen from the PC08 cell clones and A09 was chosen from the PC09 clones as they established and reached confluence most rapidly post primary isolation.

3.1.3. Morphology and Growth Characteristics of M08 and A09 Monoclonal Cell Lines

The morphology of M08 and A09 cells post initial isolation is shown in Figure 3.6. Both cell lines demonstrate small, tightly tessellating polygonal keratinocytes.

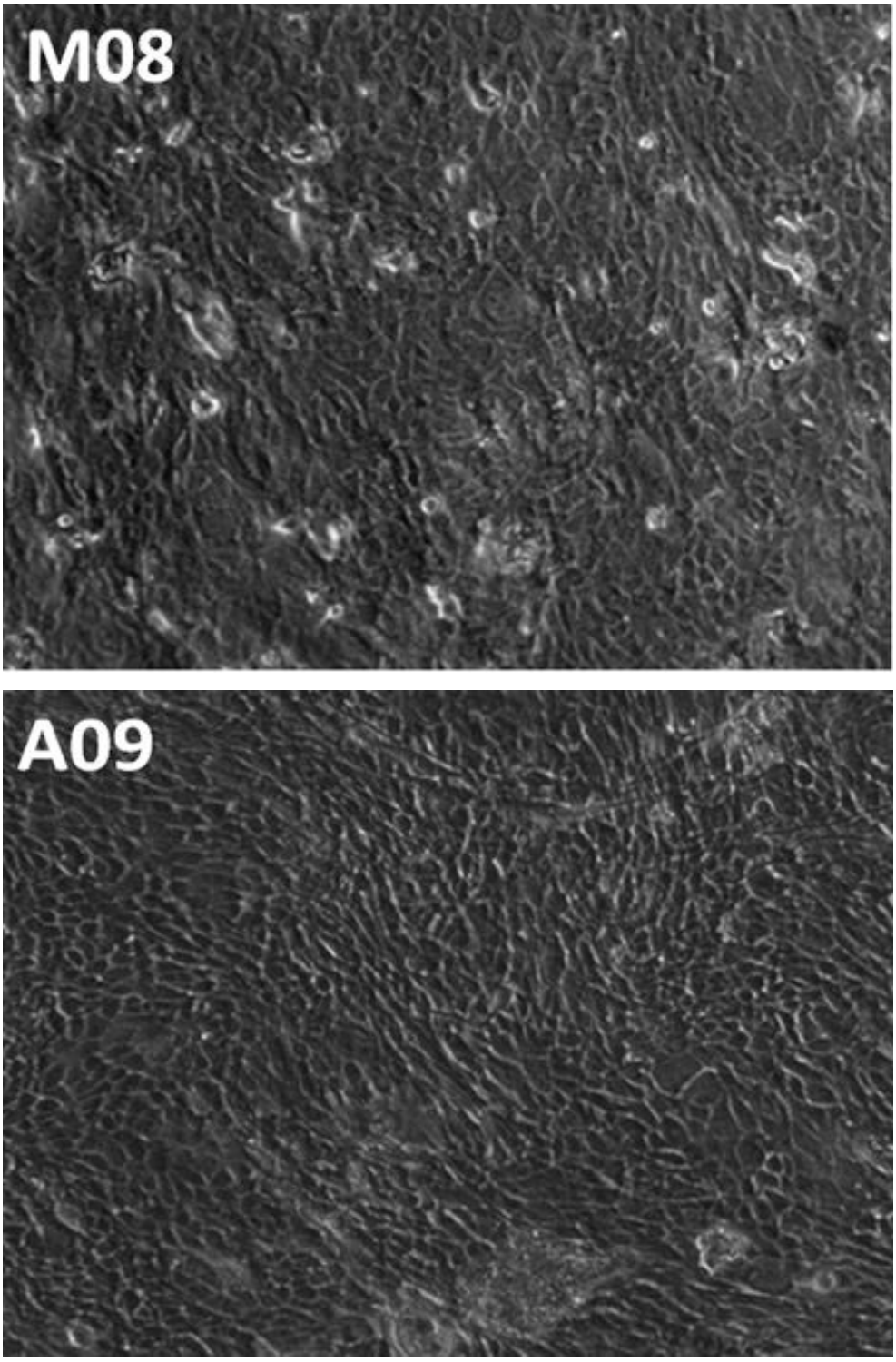

Images kindly provided by Tiffany Onions of the HPV Research Group, Cardiff University

Figure 3.6. Morphology of Clonal Cell Lines M08 and A09 at First Passage Post Isolation

Clonal cell lines were cultured in 6 cm tissue culture dishes and images taken at ~80% confluence (100X magnification). Initial cultures of M08 and A09 began at passage 4.

For preliminary phenotypic characterization, M08 was cultured for 5 passages post initial isolation, which lasted 63 days with an estimated 25.0 total number of population doublings (PD). A09 was cultured for 7 passages post initial isolation, which lasted 84 days and underwent an estimated 36.2 PD. The mean population doubling time (DT) was 1.69 days for M08 from passage 5 to passage 9; and 1.76 days for A09 from passage 5 to passage 11. This data is summarized in Table 3.1

Table 3.1. Growth Characteristics of M08 and A09 Clonal Cell Lines Post Initial Isolation

Clone	Short Term Culture (Passage)		Total Time in Culture (days)	Total PD	Mean DT (days)
	Start	Finish			
M08	5	9	63	25.0	1.69
A09	5	11	84	36.2	1.76

Data kindly provided by Tiffany Onions of the HPV Research Group, Cardiff University

M08 and A09 were selected for short-term culture (5 and 7 passages respectively). The table shows the total number of days in culture, the total calculated number of PD during this period and the calculated mean DT.

To demonstrate the difference in growth kinetics between M08 and A09, growth curves and corresponding photomicrographs are shown in Figure 3.7. When seeded at 5 x 10^5 cells in a 6 cm tissue culture dish M08 cells displayed a greater seeding efficiency when compared to A09 cells, where the cell count 12 hours post seeding was half of the initial seeding inoculum for A09 cells. Additionally, M08 cells appeared to grow more efficiently than A09 cells, which can be seen in the greater slope of the growth curve between 36 and 60 hours for M08 cells when compared to the same region of the growth curve for A09 cells in Figure 3.7 (A). The morphology of M08 cells 12 and 36 hours post seeding appeared to be typical polygonal with “cobblestone” effect. The morphology of A09 cells 12 and 36 hours post seeding appeared to be more striated and elongated with an almost fibroblast like effect.

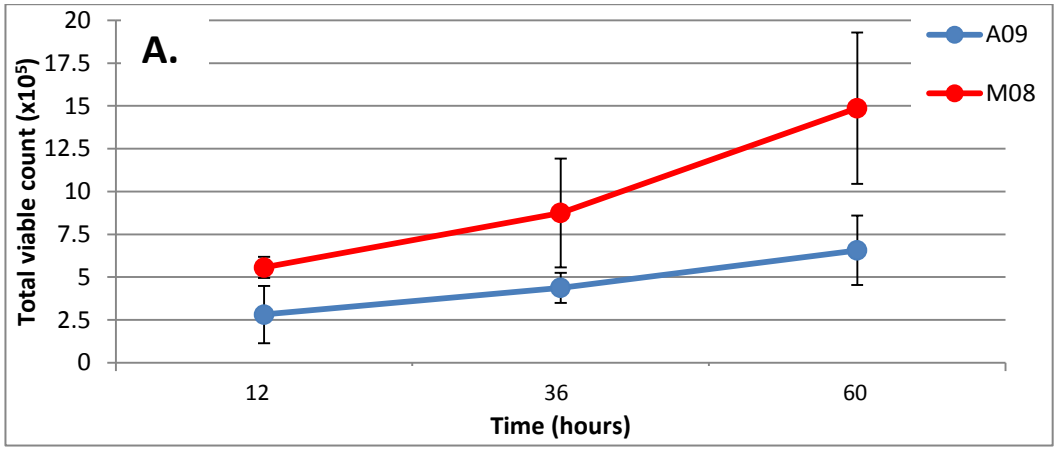

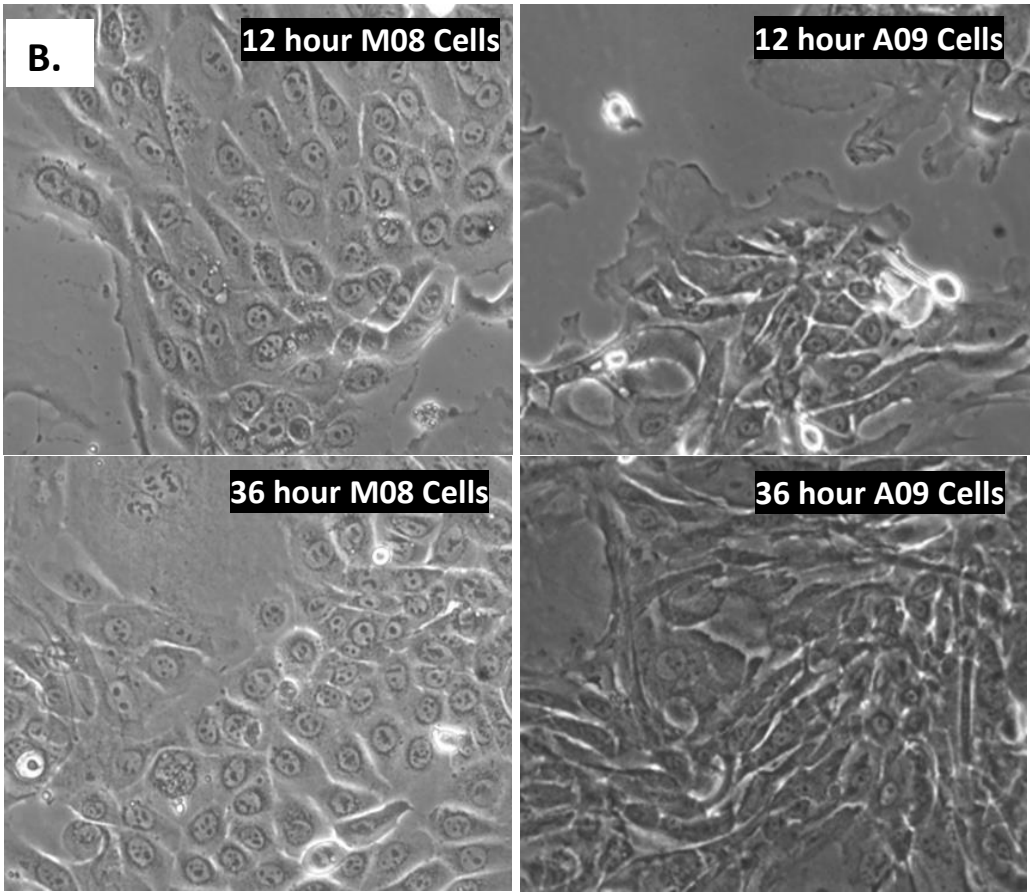

Images and data kindly provided by Tiffany Onions of the HPV Research Group, Cardiff University

Figure 3.7. Growth Kinetics and Morphology of M08 and A09 Cells

(A) Mean viable cell counts of passage 11 M08 and A09 cells 12, 36, and 60 hours post seeding at 5 x 10^5 cells in a 6 cm tissue culture dish. Data was calculated from triplicate cell counts of 2 separate experiments. Error bars = SEM. (B) M08 and A09 cell morphology 12 and 36 hours post initial seeding corresponding to growth curves in (A) (320X magnification). Note: For this experiment M08 cells were cultured further than initial passage 5 to passage 9 as descried in Table 3.1 to compare to A09 data.

3.1.4. HPV Gene Expression Profile of M08 and A09 Cell Lines

Relative quantification (RQ) of the HPV genes: *E2, E4, E5, E6* and *E7*, was assessed using RNA extracted from clonal cell lines at each passage during short-term culture. Expression of HPV genes was normalised to stable house-keeping genes *TBP2* and *HPRT*. Once calculated, the RQ of the HPV genes in the clonal cell lines was evaluated by comparing to CaSki cDNA as a standard. The RQ of *E2, E4, E5, E6* and *E7* in the M08 and A09 clonal cell lines over a range of passages is shown in Figure 3.8. mRNA for *E2, E4* and *E5* was undetectable in M08 cells, however, mRNA levels of *E6* and *E7* remained relatively constant with increasing passage number. All HPV gene transcripts were detected in the A09 cell line with stable expression values across all passages examined.

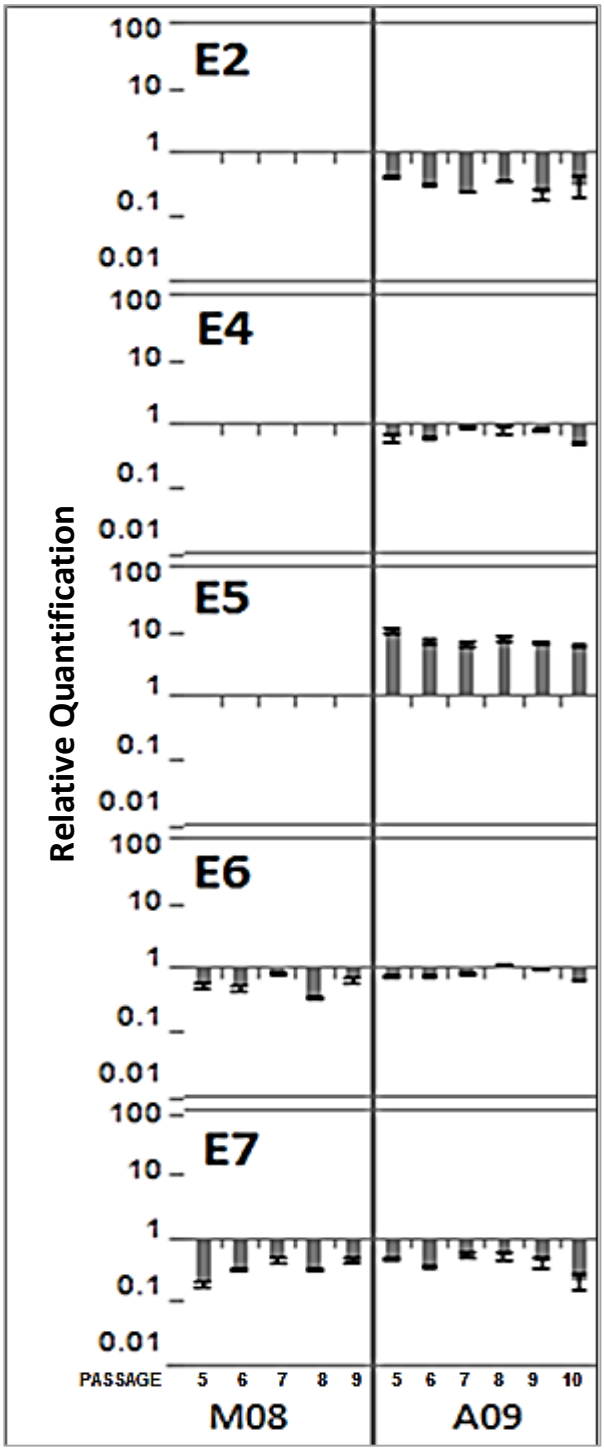

Data kindly provided by Tiffany Onions of the HPV Research Group, Cardiff University

Figure 3.8. *E2, E4, E5, E6*, and *E7* RQ during Short-Term Culture of M08 and A09 Cell Lines

HPV gene expression was investigated in passage 5 to 9 in M08 cells and passage 5 to 10 in A09 cells. Expression is relative to CaSki; a value of 1 indicates the same level of expression detected in the CaSki cell line. No data signifies that transcripts were not detected for a particular gene. Error bars signify SEM.

3.1.5. HPV DNA Integration Status of M08 and A09 Cells

The possibility of HPV DNA integration in M08 and A09 clonal cell line DNA was assessed using several different assays by Tiffany Onions of the HPV Research Group at Cardiff University. In the DIPS assay, adapters are ligated to common restriction endonuclease cut sites in the HPV and human genomes. A PCR step using adapter specific primers amplifies HPV:human DNA fusions (Luft et al., 2001). The APOT assay amplifies HPV mRNAs in order to detect and differentiate HPV:human fusion transcripts (Klaes et al., 1999). APOT and DIPS are complemented by *E2* PCRs, which are a series of overlapping PCRs that cover the entire *E2* gene (Collins et al., 2009). The assays were carried out on the first and last passage post initial clonal cell isolation for both cell lines (passage 5 and 9 for M08 and passage 5 and 11 for A09).

The results of these experiments indicated that A09 had a fully intact *E2* gene with no genomic disruption detected by DIPS. APOT data for the A09 cell line indicated an episomal transcript consisting of E7-E1 spliced to E4. On the other hand *E2* was not amplified in the M08 cell line suggesting a disruption in this gene. DIPS data for the M08 cell line indicated viral disruption at nucleotide 1194 of the HPV16 genome (E1 region) with antisense integration at locus 3q28, which was confirmed by APOT. These results were found in both passages examined for both cell lines.

These data indicate that HPV16 DNA is episomal in the A09 cell line and integrated in the M08 cell line. However, these results had not been conclusively confirmed by Southern blotting at the time of submission of this thesis.

3.2. Mycoplasma Testing

Mycoplasmas are the smallest free-living micro-organisms known (Taylor-Robinson and Bebear, 1997). They are parasitic prokaryotes that lack a true cell wall and are classed as mollicutes (Taylor-Robinson and Bebear, 1997). Mycoplasma contamination of cell culture is a common and serious problem as they can cause biochemical and metabolic changes in infected cell lines. Infection cannot be detected macroscopically or even with the aid of a normal light microscope. For this project mycoplasma detection was carried out using a Venor®GeM mycoplasma PCR detection kit, which uses PCR to test for mycoplasma DNA in the media of cell cultures. Mycoplasma monitoring of all cell types in culture within the HPV research group laboratory was carried out regularly (every 1 - 2 months). The M08, A09, 3T3 and HeLa cell lines remained mycoplasma free throughout the project. Infection of SiHa and C33A cell lines occurred at one point during the project and all stocks were replaced with new uncontaminated stocks obtained from the ATCC.

3.3. *TP53* Mutational Status of the NHIST Cell Lines

There is minimal selective pressure for mutation in the *TP53* gene in HPV associated gynaecological neoplasia due to the degradation of the p53 protein by E6; however, it was important to validate the exact *TP53* status of the HPV positive cell models used in the Cidofovir dosing studies as the central hypothesis was Cidofovir could reactivate a p53 response. The *TP53* gene of the M08 and A09 NHIST cell lines was sequenced according to "Detection of *TP53* mutations by direct sequencing" IARC protocol (IARC, 2010 Update). Briefly, 13 PCR reactions, with primer sets designed to target exons 2 to 11 of the *TP53* gene, were carried out on DNA from M08 and A09 cells. The PCR products were purified by gel band purification and sequenced in both directions. The resulting sequences were aligned with the *TP53* mRNA sequence NM_000546.4 and the *TP53* genomic reference sequence NC_000017.9. Any mismatches with the reference sequences were cross referenced to the IARC *TP53* Database (IARC, November 2012), which contains a compilation of *TP53* gene variations (both Single Nucleotide Polymorphisms (SNPs) and mutations) identified in human populations and tumour samples from peer-reviewed literature.

Out of 52 sequencing reactions (13 forward and reverse for both A09 and M08 DNA samples) 46 were successful. For the 6 reactions that failed, the corresponding opposite direction reactions were available and allowed sequence analysis of those particular regions/exons. The sequences (n = 46) were aligned with the mRNA reference sequence NM_000546.4. The possible SNPs/mutations from this step are outlined in Table 3.2. One mutation (c.670del1(C)) was present in both A09 and M08 DNA. This mutation was queried in the IARC *TP53* Database, which gave the results outlined in Table 3.3.

Table 3.2. Possible *TP53* gene SNPs/Mutations in A09 and M08 DNA

Sample	Primer	cDNA Number †	Exon Number
A09	P-326	c.215G>C ◊	4
	P-327	c.215G>C ◊	4
	P-239	c.674_675insG	6
	P-E11Re	c.1097G>T	11
	P-E11Re	c.1094del1(T)	11
	P-238	c.670del1(C)	6
	P-313	c.670del1(C) ◊	6
	P-333	c.670del1(C) ◊	6
M08	P-236	c.674_675insG	6
	P-238	c.670del1(C)	6
	P-313	c.670del1(C) ◊	6
	P-333	c.670del1(C) ◊	6

† c. denotes position on the mRNA (cDNA) reference sequence NM_000564.4. It is important to note that the sequences were searched against NM_000546.4 but the base positions used in the IARC TP53 database corresponded to NM_000546.1 which started 197 bases later than NM_000546.4. The above cDNA base positions are corrected by 197 nucleotides.

◊ This possible SNP/mutation was found in both the forward and reverse sequencing reactions

Table 3.3. IARC *TP53* Database Mutation Information for deletion c.670del1(C)

cDNA description	Protein Description	Exon Number	Effect	Somatic Count	Germline Count	Cell Line Count
c.670del1	-	6	Frame Shift	1	0	0

cDNA Description = Mutation nomenclature according to Human Genome Variation Society (HGVS) standards based on NM_000546.4 sequence. Protein Description = Mutation description at the protein level as recommended by HGVS and using the Uniprot reference sequence P04637. Exon Number = TP53 gene exon number. Effect = Effect of the mutation; Frame Shift changes the amino acid sequence from the site of the mutation. Somatic Count = Number of tumours reported to carry this somatic mutation. Germline Count = Number of tumours reported to carry this germline mutation. Cell Line Count = Number of cell lines reported to carry this mutation.

The c.670del1 mutation was a frame shift mutation in exon 6, which codes for part of the DNA binding region of the protein and according to the database was found once before in a somatic tumour. It appeared to be a rare mutation with possible significant effect on the translated protein. However, it was found in both A09 and M08 DNA. This raised concerns about possible contamination between the DNAs, although negative controls for the PCR reactions were negative and the initial electropherograms for these samples and primer sets appeared clean with single peaks at each base position. To check the consistency of these results, the process was repeated with a different extraction of A09 and M08 DNA using primer sets P-326/P-327 which flanked exon 4 and P-237/P-238 which flanked exon 6. The exon 4 primer set was used as a control as the SNP c.215G>C appeared specifically in the A09 sample in the initial sequences and not in the M08 sample (as can be seen in Table 3.2). On the repeat, negative controls were again negative indicating there was no contamination of the primers or reagents. This can be seen on the gel image of the purified PCR products in Figure 3.9.

The repeat sequences were identical to the initial sequences with c.670del1 appearing in both samples and c.215G>C only appearing in A09. The sequences which contained c.670del1 were aligned with mRNA reference sequences NM_000546 to NM_000546.5, but the deletion persisted to appear when aligned to each sequence. The sequences that contained c.670del1 were then re-aligned with the genomic reference sequence NC_000017.9 and the updated version, NC_000017.10, and 100% identities were found with no deletions. This result suggested a difference between the mRNA and gDNA reference sequences, which was confirmed by alignment of the mRNA reference sequence NM_000546.4 and the gDNA reference sequence NC_000017.9. This can be seen in Figure 3.10.

The remaining sequences with possible SNPs/mutations were realigned with the gDNA reference sequence, NC_000017.9. This filtered out several of the possible SNPs/mutations which were derived from alignment with the mRNA reference sequence only. Upon re-examination of the electropherograms of the remaining mismatches c.215G>C in sample A09 (P-326/P-327 for exon 4) was the only true mismatch. This SNP can be seen on sections of the electropherograms outlined in Figure 3.11.

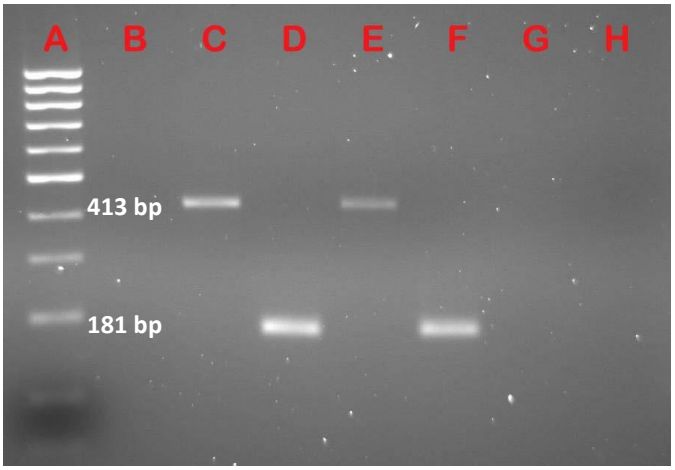

Lane	Content
A	100 bp Ladder
B	Blank lane
C	A09 primer set for Exon 4 (413 bp)
D	A09 primer set for Exon 6 (181 bp)
E	M08 primer set for Exon 4 (413 bp)
F	M08 primer set for Exon 6 (181 bp)
G	Negative control for Exon 4 PCR
H	Negative control for Exon 6 PCR

Figure 3.9. Gel Image of Purified Products of Repeat PCR for *TP53* Sequencing Primer Sets P-326/P-327 (Exon 4) and P-237/P-238 (Exon 6)

The repeat PCR on different DNA extractions produced the same results as the initial PCR ruling out contamination of DNA samples. The exon 4 primer set was used as a control as the SNP c.215G>C appeared specifically in the A09 sample in the initial sequences and not in the M08 sample, whereas, the frame shift deletion at cDNA position 670 appeared in both cell lines.

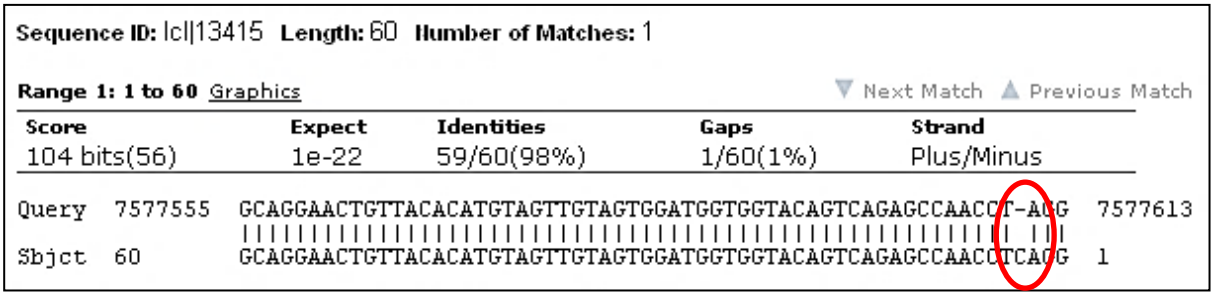

Figure 3.10. Alignment of genomic DNA Reference Sequence NC_000017.9 against 60 bases from the cDNA Reference Sequence NM_000546.4

In this figure the "Query" (top) sequence is the gDNA reference sequence NC_000017.9. The "Sbjct" (Subject – bottom) is 60 nucleotides taken from the mRNA reference sequence NM_000546.4 which contained the apparent deletion (circled in red).

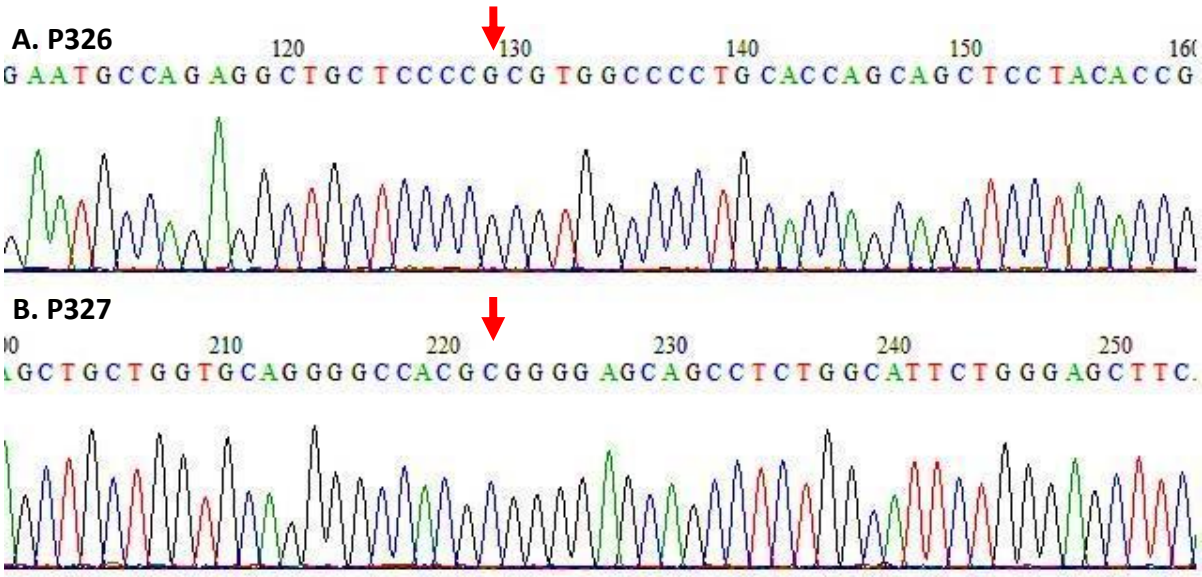

Figure 3.11. Electropherogram Sections with Forward (P-326) and Reverse (P-327) Primers for A09 DNA *TP53* Sequencing

Electropherograms showing sections of TP53 exon 4 DNA for the A09 cell line. The red arrows highlight the site of the SNP in both forward and reverse sections of DNA. Black G = Guanine; Blue C = Cytosine; Red T = Thymine; Green A = Adenine.

The single peak observed at the substitution site indicates homozygous substitution. The SNP, c.215G>C, was identified in the IARC *TP53* Database (Table 3.4). This SNP had an NCBI dbSNP link rs1042522.

Table 3.4. SNP information for c.215G>C as obtained from the IARC *TP53* Database

Primer	cDNA Description	Genomic DNA Description	Exon	Protein Description	Protein Domain	Effect
P-326 (forward) P-327 (reverse)	c.215G>C	g.7520197C>G	4	p.R72P	Proline Rich	Missense

cDNA description as per reference sequence NM_000546.4 corrected by 197 nucleotides; Genomic DNA description as per reference sequence NC_000017.9; Protein description as per reference sequence P04637; Protein domain is the domain in which the SNP occurs; This SNP occurs in the proline rich domain of the p53 protein; Effect is missense on the translated protein resulting in the substitution of a proline with an arginine amino acid at codon 72.

The data for c.215G>C / g.7520197C>G obtained from the linked Reference SNP Cluster Report, rs1042522, classed c.215G>C / g.7520197C>G as a single nucleotide variation (SNV) with the ancestral allele being C. Minor Allele Frequency (MAF) is defined as the second most frequent allele for a particular SNP using the current default global population, which is genotype data from 1094 worldwide individuals in the 1000 Genomes phase 1 project (1000Genomes, 2008 - 2012). For rs1042522 the MAF is G=0.398/869, which indicates that G has a frequency of 39.8%. This SNP results in the substitution of a proline with an arginine at position 72 of the p53 protein and is also referred to as Arg72Pro (Bojesen and Nordestgaard, 2008).

3.4. *E6* and *E7* Transcription Relative to Cell Confluence

Prior to the treatment of the NHIST cell lines with ANPs, it was necessary to examine any changes in oncogene expression of untreated cells in response to cell confluence. This was required to determine the appropriate duration of treatment and degree of confluence the cells should be allowed to reach before examination of oncogene transcription levels in response to treatment. The primary focus of this project was VIN, hence the NHIST vulval cell line, M08, was used for dosing optimization studies. In brief, the cells were cultured to reach confluences of 50%, 75%, 100% and 100% plus one week, and then RNA was extracted. The RNA was reverse transcribed and cDNA was subjected to RT-qPCR to examine *E6* and *E7* transcription levels.

Amplification curves for *E6* and *E7* at various M08 cell confluences are outlined in Figure 3.12 (A) and (B) respectively. *E6* and *E7* transcription levels corresponding to cell confluence in the M08 cell line are shown in Figure 3.12 (C). It can be seen that transcription of both oncogenes was relatively low at 50% confluence, but tripled and peaked at 75% confluence. At 100% confluence *E6* and *E7* transcript levels were similar to those of 75% confluence, but decreased following one week of culture at 100% confluence.

Statistical analyses on changes in RQ between different confluences are outlined in Table 3.5. A significant increase in RQ was observed between 50% and 100% confluence for both *E6* and *E7*. A significant decrease in *E6* RQ was also observed between 100% confluence and 100% confluence plus 1 week.

(A) *E6* Amplification Plot

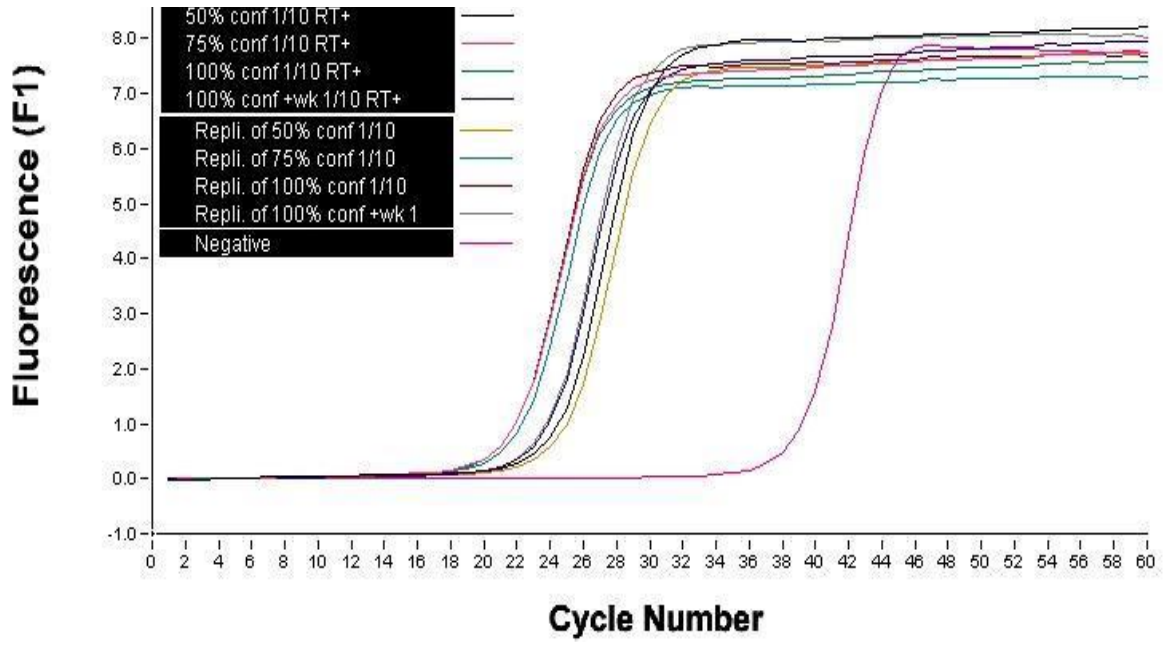

(B) *E7* Amplification Plot

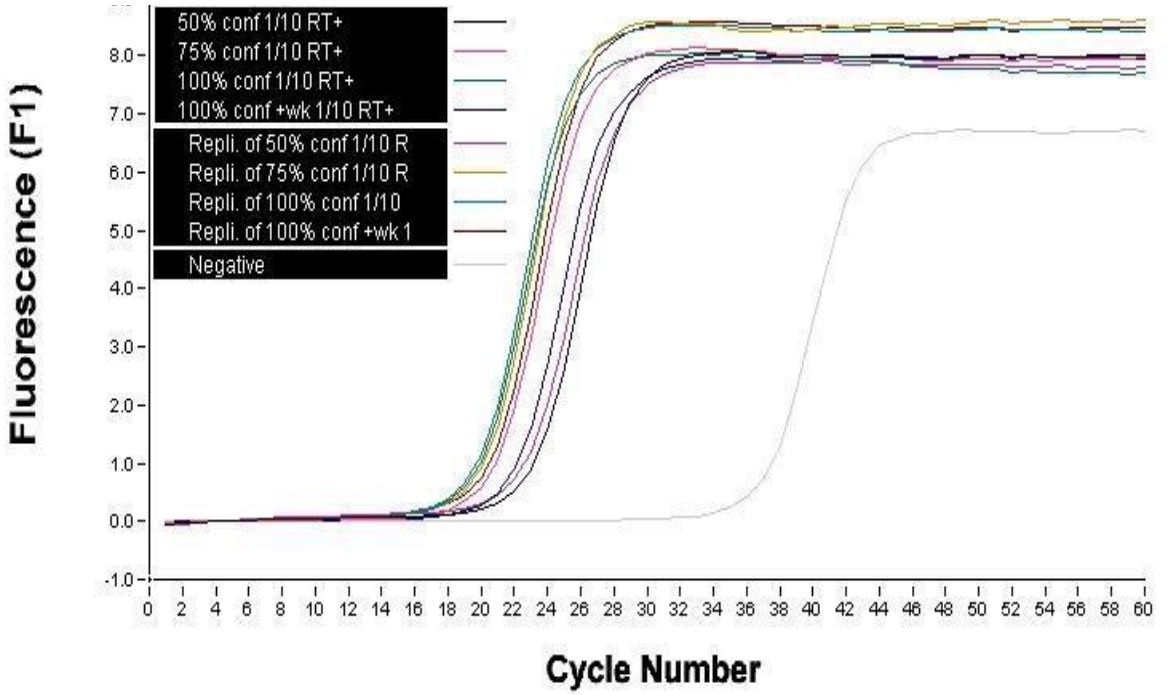

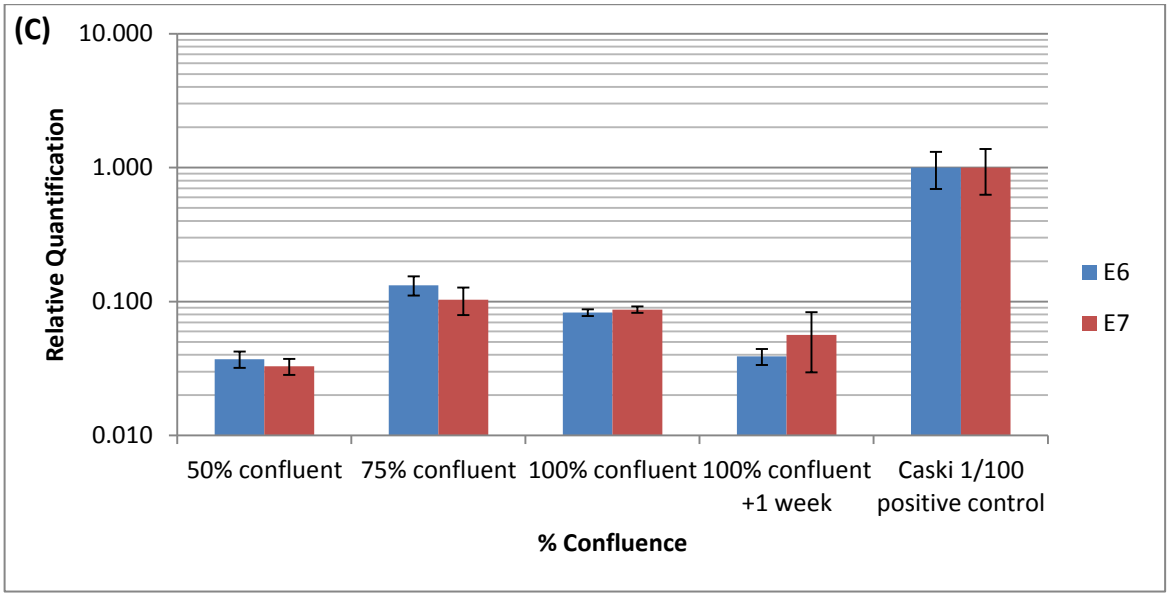

Figure 3.12. *E6* and *E7* RQ in M08 Cells at Various Degrees of Confluence

(A) Raw RT-qPCR amplification plot for E6 mRNA levels for M08 cells at 50%, 75%, 100% and 100% plus 1 week confluence including intra-experimental repeats and negative control (water). (B) Raw RT-qPCR amplification plot for E7 mRNA levels for M08 cells at 50%, 75%, 100% and 100% plus 1 week confluence including intra-experimental repeats and negative control (water). (C) E6 and E7 RQ for M08 cells at various degrees of confluence represented on a logarithmic scale. Transcript levels were calculated with Biogazelle qBase+ software using the Vandesompele equation (Vandesompele et al., 2002, Hellemans et al., 2007). E6 and E7 Ct values were normalized to housekeeping genes HPRT and TBP2. RQ values are the mean of duplicate inter-experimental repeats and error bars represent SEM. RQ values are presented on a logarithmic scale to compare with those of CaSki standard DNA (1/100 dilution).

Table 3.5. p-Values for *E6* and *E7* RQ differences between M08 Cell Confluences

	p-Values for *E6* RQ differences				**p-Values for *E7* RQ differences**			
Confluence	75%	100%	100% + 1 week	CaSki	75%	100%	100% + 1 week	CaSki
50%	0.052	0.023	0.804	0.093	0.104	0.017	0.490	0.139
75%		0.162	0.054	0.117		0.581	0.323	0.160
100%			0.025	0.104			0.376	0.155
100% + 1 week				0.094				0.146

Statistical analysis was carried out using GraphPad QuickCalcs software (GraphPad Software, Inc., California, USA). p-Values were calculated with 95% confidence intervals using a two-tailed unpaired t-test. For each confluence condition n = 2; for CaSki positive control standard n = 3. p < 0.05 indicates statistical significance (red text) and the difference in RQ levels between various conditions is unlikely to have occurred by chance. p > 0.05 indicates that the difference is not statistically significant (green text).

3.5. Culture of NHIST Cells with and without 3T3 Feeder Cells

Feeder cells are often used in the culture of primary human keratinocytes and short term cell lines to provide connective tissue factors to supplement and support keratinocyte proliferation and colony formation (Stanley and Parkinson, 1979). This study was carried out to examine if the NHIST cell lines could be cultured effectively without 3T3 feeder cells for use in the dosing studies. It was desirable to culture the NHIST cells in the absence of 3T3 feeder cells in the dosing experiments for several reasons. Firstly, it was unknown what effect the test compounds could have had on the feeder cells. Secondly, this would avoid the risk of contamination with feeder cell material during the downstream processing of NHIST cell material. Finally, the presence of feeder cells could skew viable NHIST cell counts. To examine this two identical inocula of 5×10^5 M08 cells were cultured separately with and without 3T3 feeder cells in 10 cm tissue culture plates. The two cultures were evaluated each day in terms of growth and morphology. After eight days, when both cultures had reached 80 – 100% confluence, RNA was extracted, reverse transcribed and subjected to RT-qPCR to quantify *E6* and *E7* transcripts.

E6 and *E7* transcript levels for M08 cells cultured with and without feeder cells are shown in Figure 3.13. Statistical analysis indicated *E6* and *E7* transcript levels in M08 cells grown in the absence of feeder cells were not significantly different to those in M08 cells grown with feeder cells (Table 3.6). Microscopic examination of the cultures suggested that cultures grown without 3T3 feeder cells initially grew more slowly than cells grown with feeder cells. Photomicrographs of M08 cells cultured with and without feeder cells for 6 and 8 days are shown in Figure 3.14. On day 6 cells cultured with feeder cells appeared more confluent and regularly shaped in comparison to those cultured without feeder cells. By day 8 both cultures were fully confluent; however, the cells cultured without feeder cells appeared to diversify into two morphologically distinct populations. One population resembled normal tightly packed tessellating polygonal keratinocytes with typical “cobblestone” appearance. The other population appeared irregular in morphology and exhibited large hypertrophic keratinocytes with a “fried egg” effect.

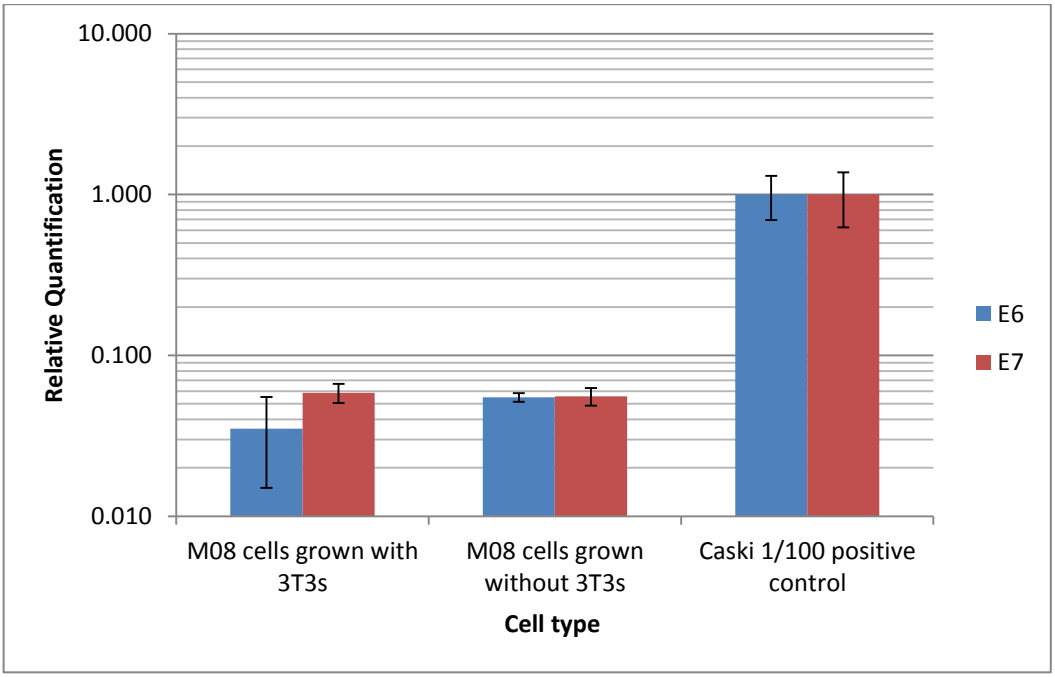

Figure 3.13. *E6* and *E7* RQ in M08 Cells cultured with and without 3T3 Feeder Cells for 8 Days

Transcript levels were calculated with Biogazelle qBase+ software using the Vandesompele equation (Vandesompele et al., 2002, Hellemans et al., 2007). E6 and E7 Ct values were first normalized to housekeeping genes HPRT and TBP2, then scaled to those of CaSki DNA standard (1/100 dilution) and presented on a logarithmic scale. RQ values are the mean of duplicate inter-experimental repeats and error bars represent SEM.

Table 3.6. p-Values for *E6* and *E7* RQ differences between M08 Cells cultured with and without 3T3 Feeder Cells

	E6	**E7**
p-Value	0.427	0.804

Statistical analysis was carried out using GraphPad QuickCalcs software (GraphPad Software, Inc., California, USA). p-Values were calculated with 95% confidence intervals using a two-tailed unpaired t-test. n = 2 for M08 cells cultured with 3T3 feeder cells and M08 cells cultured without 3T3 feeder cells after 8 days. p-Values > 0.05 indicate that the difference in both E6 and E7 RQ between M08 cells cultured with and without 3T3 feeder cells was not statistically significant.

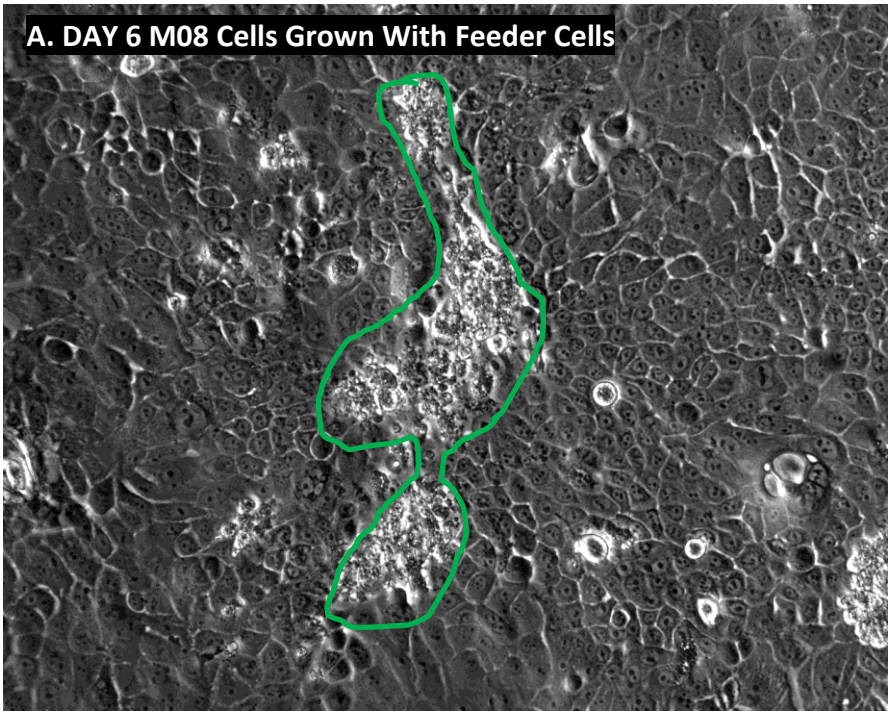
A. DAY 6 M08 Cells Grown With Feeder Cells

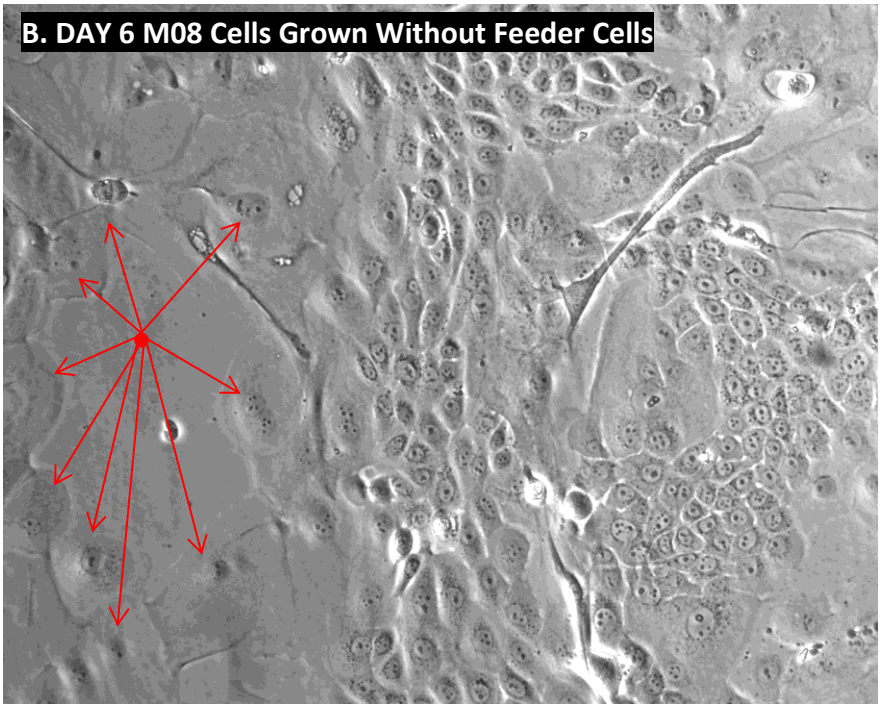
B. DAY 6 M08 Cells Grown Without Feeder Cells

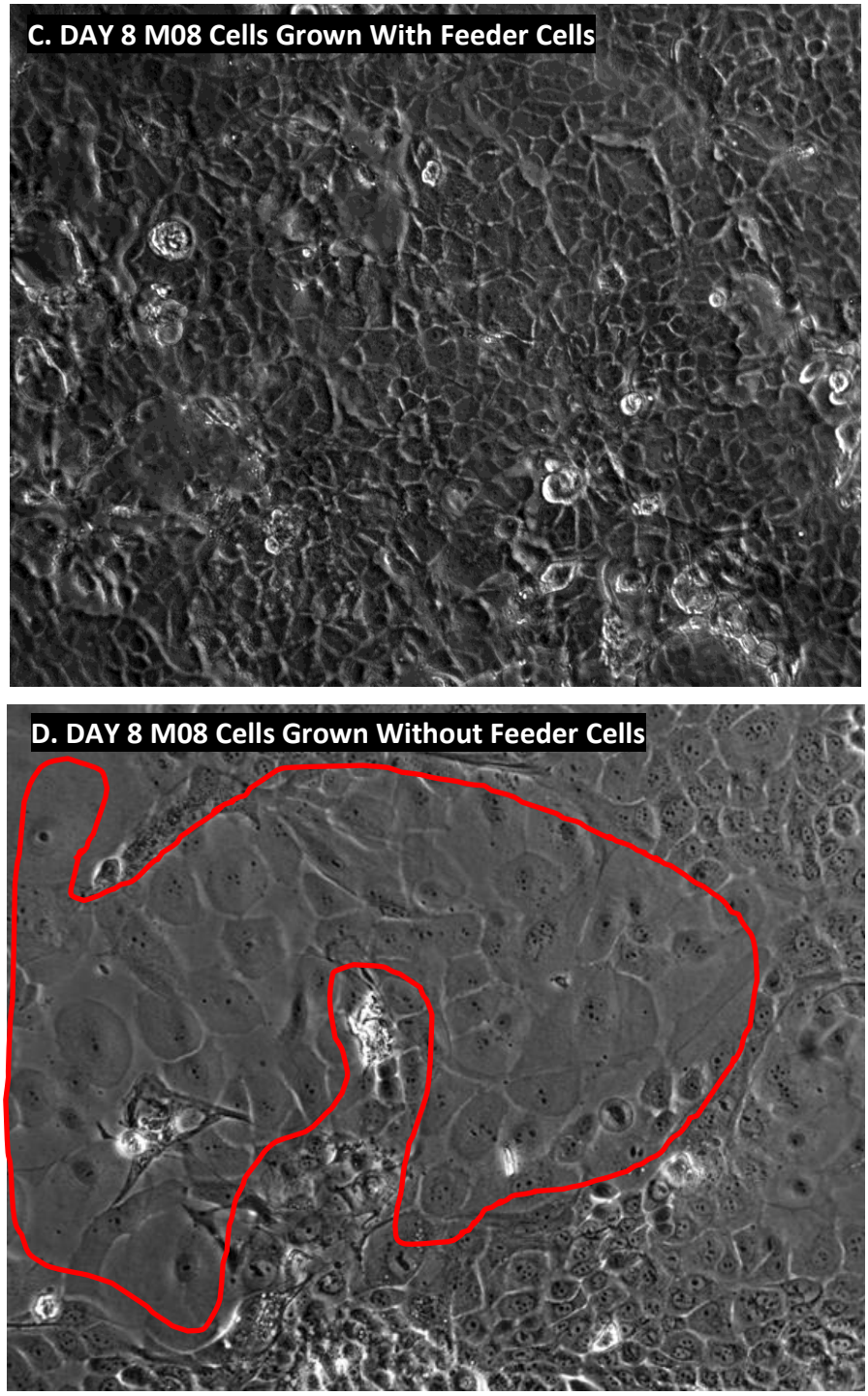

Figure 3.14. M08 Cells Cultured with and without 3T3 Feeder Cells for 6 and 8 Days

320X magnification using bright field light microscopy. (A) M08 cells on day 6 cultured in the presence of feeder cells, green line encloses a ridge of displaced feeder cells. (B) M08 cells on day 6 cultured in the absence of feeder cells, red arrows highlight atypical hypertrophic morphology. (C) M08 cells on day 8 cultured in the presence of feeder cells; feeders fully displaced. (D) M08 cells on day 8 cultured in the absence of feeder cells, red line encloses a second population of hypertrophic keratinocytes with "fried egg" effect.

3.6. Initial Inoculum of NHIST Cells for use in Dosing Studies

To use the NHIST cell lines without feeder cells in the dosing studies, seeding cell densities that would allow the cells to grow efficiently were determined. This was necessary as if the initial inoculum was too high, cells could become confluent before the end of the experiment, but if the initial inoculum was too low cells might not grow effectively. Three inocula were examined; 5,000, 7,000 and 10,000 M08 cells/well in 96 well plates. Cidofovir treatment of the M08 cell line was used to optimize the inocula. The cells were examined microscopically every day for 6 days and cell growth and morphology were assessed. On day 0 (after a 24 hour attachment period, when cells were treated with Cidofovir), day 3 and day 6 viability readings were recorded using the Trypan Blue dye exclusion method. Growth curves for the three initial cell densities are presented in Figure 3.15.

Each initial inoculum produced interpretable results with clear dose response relationships to Cidofovir concentration. The 7,000 and 10,000 initial cell inocula grew more effectively earlier (day 3) in comparison to the 5,000 cell inoculum; however, the untreated control cells were confluent by day 6 for these inocula. For the 5,000 cell inoculum, the untreated cells were not confluent by day 6.

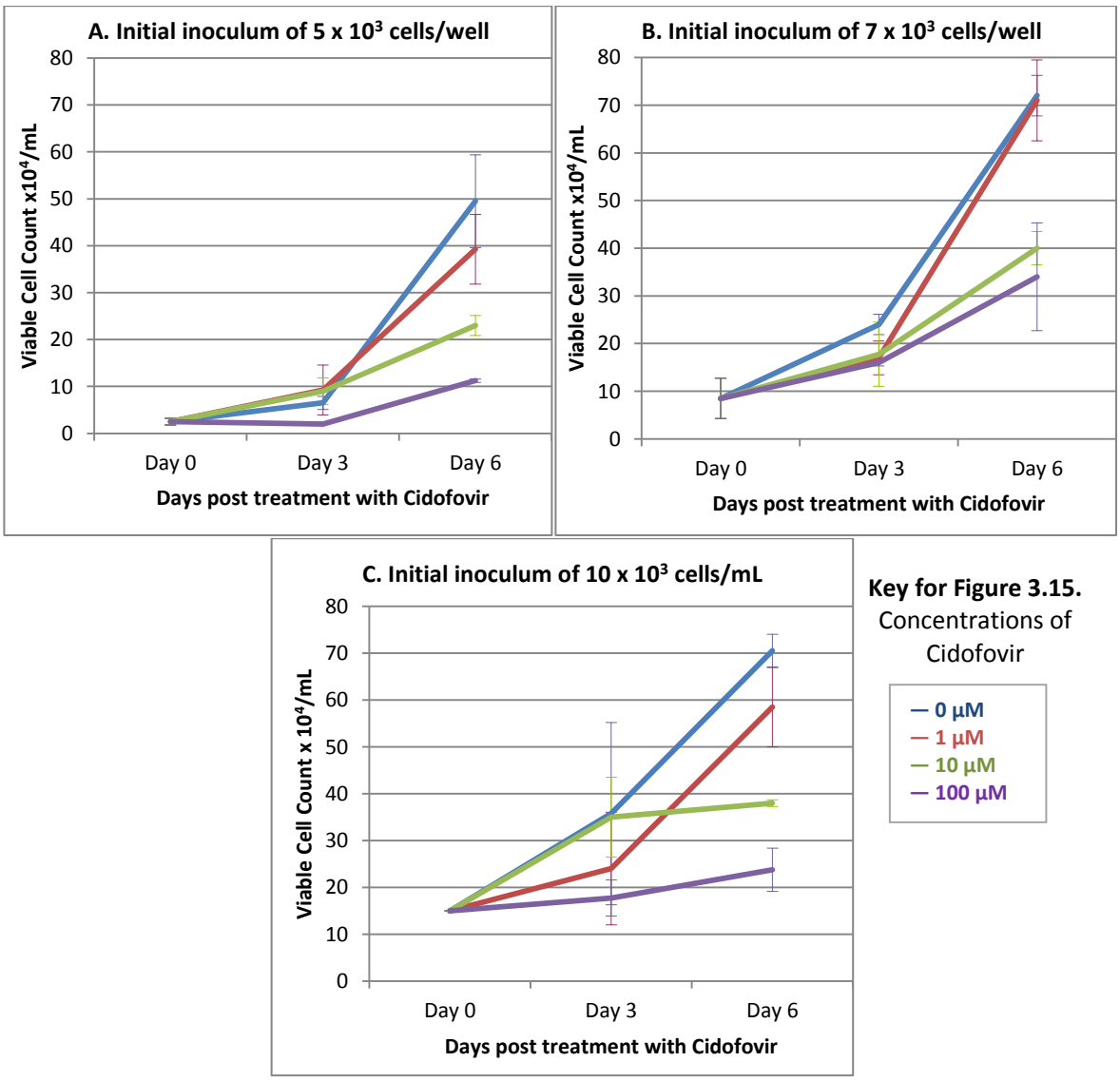

Figure 3.15. M08 Viable Cell Count per mL with Three Different Initial Cell Inocula

All cells were seeded in 96 well plates. Growth curves were constructed using viable cell counts that were obtained using Trypan blue manual counting 24 hours post seeding (Day 0); and 3 and 6 days thereafter. The growth curves show a dose dependant increase in viable cell number over the 6 day period. Initial inocula of 7,000 (B) and 10,000 (C) cells per well were better established by day 3; however, the untreated control samples were confluent by day 6 with these initial inocula. An initial inoculum of 5,000 cells per well (A) did not reach confluence by day 6. Error bars represent standard deviation of viable cell counts per mL for the mean of triplicate wells (each singular well was counted in duplicate).

3.7. Optimal Method of Assessment of Cell Viability

To determine the IC50 concentrations of the compounds in the various cell lines it was necessary to determine the number of viable cells following treatment. Three methods of assessing cell viability were employed; CellTiter 96® AQueous One MTS Solution Reagent (Promega, Southampton, UK), manual cell counting using the Trypan Blue dye exclusion method and automated cell counting using 7-AAD staining and flow cytometry. These methods were optimized using mycoplasma free SiHa cells as they were quick and easy to grow, unlike primary and NHIST cell lines that were of limited stocks.

Initially the CellTiter 96® AQueous One MTS Solution Reagent (Promega, Southampton, UK) was used to assess viability of cells treated with Cidofovir. However, increased absorbance (which the manufacturer markets as being proportional to viability) was consistently observed in cells treated with up to 30 µM Cidofovir compared to the untreated cells. However, when these cells were viewed microscopically they appeared less confluent than the untreated control cells. An example of this effect is shown in Figure 3.16. Figure 3.17 shows microscopic images complementary to Figure 3.16 (B).

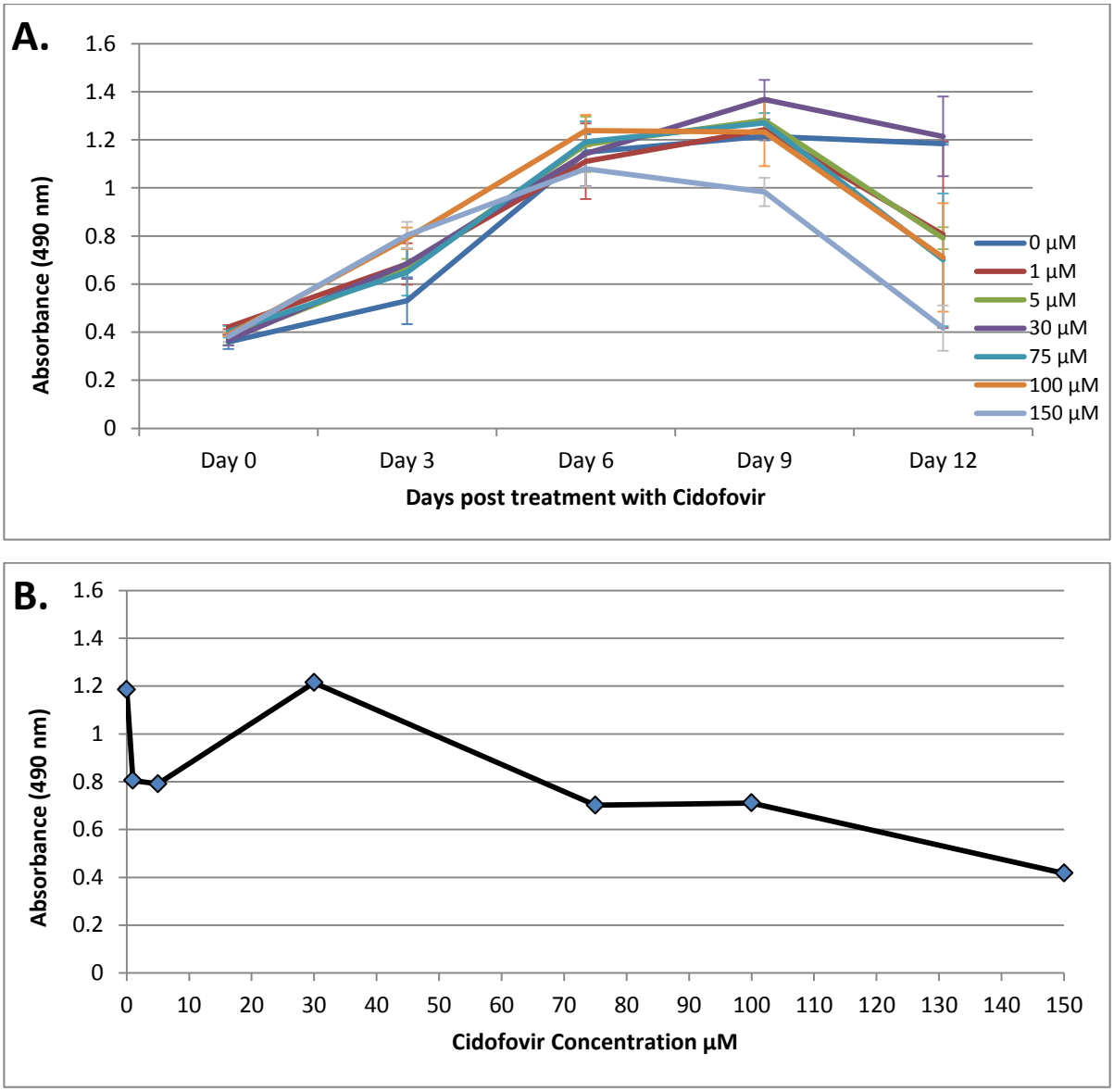

Figure 3.16. CellTiter 96® AQueous One MTS Solution Reagent Absorbance values for SiHa Cells Treated with Cidofovir

(A) Absorbance for untreated SiHa cells and SiHa cells treated with six concentrations of Cidofovir over a 12 day period. Absorbance for all samples peaked from day 6 to day 9 and decreased on day 12. (B) Absorbance of SiHa cells treated with various concentrations of Cidofovir on Day 9. A typical dose dependant decrease in absorbance was not observed and a peak in absorbance was found for 30 µM Cidofovir. Absorbance at 490 nm was read 3.5 hours after the addition of the CellTiter 96® AQueous One MTS Solution Reagent. The absorbance readings of the test wells were normalized to blank wells which contained culture media spiked with the relevant concentration of Cidofovir.

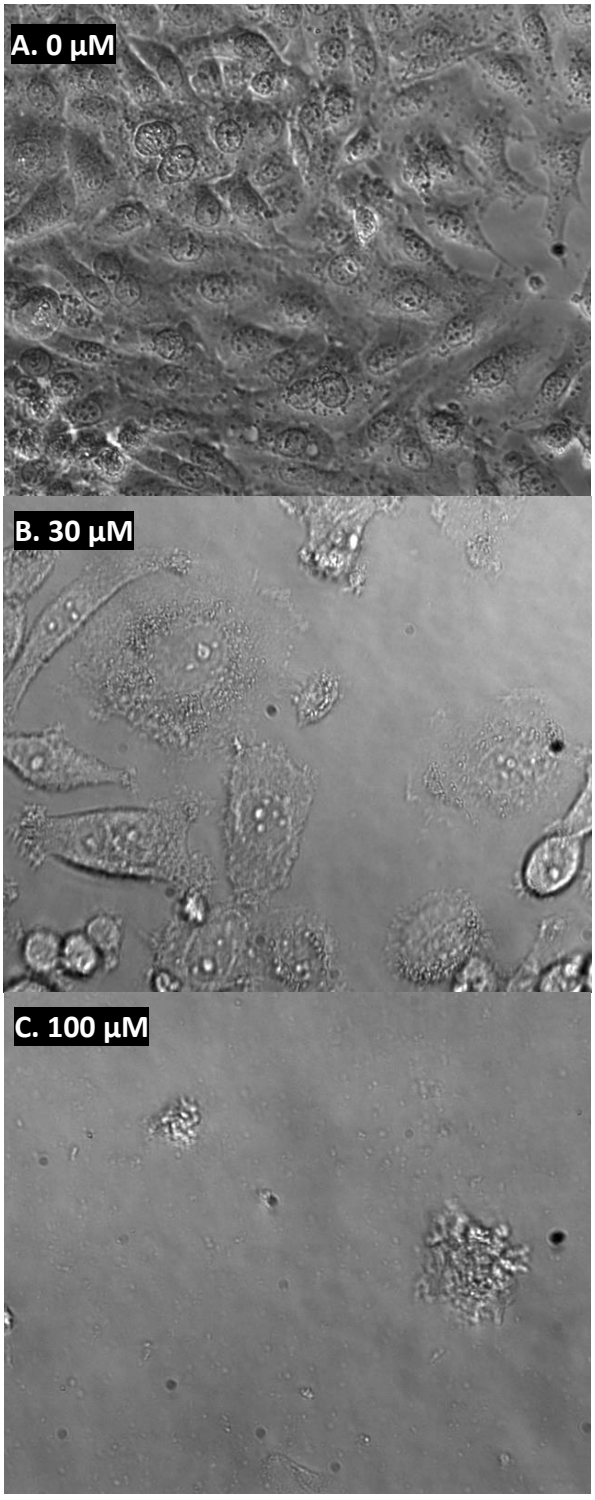

Figure 3.17. SiHa Cell Photomicrographs 9 Days post Treatment with Cidofovir

Photomicographs at 320X magnification using bright field light microscopy 9 days post treatment with Cidofovir equivalent to the absorbance trend line in Figure 3.16 (B). A = 0 µM Cidofovir (untreated), B = 30 µM Cidofovir, C = 100 µM Cidofovir. The figures show a decrease in live cell number with a corresponding increase in Cidofovir concentration, which was not found using the MTS reagent in Figure 3.16 (B).

The graphs of MTS absorbance (Figure 3.16) and photomicrographs (Figure 3.17) appear to show contradictory trends. To address this issue, viable cell counts were performed using an alternative method. SiHa cells were treated with Cidofovir for up to 6 days; on day 3 and day 6 cell viability was assessed using the Trypan Blue dye exclusion manual method of cell counting.

Figure 3.18 (A) shows SiHa cell viability obtained using the Trypan blue manual cell counting method. In contrast to the absorbance data obtained with the MTS reagent, the manual cell counting method displayed dose response consistent with Cidofovir concentration, and the data were constant with the results of microscopic analysis. It was therefore decided that cell counting was a more appropriate method of determining cell viability in comparison to the MTS method. However, due to the large number of compounds that needed to be assessed, in several different cell lines, in triplicate, it was decided that a higher throughput method was needed. Thus, automated cell counting using 7-AAD flow cytometry was used. The data obtained using automated cell counting with SiHa cells can be seen in Figure 3.18 (B.). Similar dose response trends were obtained using the manual and automated cell counting methods, hence it was decided to use automated cell counting using 7-AAD flow cytometry for the prodrug screen.

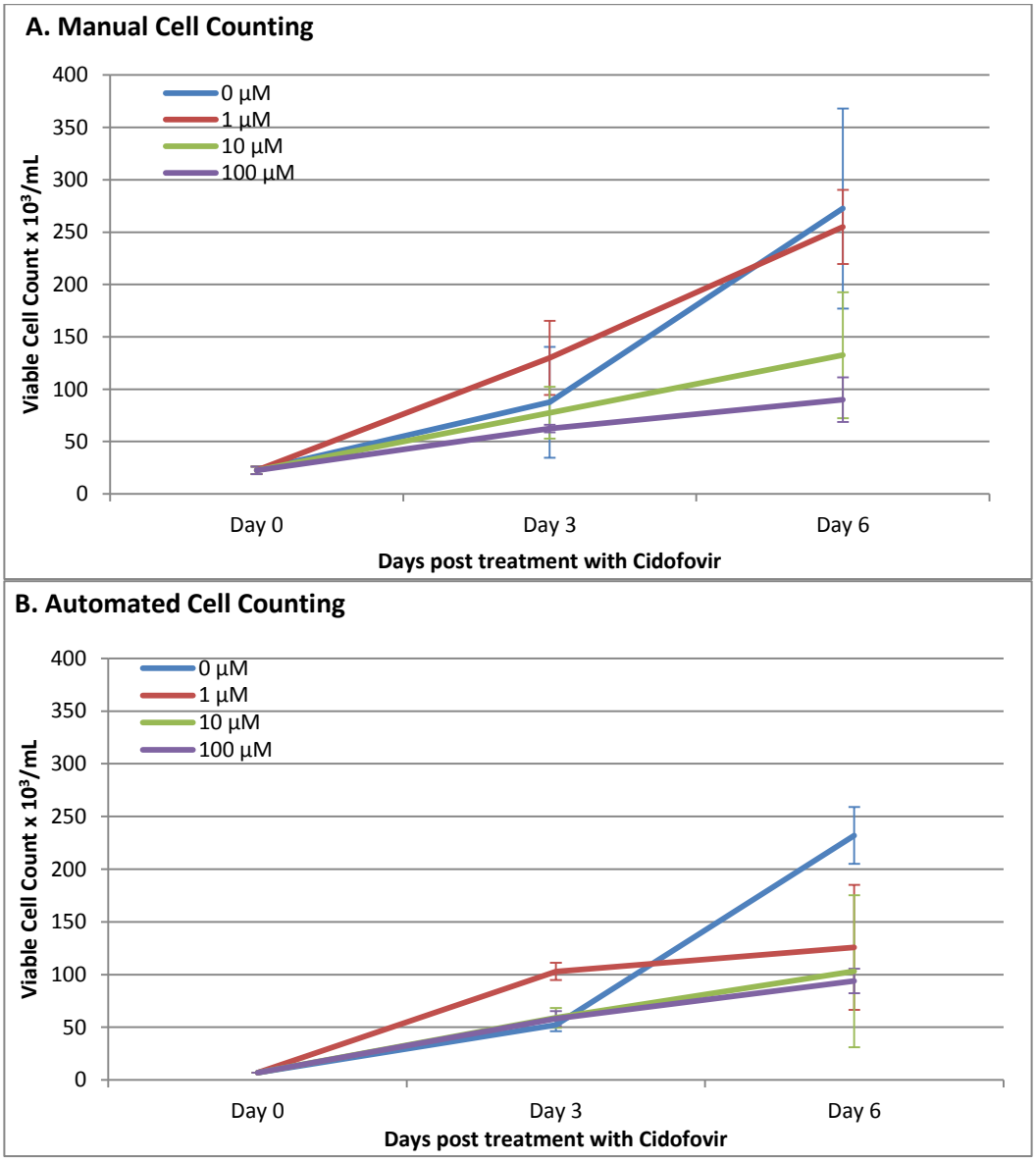

Figure 3.18. Two Methods of Cell Counting in SiHa Cells Following Cidofovir Treatment

(A) Number of SiHa viable cells per mL determined by Trypan blue dye exclusion manual cell counting (*B) Number of SiHa viable cells per mL determined by flow cytometry using 7-AAD automated cell counting. Viability readings were recorded at the time of Cidofovir treatment (Day 0) and 3 and 6 days thereafter. Error bars represent standard deviation of viable cell counts for the mean of triplicate wells. Both methods of cell counting showed similar trends in dose response of SiHa cells to three log concentrations of Cidofovir. Automated cell counting was chosen for future experiments as it allowed for the analysis of a greater volume of cells as well as allowing for analysis of other cellular characteristics in comparison to manual counting using Trypan blue staining.*

3.8. Discussion

Validation of the VIN and VaIN NHIST Clonal Cell Lines

A number of clonal cell lines were successfully isolated from heterogeneous cell lines, PC08 and PC09, which were derived from a VIN3 and a VaIN3 biopsy respectively. For use in the compound dosing and mechanism of action studies for this project the fastest growing clone from each parental heterogeneous cell line was selected. M08 was selected from the PC08 clones and A09 was selected from the PC09 clones. Both clones appeared to have similar tessellating polygonal morphologies with "cobblestone" effect post initial isolation from parental heterogeneous cell lines (Figure 3.6). However, with continued short term culture slight differences in their growth and morphological characteristics were observed. M08 had a greater seeding efficiency and growth rate when compared to A09 (Figure 3.7 (A)). Additionally, M08 had a slightly shorter mean doubling time of 1.69 days compared to 1.76 days for A09. At passage 11 A09 displayed a slightly elongated and striated morphology when compared to the prominent polygonal "cobblestone" morphology of M08 (Figure 3.7 (B)).

In terms of molecular characteristics, M08 cells did not express *E2, E4* and *E5;* however they did express *E6* and *E7* at a relatively stable level over 5 short term passages (Figure 3.8). A09 expressed *E2, E4, E5, E6* and *E7* at relatively stable levels over 6 short term passages (Figure 3.8). These data, together with the results of DIPS, APOT and *E2* PCRs, suggest that the M08 line contained integrated HPV16 only. The results of these assays indicated that A09 contained episomal HPV16 only; however, these results had not been conclusively confirmed by Southern blotting at the time of submission of this thesis.

Mycoplasma Status of Cell Lines

Mycoplasma testing of the cell lines was carried out regularly (every 1 to 2 months) during the project. If a positive result was found for a particular cell line, a new stock was obtained from the ATCC and all contaminated stocks were removed from liquid nitrogen storage. The NHIST cell lines derived from the VIN and VaIN biopsies did not test positive for mycoplasma. Stringent aseptic technique was employed during cell culture. As the main focus of this project was to evaluate nucleoside analogue drugs in cell lines,

mycoplasma testing was particularly important as mycoplasma infection can affect the metabolism of these analogues by interfering with their phosphorylation. Bronckaers et al., 2008 , found that several pyrimidine nucleoside analogues, including 5-trifluorothymidine (TFT), 5-fluoro-2'-deoxyuridine (FdUrd) and 5-halogenated 2'-deoxyuridines are susceptible to degradation to their inactive base forms by Mycoplasma hyorhinis encoded thymidine phosphorylase in MCF-7 breast carcinoma cells. The mycoplasma encoded enzyme dramatically reduced the cytostatic activity of the compounds causing a reduction in the formation of active metabolites and/or reduced drug incorporation into nucleic acids in infected cells compared with uninfected cells. Consequently, routine mycoplasma testing was essential to ensure all cell lines used in the dosing and mechanism of action studies were mycoplasma free.

TP53 Mutational Status of the NHIST Cell Lines

TP53 sequencing indicated that the coding regions, exons 2 – 11, of *TP53* in M08 and A09 cell lines were wild type and not mutated. This result was consistent with the lack of selective pressure for mutation in *TP53* in HPV positive cells. An SNV, c.215G>C/g.7520197C>G or Arg72Pro, was found in exon 4 of the A09 DNA and had a frequency of 39.8% in a sample of global population.

Although 6 out of 52 sequencing reactions failed, there were still the alternative direction sequences for those samples and upon examination of the singular sequences aligned to the reference sequences no mismatches were found. Additionally, Arg72Pro was found in both forward and reverse sequencing reactions in both the initial PCR product and the repeat PCR product, which used independently extracted DNA. Although the majority of *TP53* mutations are found within exons 5 - 8, IARC recommended screening of at least exons 4–10, including the splice junctions, so that less than 1% of mutations may be missed, which was why this protocol was chosen to evaluate the M08 and A09 samples.

During the DNA sequence analysis inconsistencies were found within the IARC *TP53* Database and between the gDNA and mRNA (cDNA) reference sequences. The nucleotide numbering of cDNA positions in the IARC *TP53* Database was 197 bases too high, which could lead to erroneous interpretations of possible SNPs/mutations. A difference was also

observed between the gDNA exon reference sequence and the mRNA reference sequence. The deletion which highlighted this non-conformance, c.670del1 (numbered from the 197 nucleotide corrected mRNA reference sequence NM_000546.4), is a rare somatic frame shift mutation which was unlikely to have occurred in cell lines derived from two individual patients led to further analysis. Upon comparison of the mRNA and gDNA reference sequences the mRNA reference sequence was found to have an extra base. As it is likely that *TP53* is sequenced more frequently from gDNA rather than mRNA/cDNA, and because the *TP53* gene was sequenced from gDNA in this study, the gDNA reference sequence was used in the bioinformatic analysis.

Published data regarding the *TP53* polymorphism at codon 72 (rs1042522) is contradictory. Functional differences between the Arg72 and Pro72 variants have been reported. The Arg72 variant was found to induce apoptosis more effectively than the Pro72 variant (Dumont et al., 2003), whereas, the Pro72 variant was found to be more efficient at activating p53 dependent DNA-repair genes (Siddique and Sabapathy, 2006).

A significant increase in the Arg72 variant with increase in latitude has been shown, although the selective pressure maintaining this gradient is unknown (Beckman et al., 1994). With regards to HPV and gynaecological disease, one particular study by Storey et al., 1998 , found that E6 proteins from both high-risk and low-risk HPV types are more efficient at targeting the p53 Arg72 variant for ubiquitin-mediated degradation compared with the Pro72 variant. Additionally, through a PCR and sequencing based assay, they found a high prevalence of the homozygote Arg72 variant in patients with cervical tumours (n = 30, material derived from frozen paraffin embedded samples) compared with healthy individuals (n = 41, material derived from whole blood), of whom the majority were heterozygous. They estimated that individuals homozygous for Arg72 were 7 times more susceptible to HPV associated tumorigenesis than heterozygote individuals (Storey et al., 1998). However another study by Rosenthal et al., 2000 , designed to evaluate the correlation between the *TP53* codon 72 polymorphism and HPV-associated neoplasia outside the cervix, observed a lower frequency of homozygote individuals for the Arg72 variant in HPV-associated vulval cancer (n = 52) and VIN (n = 48) patients than in healthy controls (n = 246) and suggested that Arg72 homozygote individuals had a lower

risk of developing vulval neoplasia, compared with heterozygote or Pro72 homozygote woman. This study also used material from paraffin embedded tissue for the disease cohort, blood samples from the healthy cohort and PCR analysis (Rosenthal et al., 2000). In 2009, however, a meta-analysis of 49 individual studies estimated odds ratios using logistic regression, stratification by study and ethnic origin for individual data sets (Klug et al., 2009). Subgroup analyses for infection with HPV, material used to determine *TP53* genotype, racial background, study quality and Hardy–Weinberg equilibrium were also performed. This demonstrated that the frequency of the arginine allele in women with invasive cancer was most likely due to errors in study methods not clinical or biological factors. When the analysis was confined to methodologically sound studies no connection was found between cervical cancer and *TP53* codon 72 polymorphism (Klug et al., 2009).

To conclude, there is diverse literature concerning the association of the *TP53* rs1042522 SNP with various HPV positive and negative neoplasias. As this study only examined two HPV positive gynaecological samples, with one being homozygous for proline at codon 72 and the other homozygous for arginine at codon 72, no conclusions can be made as to the prevalence and functional significance of rs1042522 in women with HPV associated gynaecological neoplasia. The final conclusion for this section of work was that both the M08 and A09 cell lines used in the Cidofovir dosing experiments were wild type for *TP53.* Hence they are appropriate models in which to investigate the hypotheses that Cidofovir can reactive a p53 response.

Future work might include determining the prevalence of the codon 72 SNP in the RT3VIN cohort and correlating this with treatment response and HPV status. As it has been previously demonstrated that the Arg72 variant is more susceptible to degradation by E6 perhaps heterozygous or homozygous woman for Pro53 respond differently to treatment as they may be better able to induce a p53 response (if the Pro53 allele is still functionally intact).

E6 and E7 Transcription Relative to Cell Confluence

In the cell confluence studies, it was found that at 50% confluence *E6* and *E7* transcription was lowest and from 75% to 100% confluence it was greatest. There was a significant

increase in *E6* and *E7* transcription from 50% to 100% confluence. This high level of transcription may be attributed to the exponential growth of the cells at this point. One week after 100% confluence was reached, transcript levels decreased, possibly due to cell senescence as a result of culture surface saturation as well as cell death.

A recent study by Isaacson Wechsler et al., 2012 , also demonstrated differences in *E6* and *E7* transcription with regards to cell confluence. Parental HPV16 transfected NIKS cells, 3 HPV16 positive clones representing HSIL and 3 HPV16 positive clones representing LSIL were grown in monolayer culture to a range of different cell densities before harvesting. Unlike the HSIL-like clones, the LSIL-like clones did not appear to continue to divide effectively post 100% confluence, which suggested that they were sensitive to contact inhibition. Similarly, the HSIL-like clones displayed an increase in *E6* and *E7* when they reached confluence, contrasting what was observed for the LSIL-like clones. Furthermore, it was found that the E6 target, cellular p53, decreased more prominently post 100% confluence in the HSIL-like clones compared to the LSIL-like clones. Another study by Laurson and Raj, 2011 , also found levels of *E7* to be elevated in confluent cells. The findings from both of these studies agree with the data presented here. As VIN3 is the stage prior to invasive disease it is similar to HSIL and has a highly proliferative phenotype. As the focus of this study was to assess *E6* and *E7* transcript levels relative to cell confluence it did not assess mitotic numbers one week post confluence; therefore, a valid conclusion on the contact inhibition status of the M08 cell line cannot be made, but would prove valuable as future work in light of the data presented by Isaacson Wechsler et al., 2012.

The findings from the confluence study confirmed the influence cell density had on levels of oncogene transcription and emphasised the importance of standardisation of conditions for the dosing studies. Based on the data outlined in Figure 3.12, optimal experimental conditions were chosen to examine *E6* and *E7* expression in the NHIST cell lines in response to treatment. Time periods of 12, 36 and 72 hours post treatment were selected for analysis of *E6* and *E7* transcription to ensure minimal differences in the confluences between the treated and untreated cells (where cells were allowed to adhere to the tissue culture surface 24 hours prior to dosing). A maximum cell culture period of

4.5 days would equate to less than three population doublings for both M08 and A09 cells (Table 3.1). Minimizing differences in cell confluence between treated and untreated cells by limiting the number of population doublings in a dosing study may avert potential skewing of transcript normalization, where change in oncogene expression of treated cells is normalized to that of the untreated control cells.

Culture of NHIST Cells with and without 3T3 Feeder Cells

It was found that the M08 NHIST cell line could be cultured effectively without feeder cells when inoculated at a standard concentration, although M08 cells grown with feeder cells became fully confluent sooner than M08 cells grown in the absence of feeder cells. Additionally, M08 cells grown without feeder cells exhibited hypertrophic morphology with a "fried egg" effect. "Fried egg" morphology is associated with cytoplasmic extension resulting in cell motility and locomotion (Alt and Dembo, 1999). It is possible that the M08 cells cultured in the absence of feeder cells had more room to expand, which may have resulted in this hypertrophic morphology.

An important consideration was that culture of primary and short term HPV immortalized human keratinocytes without feeder cells may promote episome loss. A study by Dall et al., 2008 , reported loss of episomal HPV DNA from W12s, a naturally HPV transformed cell line derived from a cervical intraepithelial neoplasia, following growth without feeder cells for 15 and 25 population doublings. However, as the mechanism of action studies in this project lasted a maximum of 4.5 days, which equates to less than 3 population doublings for the M08 and A09 NHIST cell lines, episome loss was unlikely. On the other hand, it may be speculated that general stress induced in cells by culturing them without feeder cells may be mistaken for stress induced by compound dosing. This effect could interfere with the compound mechanism of action results. However, as the untreated and treated cells in the mechanism of action studies were cultured in the exact same conditions such potential stress responses are controlled for. It was therefore decided that the NHIST lines could be grown in the absence of feeder cells for the dosing and mechanism of action studies.

Initial Inoculum of NHIST Cells for use in Dosing Studies

In a 96 well plate format the optimal initial inoculum of NHIST cell lines was found to be 5,000 cells per well. This value had to be a balance between the number of cells required to effectively initiate proliferation and the number of cells that would reach 100% confluence during the experimental period. This differed from experimental set up using transformed cell lines as they did not need a minimal cell density before they could divide effectively presumably because these cells were derived from cancer and the NHIST cell lines were derived from intraepithelial neoplasia biopsies. This may suggest that the NHIST cell lines rely on paracrine cell signalling, which would also explain their preference for growth in the presence of feeder cells. For mechanism of action studies, cells were grown in larger vessels and optimal initial inocula were adjusted per culture area when culturing cells in 6 cm and 10 cm culture dishes.

Optimal Method of Assessment of Cell Viability

The optimum method of assessment of cell viability in response to compound treatment was found to be cell counting. Cidofovir was used in the optimization process as it was the main subject of this investigation and results could be compared to published data. Transformed cervical cancer cells were used in the optimization process as they were more robust and easy to work with compared to short term or primary cell lines. Three different methods were assessed to determine viability of cells in response to treatment. CellTiter 96® AQueous One MTS Solution Reagent assay was initially selected as the quickest and easiest assay to perform, as well as providing high through-put; however the results it produced were consistently contradicted by microscopic assessments and did not show a linear dose response to Cidofovir concentration. The reason for this inconsistency is unclear. MTS reagent was added to compound-spiked media with no cells to control for background interference, thus the irregular results do not appear to be due to a reaction between Cidofovir and the MTS reagent. An alternative explanation might be that treatment with Cidofovir resulted in a small population of large, highly metabolically active cells.

Manual and automated cell counting methods were then evaluated and both showed linear dose responses to Cidofovir treatment. Both methods provided cell counts but the

automated cell counting method using flow cytometry had the advantage of counting a far greater number of cells in comparison to the manual method. Furthermore, automated cell counting using flow cytometry gave the option of examining a large range of cellular characteristics.

Apart from confirming the best method to assess viability of treated cells, these experiments also proved beneficial in optimization of the dosing system. For instance, initially cells were treated for up to 12 days with up to 6 different concentrations of compound (Figure 3.16 (A) - MTS method). However, upon re-evaluation of the system, it was found that a shorter experimental duration provided better data to calculate IC50 values. This was because after one week in culture, the untreated cells and the cells treated with very low concentrations of compound became over confluent and began to die of their own accord, thus skewing inhibitory concentration values.

4. The Effects of Acyclic Nucleoside Phosphonate and ProTide Treatment on the Growth of HPV Positive Cell Lines

The compounds analysed in this chapter include: Cidofovir, cyclic Cidofovir, one cyclic Cidofovir ProTide analogue, Adefovir, two ProTide analogues of Adefovir, Tenofovir and three ProTide analogues of Tenofovir. The experiments were designed to investigate the specificity of Cidofovir for HPV transformed lines and to investigate the activity of Cidofovir and the other ANPs in the NHIST cell lines.

4.1. Cidofovir Specificity and Dose Range Finding

Hypotheses

i. *Cidofovir displays anti-growth activity in NHIST cell lines*
ii. *IC50 values obtained for Cidofovir in NHIST cell lines are similar to those outlined in previously published literature*

Cidofovir has shown promise in the treatment of HPV positive cell lines and lesions (Tristram and Fiander, 2005, Snoeck et al., 2000); additionally, some studies have reported specificity of Cidofovir to HPV positive cells (Andrei et al., 2001, Abdulkarim et al., 2002). To test these hypotheses the specificity of Cidofovir to NHIST cell lines was examined and IC50 concentrations of Cidofovir were determined for use in subsequent mechanism of action studies. Cidofovir dosing was examined in the NHIST cell lines and untransformed HPV negative HEKs. M08 and A09 cells were seeded at 5 x 10^3 cells/well in 96 well plates. HEKs were seeded at 3.5 x 10^4 cells/well in 24 well plates. After an initial attachment period of 24 hours M08 and A09 cells were treated with 0, 1, 5, 10 and 100 µM Cidofovir in triplicate and HEKs were treated with 0, 1, 10 and 100 µM Cidofovir in duplicate. HEKs were treated in 24 well plates as they were easier to work with in larger numbers. An extra concentration of Cidofovir (5 µM) was used in the M08 and A09 cell lines as previous work had suggested Cidofovir had an IC50 value between 1 and 10 µM in the M08 cell line (results section 3.6; Figure 3.15). Viable cells were counted 48 and 96 hours post treatment for each cell type using Trypan blue staining.

4.1.1. Growth and Morphology of NHIST Cells Post Cidofovir Treatment

Ninety-six hour dose response curves and photomicrographs of cellular morphology 96 hours post Cidofovir treatment of M08, A09 and HEK cells are shown in Figures 4.1, 4.2 and 4.3 respectively.

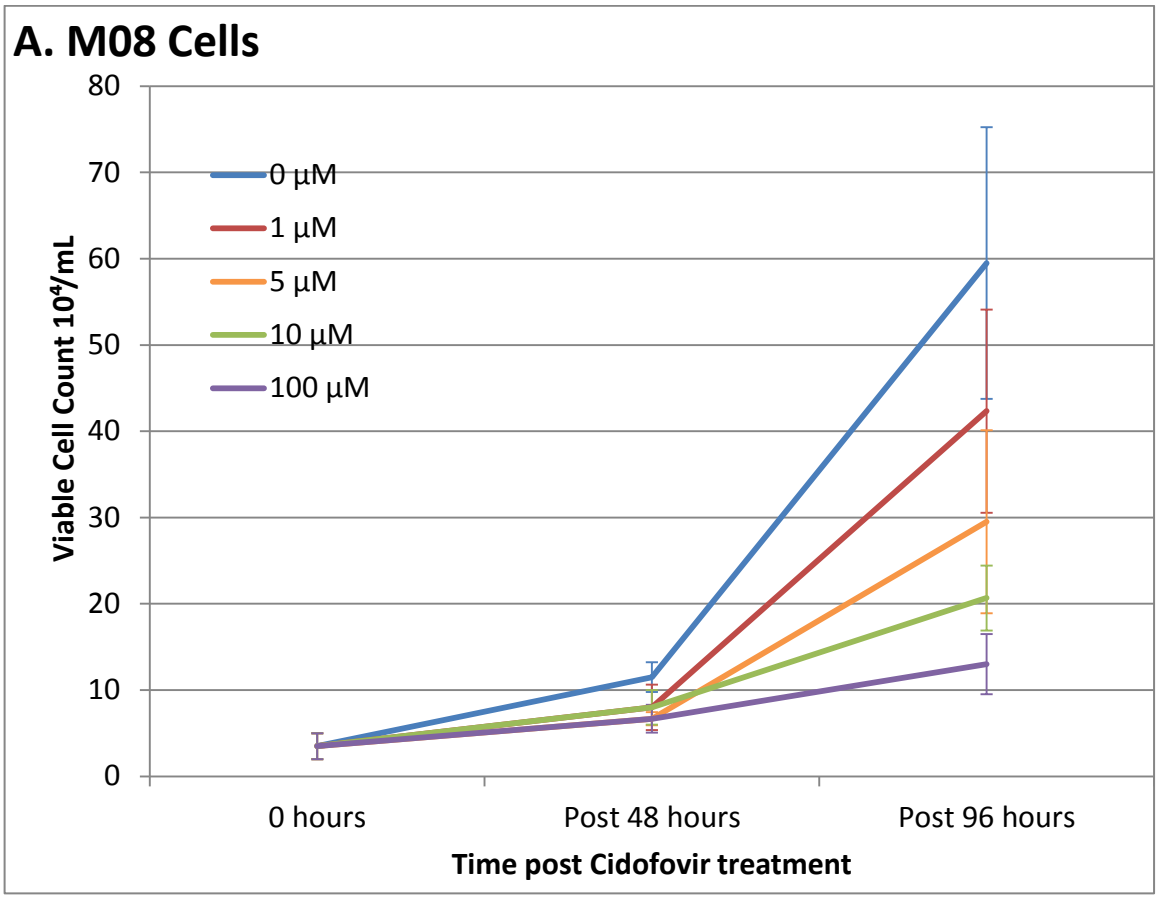
A. M08 Cells
80
70
60
50
40
30
20
10
0
Viable Cell Count 10⁴/mL
0 µM
1 µM
5 µM
10 µM
100 µM
0 hours
Post 48 hours
Post 96 hours
Time post Cidofovir treatment

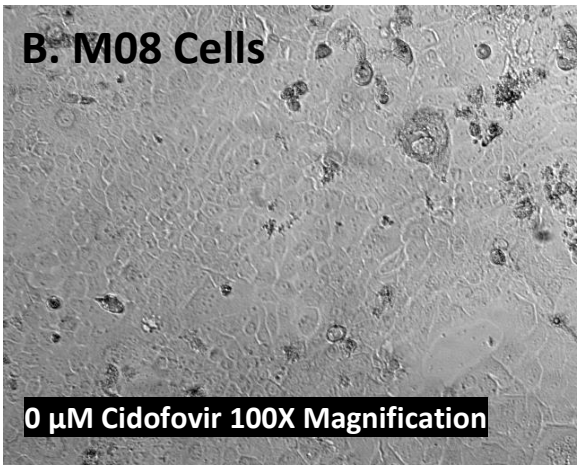
B. M08 Cells
0 µM Cidofovir 100X Magnification

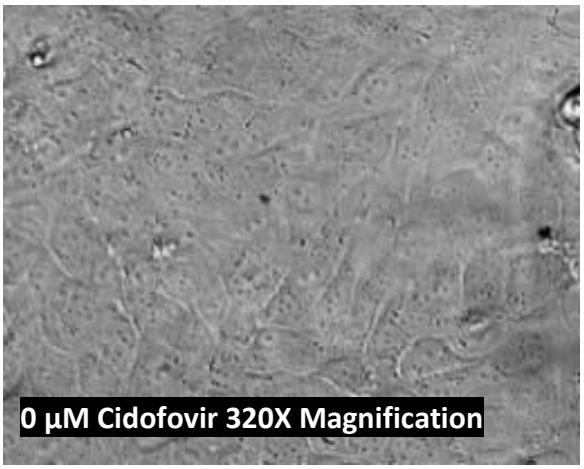
0 µM Cidofovir 320X Magnification

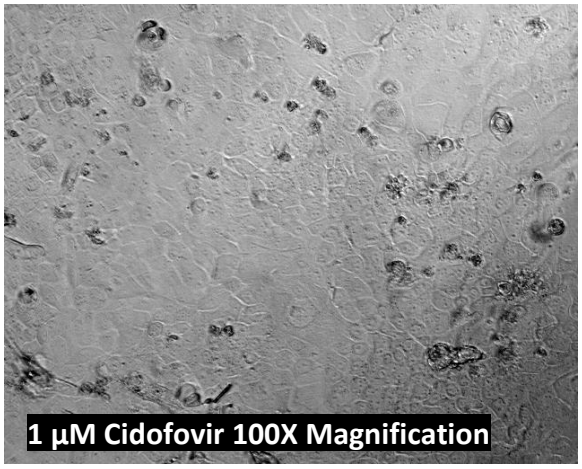
1 µM Cidofovir 100X Magnification

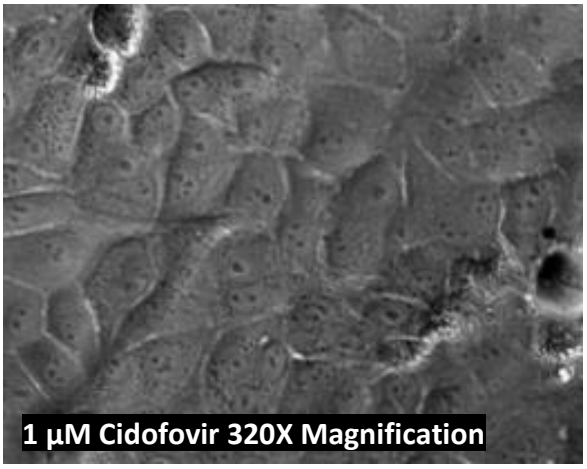
1 µM Cidofovir 320X Magnification

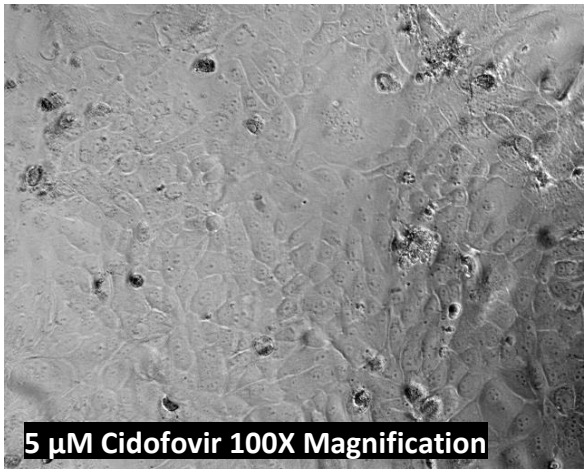
5 µM Cidofovir 100X Magnification


5 µM Cidofovir 320X Magnification

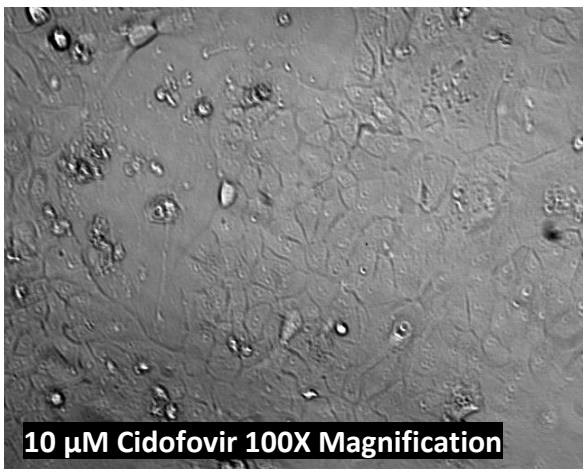
10 µM Cidofovir 100X Magnification


10 µM Cidofovir 320X Magnification

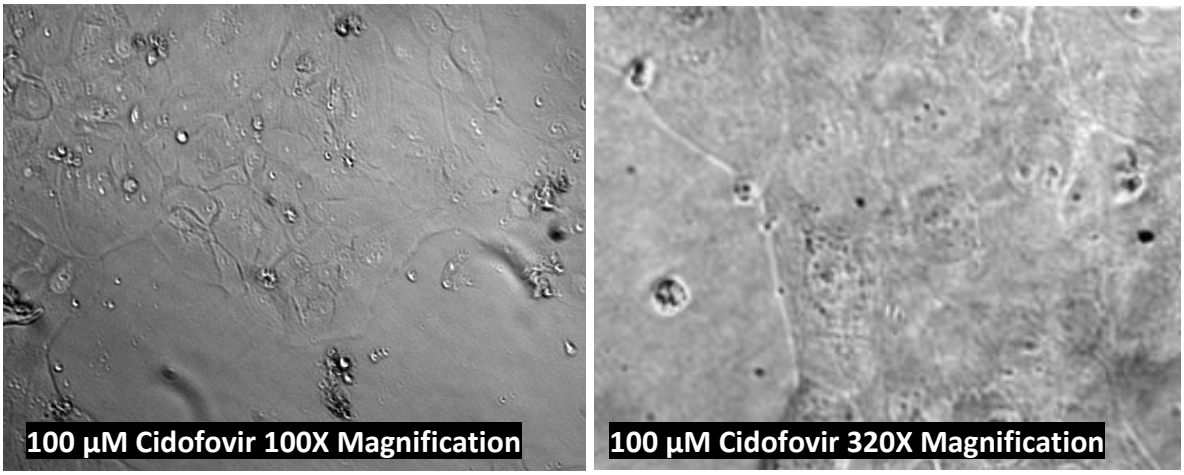

Figure 4.1. M08 Cell Viability and Morphology in Response to Cidofovir Treatment over a 96 Hour Time Frame

(A) Growth curves of M08 cells treated with 4 concentrations of Cidofovir over a 96 hour period. Cells were seeded at 5 x 10^3 cells per well in 96 well plates. After a 24 hour attachment period cells were treated with 0 µM, 1 µM, 5 µM, 10 µM and 100 µM Cidofovir in triplicate wells for each condition. Viability was assessed 48 and 96 hours post treatment by manual cell counting using Trypan blue staining. Error bars represent standard deviation of the mean viable cell count per mL of triplicate wells for each condition. (B) Photomicrographs illustrate M08 cell morphology 96 hours post treatment with 4 concentrations of Cidofovir. Images were captured using bright field microscopy. Images at 100X magnification show cells floating in media for each condition and decreasing cell confluence with higher concentrations of Cidofovir. Images at 320X magnification show morphology of cells treated with all conditions, where an increase in cell size can be seen in cells treated with higher concentrations of Cidofovir.

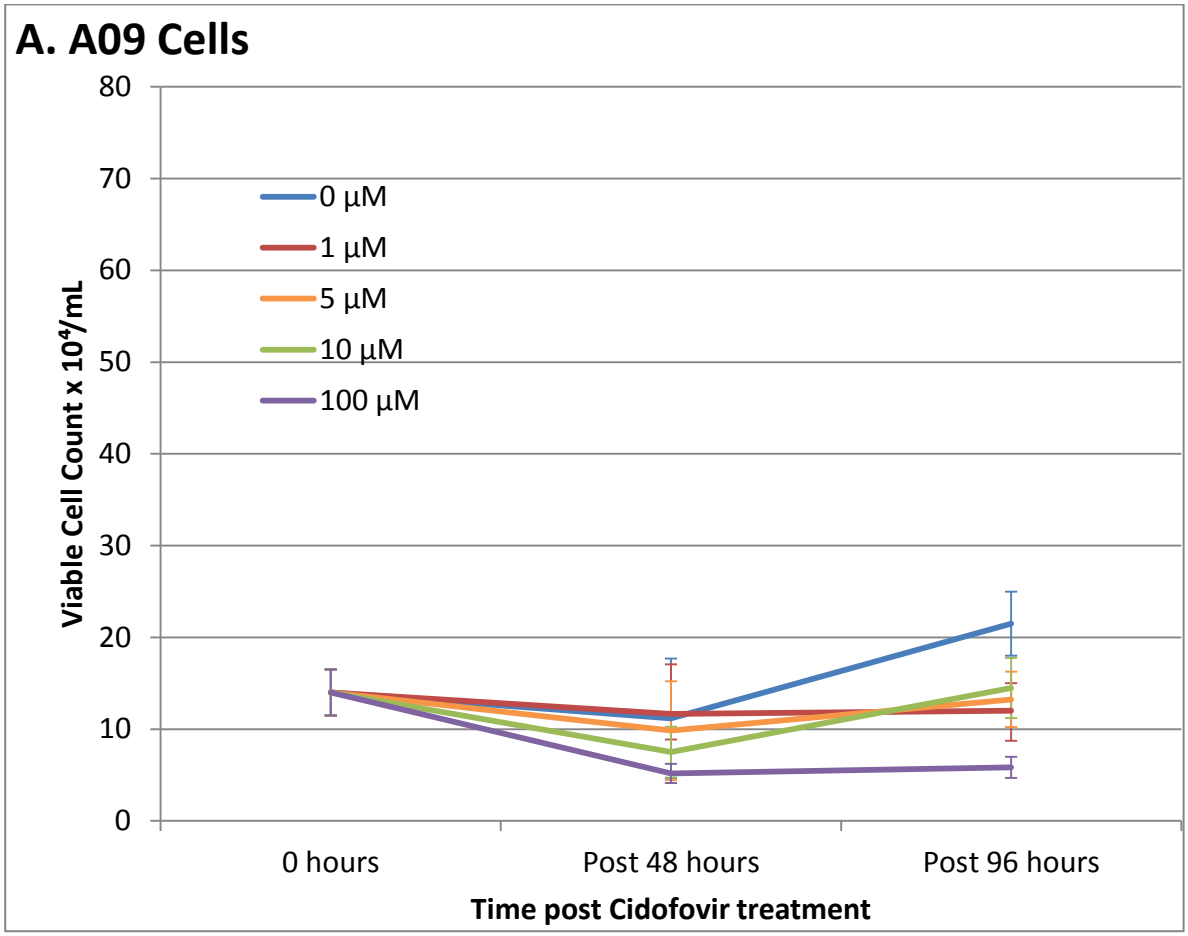
A. A09 Cells
80
70
60
50
40
30
20
10
0
Viable Cell Count x 10⁴/mL
0 µM
1 µM
5 µM
10 µM
100 µM
0 hours
Post 48 hours
Post 96 hours
Time post Cidofovir treatment

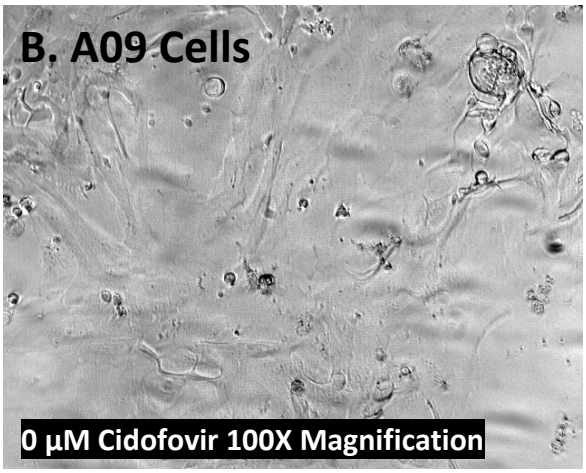
B. A09 Cells
0 µM Cidofovir 100X Magnification

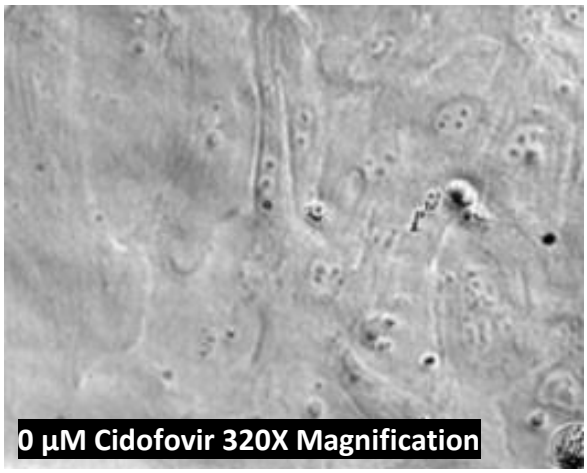
0 µM Cidofovir 320X Magnification

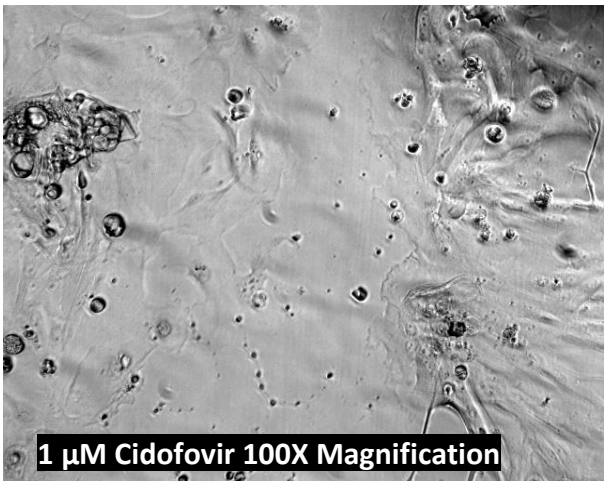
1 µM Cidofovir 100X Magnification


1 µM Cidofovir 320X Magnification

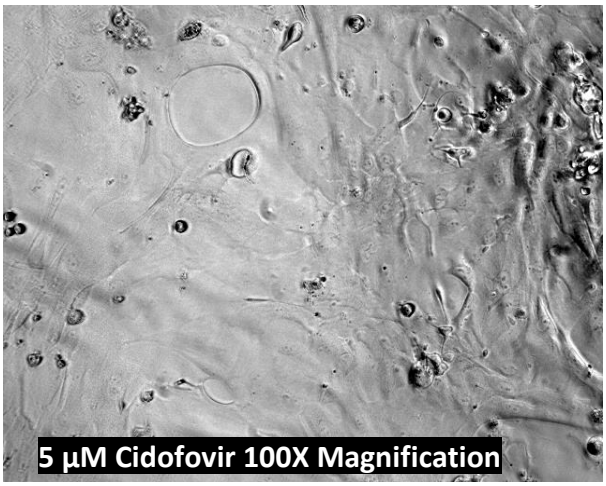
5 µM Cidofovir 100X Magnification

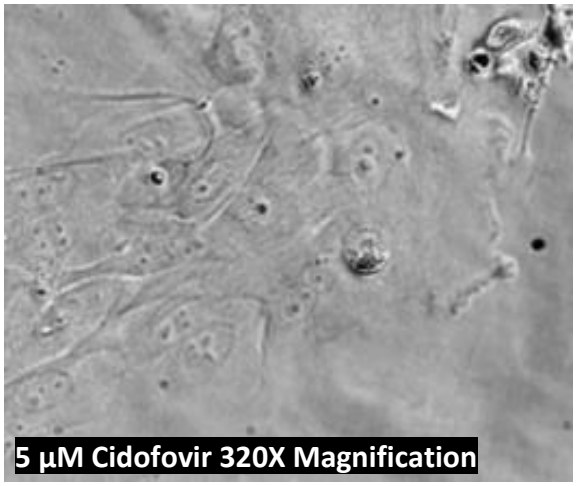
5 µM Cidofovir 320X Magnification

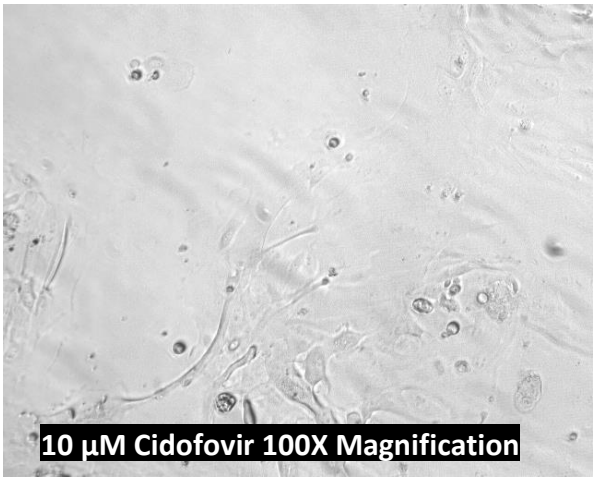
10 µM Cidofovir 100X Magnification


10 µM Cidofovir 320X Magnification

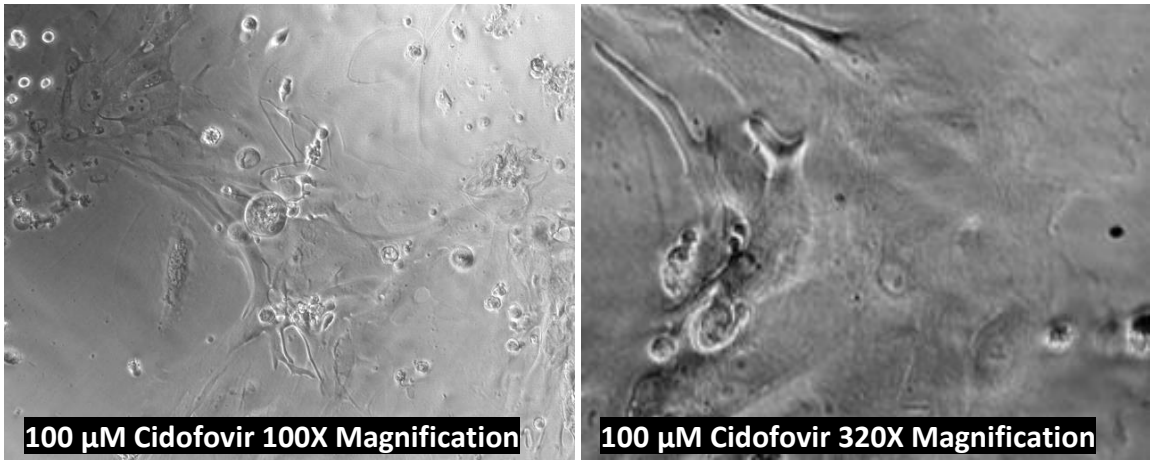

Figure 4.2. A09 Cell Viability and Morphology in Response to Cidofovir Treatment over a 96 Hour Time Frame

(A) Growth curves of A09 cells treated with 4 concentrations of Cidofovir over a 96 hour period. Cells were seeded at 5 x 10^3 cells per well in 96 well plates. After a 24 hour attachment period cells were treated with 0 µM, 1 µM, 5 µM, 10 µM and 100 µM Cidofovir in triplicate wells for each condition. Viability was assessed 48 and 96 hours post treatment by manual cell counting using Trypan blue staining. Error bars represent standard deviation of the mean viable cell count per mL of triplicate wells for each condition. (B) Photomicrographs illustrate A09 cell morphology 96 hours post treatment with 4 concentrations of Cidofovir. Images were captured using bright field microscopy. Images at 100X magnification show cells floating in media for each condition. Images at 320X magnification show cells in each condition with an elongated morphology.

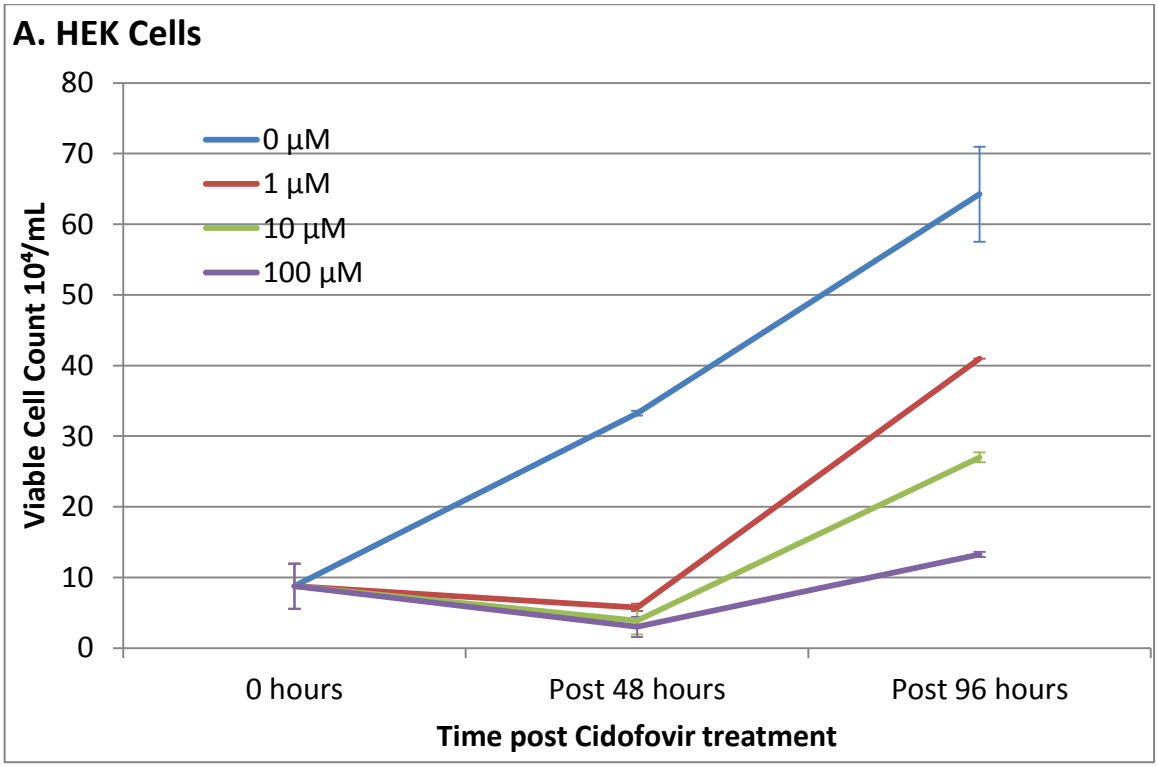
A. HEK Cells
80
70
60
50
40
30
20
10
0
Viable Cell Count 10^4/mL
0 µM
1 µM
10 µM
100 µM
0 hours
Post 48 hours
Post 96 hours
Time post Cidofovir treatment

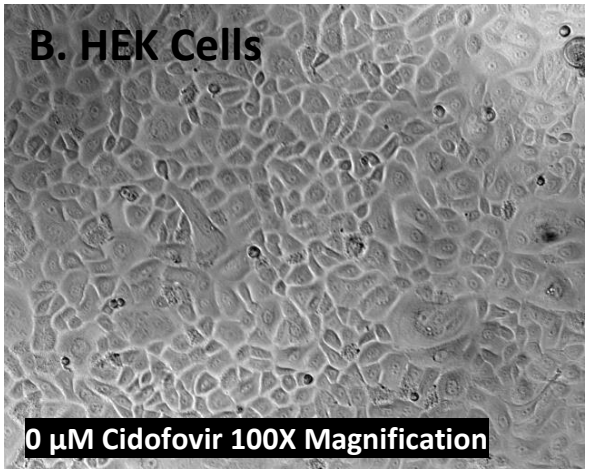
B. HEK Cells
0 µM Cidofovir 100X Magnification


0 µM Cidofovir 320X Magnification

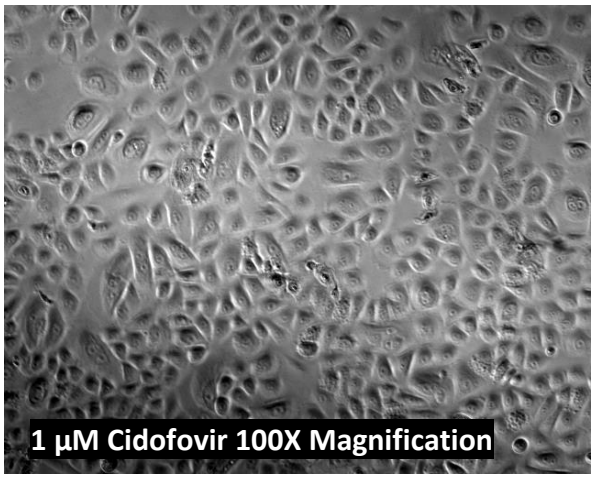
1 µM Cidofovir 100X Magnification

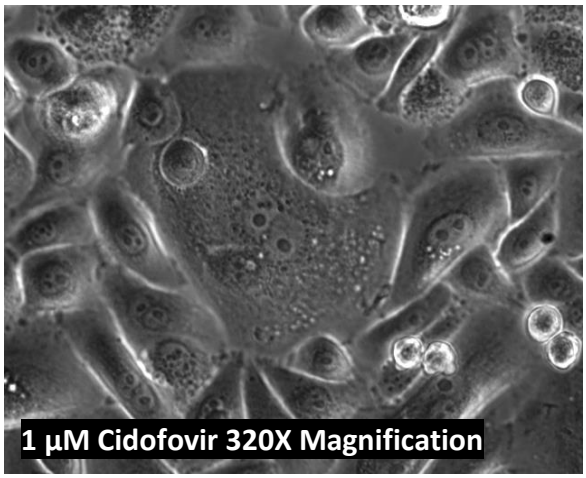
1 µM Cidofovir 320X Magnification

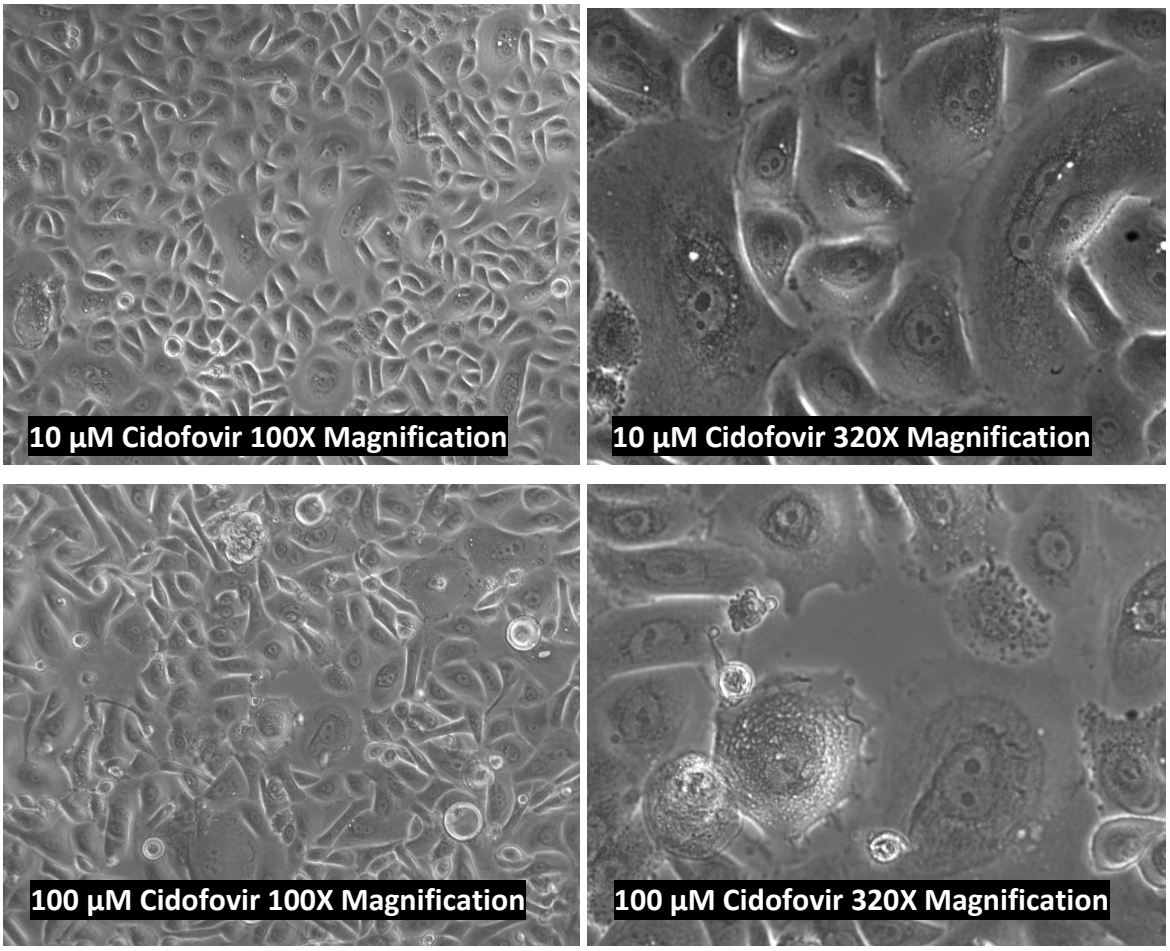

Figure 4.3. HEK Cell Viability and Morphology in Response to Cidofovir Treatment over a 96 Hour Time Frame

(A) Growth curves of HEK cells treated with 3 concentrations of Cidofovir over a 96 hour period. Cells were seeded at 3.5 x 10^4 cells per well in 24 well plates. After a 24 hour attachment period cells were treated with 0 µM, 1 µM, 10 µM and 100 µM Cidofovir in duplicate wells for each condition. Viability was assessed 48 and 96 hours post treatment by manual cell counting using Trypan blue staining. Error bars represent standard deviation of the mean viable cell count per mL of duplicate wells for each condition. (B) Photomicrographs illustrate HEK cell morphology 96 hours post treatment with 3 concentrations of Cidofovir. Images were captured using bright field microscopy. Images at both 100X and 320X magnification show hypertrophic cells with increasing Cidofovir concentration.

The M08 cell dose response curve in Figure 4.1 (A) indicates that Cidofovir did not produce a notable differential inhibitory effect until 96 hours post treatment in this cell line. This can be seen in the photomicrographs in Figure 4.1 (B), where increasing Cidofovir concentration caused a decrease in cell confluence and an increase in cell size.

Similar to M08 cells, a differential inhibitory effect by Cidofovir in A09 cells was not seen until 96 hours post treatment (Figure 4.2 (A)). This was not clear in the photomicrographs due to the low number of viable cells and smaller differential effect between different concentrations of Cidofovir (Figure 4.2 (B)).

From the HEK dose response curve (Figure 4.3 (A)) a prominent decrease in viable cell number was observed for each concentration of Cidofovir at 48 hours. However, by 96 hours the HEK cells appear to have recovered but grew in a dose dependent manner. The photomicrographs in Figure 4.3 (B) show HEKs decreasing in cell number and increasing in cell size in a Cidofovir dose dependent manner.

4.1.2. Cidofovir IC50 Values in NHIST Cell Lines

Cell count data was used to calculate Cidofovir IC50 values for M08, A09 and HEK cells 48 and 96 hours post treatment (Table 4.1). Cidofovir did not produce 50% inhibition of M08 cell growth with the concentrations used at 48 hours; however, an IC50 value of 5 µM was calculated for M08 cells 96 hours post Cidofovir treatment. In A09 cells an IC50 value of 84 µM was found at 48 hours; this reduced to 21 µM 96 hours post Cidofovir treatment. An IC50 value of 0.6 µM was calculated 48 hours post treatment for HEKs; however, this increased 10 fold to 6.6 µM by 96 hours post Cidofovir treatment.

Table 4.1. Cidofovir IC50 values for M08, A09 and HEK cells 48 and 96 hours post treatment

	M08 (HPV16+) IC50		**A09 (HPV16+) IC50**		**HEK (HPV-) IC50**	
	48 hours	**96 hours**	**48 hours**	**96 hours**	**48 hours**	**96 hours**
µM	-	5	84	21	0.6	6.6

4.2. Effects of Cyclic Analogues of Cidofovir on HPV Positive and Negative Transformed Cell Lines

Hypothesis

Cyclic ProTide analogues of Cidofovir have increased anti-growth activity compared with acyclic parent Cidofovir in HPV positive cell lines

Previous studies suggest Cidofovir may be an effective treatment for HPV associated neoplasia (Tristram and Fiander, 2005, Snoeck et al., 2000). This study focused on modifying Cidofovir using the ProTide approach in order to increase its efficacy. ProTide technology was applied to the compound in order to mask the negative charge on the phosphonate moiety, thus allowing it to enter cells more readily. However, the synthesis of the ProTide derivative of Cidofovir in its acyclic form was not achieved due to nucleophilic attack on the phosphonate group by a hydroxymethylene side chain. The chemical structure of Cidofovir before manipulation is outlined in Figure 4.4 (A).

In order to avoid the displacement of the masking group on the phosphonate moiety by the hydroxymethylene side chain, cyclic Cidofovir was synthesised and its amidate derivative was obtained by reaction with the benzyl ester of L-Alanine. The chemical structures of cyclic Cidofovir (salt) and its ProTide amidate derivative are shown in Figure 4.4 (B) and Figure 4.4 (C) respectively.

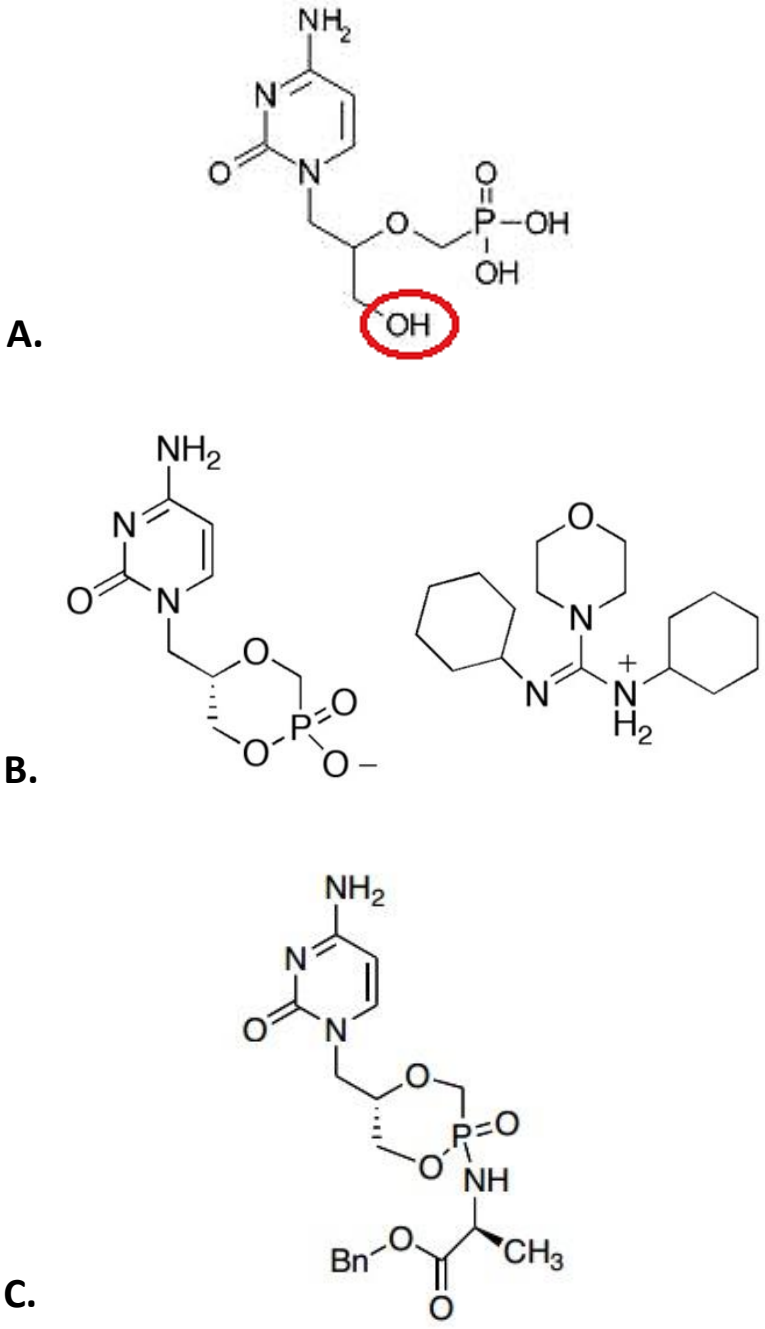

Figure 4.4. Chemical structure of Cidofovir, cyclic Cidofovir and cyclic Cidofovir Amidate (ProTide)

(A) Chemical structure of Cidofovir; the red ring highlights the site of attachment for the hydroxymethylene side chain. (B) Chemical structure of Cyclic Cidofovir; Cyclic Cidofovir is the structure on the left hand side; its salt is the structure on the right hand side. (C) Chemical structure of cyclic Cidofovir amidate (ProTide); the amidate moiety is attached to the phosphonate group of cyclic Cidofovir.

The cyclic compounds were examined for improved growth inhibitory efficacy in comparison to Cidofovir in HeLa (HPV18 positive) and C33A (HPV negative) cells. The cells were subjected to treatment with 0, 1, 10 and 100 µM Cidofovir, cyclic Cidofovir and cyclic Cidofovir amidate in triplicate in 96 well plates. Viable cell counts were performed prior to treatment (0 hours) and 48 and 96 hours post treatment. Viability was assessed using Trypan blue dye exclusion manual counting.

4.2.1 Growth of HeLa and C33A cells with Cidofovir, cyclic Cidofovir and cyclic Cidofovir Amidate Treatment

The results of the Cidofovir, cyclic Cidofovir and cyclic Cidofovir amidate dosing are outlined in Figure 4.5 (A), (B) and (C) respectively. There appears to be minimal variation in dose response between the three compounds in HeLa and C33A cell lines.

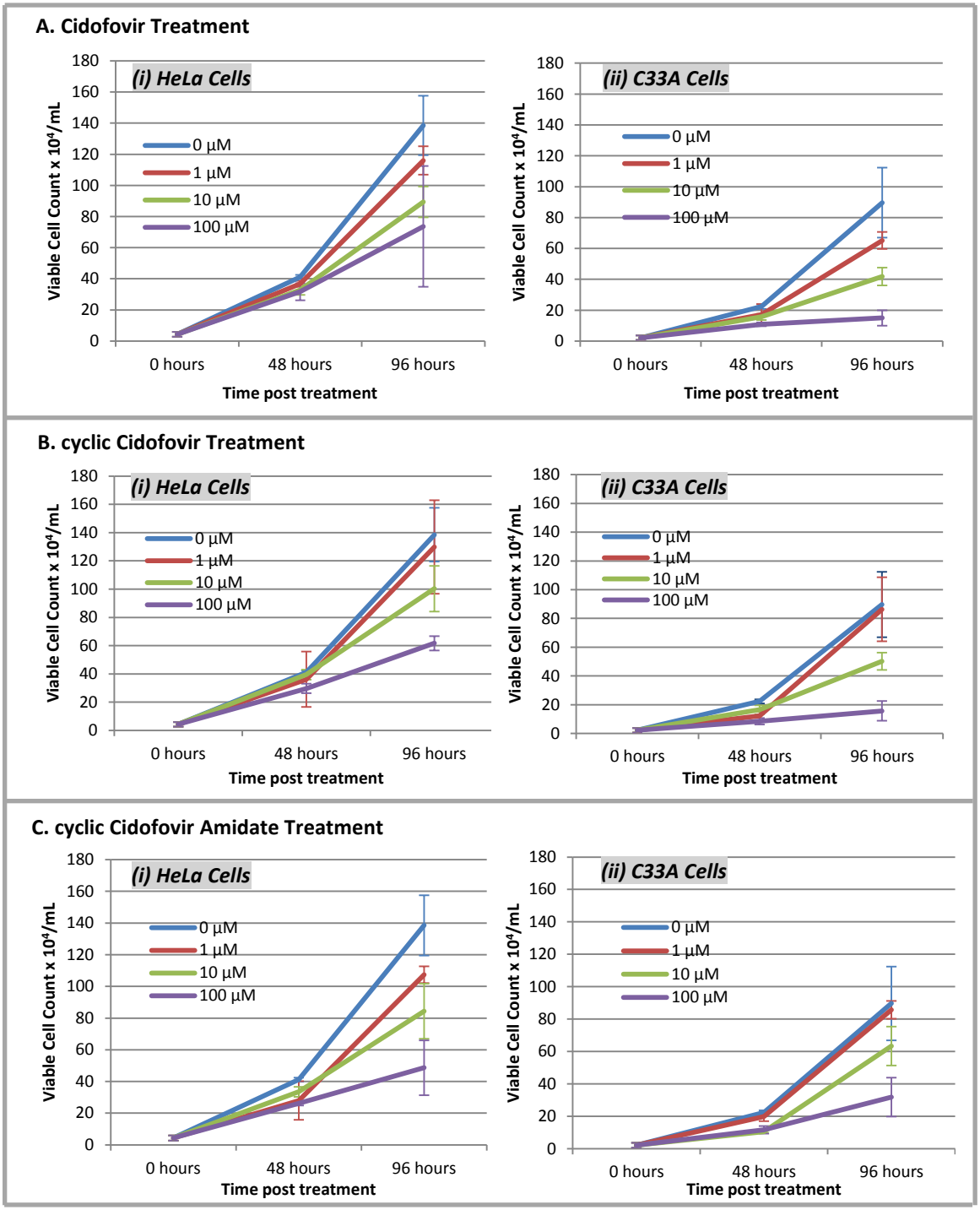

Figure 4.5. HeLa and C33A cell growth 48 and 96 hours post Cidofovir, cyclic Cidofovir and cyclic Cidofovir amidate (ProTide) treatment

(i) HeLa and (ii) C33A growth curves post (A) Cidofovir, (B) cyclic Cidofovir and (C) cyclic Cidofovir amidate (ProTide) treatment. Both cell types were seeded at 5 x 10^2 cells per well in 96 well plates. After an attachment period of 24 hours cells were treated with 0 µM, 1 µM, 10 µM and 100 µM of each compound in triplicate. The number of viable cells per mL was recorded 48 and 96 hours post treatment using Trypan blue manual cell counting. Error bars represent standard deviation of the mean of triplicate wells for each condition.

4.2.1. IC50 Values for HeLa and C33A Cells Treated with Cidofovir, cyclic Cidofovir and cyclic Cidofovir amidate (ProTide)

The IC50 values presented in Table 4.2 were calculated from the dose response curves outlined in Figure 4.5.

Table 4.2. IC50 values for Cidofovir, cyclic Cidofovir and cyclic Cidofovir amidate (ProTide) in HeLa and C33A cells

Compound	IC50 for HeLa Cells (HPV+) µM		IC50 for C33A Cells (HPV-) µM	
	48 hours	96 hours	48 hours	96 hours
Cidofovir	-	-	92	9
Cyclic Cidofovir	-	83	-	24
Cyclic Cidofovir amidate	-	46.5	-	62

Table 4.2 shows that at the doses examined, Cidofovir did not reduce HeLa cell counts by 50% over a period of 96 hours. Less than 50% reduction in cell counts was also seen at 48 hours for both cyclic Cidofovir and cyclic Cidofovir amidate in HeLa cells. At 96 hours, cyclic Cidofovir had an IC50 value of 83 µM, and cyclic Cidofovir amidate had an IC50 value of 46.5 µM. From this data it would appear that the cyclic compounds are more active than unmodified Cidofovir, with the ProTide analogue producing 50% inhibition at nearly half the concentration of cyclic Cidofovir.

With the C33A cell line, Cidofovir did have a 50% inhibitory effect, with IC50 values of 92 µM and 9 µM at 48 and 96 hours respectively. No IC50 effect was seen at 48 hours for either cyclic Cidofovir or the cyclic Cidofovir amidate in the C33A cell line. An IC50 value of 24 µM with cyclic Cidofovir was observed at 96 hours and an IC50 value of 62 µM was observed with the cyclic Cidofovir amidate at the same time. This data suggests that the cyclic compounds are not as effective as unmodified Cidofovir in the HPV negative C33A cells.

These IC50 values vary between the two cell lines as well as between the 3 compounds examined. Cidofovir had no 50% inhibitory effect on HeLa cells over the experimental time period, where as it did on the C33A cells with a 10 fold decrease in IC50 concentration from 48 to 96 hours. Neither cyclic compound produced an IC50 effect after 48 hours in either cell line. At 96 hours the cyclic amidate was more active than cyclic Cidofovir in HeLa cells, but in C33A cells the opposite was observed. The HPV negative C33A cells

appeared to be more sensitive to all compounds compared to the HPV positive HeLa cells, which is most likely due to genetic differences between the two cell lines.

The inconsistency of these results raised questions regarding the experimental materials. Upon chemical re-evaluation of the amidate derivative of cyclic Cidofovir by ^{31}P-NMR and TLC analysis in the Welsh School of Pharmacy, it was found that the compound re-opened to its acyclic form by a hydrolysis reaction.

4.3. Adefovir and Tenofovir ProTide Screen

Hypothesis

ProTide analogues of Adefovir and Tenofovir are more efficient at inhibiting cell growth in HPV positive immortalized cell lines in comparison to the parent compounds from which they were derived

As the chemical structure of Cidofovir would not allow chemical manipulation to form acyclic ProTide analogues it was decided to modify the Cidofovir sister compounds, Adefovir and Tenofovir. Like Cidofovir, Adefovir and Tenofovir are ANP compounds but are derived from an adenine nucleobase. Adefovir in its oral prodrug form, Adefovir dipivoxil (Hepsera)**,** is FDA approved for the treatment of HBV infections, and the prodrug form of Tenofovir, Tenofovir disoproxil fumarate (TDF, Viread), is approved for the treatment of HIV and HBV infections (De Clercq, 2011b). In theory, ProTide compounds should be more effective than their parent compounds as the negative charge on their phosphate group is masked to allow more efficient entry into cells.

Three ProTide analogues of Tenofovir and two ProTide analogues of Adefovir were made in the Welsh School of Pharmacy. These ProTide analogues along with their parent compounds were examined at 1 µM, 10 µM and 100 µM concentrations in triplicate 3 and 6 days post treatment in SiHa (HPV 16 positive), HeLa (HPV 18 positive) and C33A (HPV negative) cell lines. Viable cell counts in treated lines were determined using 7-AAD flow cytometry, cell size was assessed using the forward scatter parameter in flow cytometry and morphology was assessed by bright field microscopy.

4.3.1. ProTide Screen

A summary of IC50 values obtained in the ProTide screen are outlined in Table 4.3.

Table 4.3. ProTide Analogue and Adefovir and Tenofovir Parent Compound IC50 Values for SiHa, HeLa and C33A Cells 3 and 6 days Post Treatment

	SiHa (HPV 16+)			HeLa (HPV 18+)			C33A (HPV -)		
Compound	IC50 (µM)		Effect on cell size ‡	IC50 (µM)		Effect on cell size ‡	IC50 (µM)		Effect on cell size ‡
	Day 3	Day 6		Day 3	Day 6		Day 3	Day 6	
Tenofovir	0	0	-	0	0	-	0	**10**	-
TNF Pro cf3472	**0.73**	**0.77**	++	**0.54**	**0.5**	++	**0.7**	**0.79**	++
TNF Pro cf3473	0	**0.93**	++	**0.53**	**5.6**	++	**7.6**	**0.8**	++
TNF Pro cf3474	**7.8**	**5.9**	++	**6.2**	**6**	++	**6**	**0.7**	++
Adefovir	**45**	**10**	++	0	0	+	**7.8**	**0.94**	+
ADF Pro cf3475	**0.6**	**0.5**	+++	**0.5**	**0.5**	+++	**0.54**	**0.5**	+++
ADF Pro cf3476	**0.66**	**0.55**	+++	**0.6**	**6.4**	++	**0.84**	**0.62**	++

Viable cell numbers to calculate IC50 values were determined by flow cytometry using 7-AAD staining. Cells were seeded at 5 x 10^2 cells per well in 96 well plates. After an attachment period of 24 hours cells were treated in triplicate with 3 log concentrations of the test compounds. Three days post initial treatment viability was measured for each condition in triplicate and the remaining wells had a media change/second dose of test compound. Three days post the second treatment (6 days post initial treatment) a second viability measurement was obtained for each condition in triplicate. IC50 values were calculated from percentage kill plots using the equation of the line; Y = MX + C. IC50 values in red text highlight sub micromolar concentrations. IC50 values in green text highlight concentrations of 1 µM or greater.

‡ Effect on cell size and morphology:

- *No effect*

+ *Slight effect, cells starting to become bigger*

++ *Cells are moderately swollen and granular*

+++ *Cells extremely swollen and granular*

As can be seen from Table 4.3 the Tenofovir parent compound had the least effect on the three cell lines. However, an inhibitory effect was observed on day 6 in the C33A cells. This contrasted with the Tenofovir ProTide analogue, TNF Pro cf3472, which displayed sub-micromolar IC50 values for each cell line at each time point. A moderate effect on cell size and morphology was also observed with this compound. The second Tenofovir ProTide analogue, TNF Pro cf3473, showed inconsistent results over the 3 cell lines at both time points. For example, no IC50 value was found on day 3 in the SiHa cell line with concentrations as high as 100 µM, but 3 days later a 50% inhibitory effect was seen with just under 1 µM concentration of the compound. In the HeLa cell line, 3 days after treatment an IC50 value of 0.53 µM was found but 3 days later it increased 10 fold to 5.6 µM, which directly contradicted what was found in the C33A cell line, with an IC50 concentration of 7.6 µM on day 3 but 10 fold lower at 0.8 on day 6. However, a moderate effect on cell size and morphology was observed in each cell line. The final Tenofovir ProTide, TNF Pro cf3474, like TNF Pro cf3472 showed stable IC50 values over the three cell lines, with a 10 fold decrease in IC50 on day 6 in the C33A cell line. A moderate effect on cell size and morphology was observed in each cell line with this compound.

Adefovir produced IC50 values of 45 µM and 10 µM on day 3 and day 6 respectively in the SiHa cell line and IC50 values of 7.8 µM and 0.94 µM on day 3 and day 6 respectively in C33A cells. The compound displayed an effect on cell size and cell morphology in each cell line but did not produce an IC50 value in HeLa cells. The first Adefovir ProTide analogue, ADF Pro cf3475, displayed the greatest effect on the three cell lines with consistent IC50 values between 0.5 and 0.6 µM at both time points in each of the cell lines and the greatest effect on cell size and morphology for each cell line also. Similarly, the second Adefovir ProTide analogue, ADF Pro cf3476, showed a prominent inhibitory effect on each cell line with mostly sub-micromolar IC50 values except in the HeLa cell line on day 6. This analogue also caused a significant effect on cell size and morphology in each cell line which appeared to be more pronounced in the SiHa cell line.

Examining the data as a whole, the Tenofovir parent compound had the least effect on viable cell counts and the Adefovir ProTide compound, ADF Pro cf3475, had the most pronounced effect. It would also appear from these cell models that none of the

compounds were specific to HPV positive cell lines. In fact the HPV negative cell line, C33A, appeared to be the most susceptible in that each of the 7 compounds produced an inhibitory effect. The Adefovir ProTide analogues appeared to have a greater effect in comparison to the Tenofovir ProTide analogues as a collection, which may reflect the greater activity of the Adefovir parent compound. Each ProTide daughter compound for both Adefovir and Tenofovir had far greater growth inhibitory effects on the cell lines examined in comparison to their respective parent compounds.

To highlight the difference in efficacy between parent Adefovir and ADF Pro cf3475 flow cytometry plots, growth curves and photomicrographs are shown in the following sections using SiHa cells as an example.

4.3.2. Effect of Adefovir and ADF Pro cf3475 on SiHa Cell Viability

The increased efficacy of the ADF Pro cf3475 compound relative to Adefovir was demonstrated by flow cytometry. Figure 4.6 depicts flow cytometry plots of 7-AAD fluorescence versus forward scatter for SiHa cells treated with (A) 10 µM Adefovir and (B) 10 µM ADF Prof Cf3475.

The dose response plots outlined in Figure 4.7 were derived from the viable cell count data obtained using 7-AAD flow cytometry. Viable counts for SiHa cells 3 and 6 days post treatment with (A) Adefovir and (B) ADF Pro cf3475 are shown in Figure 4.7. All concentrations of ADF Pro cf3475 had an inhibitory effect on SiHa cells as early as 3 days post treatment.

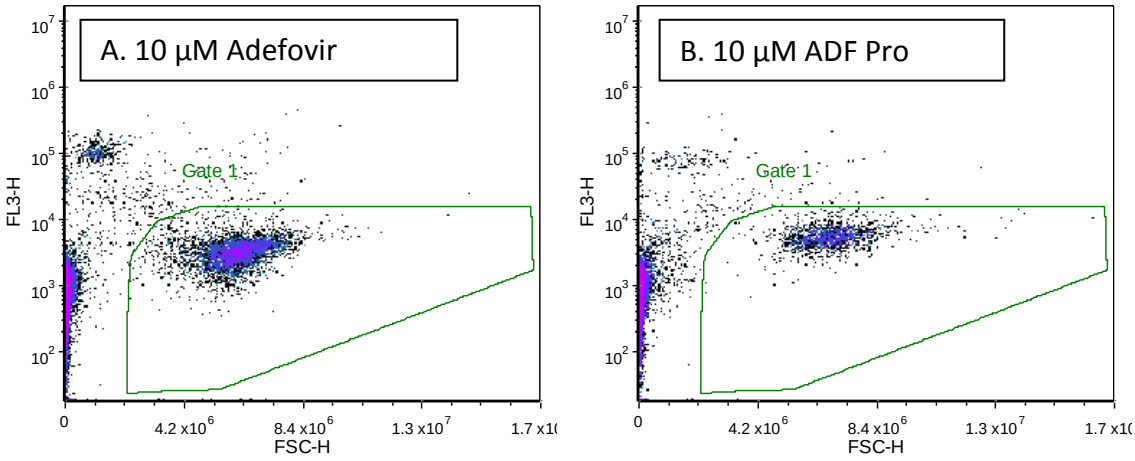

Figure 4.6. Dot Plots of 7-AAD Fluorescence versus Forward Scatter for SiHa Cells 3 days post Treatment with Adefovir and ADF Pro cf3475

7-AAD flourescence is displayed on a log scale on the y axis, forward scatter is displayed on the x axis."Gate 1" encloses the viable cell population used to determine number of viable cells per mL for (A) Adefovir and (B) ADF Pro cf3475 3 days post treatment.

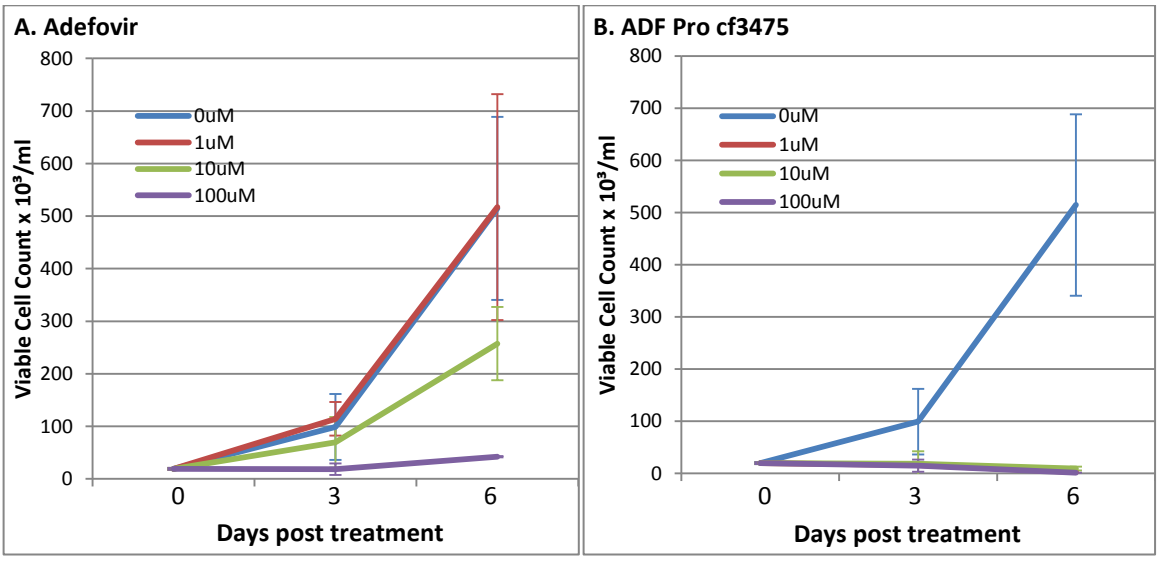

Figure 4.7. Dose Response Growth Curves of SiHa Cells Treated with Adefovir and ADF Pro cf3475

Growth curves of SiHa cells treated with (A) Adefovir and (B) ADF Pro cf3475. SiHa cells were seeded at 5 x 10^2 cells per well in 96 well plates and were allowed to adhere for 24 hours before treatment with 3 log concentrations of both Adefovir and ADF Pro cf3475 in tiplicate. Cell viability was determined by 7-AAD staining and quantification on an Accuri C6 flow cytometry instrument 3 and 6 days post treatment. Error bars represent standard deviation of the mean number of viable cells per mL for triplicate wells.

4.3.3. Effect of Adefovir and ADF Pro cf3475 on SiHa Cell Size and Morphology

Adefovir and ADF Pro cf3475 treatment of SiHa cells resulted in a noticeable effect on cell size, which was quantified by flow cytometry using the forward scatter parameter. In Figure 4.8 (A), SiHa cells treated with Adefovir were larger than the untreated control cells particularly at 10 and 100 µM. Figure 4.8 (B), on the other hand, shows SiHa cells were considerably larger compared to untreated cells at concentrations of 1 and 10 µM ADF Pro cf3475. Cells treated with 100 µM ADF Pro cf3475 were smaller.

In addition to effect on cell size, both compounds produced noticeable effects on SiHa cell morphology (photomicrographs in Figure 4.9). Treated cells were larger than the untreated cells particularly with ADF Pro cf3475, where a proportional increase in cell size was observed with increasing concentration of compound; with the exception of 100 µM where the majority of cells appeared to be dead.

When viewed by light microscopy, apoptosing cells appear to shrink and exhibit membrane blebbing (Kerr et al., 1972). Distinct from apoptosing cells, necrotic cells and cells undergoing senescence display similar morphological characteristics. For example, necrotic cells exhibit cell swelling, cytoplasmic vacuolation and eventually disruption of the cell membrane (Edinger and Thompson, 2004, Golstein and Kroemer, 2007). Similarly, senescing cells also become larger in size, flatten out and lose their original shape (Ben-Porath and Weinberg, 2004). From this it would appear that the cells, which increased in size and decreased in number, were either displaying necrotic or senescent characteristics in response to treatment with the compounds. Photomicrographs for Figure 4.9 were taken at X320 magnification using bright field microscopy.

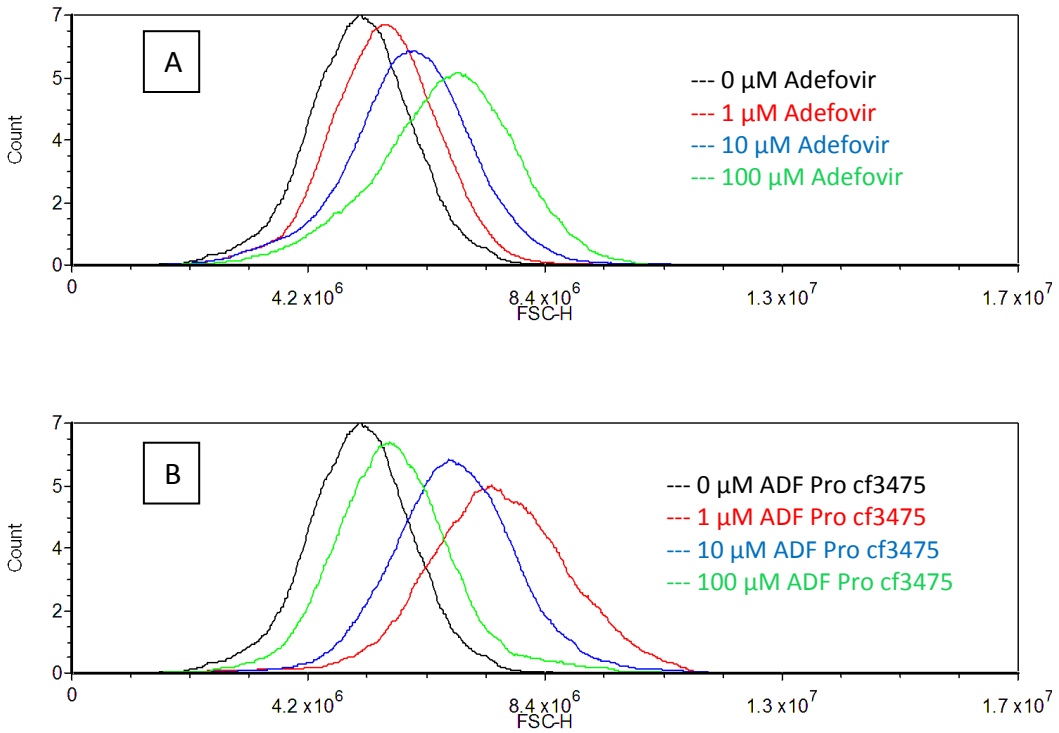

Figure 4.8. Histograms showing changes in SiHa cell size 3 days post treatment with Adefovir and ADF Pro cf3475

Increases in SiHa cell size three days post treatment with three log concentrations of (A) Adefovir and (B) ADF Pro cf3475. Cell size was determined by the median forward scatter value for each viable population of cells, as gated on using 7-AAD staining. Increases in forward scatter are proportional to increases in cell size from the left hand side of the x axis to the right hand side. Histogram curves were subjected to "smoothing" to account for low numbers of viable cells in samples that were treated with high concentrations of compound.

A. 3 Days

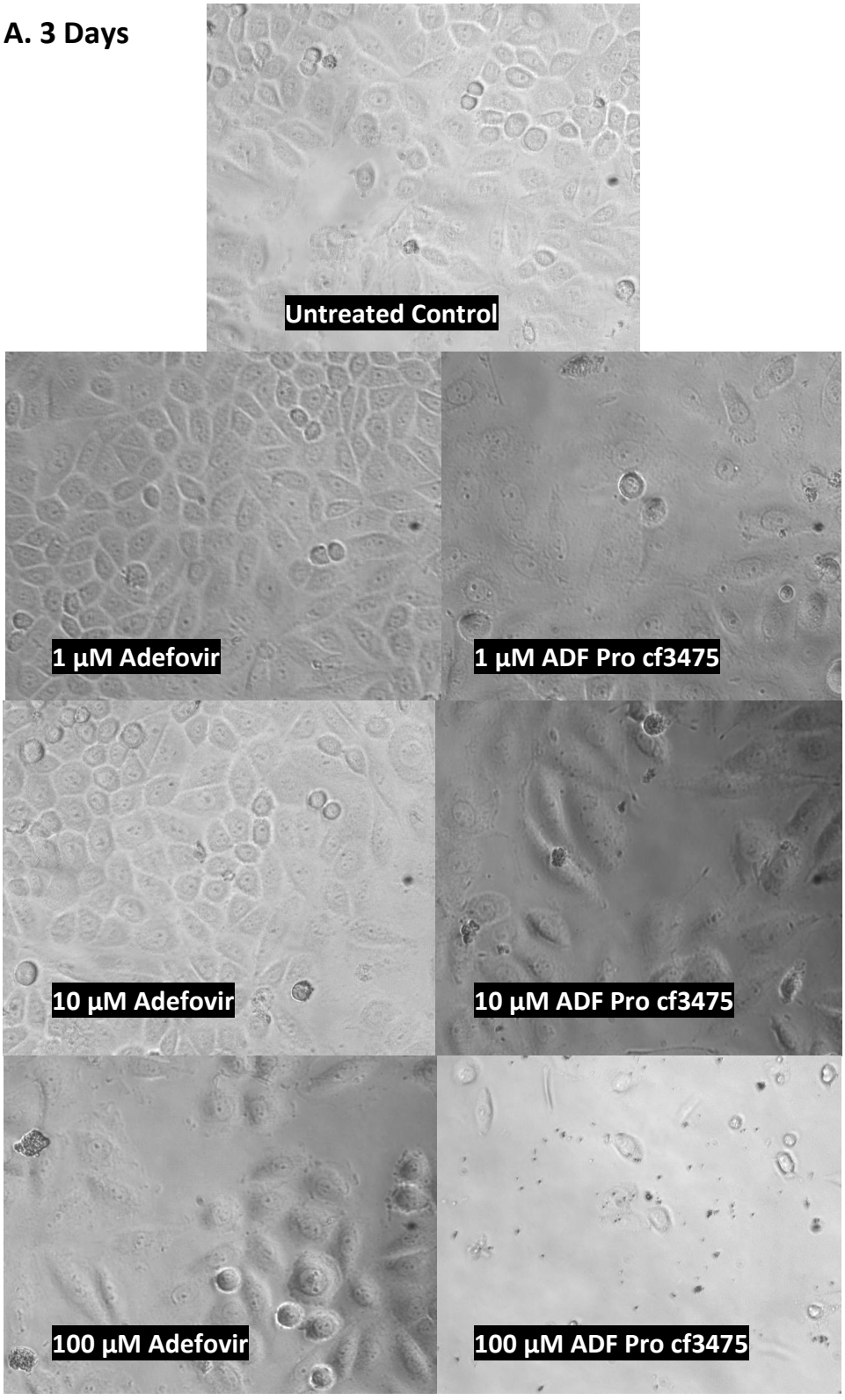
Untreated Control
1 µM Adefovir
1 µM ADF Pro cf3475
10 µM Adefovir
10 µM ADF Pro cf3475
100 µM Adefovir
100 µM ADF Pro cf3475

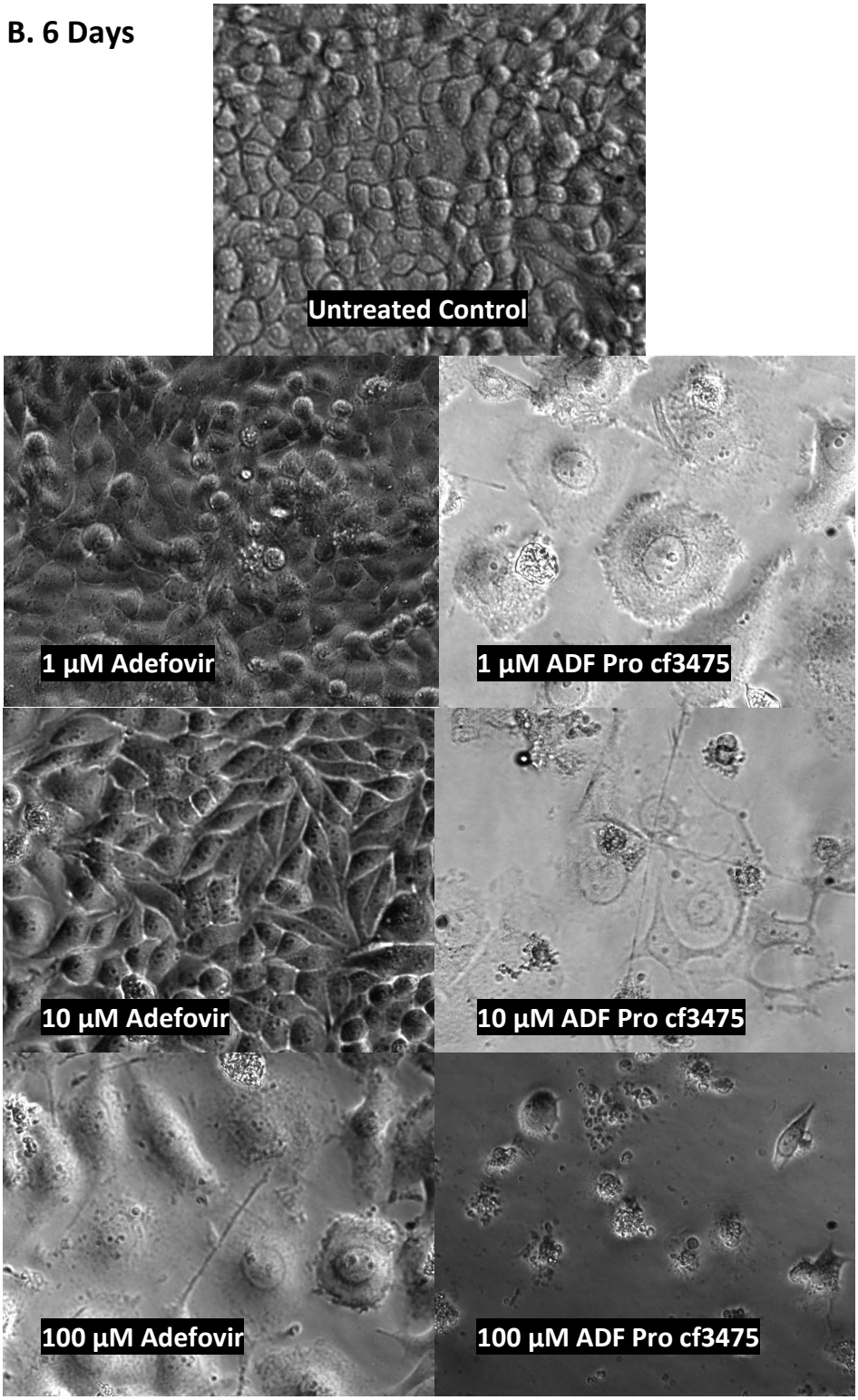

Figure 4.9. SiHa morphology 3 and 6 days post Adefovir and ADF Pro cf3475 treatment

SiHa cell morphology at 320X magnification using bright field microscopy; (A) 3 days, and (B) 6 days post Adefovir and ADF Pro cf3475 treatment. A proportional increase in cell size was observed with increasing concentration of both compounds with the exception of 100 µM ADF Pro cf3475, where cell debris was observed at both time points.

4.3.4. Disease Model Specificity of the Most Effective Compounds

The compounds that displayed the greatest degree of efficacy, ADF Pro cf3475 and ADF Pro cf3476, were further examined at lower concentrations (0.01 to 5 µM) to identify any specificity to cell models representing normal (HEK cells), neoplastic (short term M08 cells) and malignant (SiHa cells) disease types.

SiHa cells were seeded at 5 x 10^2 cells per well in 96 well plates; M08 cells were seeded at 5 x 10^3 cells per well in 96 well plates; HEKs were seeded at 3.5 x 10^4 cells per well in 24 well plates. After an initial attachment period of 24 hours all cell types were treated with 0.01 µM, 0.05µM, 0.1 µM and 1 µM ADF Pro cf3475 in triplicate; and 0.05 µM, 0.1 µM, 1 µM and 5 µM ADF Pro cf3476 in triplicate. Two and 4 days post treatment cell viability was assessed by Trypan blue staining and manual cell counting for each condition in triplicate to calculate viable cell counts per mL. Percentage kill plots were constructed and IC50 values for both compounds were derived and outlined in Table 4.4. Response to treatment with ADF Pro cf3475 and ADF Pro cf3476 did not differ markedly between the normal, neoplastic or malignant cell types. At both time points ADF Pro cf3475 appeared to have lower IC50 concentrations in the 3 cell types compared to ADF Pro cf3476.

Table 4.4. IC50 values for ADF Pro cf3475 and ADF Pro cf3476 in SiHa, M08 and HEK Cells two and four days post Treatment

Cell Line	HPV Status	Phenotype	IC50 ADF Pro cf3475 (µM)		IC50 ADF Pro cf3476 (µM)	
			2 days	4 days	2 days	4 days
SiHa	HPV 16	Malignant	0.17	0.09	1.06	0.83
M08	HPV 16	Neoplastic	0.68	0.05	1.04	0.82
HEK	Negative	Normal	0.08	0.08	0.34	0.30

IC50 values in red text highlight sub micromolar concentrations. IC50 values in green text highlight concentrations of 1 µM or greater.

4.4. Discussion

Cidofovir Specificity and Dose Range Finding

The main finding of the Cidofovir specificity study was that the compound did not produce a specific inhibitory effect in NHIST cell lines compared to HPV negative HEKs. In Cidofovir treated HEK cells at 48 hours the number of viable cells was reduced, but by 96 hours they appeared to have recovered but proliferated in a dose dependant manner. This could perhaps be due to the fact that these cells have functional stress response pathways. The initial assault with the compound may have caused substantial apoptosis but recovery/cell survival pathways may have been reactivated thereafter, which may be why viability increased by 96 hours.

The A09 NHIST cell line grew less efficiently than the M08 cell line. As both cell lines were cultured in the exact same conditions this may have been due to genetic differences between the two cell lines. M08 has a disruption in its *E2* gene, which can result in over-expression of *E6* and *E7*. On the other hand, A09 has an intact *E2* gene, whose protein product can suppress *E6* and *E7*. However, when baseline levels of *E6* and *E7* in the M08 and A09 clones were assessed the difference between them was minimal (Section 3.1.4.; Figure 3.8). There was also a considerable difference in cell morphology between the A09 and M08 cell line. Even though both cells lines were used in the dosing experiment from passages 7 to 10, the A09 cells appeared to resemble earlier passage heterogeneous cells, with morphology closer to cells from the initial biopsy (PC09 cell line; Section 3.1.1.; Figure 3.1 (B)). An IC50 concentration was obtained at 96 hours for A09 cells, but estimation of this value may have been confounded due to low cell counts in the control/untreated cells. The apparent greater sensitivity of M08 cells to Cidofovir may hence only reflect differences in growth rates between the M08 and A09 cell lines. Similarly, the increase in IC50 with time, observed in the HEK cells, may be caused by inaccurate estimation of the IC50 at 48 hours.

With regards to previous published studies, Andrei et al., 1998 , examined IC50 values of Cidofovir in HPV33 transfected cervical keratinocytes (CK-1 cell line) as well as CaSki (HPV16), HeLa (HPV18), SiHa (HPV16) and C33A (HPV negative) transformed cell lines. The authors reported IC50 values in µg/mL at 3 and 7 days post Cidofovir treatment using cell

counts as determined by a Coulter counter. For the SiHa, HeLa and CaSki HPV positive transformed cell lines they reported IC50 values between 26 and 143 μg/mL on day 3 and IC50 values between 0.7 and 2 μg/mL on day 7. For the HPV33 positive cervical keratinocytes they reported an IC50 of 52 μg/mL on day 3 and 0.7 μg/mL on day 7. Finally they reported an IC50 value of 32 μg/mL on day 3 and 1.4 μg/mL on day 7 in C33A cells. From this data it can be seen that the IC50 of Cidofovir in each cell line drops considerably at day 7 compared to day 3. This is a trend which is also seen in the M08 and A09 cell line IC50 values between day 2 and day 4. The IC50 values on day 3 in the Andrei et al. study were much higher than the IC50 values observed on day 4 for the M08, A09 and HEK cell lines in this study.

A different study by Abdulkarim et al., 2002 , examined Cidofovir selectivity in HPV positive cell lines in terms of mechanism of action rather than cell viability. The authors examined induction of p53 and pRb protein levels following Cidofovir treatment in Me180 and HeLa (both HPV positive) and C33A (HPV negative) cell lines, and observed induction of p53 protein in HeLa cells 3 days post treatment with 1, 10 and 100 μg/mL Cidofovir but not in C33A cells. However, they had previously concluded through a p53 functional assay in yeast that *TP53* in C33A was mutated, which may be a reason for the apparent selectivity.

A strength of the Cidofovir specificity study includes the HEK cells as the HPV negative control cell line. The HEK cells are untransformed and thus are a better genotypic representation of “normal” HPV negative cells that would occur *in vivo.* Abdulkarim et al., 2002, identified specificity of Cidofovir to HPV positive cells using transformed C33A cells as a HPV negative counterpart. C33A cells are derived from a cervical cancer and while HPV negative they cannot be considered an accurate model of “normal” HPV negative cells. Furthermore, as a transformed cell line, C33A cells could be resistant to drug treatment due to mutated DNA damage/stress response pathways or up or down regulation of nucleoside metabolising enzymes. Abdulkarim et al., 2002, examined the *TP53* status of the cell lines they used to assess cellular response to Cidofovir and found that the C33A cell line had a mutation in this gene. Consequently, another strength of this study was that M08 and A09 cell lines were previously found to be *TP53* wild-type and as

the HEKs were primary human epidermal keratinocytes derived from a neonate of less than two weeks old they are unlikely to carry a *TP53* mutation. Additionally, as this study was to model Cidofovir treatment in vulval and vaginal intraepithelial neoplasia rather than invasive cancer, the M08 and A09 NHIST cell lines were more similar models of the disease compared to other HPV positive transformed cell lines.

A limitation of the Cidofovir specificity study includes the broad range of Cidofovir concentrations used. A narrower range of concentrations would give more precise IC50 values. M08 and A09 cells were treated with an extra concentration of Cidofovir (5 µM) as previous work had suggested Cidofovir may cause 50% growth inhibition in these cells with less than 10 µM. Additionally, HEK cells were assayed in duplicate rather than triplicate as work with the HEKs was carried out in 24 well plates rather than 96 well plates and the larger volumes meant a decrease in throughput. However, as the main reason for using the HEKs was to examine if Cidofovir had any effect on a HPV negative untransformed cell line, the duplicate repeats were deemed sufficient. Nevertheless, although the HEKs are a better representation of a HPV negative cell line in comparison to C33A cells, they may not be the best representation of a HPV/neoplasia-free vulval and vaginal cell line as they are primary cells derived from neonatal foreskin. A better model to test the specificity of Cidofovir may be by transfection of a portion of the HEKs with HPV, therefore having two genetically identical cell lines but one HPV transformed and the other HPV negative. The final disadvantage of the study was that it was carried out in 2D monolayer cell culture. This is not representative of an *in vivo* state due to lack of physical barriers and immune system and thus would not exemplify a true VIN lesion. Better models would include raft culture, which would show drug effect on the different layers of epithelium or *in vivo* animal models, which would have the advantage of having an immune system and ability to produce an inflammatory response.

Future work from the Cidofovir specificity study would involve a better model to measure the specificity of the compound. Either HPV transfected HEKs in monolayer culture or raft cultures to obtain a better *in vivo* representation. To conclude on the Cidofovir specificity study, selectivity of the compound to HPV immortalized cells was not demonstrated in this model but IC50 values for use in the mechanism of action studies were obtained.

Examination of Cyclic Analogues of Cidofovir

The main finding of the cyclic Cidofovir ProTide analogue study was that the cyclic Cidofovir compounds produced a 50% growth inhibitory effect in the HeLa cell line compared with unmodified Cidofovir, which did not produce a 50% growth inhibitory effect at either time point in HeLa cells. Contrastingly, in the C33A cell line, unmodified Cidofovir appeared to produce 50% inhibition at lower concentrations, at both time points, compared to the cyclic compounds. There was no HPV specificity or pattern with regards to response to treatment between the two lines with all three compounds. As unmodified Cidofovir and the two cyclic compounds had an inhibitory effect on the C33A cells, it would appear this cell line was more sensitive to treatment.

Similar studies have compared Cidofovir analogues, both cyclic and acyclic, to unmodified Cidofovir and have found variable results depending on analogue type and experimental model used. Hostetler et al., 2006 , synthesized three novel analogues of Cidofovir and found all three to be more efficient at arresting cell proliferation in the cervical cancer lines, CaSki, Me-180 and HeLa. Cell proliferation was measured by an XTT assay, which is a colorimetric tetrazolium salt based assay that detects cellular metabolic activities similar to MTS (Scudiero et al., 1988). Hostetler et al., 2006, found two of the novel compounds to be up to 17,000 times more active than Cidofovir at inhibiting the proliferation of cervical cancer cells. However, they did not demonstrate specificity to HPV positive cell lines as C33A cells and primary human foreskin fibroblasts were also susceptible. They speculated that the increase in efficacy was due to increased cellular uptake of the novel analogue compounds.

In a different study by the same group (Beadle et al., 2002), hexadecyloxypropyl and octadecyloxyethyl novel analogues of cyclic Cidofovir and Cidofovir were synthesized and found to have 2.5- to 4-log increases in anti-CMV activity when compared to their respective parent compounds. They also suggested that the increase in anti-viral activity of these novel compounds may be partially due to greater cell permeability. Anti-viral activity was determined by a DNA reduction assay with MRC-5 human lung fibroblast cells or by a plaque reduction assay with human foreskin fibroblast cells infected with different strains of HCMV. Although the novel cyclic analogues were much more active than parent

cyclic Cidofovir, they were less active than the corresponding novel analogues of Cidofovir. Both cyclic Cidofovir and Cidofovir parent compounds had similar activities.

Both of these *in vitro* studies (Beadle et al., 2002, Hostetler et al., 2006) agree that analogues of Cidofovir have greater anti-proliferative activities compared to their parent compounds. With regards to cyclic Cidofovir (Beadle et al., 2002), the novel cyclic analogues appeared to be considerably more active than parent cyclic Cidofovir and Cidofovir, where both parent cyclic Cidofovir and Cidofovir had the same activities. These results differ to the data presented here in that cyclic Cidofovir and Cidofovir both displayed contrasting activities in the HeLa and C33A cell lines. Additionally, in the study presented here, the cyclic amidate analogue appeared to be less active, albeit not by much, than parent cyclic Cidofovir in C33A cells. However, when evaluating these differences it should be highlighted that the study carried out by Beadle et al., 2002 used live CMV infected MRC-5 human lung fibroblast cells/human foreskin fibroblast cells, whereas the study presented here was carried out in HPV transformed HeLa cells and transformed C33A cells, both derived from cervical carcinomas. Therefore, the compounds may have been metabolized differently by different viruses/different cell types. As it is already known that ANP compounds have a greater affinity to virus encoded polymerases as opposed to host cell polymerases (Kramata et al., 1996 and references therein), the molecular mechanism of cellular inhibition may have differed between compounds and cell models, giving rise to the differences in compound efficiencies.

Another study by McKenna et al., 2005 , synthesized three novel analogues of cyclic Cidofovir and examined their permeability relative to parent cyclic Cidofovir and Cidofovir in a rat oral bioavailability assay examining single pass intestinal drug perfusion with portal vein blood collection. They found a 10 – 20 fold increase in permeability for the cyclic analogue derivatives relative to Cidofovir and cyclic Cidofovir. Aside to this, Cidofovir exhibited a higher rate of perfusion in comparison to unmodified cyclic Cidofovir, which was interesting as part of the negative charge on Cidofovir is eliminated by cyclization (McKenna et al., 2005), therefore in theory it would be expected that cyclic Cidofovir has the potential to be more permeable than acyclic Cidofovir. These results complemented

those of the Beadle et al., 2002 study, where they found increased efficacy of novel cyclic Cidofovir analogues by their ability to inhibit CMV infected cells.

Due to the differences in the results presented here and the results of published studies, the chemical structure of the cyclic Cidofovir amidate was re-evaluated and appeared to have degraded to its unmodified form by a hydrolysis reaction, with additional probable hydrolysis of the amino acid. It may be tentatively suggested that the hydrolysis reaction occurred during the storage (4°C) of the compound as the NMR was carried out on stock compound, not supernatant. Indeed, hydrolysis of an ester of cyclic Cidofovir has been reported as a possible product at 37°C (Oliyai et al., 1999).

Because the cyclic Cidofovir amidate analogue had degraded, a valid conclusion cannot be made as to whether unmodified Cidofovir, cyclic Cidofovir or the cyclic Cidofovir ProTide amidate was more effective at inhibiting cell growth. The HeLa cell experiment suggested the cyclic analogues were more effective but the C33A cell assay suggested the unmodified form was better at inhibiting cell growth. Future work would involve re-evaluating all compounds in their non-degraded forms.

Adefovir and Tenofovir ProTide Screen

The Adefovir and Tenofovir ProTide study evaluated the ability of ProTide analogues of these adenine derivative compounds to inhibit the growth of HPV positive and negative, transformed and untransformed cells. It also examined the effect of these compounds on cell size and morphology. The ProTide compounds were far more efficient at inhibiting growth of both HPV positive and negative cell lines in comparison to their parent compounds; most likely due to increased cellular permeability. This was seen most in the Adefovir ProTides as both daughter compounds exhibited consistent sub-micromolar IC50 values, with prominent increases in cell size and atypical morphology. There was no specificity observed for HPV positive cell lines, in fact the HPV negative cell line, C33A, appeared most sensitive. The Adefovir parent compound produced a greater effect than the Tenofovir parent compound. The two compounds that displayed greatest efficacy, ADF Pro cf3475 and ADF Pro cf3476, were further examined in cell lines representing normal, neoplastic and malignant cell types, but again no specificity was observed.

Several reports suggest that Cidofovir may be effective in treatment of HPV associated disease (Tristram and Fiander, 2005, Abdulkarim et al., 2002, Sirianni et al., 2005, Andrei et al., 1998, Andrei et al., 2001). In contrast, the ProTide compounds were completely novel and no previous studies had been carried out to examine their possible therapeutic effects in HPV positive experimental models of disease. However, collaboration with the Rega Institute for Medical Research in Leuven, Belgium, allowed for the examination of the ProTides and their parent compounds in HIV-1, HIV-2, herpes simplex virus type 1 (HSV-1), herpes simplex virus type 2 (HSV-2), CMV, varicella-zoster virus (VZV) and vaccinia virus infected cells (Pertusati et al., Submitted for publication). All the ProTide analogues were far more effective than their parent compounds and had considerable anti-HIV activity at nanomolar concentrations. In contrast to the current study, the Tenofovir ProTides had an even greater effect than the Adefovir ProTides. With regards to the DNA virus infected cells, the Tenofovir ProTides also proved to be more efficient than the Adefovir ProTides. As well as virus infected cells this study also examined inhibition by all compounds in murine leukemia cells (L1210), human $CD4^+$ T-lymphocyte cells (CEM) and HeLa cells. The results showed low micromolar IC50 values in the Tenofovir series and sub-micromolar IC50 values in the Adefovir series. The latter results were consistent with the findings of this study, where the analogues, particularly those of Adefovir, also produced a profound inhibitory effect on the HPV negative C33A cells.

Other studies have looked at Adefovir and Tenofovir treatment in HPV associated lesions. For example, Christensen et al., 2000 , examined Adefovir and Tenofovir in a cottontail rabbit papillomavirus (CRPV) domestic rabbit model and found that topical treatment with Adefovir had a marked effect on papillomas whereas Tenofovir showed no effect. Similarly, in the data presented here, Adefovir parent compound produced an anti-proliferative effect on both SiHa and C33A cell lines, whereas Tenofovir produced a growth inhibitory effect on the C33A cell line alone. This would suggest that Adefovir had a greater potency at inhibiting HPV positive cells in comparison to Tenofovir. To add to this, the Adefovir ProTide analogues produced the most profound anti-growth effects on all three cell lines examined, with the lowest IC50 concentrations out of all compounds

examined. This again indicates that the Adefovir derived compounds were more efficient at inhibiting the growth of the cells described in this study.

Historically, Adefovir and Tenofovir have been used as anti-viral compounds, with Adefovir being approved as an anti-HBV compound and Tenofovir for the treatment of both HBV and HIV (De Clercq, 2011b). These compounds produce anti-viral effects by inhibiting viral polymerases (Kramata et al., 1996 and references therein). However, In HPV associated disease episomal HPV replicates using host cell DNA polymerase (Park et al., 1994). Additionally, the risk of episome loss and integration of HPV into the human genome increases as the disease progresses (Pirami et al., 1997). ANP ProTide analogues have the negative charges on their phosphate groups masked to allow for more efficient cell permeability thus increasing their activity (Serpi et al., 2013). Once inside the target cell the blocking group is enzymatically cleaved to release the ANP, where it can be further phosphorylated to its active tri-phosphate form (Hecker and Erion, 2008). From the data presented here the exact mechanism of action of the Adefovir and Tenofovir ProTides cannot be deduced. The analogues produced a profound growth inhibitory effect on both HPV positive and negative cell lines, therefore specificity to HPV positive cells was not observed at the concentrations used. From the morphology of the treated cells, either cell senescence or necrosis could be deduced from their enlarged, flattened and vacuolar appearance. Cell senescence may have occurred via DNA damage (Di Leonardo et al., 1994) caused by possible genotoxic stress induced by the analogues. Similarly, necrosis may also have resulted by compound induced DNA strand breaks and Poly (ADP-ribose) polymerase (PARP) activation. Over-activation of PARP in response to DNA damage can result in decreased ATP, which would lead to cell death via necrosis rather than apoptosis (Ha and Snyder, 1999).

Strengths of this study include use of multiple transformed cell lines; SiHa (HPV16 positive), HeLa (HPV18 positive) and C33A (HPV negative). The HPV negative cell line allowed for the examination of possible specificity to HPV positive cell lines. Each concentration of compound was examined in triplicate and parent and daughter compound dosing were set up and analysed at the same time in the same controlled conditions. Furthermore, in the primary ProTide screen the daughter compounds

generally displayed a consistency in IC50 values (with the exception of TNF Pro cf3473 and the lower values observed for most compounds in the C33A cell line). Also, 3 different responses to treatment were examined; Cell viability by 7-AAD flow cytometry, cell size by the forward scatter parameter using flow cytometry and cell morphology by manual evaluation of cell appearance by light microscopy. These 3 components combined made for a more comprehensive evaluation of cell line response to treatment with the test compounds. After the ProTide screen, the 2 most effective compounds were further examined in three more cell lines; HEKs, M08 and SiHa at lower concentrations to gain a better indication of true IC50 values and specificity to normal and transformed cell types. This further evaluation was carried out using Trypan blue dye exclusion manual cell counting; a second method of assessment of cell viability to complement the data produced by the 7-AAD automated flow cytometry.

Weaknesses of this study include the fact that only 3 concentrations were examined for each compound. More concentrations would give more accurate IC50 values but as this study was a primary screen and as the ProTide compounds had never been examined before, 1, 10 and 100 μM were selected as a wide range of concentrations to examine growth inhibitory effects. Another weakness and probably the most important was that 2D/monolayer cell culture models are not representative of an *in vivo* state, in particular layered differentiated epithelium, which would be better represented by 3D/raft culture or an *in vivo* animal model.

To conclude on the ProTide analogue study, the hypothesis that the ProTide compounds were more effective at inhibiting HPV transformed cells in comparison to their parent compounds proved true. This may be due to more efficient cell membrane permeability. There was no specificity found for HPV positive cells, neoplastic cells or malignant cells. As a monolayer cell culture system does not contain any barriers, such as cornified epithelium, it cannot be said for certain how these compounds would be processed *in vivo.* Further work with the analogues would involve cytotoxicity evaluation and possible mechanism of action studies examining cell senescence and necrosis. Examination of the compounds in a HPV virus infected 3D/raft culture would also prove useful to see if they had an effect or specificity through the entire epithelial layer. Finally, if cytotoxicity

studies proved non-toxic, examination of the compounds in topical formulation on neoplastic lesions in animal models might also prove informative.

Several conclusions were made from the data presented in this chapter. The first conclusion was that Cidofovir did inhibit the growth of NHIST cell lines. However, the inhibitory effect caused by Cidofovir was not specific to HPV immortalized cell lines as the compound also had an effect on normal HPV negative cells. The second conclusion was that Cidofovir and its cyclic analogues displayed variation in growth inhibition of HPV18 transformed HeLa cells and the HPV negative transformed C33A cells. However, the cyclic Cidofovir amidate analogue appeared to have degraded upon re-evaluation of its chemical structure, which invalidated these findings. The third conclusion was that ProTide analogues of Adefovir and Tenofovir had a much greater inhibitory effect on cell growth in comparison to the parent compounds from which they were derived; however this effect did not appear specific to HPV positive cells.

5. Mechanism of Action of Cidofovir

Several published studies have attempted to determine the mechanism of action of Cidofovir. The mechanism of action of this acyclic nucleoside phosphonate analogue is well documented with regards to CMV infection. Once inside its target cell Cidofovir is phosphorylated twice to its active triphosphate form, which structurally mimics deoxycytidine triphosphate (dCTP). After the incorporation of two consecutive Cidofovir diphosphate molecules by CMV DNA polymerase, chain elongation is inhibited and virus replication is arrested (Xiong et al., 1997). This mechanism is consistent with the finding that the specific anti-viral activities of acyclic nucleoside phosphonates are attributed to the higher affinity of the compounds towards viral polymerases rather than host polymerase (Kramata et al., 1996, De Clercq and Holy, 2005 and references therein). However, as HPV replication uses host cell DNA polymerase, the classical mechanism of action of Cidofovir is not likely to be relevant in HPV associated disease. If Cidofovir is incorporated into both human and viral DNA it will most likely result in chain termination and stalling of replication forks, which may result in a stress or DNA damage response. Various mechanisms of action for Cidofovir in HPV associated disease have been proposed and include; inhibition of E6 and E7 oncoproteins (Amine et al., 2009, Sirianni et al., 2005), re-accumulation of p53 and pRb (Snoeck et al., 2001a), induction of apoptosis (Snoeck et al., 2001a, Donne et al., 2007) and cell cycle arrest (Abdulkarim et al., 2002). Taking into account these findings and examining them alongside the biology of HPV pathogenesis, they would all appear to be linked; repression of E6 and E7 oncoproteins would lead to re-accumulation of p53 and pRb and providing that the p53 and pRb signalling pathways are still functionally intact, would in turn lead to induction of apoptosis and/or cell cycle arrest.

Radiation treatment alone can also induce a p53 dose dependant response both *in vitro* and *in vivo* (Fei and El-Deiry, 2003). Several studies (Abdulkarim et al., 2002, Sirianni et al., 2005) have shown that Cidofovir can radiosensitize HPV positive cell lines and augment a p53 response when both treatments are combined. If correct, radiosensitisation might aid clinical management of HPV associated lesions.

This chapter describes the results of experiments that were designed to determine the mechanism of action of Cidofovir and to investigate the molecular effects of combining Cidofovir treatment with radiation, a known inducer of a p53 response, in NHIST cell lines. To examine the mechanism of action of the compound M08, A09 and HEK cells were cultured in their respective IC50 concentrations of Cidofovir (5 μM for M08, 21 μM for A09 and 6 μM for HEKs) for 6 days. At the same time M08, A09 and HEK cells were also cultured in Cidofovir free media. At -24 hours (1 day before treatment) both sets of cells were plated into 6 cm tissue culture dishes and allowed to adhere for 24 hours. At 0 hours, the cells that had been cultured in Cidofovir free media were treated with their IC50 concentration of Cidofovir, 2 Gy gamma radiation or 20 Gy gamma radiation. The cells that were previously cultured in Cidofovir spiked media were subjected to 2 Gy radiation. Two Gray radiation was used as it constitutes a clinically relevant dose (Abdulkarim et al., 2002). As the main hypothesis of the mechanism of action studies was that Cidofovir could reactivate a p53 response in HPV positive cell lines, 20 Gy radiation was used as a positive control as such a dose has been found to induce p53 accumulation in a variety of cell lines and other experimental models (Cmielova et al., 2012, Sun et al., 2005, Guo et al., 2013). The reason for pre-treating cells for 6 days with Cidofovir was to allow for ample accumulation of the compound in the cells, and in theory incorporation into the cellular DNA, before treatment with radiation. Additionally, a portion of cells cultured in the absence of Cidofovir were kept in culture to serve as negative untreated control cells for each cell type. These dosing conditions are outlined in Figure 5.1.

After 12, 36 and 72 hours of treatment all cells had protein and RNA extracted. These time points were used as significant differences in cell number were not generally observed until four days post Cidofovir treatment. Therefore, the molecular processes leading to the growth inhibitory effect would have occurred prior to day four.

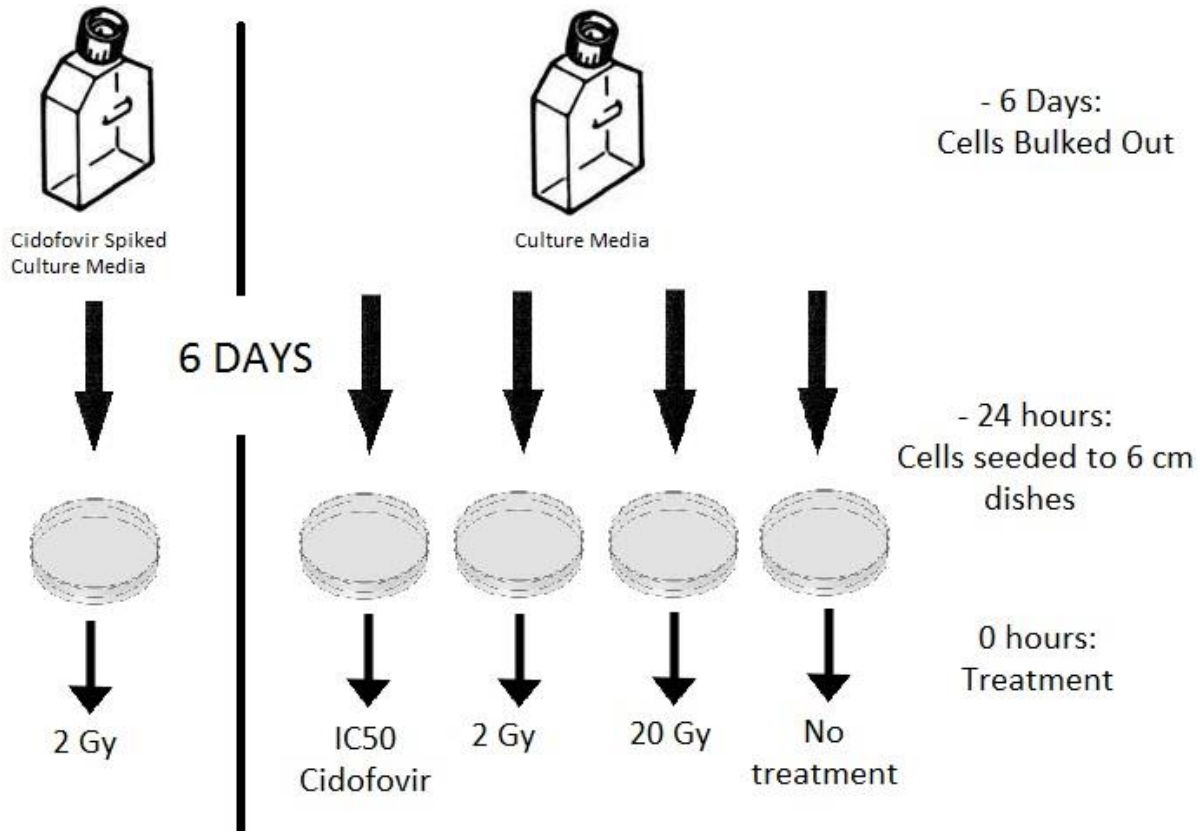

Figure 5.1. Cell Culture and Treatment Regimen for M08, A09 and HEK Cells for Mechanism of Action of Cidofovir Studies

M08, A09 and HEK cells were cultured in their respective IC50 concentrations of Cidofovir (5 μM for M08, 21 μM for A09 and 6 μM for HEKs) for 6 days. Additionally, M08, A09 and HEK cells were concurrently cultured in Cidofovir free media. At -24 hours (1 day before treatment) both sets of cells were plated into 6 cm tissue culture dishes and allowed to adhere for 24 hours. At 0 hours, the cells that had been cultured in Cidofovir free media were treated with their IC50 concentration of Cidofovir, 2 Gy gamma radiation or 20 Gy gamma radiation. Additionally, a portion of cells cultured in the absence of Cidofovir were kept in culture to serve as negative untreated control cells for each cell type. The cells that were previously cultured in Cidofovir spiked media were subjected to 2 Gy radiation. Cells in all treatment conditions had protein and RNA extracted 12, 36 and 72 hours post treatment.

5.1. Cidofovir Induction of Apoptosis and Effect of Combining Treatment with Radiation

Hypothesis

i. *Cidofovir inhibits growth of NHIST cell lines by induction of apoptosis*
ii. *Cidofovir can be used as a radiosensitizer and augment an apoptotic response in NHIST cell lines*

The dose response observed in Cidofovir treated NHIST cell lines (results section 4.1) was examined in order to further clarify the mechanism of action of the compound in these cell models. After IC50 values were determined in M08 and A09 cell lines, the possibility that Cidofovir produced an inhibitory effect by causing apoptosis was investigated. Twenty Gray gamma radiation was used as a positive control (Petit-Frere et al., 2000) and the combined effects of Cidofovir and 2 Gy gamma radiation were also assessed as 2 Gy equates to a clinically relevant dose (Abdulkarim et al., 2002). A caspase-3 activity assay kit, which used a fluorogenic substrate (Ac-DEVD-AMC) for activated caspase-3 enzyme was used to quantify apoptotic cells in all sets of conditions for each cell type at the three time points. Positive and negative assay controls were used, which included AMC and water respectively. After the caspase-3 activity assay, cleaved caspase-3 protein levels were also measured by Western blotting and densitometry.

5.1.1. Cleaved Caspase-3 Activity

The results of the caspase-3 activity assay, measured by relative florescence units (RFU), for M08, A09 and HEK cells are outlined in Figure 5.2.

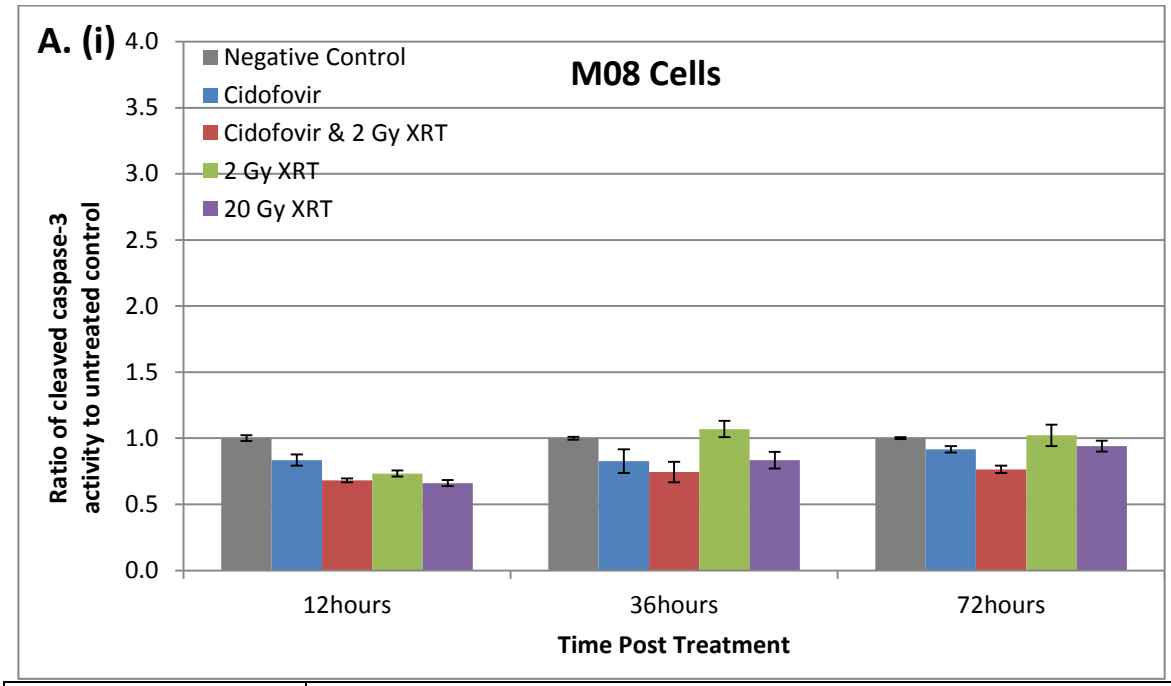

A. (ii) **Treatment Condition**	p-value for change in cleaved caspase-3 activity between untreated control cells and each treatment condition at 12, 36 and 72 hours post treatment for M08 cells		
	12 hours	**36 hours**	**72 hours**
Cidofovir	0.0141	0.1013	0.0149
Cidofovir + 2 Gy XRT	0.0001	0.0165	0.0002
2 Gy XRT	0.0004	0.2533	0.7638
20 Gy XRT	0.0001	0.0286	0.1484

B. (i)

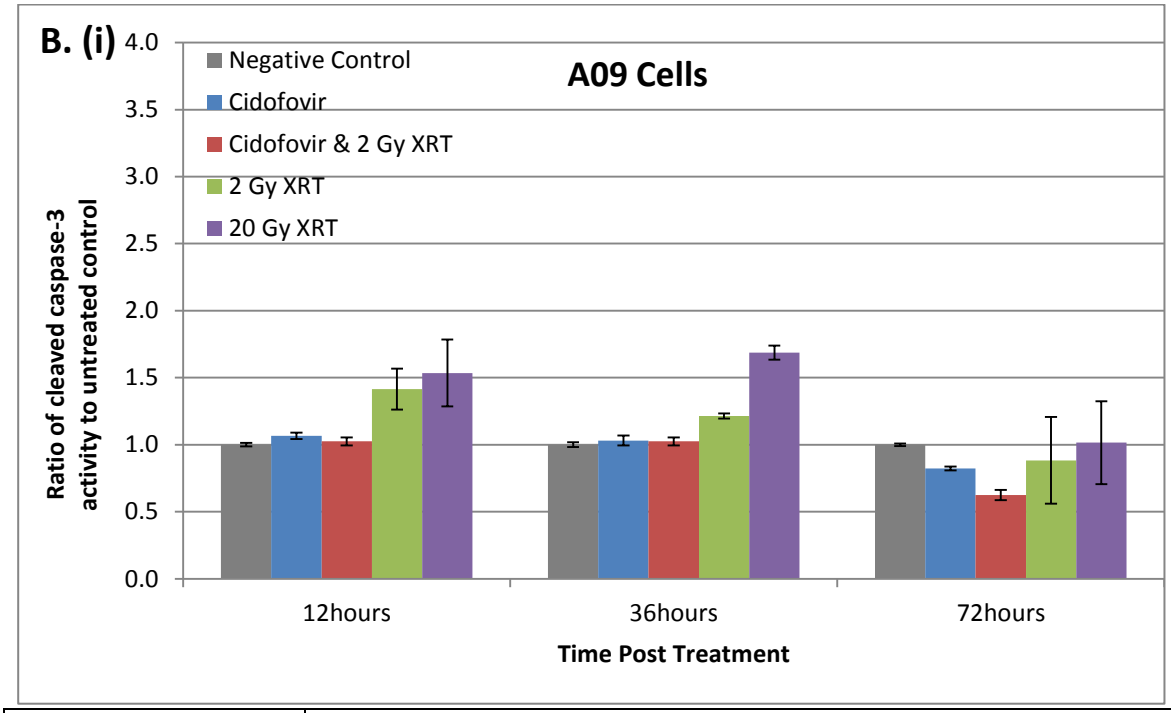

B. (ii) **Treatment Condition**	p-value for change in cleaved caspase-3 activity between untreated control cells and each treatment condition at 12, 36 and 72 hours post treatment for A09 cells		
	12 hours	**36 hours**	**72 hours**
Cidofovir	0.0513	0.4754	0.0001
Cidofovir + 2 Gy XRT	0.462	0.5008	0.0001
2 Gy XRT	0.0231	0.0005	0.6834
20 Gy XRT	0.0512	0.0001	0.9532

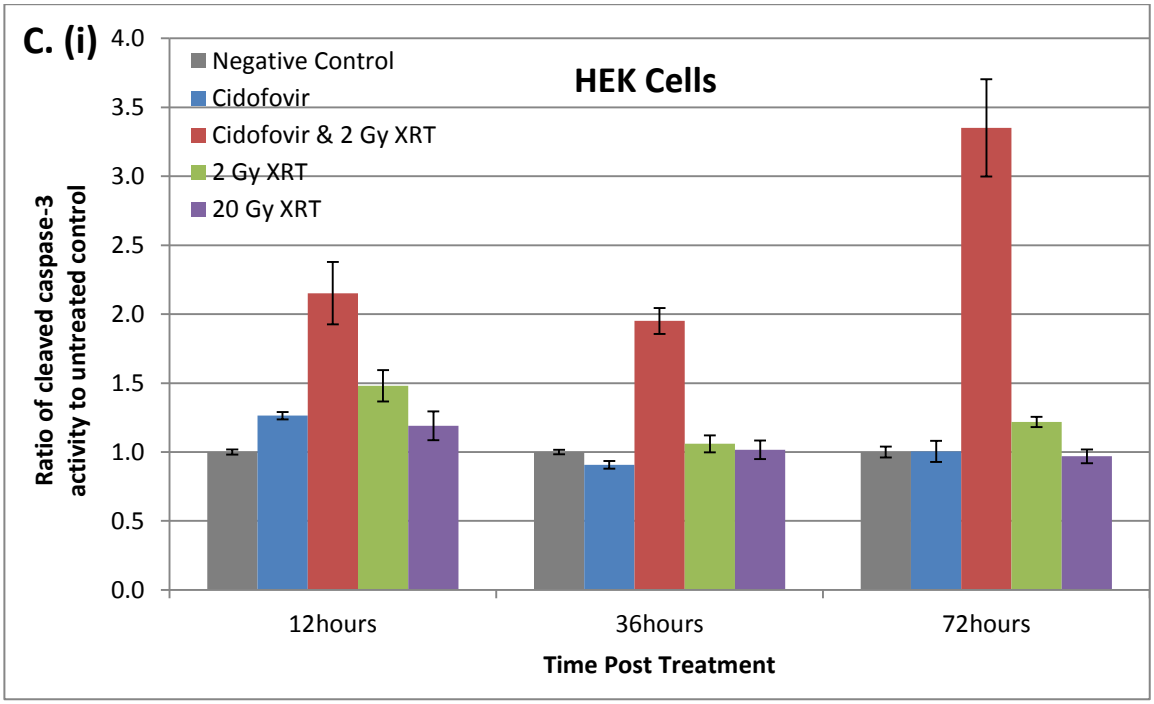

C. (ii) Treatment Condition	p-value for change in cleaved caspase-3 activity between untreated control cells and each treatment condition at 12, 36 and 72 hours post treatment for HEK cells		
	12 hours	**36 hours**	**72 hours**
Cidofovir	0.0002	0.0298	0.9601
Cidofovir + 2 Gy XRT	0.0022	0.0001	0.0006
2 Gy XRT	0.0044	0.3299	0.0124
20 Gy XRT	0.0868	0.8016	0.6416

Figure 5.2. Cleaved Caspase-3 Activity in M08, A09 and HEK cells 12, 36 and 72 hours post treatment with Cidofovir, Cidofovir combined with 2 Gy, 2 Gy and 20 Gy radiation

A. (i), B. (i) and C. (i) represent cleaved caspase-3 activity plots for each treatment condition normalised to that of the untreated control samples for M08, A09 and HEK cells respectively. Cleaved caspase-3 activity was measured by RFU with excitation at 380 nm and emission at 470 nm using a cleaved caspase-3 activity kit (Cell Signalling, Massachusetts, USA). Each treatment condition was measured in duplicate intraexperimental repeats in 2 independent experiments. XRT = radiotherapy. Error bars represent SEM of 4 repeat values. The tables in A. (ii), B. (ii) and C. (ii) show p-values for each corresponding cleaved caspase-3 activity plot for M08, A09 and HEK cells respectively. p-values were calculated for differences in cleaved caspase-3 activity between the untreated control samples and each treatment condition for each time point in the three cell lines using an unpaired two-tailed Student's t-test with 95% confidence intervals (GraphPad QuickCalcs software, GraphPad Software, Inc., California, USA). n = 4 for each condition. p-value < 0.05 (red text) = the difference in cleaved caspase-3 activity is statistically significance. p-value > 0.05 (green text) = the difference in cleaved caspase-3 activity is not statistically significant.

The M08 data set indicated a significant reduction in caspase-3 activity in all conditions compared with the untreated cells 12 hours post treatment. A similar trend was observed at 36 and 72 hours post treatment with a slight increase in caspase-3 activity at these time points in 2 Gy treated M08 cells; however, this increase was not significantly different to the untreated control samples at these time points.

In contrast to the M08 line, the A09 line did show increased caspase-3 activity compared with the negative control at 12 and 36 hours in the 2 and 20 Gy treated cells. However, the response was diminished by 72 hours. No change in caspase-3 activity was observed for Cidofovir and Cidofovir combined with 2 Gy treated cells at 12 and 36 hours post treatment; however, caspase-3 activity was significantly reduced 72 hours post treatment with these particular conditions.

Induction of caspase-3 activity was greatest in the HEKs, particularly in the combined treatment samples at each time point. At 12 hours, with the exception of the 20 Gy treated cells, all treatment conditions had significantly increased levels of caspase-3 activity compared to the untreated cells, however, this response diminished thereafter (except in the combined treatment cells).

In terms of the actual cleaved caspase-3 activity assay, positive control AMC (supplied with the kit) was highly fluorescent, which indicated that the reagents used for the assay were all working correctly.

5.1.2. Western Blotting for Total Cleaved Caspase-3

Cleaved caspase-3 Western blot images and corresponding densitometry plots using the same cell lysates that were used in the caspase-3 activity assay are outlined for the M08 and A09 cell lines in Figure 5.3. As HEK viable cell number decreased considerably after radiotherapy there was not sufficient protein concentrations to carry out Western blotting on this material.

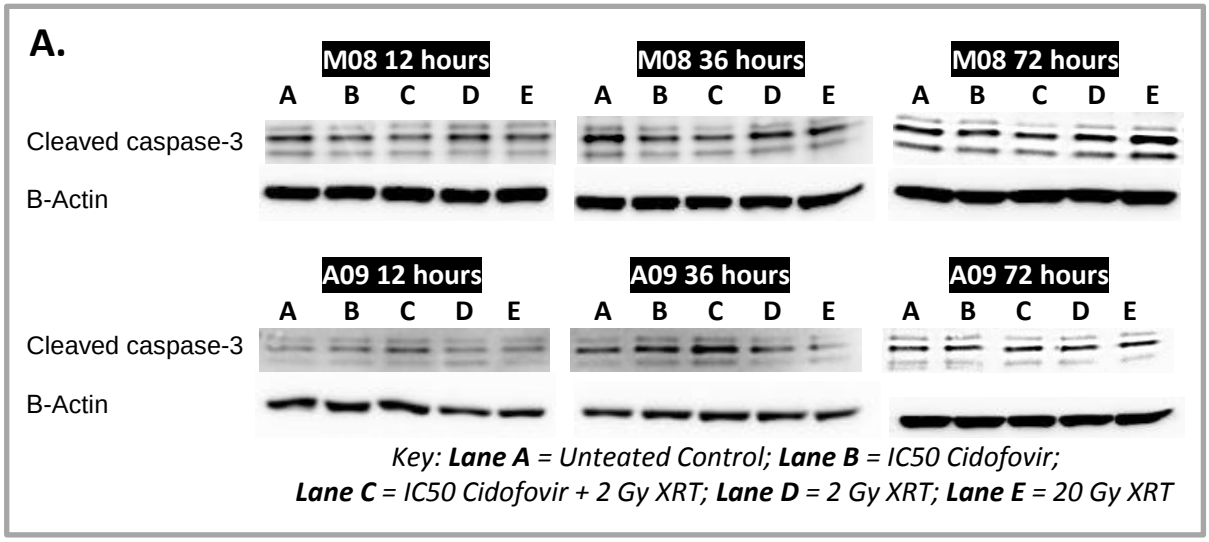

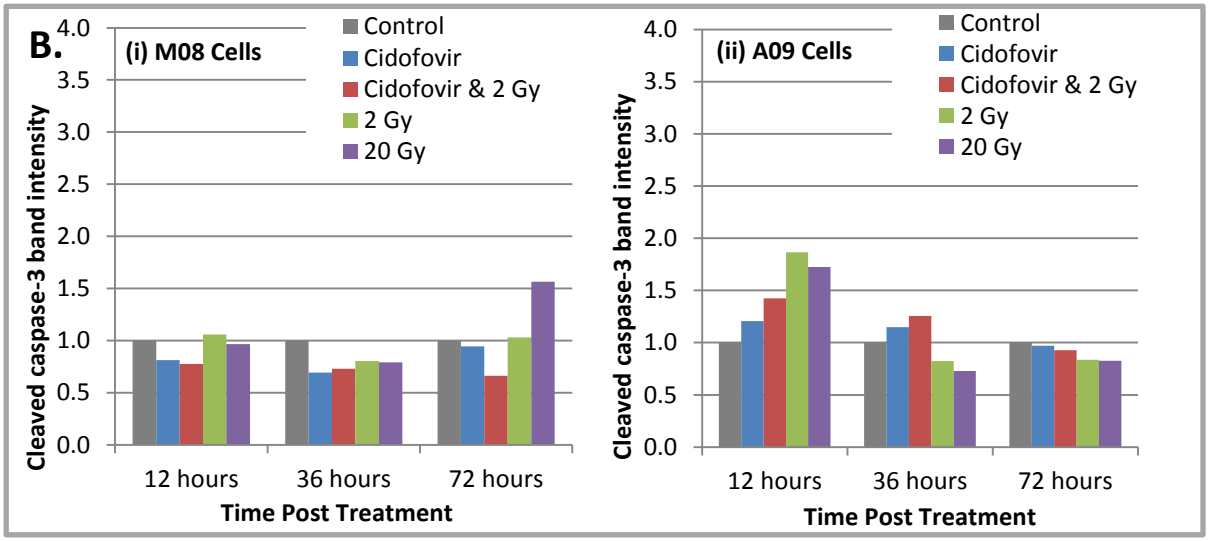

Figure 5.3. Cleaved Caspase-3 Western blot results for M08 and A09 Cells 12, 36 and 72 hours post Treatment with Cidofovir, Cidofovir combined with 2 Gy, 2 Gy and 20 Gy radiation

(A) Cleaved caspase-3 and corresponding β-actin Western blot images 12, 36 and 72 hours post treatment. Cleaved caspase-3 was imaged using a 30 minute exposure time. β-Actin was imaged using a 1 minute exposure time on the same membrane. The cleaved caspase-3 protein band was confirmed to be 17/19 kDa in size and the β-Actin protein band was confirmed to be 45 kDa in size using a MagicMark™ XP Western Protein Standard. The MagicMark™ XP Western protein standard and specificity of both antibodies can be seen in appendix 8. (B) Densitometry plots for cleaved caspase-3 band intensity for (i) M08 cells and (ii) A09 cells corresponding to Western blot membrane images in (A). Cleaved caspase-3 band intensity was first normalized to the corresponding intensity for β-Actin, before further normalization to the untreated control band for each time point. It was not possible to repeat this experiment due to insufficient protein concentrations; therefore n = 1.

A similar pattern observed in the caspase-3 activity assay was found in the cleaved caspase-3 Western blot results for the M08 cell line. In the A09 cell line an increase in cleaved caspase-3 levels was observed in the Western blot data for all treatment conditions at 12 hours; and in the Cidofovir and Cidofovir combined with 2 Gy radiation treatment conditions at 36 hours. Western blotting for cleaved caspase-3 was carried out in one single experiment due to insufficient protein concentrations. As the cleaved caspase-3 activity assay was carried out with 2 intra-experimental repeats on two separate occasions the results produced from the cleaved caspase-3 activity assay are more reliable in comparison to the cleaved caspase-3 Western blot data.

5.2. Transcription of Apoptotic Response Pathway Genes post Cidofovir Treatment

Hypothesis

Cidofovir inhibits growth of NHIST cell lines by induction of apoptosis

In addition to examining apoptosis at a protein level RT-qPCR arrays were used to examine transcription of apoptosis related genes in response to Cidofovir treatment. M08 and HEK cells were treated with 10 µM Cidofovir and 0.1 µM ADF Pro cf3475. HEKs were used as a HPV negative untransformed control line and ADF Pro cf3475 was examined due to its striking inhibitory effect (section 4.3). RNA was extracted from all samples 12 and 36 hours post Cidofovir treatment, reverse transcribed, and cDNA was evaluated in apoptosis pathway specific RT-qPCR arrays. Genes that were greater than 2 fold up/down-regulated in the initial arrays at both time points were further examined in gene specific individual RT-qPCR assays.

5.2.1. RT-qPCR Apoptosis Arrays

5.2.1.1. M08 Cell Line

The data described below shows that in the M08 line, 0.1 µM ADF Pro cf3475 had less effect on expression of apoptosis pathway specific genes compared to 10 µM Cidofovir.

5.2.1.1.1. Clustergrams for RT-qPCR Apoptosis Arrays

Figure 5.4 shows clustergrams representing co-regulated genes 12 and 36 hours post Cidofovir and ADF Pro cf3475 treatment in addition to the untreated control cells for the M08 cell line. The clustergrams display non-supervised hierarchical clustering of the entire RT-qPCR array dataset in the form of a heat map with dendrograms indicating co-regulated genes across the individually treated samples.

A.

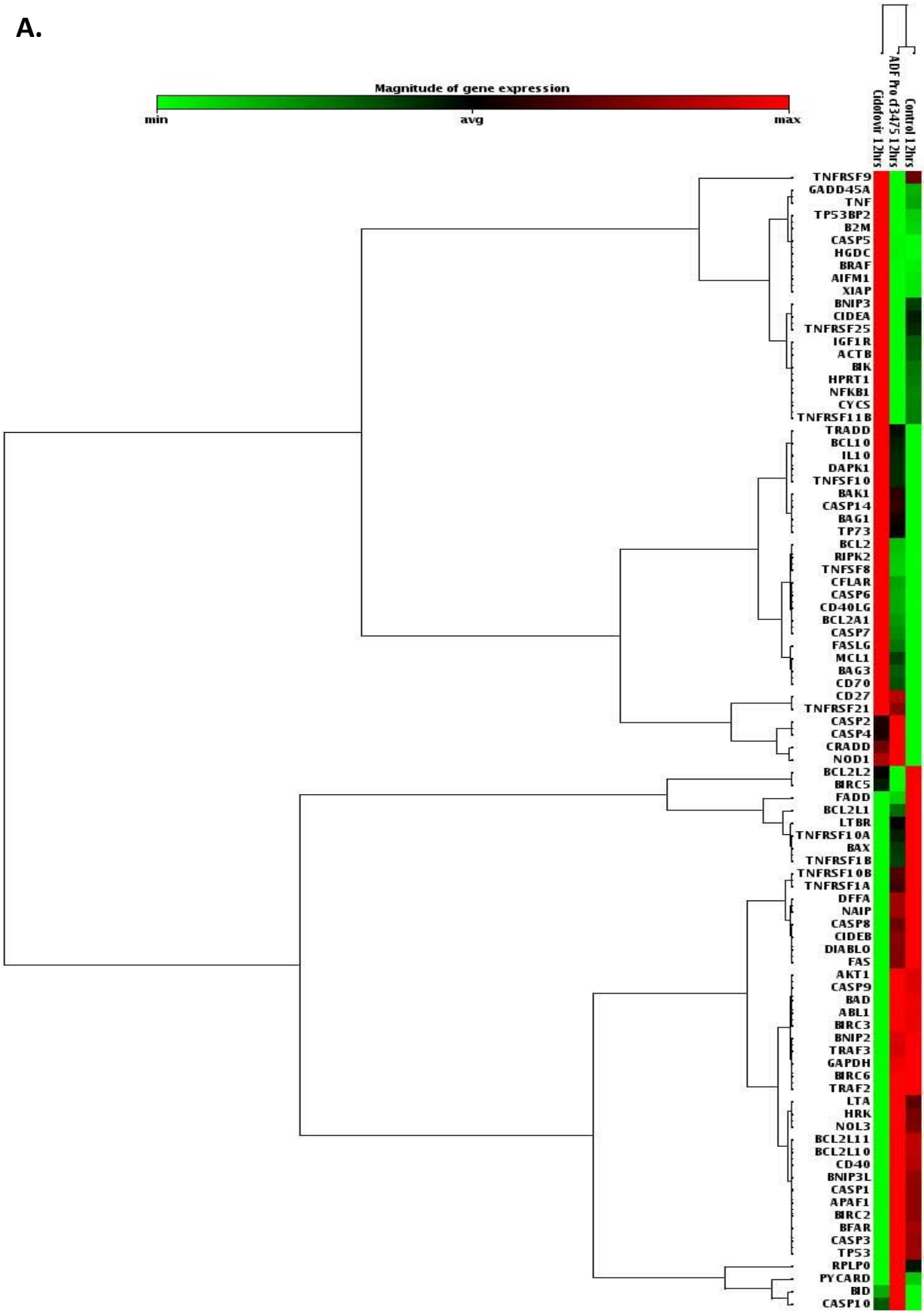
Magnitude of gene expression
min
avg
max
Cidofovir 12hrs
ADF Pro cf3475 12hrs
Control 12hrs
TNFRSF9
GADD45A
TNF
TP53BP2
B2M
CASP5
HGDC
BRAF
AIFM1
XIAP
BNIP3
CIDEA
TNFRSF25
IGF1R
ACTB
BIK
HPRT1
NFKB1
CYCS
TNFRSF11B
TRADD
BCL10
IL10
DAPK1
TNFSF10
BAK1
CASP14
BAG1
TP73
BCL2
RIPK2
TNFSF8
CFLAR
CASP6
CD40LG
BCL2A1
CASP7
FASLG
MCL1
BAG3
CD70
CD27
TNFRSF21
CASP2
CASP4
CRADD
NOD1
BCL2L2
BIRC5
FADD
BCL2L1
LTBR
TNFRSF10A
BAX
TNFRSF1B
TNFRSF10B
TNFRSF1A
DFFA
NAIP
CASP8
CIDEB
DIABLO
FAS
AKT1
CASP9
BAD
ABL1
BIRC3
BNIP2
TRAF3
GAPDH
BIRC6
TRAF2
LTA
HRK
NOL3
BCL2L11
BCL2L10
CD40
BNIP3L
CASP1
APAF1
BIRC2
BFAR
CASP3
TP53
RPLP0
PYCARD
BID
CASP10

B.

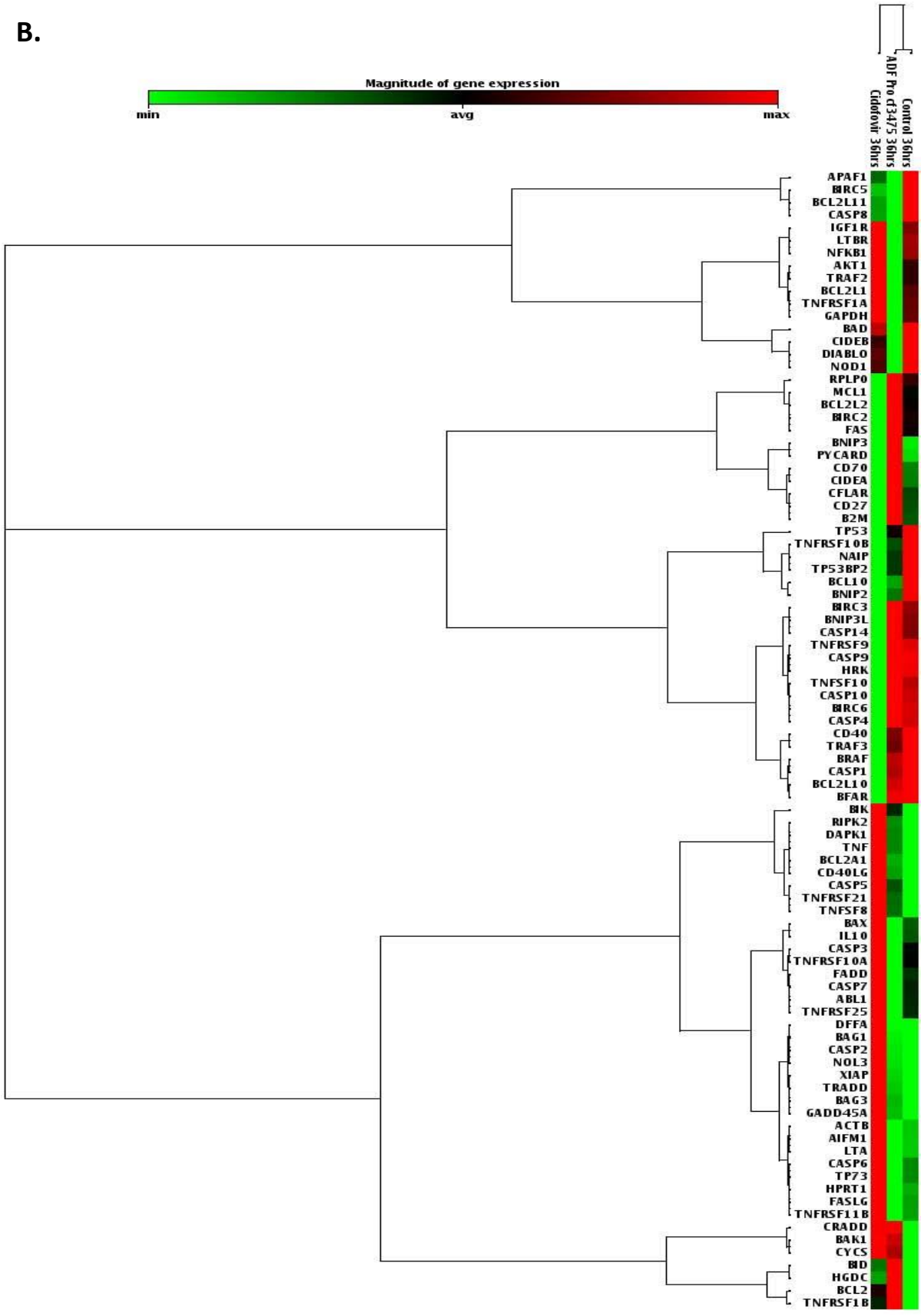
Magnitude of gene expression
min
avg
max
Cidofovir 36hrs
ADF Pro cf3475 36hrs
Control 36hrs
APAF1
BIRC5
BCL2L11
CASP8
IGF1R
LTBR
NFKB1
AKT1
TRAF2
BCL2L1
TNFRSF1A
GAPDH
BAD
CIDEB
DIABLO
NOD1
RPLP0
MCL1
BCL2L2
BIRC2
FAS
BNIP3
PYCARD
CD70
CIDEA
CFLAR
CD27
B2M
TP53
TNFRSF10B
NAIP
TP53BP2
BCL10
BNIP2
BIRC3
BNIP3L
CASP14
TNFRSF9
CASP9
HRK
TNFSF10
CASP10
BIRC6
CASP4
CD40
TRAF3
BRAF
CASP1
BCL2L10
BFAR
BIK
RIPK2
DAPK1
TNF
BCL2A1
CD40LG
CASP5
TNFRSF21
TNFSF8
BAX
IL10
CASP3
TNFRSF10A
FADD
CASP7
ABL1
TNFRSF25
DFFA
BAG1
CASP2
NOL3
XIAP
TRADD
BAG3
GADD45A
ACTB
AIFM1
LTA
CASP6
TP73
HPRT1
FASLG
TNFRSF11B
CRADD
BAK1
CYCS
BID
HGDC
BCL2
TNFRSF1B

Figure 5.4. Clustergrams for M08 Cell Gene Expression post Cidofovir and ADF Pro cf3475 Treatment

(A) Clustergram for M08 cells 12 hours post 10 µM Cidofovir and 0.1 µM ADF Pro cf3475 treatment; (B) Clustergram for M08 cells 36 hours post 10 µM Cidofovir and 0.1 µM ADF Pro cf3475 treatment. The clustergrams were constructed using the SA Bioscience Web-Based RT² Profiler™ PCR Array Data Analysis (Qiagen, Hilden, Germany). Colour coded values are displayed on the y-axis of the clustergrams based on magnitude of gene expression. The green colour at the extreme left of the colour scale correlates to the minimal value, whereas, the red colour at the extreme right of the scale correlates to the maximum value. The black colour in the middle of the colour scale represents the average magnitude of expression value for a particular gene. In the following clustergrams the software assigned the colours according to the normalized gene expression values across all samples including the negative controls. It then clustered samples that had similar values and created the colour range based on these numbers. At both time points ADF Pro cf3475 and untreated samples were clustered together according to similarities and co-regulation of the genes examined in the qPCR apoptosis arrays.

From the 12 hour clustergram (Figure 5.4 (A)) it can be seen that magnitude of gene expression for the majority of genes in the Cidofovir treated cells was the opposite of the untreated sample. Treatment with ADF Pro cf3475 produced magnitude of gene expression values similar to those of the untreated control cells or average magnitude of expression values between the untreated control cells and Cidofovir treated cells. For the Cidofovir treated cells, the SA Bioscience software clustered several genes involved in induction of apoptosis together as being minimally expressed compared to the other two samples, for example; *TNFRSF10B TNFRSF1A, DFFA, CASP8, CIDEB, DIABLO* and *FAS,* however*, NAIP*, an anti-apoptosis gene was also grouped within this cluster. On the contrary however, other inducers of apoptosis were clustered as being maximally expressed compared with the other samples, for instance; *BNIP3, CIDEA, TNFRSF25, BIK, CYCS* and *TNFRSF25*. However, anti-apoptosis genes such as *IGF1R* and *NFKB1* were also grouped with these genes.

The 36 hour clustergram also shows contrasting magnitudes of gene expression for nearly all genes treated with Cidofovir when compared to the untreated control. Magnitude of gene expression in the ADF Pro cf3475 was again similar to that of the untreated cells, but not as much as it was at 12 hours. In the Cidofovir treated cells the software clustered several minimally expressed anti-apoptosis/negative regulators of apoptosis together, for example; *MCL1, BCL2L2, BIRC2* and *FAS*. However, it also clustered several inducers/regulators of apoptosis together as being minimally expressed in comparison to the average value across all the samples analysed, for example; *BNIP3L, CASP14, TNFRSF9, CASP9, TNFSF10, CASP10* and *CASP4*. In contrast again, it clustered other inducers and regulators of apoptosis together as having maximum magnitudes of expression in comparison to the other samples, these include; *BAX, CASP3, TNFRSF10A, FADD, CASP7, ABL1* and *TNFRSF25,* as well as; *AIFM1, LTA, CASP6, TP73, FASL6* and *TNFRSF11B,* and finally; *CRADD, BAK1* and *CYCS*.

For the remainder of this chapter gene expression is discussed in terms of fold regulation. RQ, expressed as fold change, quantifies differences in the expression level of a specific target gene between different samples. Fold change values are derived from the ΔΔCt equation, where change in gene expression is measured between the untreated and

treated cells for a particular time point. Fold regulation values, on the other hand, are those which are used to present the data in a biologically meaningful way. If a fold change value of less than 1, indicating down-regulation, was plotted on a linear scale its size would be disproportional to a fold change value of greater than 1, representing-up regulation. To make fold change values less than 1 easier to interpret on a linear scale they are converted to their negative inverse value to make down-regulation more comparable to up-regulation. Therefore, when the fold change value is less than 1 its negative inverse value is the fold regulation value. When the fold change value is one or more the fold regulation value is the same as the fold change value. For the remainder of this section fold regulation values are shown for genes with greater than or equal to 2 fold up/down-regulation for a particular time point.

5.2.1.1.2. RT-qPCR Apoptosis Array Data for M08 Cells

Genes showing greater than 2 fold up- or down-regulation in M08 cells treated with both compounds are listed in Table 5.1. As seen in the clustergrams, there were minimal changes in expression of apoptosis pathway specific genes in the M08 cells treated with 0.1 µM ADF Pro cf3475 after 12 and 36 hours. The only gene with a dependable differential regulation value was *BCL2* at 36 hours post ADF Pro cf3475 treatment. On the other hand, 18 out of 84 apoptosis-related genes were differentially expressed following Cidofovir treatment in the M08 cell line after treatment periods of 12 and 32 hours. Seven genes were greater than 2 fold differentially expressed at both time points, these include: *BCL2A1, BCL2L10, BIRC3, HRK, TP53, TNFSF8* and *TNFSF10. TNFSF10* was 2 fold up-regulated at 12 hours and 2 fold down-regulated at 32 hours. There was a greater change in expression in the 36 hour Cidofovir treated sample, with *HRK* decreasing from -3.4 at 12 hours to -5.8 at 36 hours and *BIRC3* decreasing from -2.4 at 12 hours to -9 at 36 hours.

To demonstrate the raw RT-qPCR apoptosis array data, Figure 5.5 shows amplification and dissociation plots for *BCL2A1, BIRC3*, *HRK* and 5 housekeeping genes (HKGs): *ACTB, RPLPO, GAPDH, B2M* and *HPRT1*.

Table 5.1. Fold Regulation Values and Protein Function of Differentially Expressed Genes post Cidofovir and ADF Pro cf3475 Treatment of M08 Cells as determined by RT-qPCR Apoptosis Arrays

Gene	10 µM Cidofovir		0.1 µM ADF Pro cf3475		Gene product function in apoptosis
	12 hours	36 hours	12 hours	36 hours	
BCL2				2.3122†	Inhibits apoptosis (NCBI, October 2013)
BCL2A1	3.1325	2.459			Inhibits apoptosis (NCBI, September 2013c)
CD70	3.1536†				T cell activation and regulation (NCBI, September 2013f)
FASLG	2.2574‡				Positive regulator of apoptosis (NCBI, September 2013b)
IL10	2.2508‡				Immune-regulation and inflammation (NCBI, September 2013j)
TNF	2.9045‡				Positive regulator of apoptosis (NCBI, September 2013o)
TNFSF8	2.2241‡	2.1338‡			Can induce apoptosis or promote cell proliferation (NCBI, September 2013e)
TNFRSF11B		2.0743‡			DEATH domain protein (NCBI, September 2013n)
TNFRSF21		2.0072			DEATH domain protein (NCBI, September 2013u)
TNFSF10	2.324	-1.9819			Induces apoptosis in transformed and tumour cells (NCBI, September 2013r)
BCL2L10	-2.1616	-2.4394			Inhibits apoptosis (NCBI, September 2013s)
BIRC3	-2.3679	-9.1225			Inhibits apoptosis (NCBI, September 2013a)
BNIP3L		-2.0484			Inhibits apoptosis (GeneCards®, 2013)
CASP14		-11.9187			Functions in terminal keratinocyte differentiation (NCBI, September 2013t)
CIDEA		-2.0568‡	-2.1785‡	2.5459‡	Induces apoptosis (NCBI, September 2013h)
HRK	-3.385†	-5.7533			Induces apoptosis (NCBI, September 2013q)
NAIP	-2.3798				Inhibits apoptosis (NCBI, September 2013m)
TNFRSF9		-2.0789‡			TNF-receptor involved in inflammation and immunity (NCBI, September 2013k)
TP53	-3.0134	-1.9951			Tumour suppressor protein. Responds to diverse cellular stresses to regulate expression of target genes, thereby inducing cell cycle arrest, apoptosis, senescence, DNA repair, or changes in metabolism(NCBI, September 2013p)

Fold regulation values greater than 2 and less than -2 obtained in the RT-qPCR apoptosis arrays 12 and 36 hours post 10 µM Cidofovir and 0.1 µM ADF Pro cf3475 treatment of M08 cells are shown. Fold regulation values were calculated using the ΔΔCt method and fold change values less than 1.00 were converted into their negative inverse value. Red and blue texts highlight up- and down-regulation respectively.

† The average threshold cycle for this gene was greater than 30 in either the treated or un-treated sample and less than 30 in the opposite sample. Therefore, the gene's expression is low in one sample and reasonably detected in the other suggesting that the true fold-change value is at least as large as the calculated value shown.

‡ The average threshold cycle for this gene is high (> 30) in both treated and untreated samples indicating low expression values in both; this result should be treated with caution.

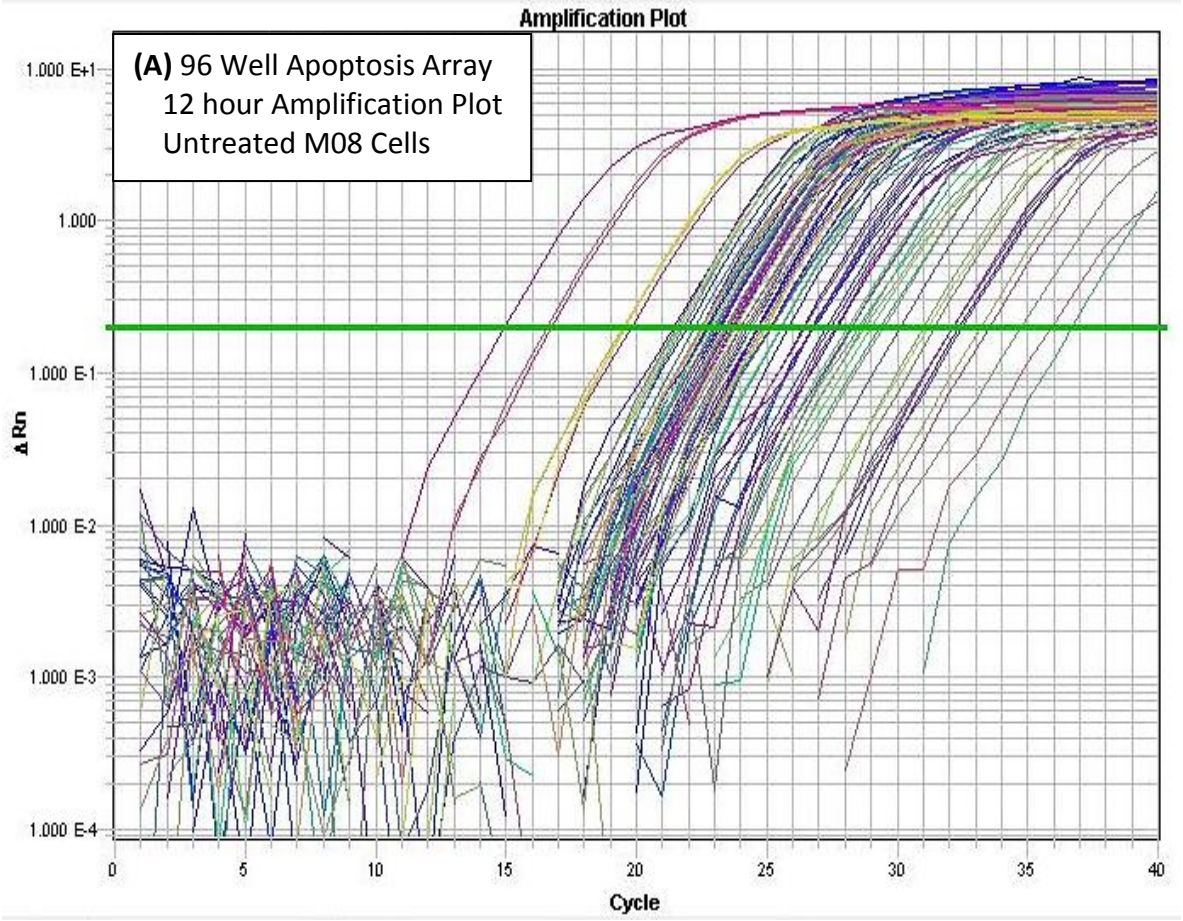
Amplification Plot
(A) 96 Well Apoptosis Array
12 hour Amplification Plot
Untreated M08 Cells
1.000 E+1
1.000
1.000 E-1
1.000 E-2
1.000 E-3
1.000 E-4
ΔRn
0
5
10
15
20
25
30
35
40
Cycle

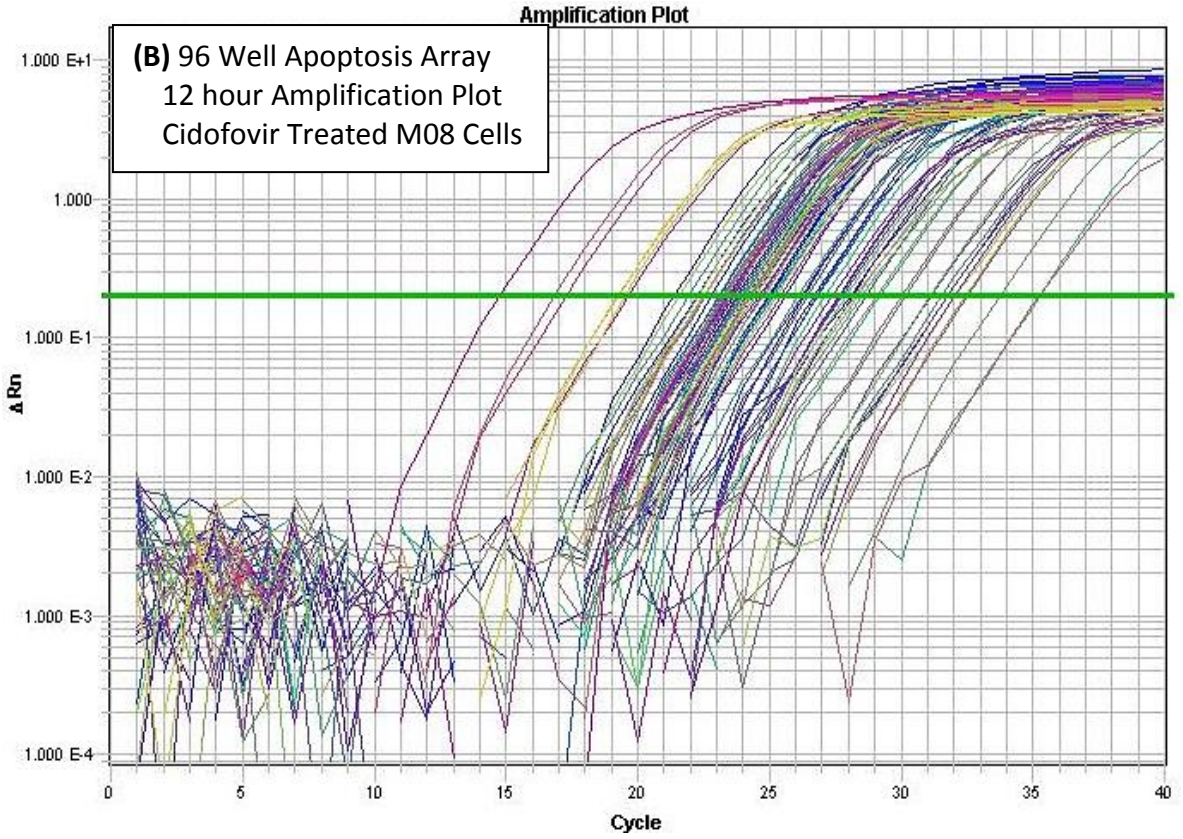
Amplification Plot
(B) 96 Well Apoptosis Array
12 hour Amplification Plot
Cidofovir Treated M08 Cells
1.000 E+1
1.000
1.000 E-1
1.000 E-2
1.000 E-3
1.000 E-4
ΔRn
0
5
10
15
20
25
30
35
40
Cycle

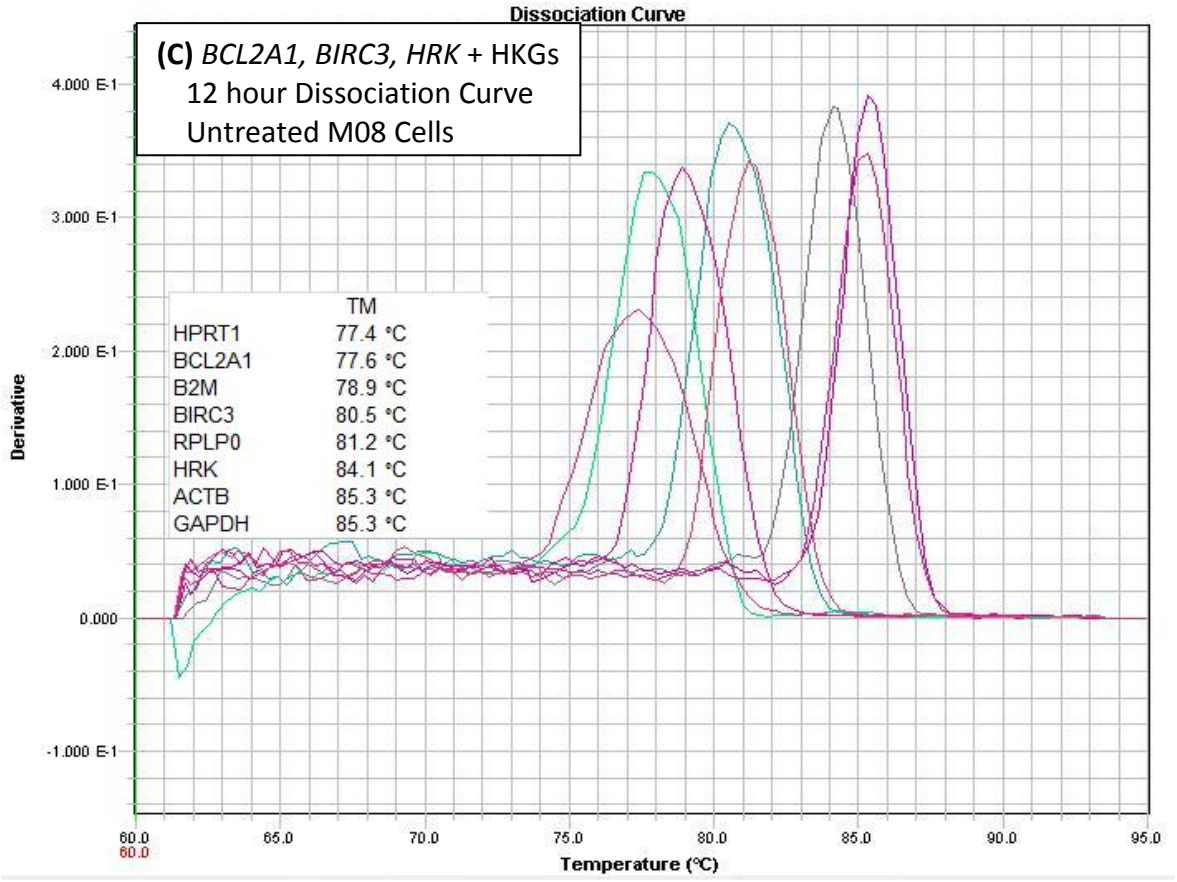
Dissociation Curve
(C) BCL2A1, BIRC3, HRK + HKGs
12 hour Dissociation Curve
Untreated M08 Cells
TM
HPRT1 77.4 °C
BCL2A1 77.6 °C
B2M 78.9 °C
BIRC3 80.5 °C
RPLP0 81.2 °C
HRK 84.1 °C
ACTB 85.3 °C
GAPDH 85.3 °C
Derivative
4.000 E-1
3.000 E-1
2.000 E-1
1.000 E-1
0.000
-1.000 E-1
60.0
65.0
70.0
75.0
80.0
85.0
90.0
95.0
Temperature (°C)

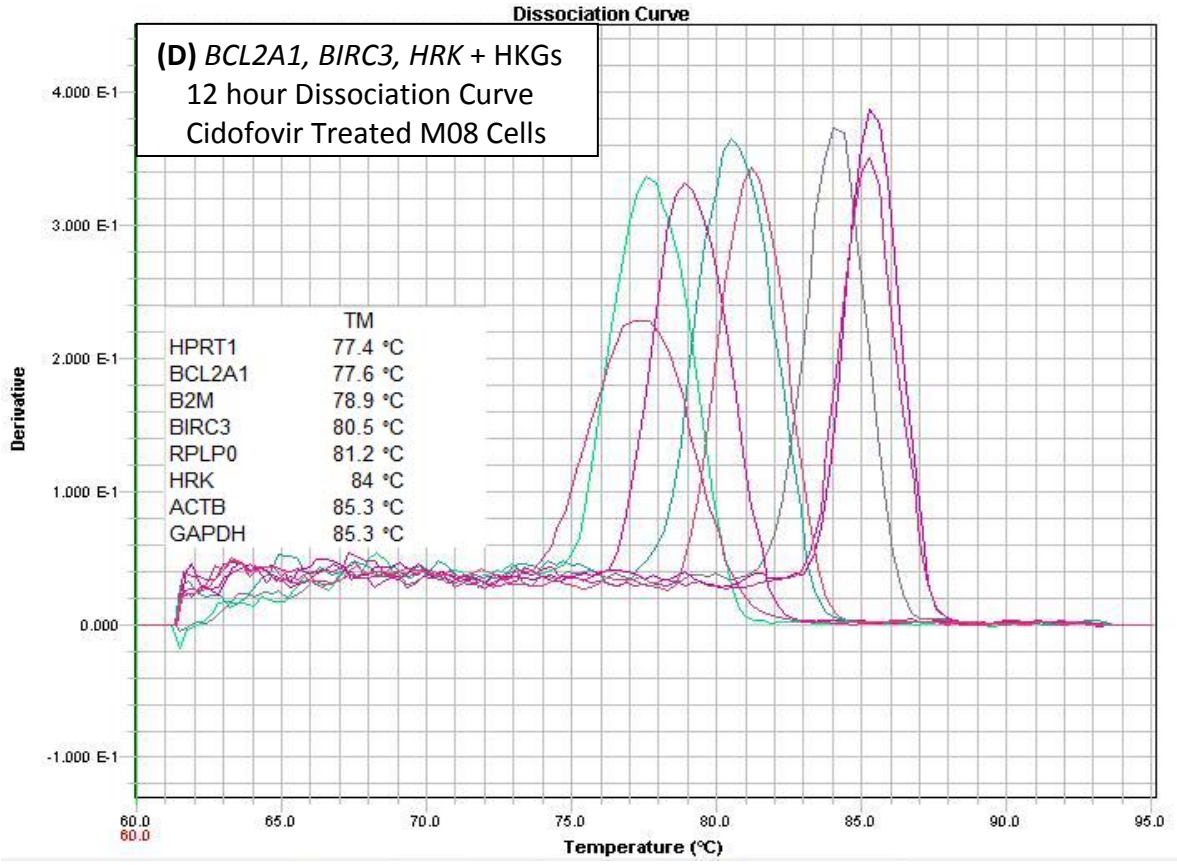
Dissociation Curve
(D) BCL2A1, BIRC3, HRK + HKGs
12 hour Dissociation Curve
Cidofovir Treated M08 Cells
TM
HPRT1 77.4 °C
BCL2A1 77.6 °C
B2M 78.9 °C
BIRC3 80.5 °C
RPLP0 81.2 °C
HRK 84 °C
ACTB 85.3 °C
GAPDH 85.3 °C
Derivative
4.000 E-1
3.000 E-1
2.000 E-1
1.000 E-1
0.000
-1.000 E-1
60.0
65.0
70.0
75.0
80.0
85.0
90.0
95.0
Temperature (°C)

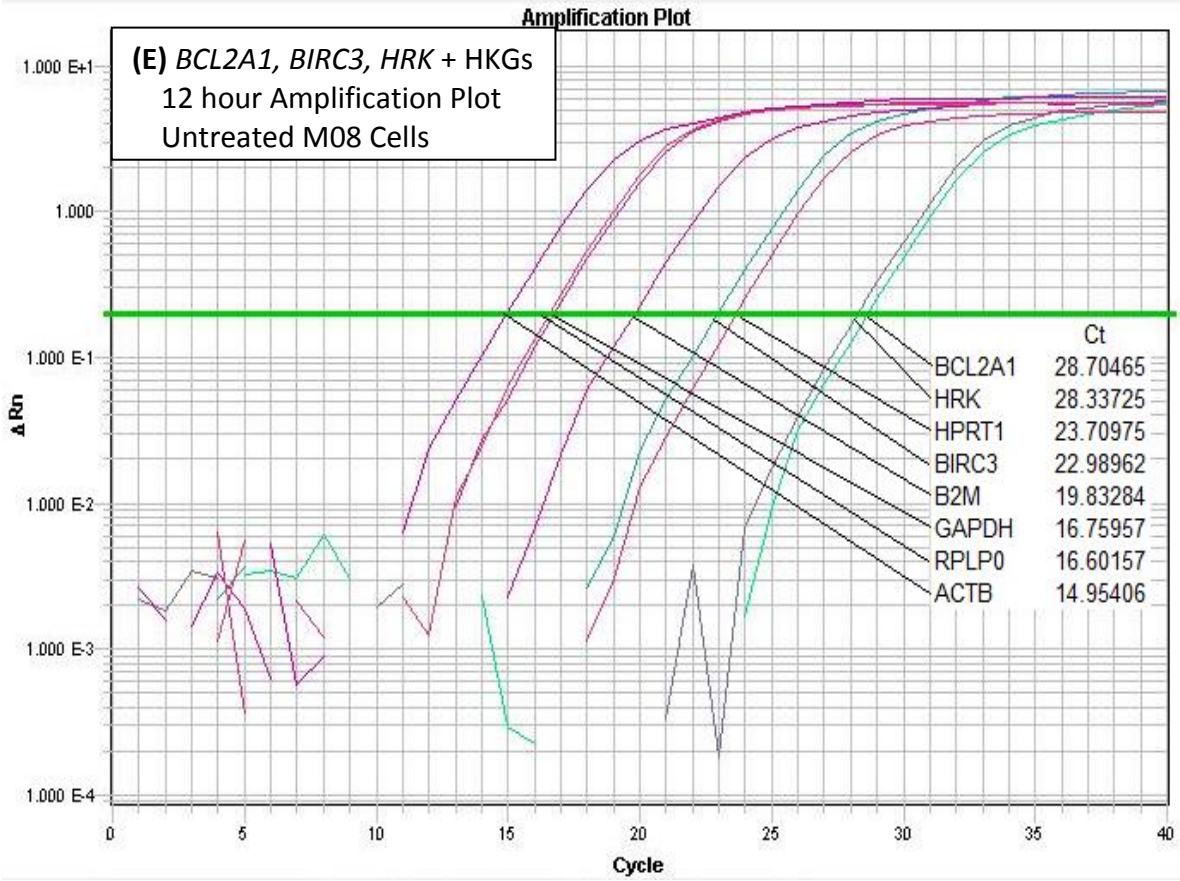
Amplification Plot
(E) BCL2A1, BIRC3, HRK + HKGs
12 hour Amplification Plot
Untreated M08 Cells
ΔRn
Cycle
Ct
BCL2A1 28.70465
HRK 28.33725
HPRT1 23.70975
BIRC3 22.98962
B2M 19.83284
GAPDH 16.75957
RPLP0 16.60157
ACTB 14.95406

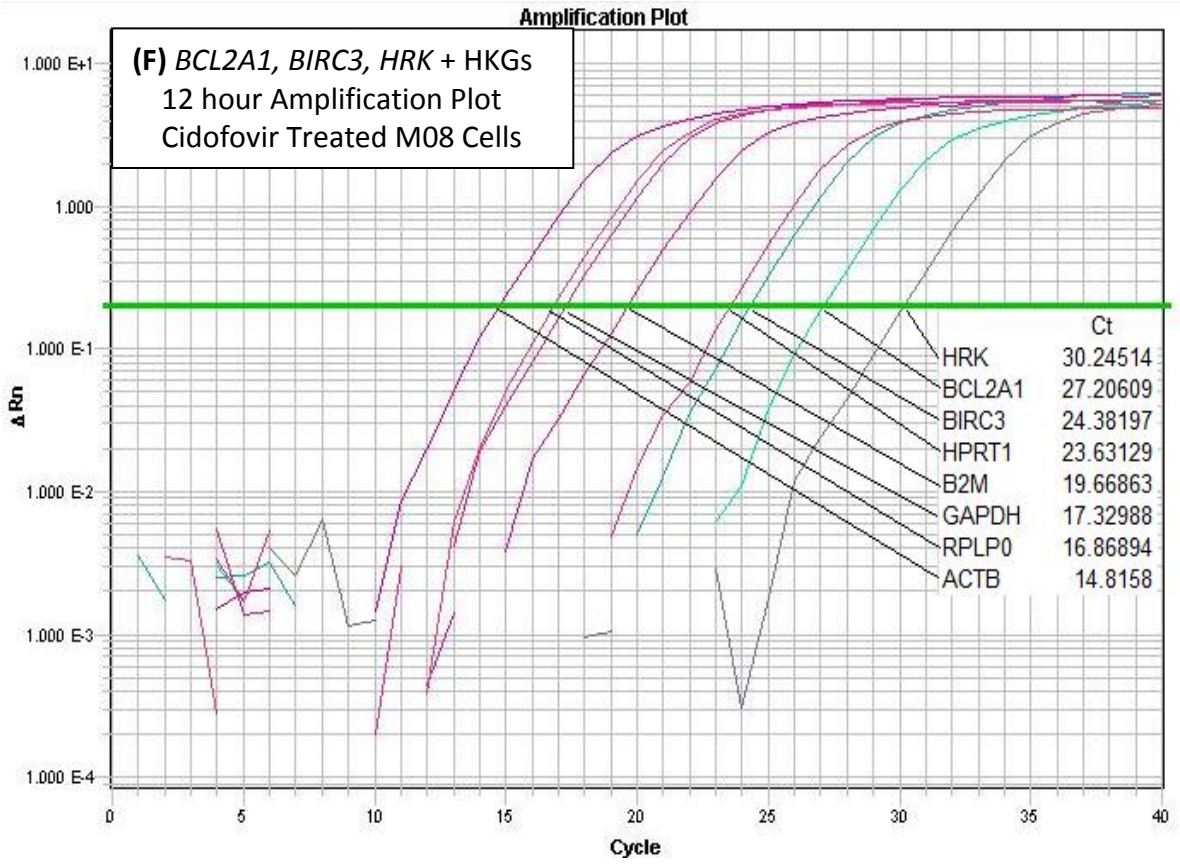
Amplification Plot
(F) BCL2A1, BIRC3, HRK + HKGs
12 hour Amplification Plot
Cidofovir Treated M08 Cells
ΔRn
Cycle
Ct
HRK 30.24514
BCL2A1 27.20609
BIRC3 24.38197
HPRT1 23.63129
B2M 19.66863
GAPDH 17.32988
RPLP0 16.86894
ACTB 14.8158

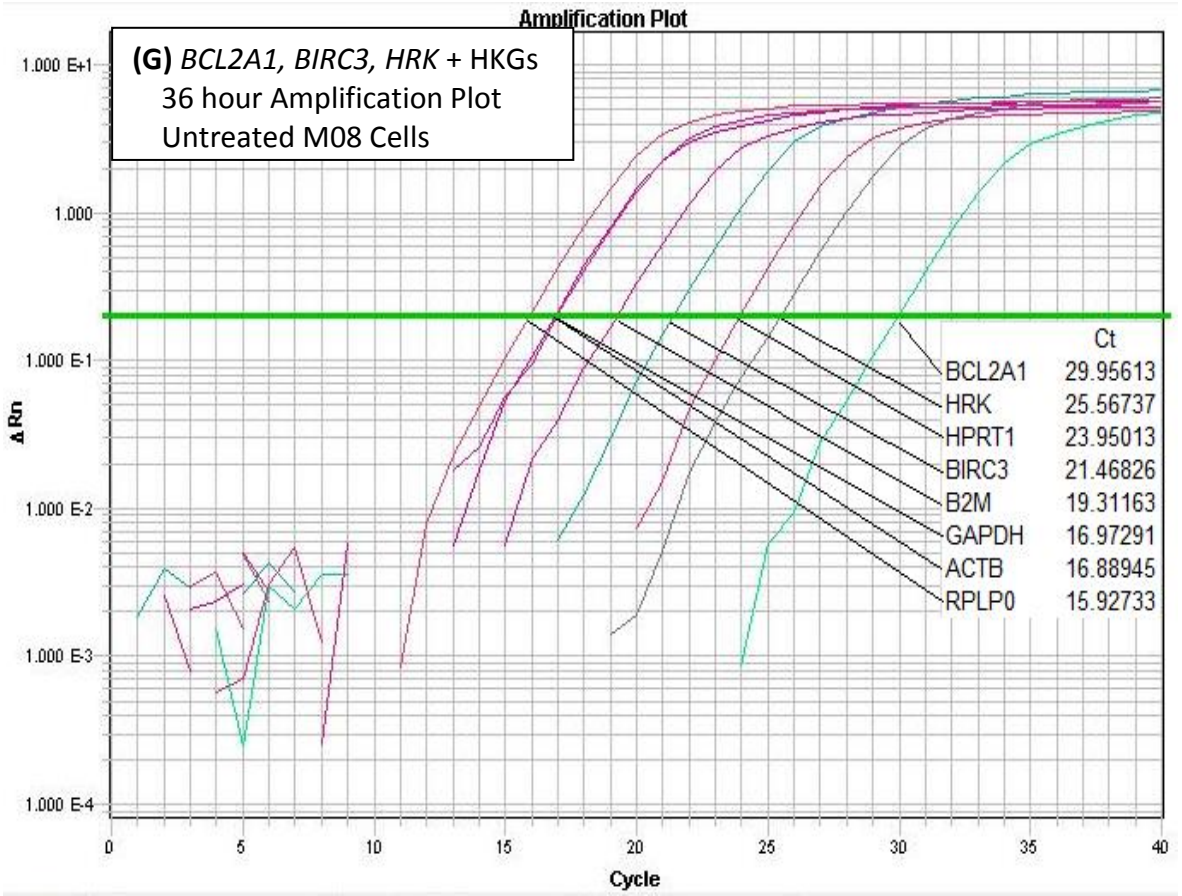
Amplification Plot
(G) BCL2A1, BIRC3, HRK + HKGs
36 hour Amplification Plot
Untreated M08 Cells
1.000 E+1
1.000
1.000 E-1
1.000 E-2
1.000 E-3
1.000 E-4
ΔRn
0
5
10
15
20
25
30
35
40
Cycle
Ct
BCL2A1 29.95613
HRK 25.56737
HPRT1 23.95013
BIRC3 21.46826
B2M 19.31163
GAPDH 16.97291
ACTB 16.88945
RPLP0 15.92733

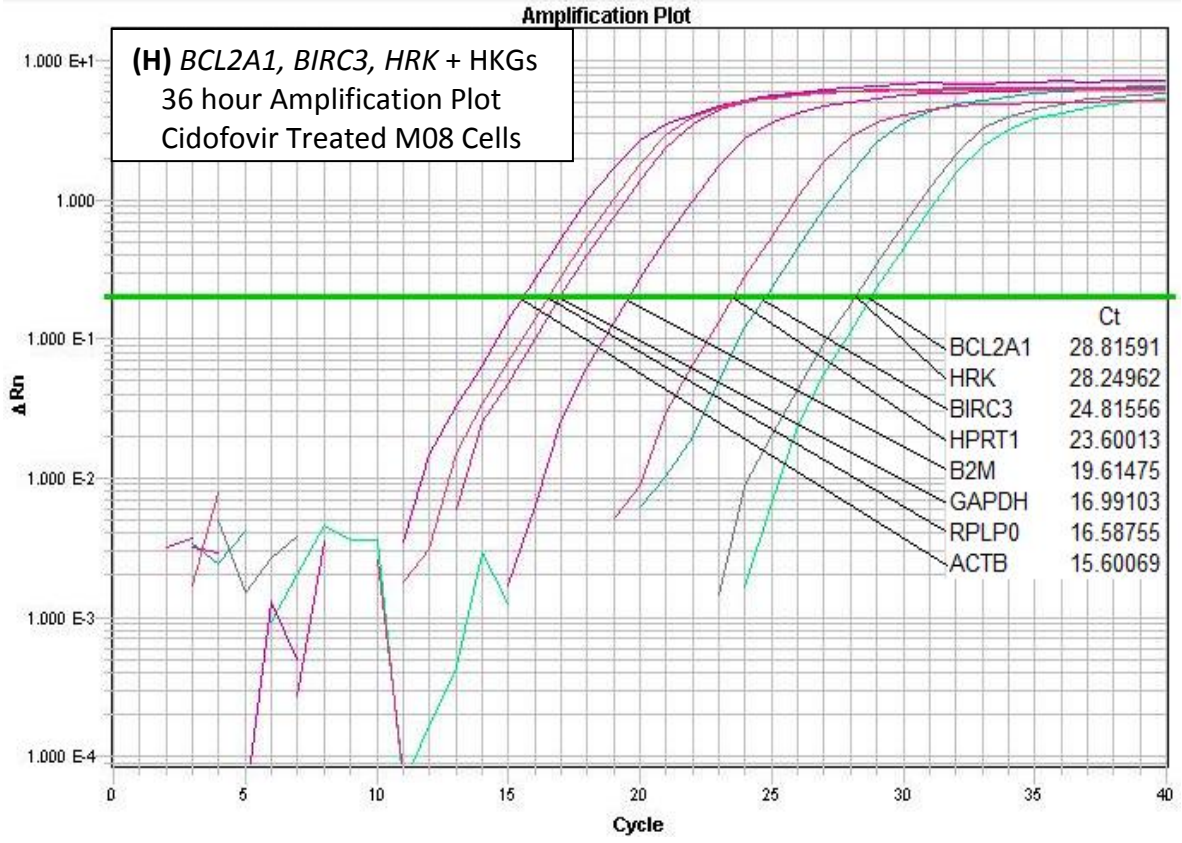
Amplification Plot
(H) BCL2A1, BIRC3, HRK + HKGs
36 hour Amplification Plot
Cidofovir Treated M08 Cells
1.000 E+1
1.000
1.000 E-1
1.000 E-2
1.000 E-3
1.000 E-4
ΔRn
0
5
10
15
20
25
30
35
40
Cycle
Ct
BCL2A1 28.81591
HRK 28.24962
BIRC3 24.81556
HPRT1 23.60013
B2M 19.61475
GAPDH 16.99103
RPLP0 16.58755
ACTB 15.60069

(I)

Gene	12 hours					36 hours				
	Untreated		Cidofovir			Untreated		Cidofovir		
	Ct	ºC	Ct	ºC	Δ Ct	Ct	ºC	Ct	ºC	Δ Ct
BCL2A1	28.70465	77.6	27.20609	77.6	1.498561	29.95613	78	28.81591	77.7	1.140213
BIRC3	22.98962	80.5	24.38197	80.5	1.39235	21.46826	80.6	24.81556	80.6	3.3473
HRK	28.33725	84.1	30.24514	84	1.90789	25.56737	84.1	28.24962	84.1	2.68225
ACTB	14.95406	85.3	14.8158	85.3	0.138264	16.88945	85.4	15.60069	85.4	1.288755
B2M	19.83284	78.9	19.66863	78.9	0.164211	19.31163	78.7	19.61475	79	0.30313
GAPDH	16.75957	85.3	17.32988	85.3	0.57031	16.97291	85.4	16.99103	85.4	0.01812
HPRT1	23.70975	77.4	23.63129	77.4	0.078457	23.95013	77.3	23.60013	77.3	0.350001
RPLP0	16.60157	81.2	16.86894	81.2	0.26737	15.92733	81.3	16.58755	81.3	0.66022

Figure 5.5. RT-qPCR Apoptosis Array Amplification and Dissociation Plots for *BCL2A1, BIRC3, HRK* and Housekeeping Genes (*ACTB, RPLPO, GAPDH, B2M* and *HPRT1*)

BCL2A1, BIRC3 and HRK exemplify differentially expressed genes in the RT-qPCR apoptosis array data 12 and 36 hours post Cidofovir treatment of M08 cells. The primary array data was analysed using SDS Software version 2.3 (SA Bioscience, Qiagen, Hilden, Germany). For amplification analysis and to obtain Ct (crossing threshold) values for all gene products the baseline parameter was set to automatic and the threshold value was manually set to 0.2. Amplification plots are presented on logarithmic scales. (A) and (B) show 96 well array amplification plots for 12 hour untreated and Cidofovir treated M08 cells respectively. (C) and (D) show derivative melting point disassociation curves for BCL2A1, BIRC3, HRK and the 5 Housekeeping genes (HKGs) (ACTB, RPLPO, GAPDH, B2M and HPRT1) in the 12 hour untreated and Cidofovir treated M08 samples respectively. The disassociation curves indicated no unspecific amplification. (E) and (F) show amplification plots for BCL2A1, BIRC3, HRK and the 5 HKGs for untreated and Cidofovir treated M08 cells after 12 hours respectively. (G) and (H) show amplification plots for BCL2A1, BIRC3, HRK and the 5 HKGs for untreated and Cidofovir treated M08 cells after 36 hours respectively. The table in (I) summarises the Ct values and melting temperatures (TM) (°C) for BCL2A1, BIRC3, HRK and the 5 HKGs in untreated and Cidofovir treated M08 cells after 12 and 36 hours. The table also shows change in Ct (ΔCt) between the untreated and Cidofovir treated samples at both time points. Due to the expense of the RT-qPCR apoptosis arrays and financial limitations each sample was assayed once only. Genes that were differentially expressed at both time points in the RT-qPCR arrays were examined further in repeat individual RT-qPCR assays.

5.2.1.2. HEK Cell Line

Unlike the M08 cells, HEKs displayed minimal changes in expression of apoptotic response pathway genes after treatment with Cidofovir at both 12 and 36 hours. However, similar to the M08 cell line there was also minimal changes in expression of apoptosis response pathway genes in HEKs treated with 0.1 µM ADF Pro cf3475 at 12 and 36 hours. These data can be seen in Table 5.2. *BCL2A1, CD27, HRK* and *LTA* all had relatively high Ct values in both treated (Cidofovir and/or ADF Pro cf3475) and untreated HEKs. Consequently, the only gene that displayed a reliable fold regulation value in HEKs was *DAPK1*, which was 2 fold up-regulated at 36 hours with both treatments.

Table 5.2. Fold Regulation Values and Protein Function of Differentially Expressed Genes post Cidofovir and ADF Pro cf3475 Treatment in HEK Cells as determined by RT-qPCR Apoptosis Arrays

Gene	10 µM Cidofovir		0.1 µM ADF Pro cf3475		Gene product function in apoptosis
	12 hours	36 hours	12 hours	36 hours	
BCL2A1	-2.8932‡		-2.7719‡		Inhibits apoptosis (NCBI, September 2013c)
CD27	2.1832‡		2.3335‡		Induces apoptosis (NCBI, September 2013d)
DAPK1		2.1058		2.7517	Induces apoptosis (NCBI, September 2013i)
HRK				2.5532‡	Induces apoptosis (NCBI, September 2013q)
LTA		2.3404‡			Induces apoptosis (NCBI, September 2013l)

Fold regulation values greater than 2 and less than -2 obtained in the RT-qPCR apoptosis arrays 12 and 36 hours post 10 µM Cidofovir and 0.1 µM ADF Pro cf3475 treatment of HEK cells are shown. Fold regulation values were calculated using the ΔΔCt method and fold change values less than 1.00 were converted into their negative inverse value. Red and blue texts highlight up- and down-regulation respectively.

‡ The average threshold cycle for this gene is high (> 30) in both treated and untreated samples indicating low expression values in both; this result should be treated with caution

.

5.2.2. Individual RT-qPCR Assays

From the RT-qPCR apoptosis array results, the genes that were differentially expressed 12 and 36 hours post Cidofovir treatment of M08 cells were validated in triplicate in separate individual RT-qPCR assays. These genes were *BCL2A1, BCL2L10, BIRC3, HRK* and *TP53. CDKN1A* (NCBI, September 2013g) was also examined in an individual RT-qPCR assay as it is a direct transcriptional target of p53 protein.

Although differentially expressed at both time points, *TNFSF8* was not assayed further as it displayed high Ct values in both the untreated and treated samples at both times points. *TNFSF10* was also not examined further as it was up-regulated at 12 hours and down-regulated at 36 hours. Fold regulation values for the genes examined in the individual RT-qPCR assays are listed in Table 5.3, and displayed graphically in Figure 5.6. The individual RT-qPCR assay results showed the same trends as the RT-qPCR apoptosis arrays (with the exception of *BCL2L10*, which was not down-regulated at 12 hours but was at 36 hours). *CDKN1A* was slightly up-regulated at 12 hours but greater than 3 fold down-regulated at 36 hours. *BCL2A1* was up-regulated by 2 fold at both time points. *BIRC3, HRK* and *TP53* were down-regulated at both time points

Table 5.3. Fold Regulation Values of Differentially Expressed Genes post Cidofovir Treatment of M08 Cells as determined by Individual RT-qPCR Assays

Gene	12 hour fold regulation value	36 hour fold regulation value
BCL2A1	2.246542	1.937273
BCL2L10	1.282695	-8.47386
BIRC3	-2.428559	-22.9953
HRK †	-10.33652	-18.155
TP53	-4.293396	-3.55173
CDKN1A	1.74351	-3.21667

Fold regulation values from the individual RT-qPCR assays 12 and 36 hours post 10 µM Cidofovir treatment of M08 cells are shown. Fold regulation values were calculated using the ΔΔCt method and fold change values less than 1.00 were converted into their negative inverse value. Red and blue texts highlight up- and down-regulation respectively.

† The average threshold cycle for HRK was greater than 30 in either the treated or un-treated sample and less than 30 in the opposite sample. Therefore, the gene's expression is considerably low in one sample and reasonably detected in the other suggesting that the true fold-change value is at least as large as the calculated value shown.

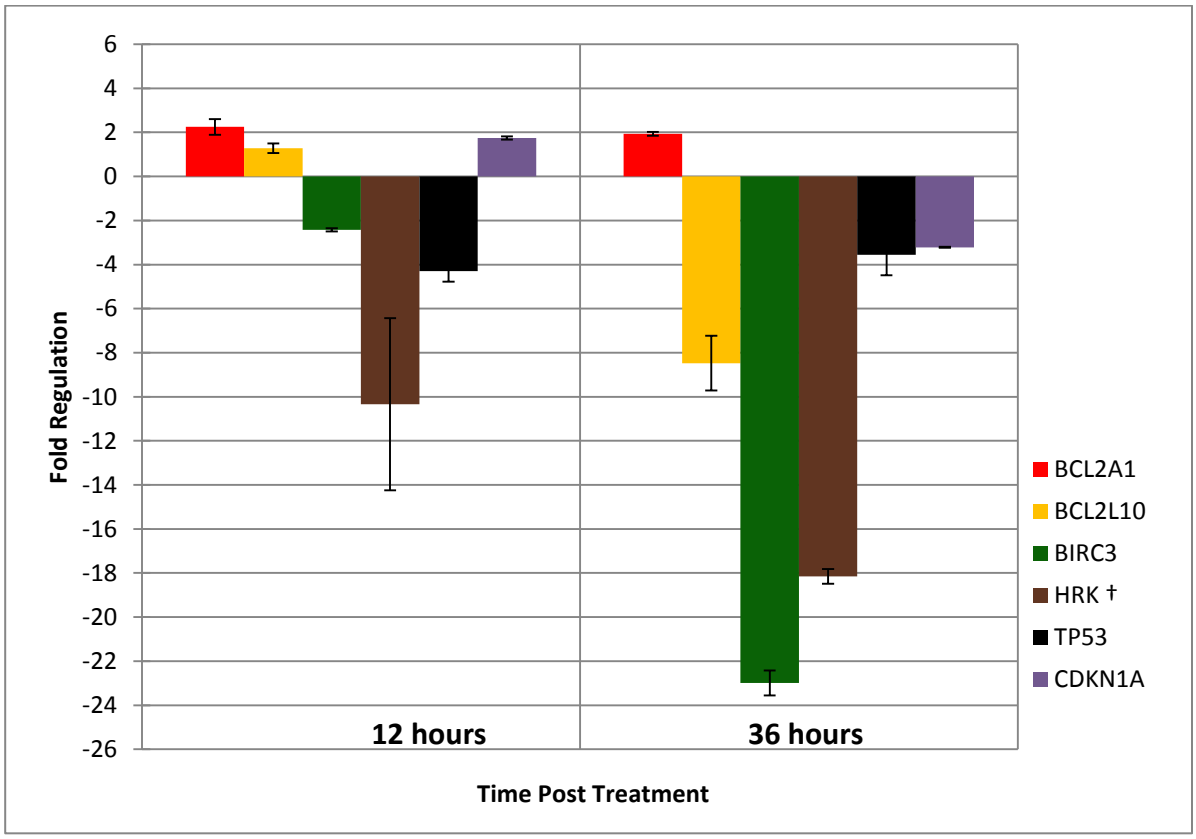

Figure 5.6. Fold Regulation of Differentially Expressed *BCL2A1, BCL2L10, BIRC3, HRK, TP53* and *CDKN1A* post Cidofovir Treatment of M08 Cells as determined by Individual RT-qPCR Assays

The RT-qPCR apoptosis arrays found that BCL2A1, BCL2L10, BIRC3, HRK, and TP53 were differentially expressed at both time points in Cidofovir treated M08 cells. This result was validated with individual RT-qPCR assays using the same primer sets as those that were used in the RT-qPCR arrays. CDKN1A was also examined as it is a direct transcriptional target of p53 protein. Fold regulation values were calculated using the ΔΔCt method and fold change values less than 1.00 were converted into their negative inverse value. Fold regulation is presented on a linear scale. Each gene was analysed in triplicate and error bars represent SEM for triplicate values.

† The average threshold cycle for HRK was greater than 30 in either the treated or un-treated sample and less than 30 in the opposite sample. Therefore, the gene's expression is considerably low in one sample and reasonably detected in the other suggesting that the true fold-change value is at least as large as the calculated value shown. The large error bar on HRK gene expression at 12 hours was because the Ct value of the treated sample was greater than 35 indicating considerably reduced expression.

5.3. Total and Phospho-p53 Re-Accumulation in Cidofovir and Radiation Treated NHIST Cell Lines

Hypothesis

i. *Growth inhibition of Cidofovir treated NHIST cell lines is due to re-accumulation of total and phosphorylated-p53*
ii. *Cidofovir treatment combined with radiation can augment a p53 protein response in NHIST cell lines*

As a decrease in *TP53* transcription was observed in the RT-qPCR apoptosis arrays and individual RT-qPCR assays in the Cidofovir treated M08 cell line, but not in the Cidofovir treated HEK line, a selective effect on *TP53* transcription in HPV positive cells lines was speculated. To examine if the decreased transcription of *TP53* in response to treatment with Cidofovir had an effect at the protein level, and to examine the possible synergistic effect of combining Cidofovir treatment with a clinically relevant dose of radiation, levels of total and phosphorylated p53 and p21 protein were examined. M08 and A09 cell lysates from all treatment conditions outlined previously in Figure 5.1 were subjected to Western blotting and densitometric analysis for p53, phospho-p53 and p21 proteins. Phosphorylated p53 was evaluated to examine if any of the treatment conditions could activate p53, if change in total p53 levels were found. p21 was examined as it is a transcriptional target of phosphorylated p53. Due to low viable cell numbers post irradiation it was not possible to carry out Western blotting on irradiated HEK cells. Hence for this experiment, only untreated and Cidofovir treated HEKs were examined for p53, phospho-p53 and p21 proteins.

5.3.1. NHIST Cell Lines

Total p53, phospho-p53 and p21 Western blot images and densitometry plots for treated M08 and A09 cell lines are outlined in Figure 5.7.

A. Total p53, phospho-p53, p21 and β-Actin Western blot images

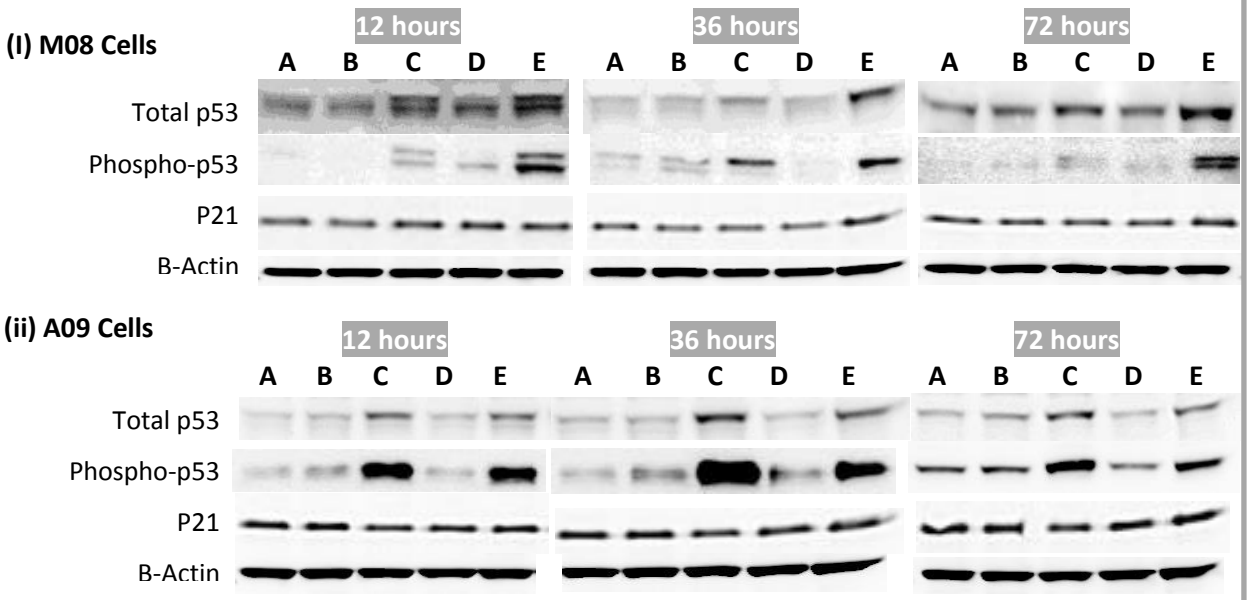

Key: ***Lane A*** *= Untreated Control;* ***Lane B*** *= IC50 Cidofovir;*
Lane C *= IC50 Cidofovir + 2 Gy XRT;* ***Lane D*** *= 2 Gy XRT;* ***Lane E*** *= 20 Gy XRT*

B. Total p53 densitometry

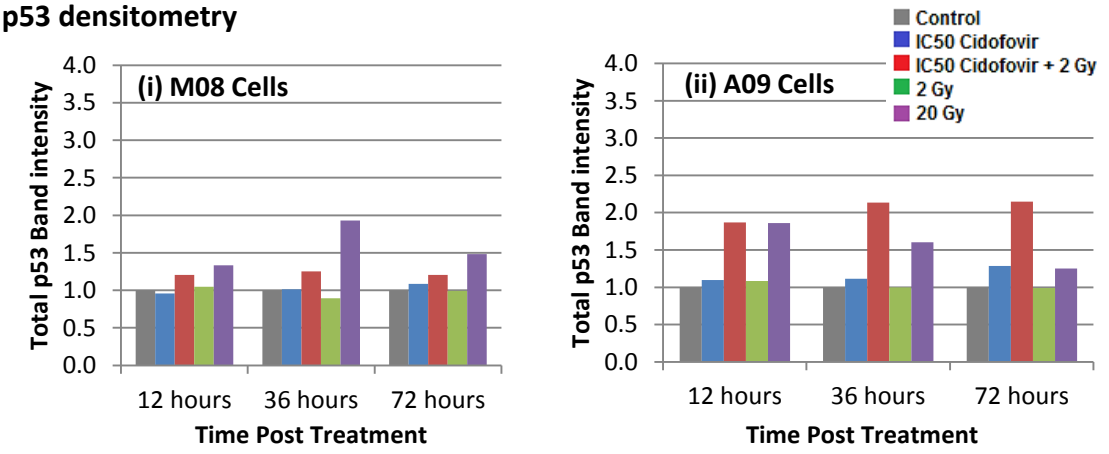

C. Phospho-p53 densitometry

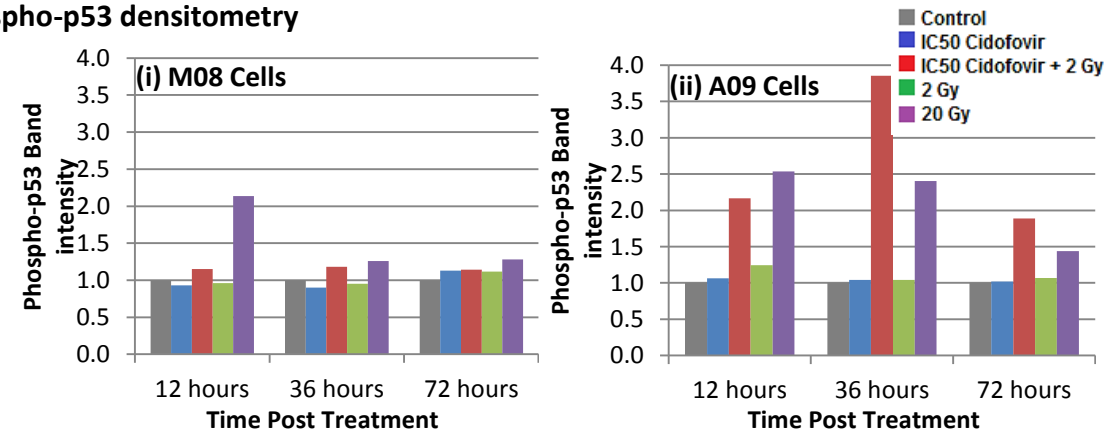

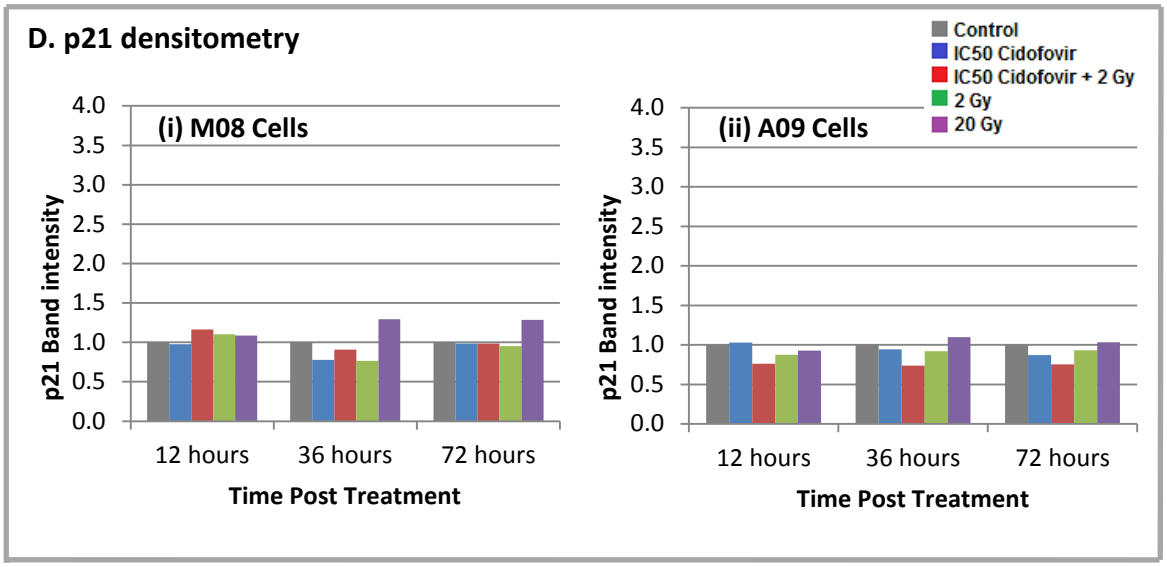

Figure 5.7. Total p53, phospho-p53 and p21 Western blot Images and Densitometry Plots for M08 and A09 Cells Treated with Cidofovir, Cidofovir combined with 2 Gy, 2 Gy and 20 Gy Radiation over a 72 Hour Time Frame

(A) Total p53, phospho-p53 and p21 Western blot images for (i) M08 and (ii) A09 cells 12, 36 and 72 hours post teatment with the conditions outlined in Figure 5.1. Total p53 and p21 blotting were carried out on a separate membrane to phospho-p53. All membranes were probed for β-Actin to normalize for sample loading differences. Total p53, p21 and β-Actin were imaged using a 1 minute exposure time. Phospho-p53 was imaged using a 30 minute exposure time. The β-Actin bands shown in this figure correspond to the same membrane as total p53 and p21. β-Actin for phospho-p53 for the M08 and A09 samples can be seen in Figure 5.3. Total and phospho-p53 were confirmed to be 53 kDa, p21 was confirmed to be 21 kDa and β-Actin was confirmed to be 45 kDa using a MagicMark™ XP Western Protein Standard. The MagicMark™ XP Western Protein Standard and specificity of all antibodies can be seen in appendix 8.1.The total and phospho-p53 doublets, observed in the M08 cell line, may be due to different phosphorylated isoforms of the protein. Due to the limitations of low protein concentrations n = 1 for all samples; however, trends in protein levels can be found through the three different time points examined for each cell line.

(B) Densitomety plots for total p53 band intensities corresponding to the Western blot images for M08 and A09 cells in (A). (C) Densitomety plots for phospho-p53 band intensities corresponding to the Western blot images for M08 and A09 cells in (A). (D) Densitomety plots for p21 band intensities corresponding to the Western blot images for M08 and A09 cells in (A). All protein band intensities were first normalized to the corresponding intensity for β-Actin on the same nitrocellulose membrane, before further normalization to the untreated control band for each time point.

From these analyses, it appeared that Cidofovir on its own had no effect on the accumulation of total p53 in M08 cells. However, Cidofovir combined with 2 Gy radiation did produce a slight increase in total p53 at each time point. An increase in total p53 was also observed in the 20 Gy positive control cells at each time point. Cidofovir treatment of M08 cells had no effect on phospho-p53 levels. None of the treatment conditions produced a differential effect on the p21 protein levels observed in the M08 cell line.

In comparison to the M08 cell line, a more prominent response in total and phospho-p53 was observed in the A09 cell line. A large increase in these proteins was observed in both the combination treated sample and 20 Gy positive control. Phospho-p53 levels peaked at 36 hours in the combined treatment sample. Similar to M08, no differences in p21 levels were observed in the A09 cell line at each time point.

5.3.2. HEK Cell Line

Total p53, phospho-p53 and p21 Western blot images and densitometry plots for HEKs treated with and without Cidofovir are outlined in Figure 5.8. This data indicated Cidofovir had minimal effect on accumilation of total p53, phospho-p53 and p21 protein levels in HEK cells.

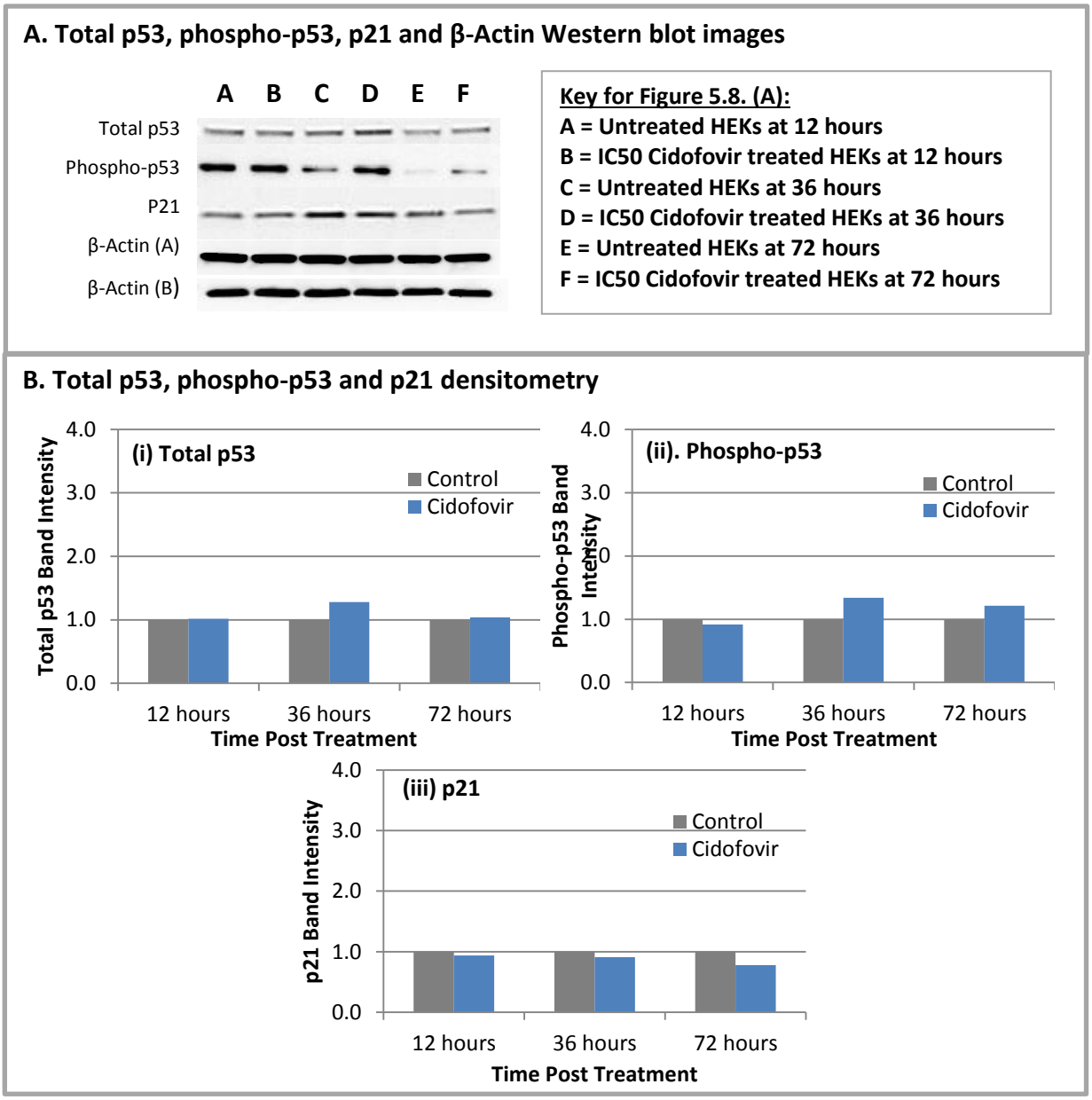

Figure 5.8. Total p53, phospho-p53 and p21 Western blot Images and Densitometry Plots for Cidofovir Treated HEK Cells over a 72 Hour Time Frame

(A) Total p53, phospho-p53 and p21 Western blot images for HEK cells 12, 36 and 72 hours post Cidofovir teatment. p53 and p21 proteins were imaged using a 1 minute exposure time. Phospho-p53 was imaged using a 30 minute exposure time. β-Actin was imaged using a 1 minute exposure time. B-Actin (a) corresponds to the same membrane as p53 and p21. β-Actin (b) corresponds to the same membrane as phospho p53. Specifiicty of all antibodies used can be found in appendix 8. (B) Band intensities for (i) Total p53, (ii) Phospho-p53 and (iii) p21 in HEK cells post Cidofovir treatment. Intensities were first normalized to the corresponding intensity for β-Actin on the same nitrocellulose membrane, before further normalization to the untreated control band for each time point.

5.4. *E6, E7, TP53* and *p21/CDKN1A* Transcription Levels in Cidofovir and Cidofovir Combined with Radiation Treated NHIST Cell Lines

Hypotheses

i. *The increases in total and phosphorylated-p53 levels in Cidofovir and Cidofovir combined with radiation treated NHIST cell lines are due to decreases in E6 expression*
ii. *Increases in total and phosphorylated-p53 levels in Cidofovir and Cidofovir combined with radiation treated NHIST cell lines result in increased p21/CDKN1A transcription*

The p53 western blotting results showed that Cidofovir combined with radiation caused a re-accumulation of total and phosphorylated-p53, particularly in the A09 line. The molecular pathology of HPV associated cellular proliferation involves E6 and E7 degradation of tumour suppressor proteins p53 and pRb. Therefore, the apparent increase in total and phosphorylated p53 may have been due to combination treatment causing a decrease in *E6/E7* expression. mRNA from M08 and A09 cells treated with the same conditions as the Western blotting experiments (as described in Figure 5.1) was reverse transcribed and the resultant cDNA was subjected to RT-qPCR analysis to examine *E6, E7, TP53* and *CDKN1A* transcription levels, which are outlined in Figure 5.9. Table 5.4 lists p-values for change in *E6, E7, TP53* and *CDKN1A* transcription levels between the untreated control samples and each treatment condition for M08 and A09 cells.

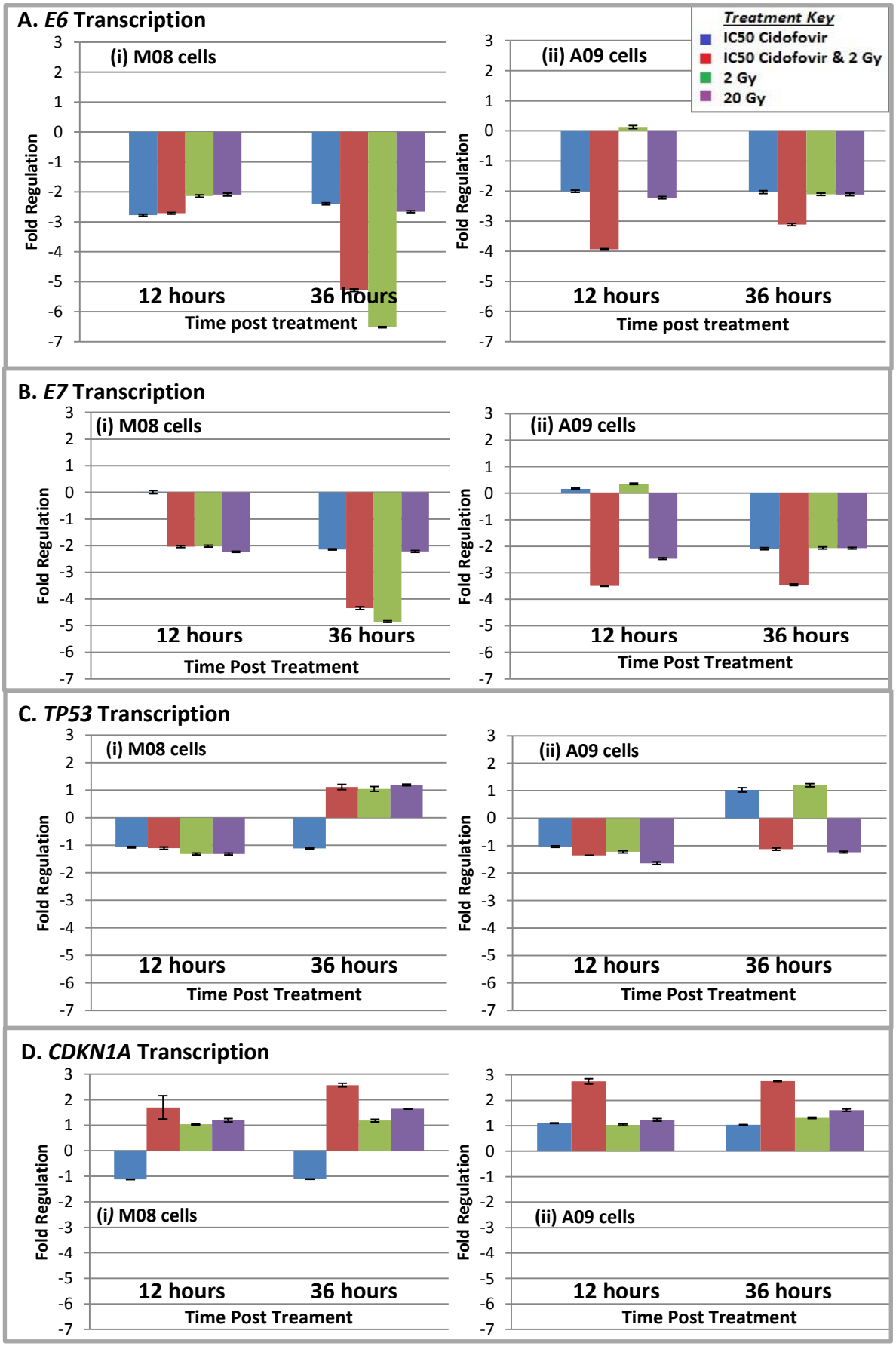
A. E6 Transcription
(i) M08 cells
(ii) A09 cells
Treatment Key
IC50 Cidofovir
IC50 Cidofovir & 2 Gy
2 Gy
20 Gy
Fold Regulation
12 hours
36 hours
Time post treatment
B. E7 Transcription
(i) M08 cells
(ii) A09 cells
Fold Regulation
12 hours
36 hours
Time Post Treatment
C. TP53 Transcription
(i) M08 cells
(ii) A09 cells
Fold Regulation
12 hours
36 hours
Time Post Treatment
D. CDKN1A Transcription
(i) M08 cells
(ii) A09 cells
Fold Regulation
12 hours
36 hours
Time Post Treament
Time Post Treatment

Figure 5.9. *E6, E7, TP53* and *CDKN1A* Fold Regulation for M08 and A09 Cells 12 and 36 Hours Post Treatment with Cidofovir, Cidofovir & 2 Gy, 2 Gy and 20 Gy radiation

Fold regulation relative to untreated control samples (which equate to 0 on the X axes) for (A) E6, (B) E7, (C) TP53 and (D) CDKN1A for M08 and A09 cells treated with a variety of conditions as outlined in Figure 5.1. Each sample was analysed in triplicate for each gene and error bars represent SEM. Before conversion to E6 and E7 fold regulation, fold change was calculated using qBase+ software (Biogazelle, Gent, Belgium). Before conversion to TP53 and CDKN1A fold regulation, fold change was calculated manually using the ΔΔCt equation.

Table 5.4. p-values for Change in *E6, E7, TP53* and *CDKN1A* Transcription between Untreated Control Samples and Cidofovir, Cidofovir & 2 Gy, 2 Gy and 20 Gy radiation Treatment Conditions for M08 and A09 Cells

Gene	M08 12 hour p-value				M08 36 hour p-value			
	Cidofovir	Cidofovir + 2 Gy	2 Gy	20 Gy	Cidofovir	Cidofovir + 2 Gy	2 Gy	20 Gy
E6	0.0019	0.0022	0.1347	0.332	0.0108	0.0003	0.0001	0.0027
E7	0.8744	0.5162	0.7952	0.0089	0.0283	0.0004	0.0001	0.0213
TP53	0.0826	0.1152	0.0041	0.0044	0.0629	0.2946	0.6864	0.0095
CDKN1A	0.0003	0.1356	0.2599	0.0346	0.0044	0.0001	0.0235	0.0001
Gene	**A09 12 hour p-value**				**A09 36 hour p-value**			
	Cidofovir	Cidofovir + 2 Gy	2 Gy	20 Gy	Cidofovir	Cidofovir + 2 Gy	2 Gy	20 Gy
E6	0.9398	0.0003	0.1483	0.0504	0.5962	0.0007	0.1735	0.1497
E7	0.3299	0.0144	0.0704	0.0982	0.2124	0.0002	0.3521	0.2555
TP53	0.6037	0.0028	0.0343	0.0045	0.8366	0.1036	0.0368	0.0121
CDKN1A	0.059	0.0001	0.5443	0.0189	0.3403	0.0001	0.0019	0.0003

The table shows p-values for change in E6, E7, TP53 and CDKN1A transcription between the untreated control sample and each treatment conditions for M08 and A09 cells. p-values were calculated using an unpaired two-tailed Student's t-test with 95% confidence intervals (GraphPad QuickCalcs software, GraphPad Software, Inc., California, USA). n = 3 for each condition. p-value < 0.05 (red text) = the difference in transcription levels is statistically significance. p-value > 0.05 (green text) = the difference in transcription levels is not statistically significant.

As can be seen from Figure 5.9 (A) and Table 5.4, *E6* was significantly down-regulated in Cidofovir and Cidofovir combined with 2 Gy radiation treated M08 cells 12 hours post treatment. *E6* was significantly down-regulated in all treatment conditions 36 hours post treatment of M08 cells. A similar effect was observed in the A09 cell line; however, Cidofovir combined with 2 Gy radiation was the only treatment condition that produced significant down-regulation of *E6* at both time points.

Figure 5.9 (B) and Table 5.4 show differential expression of *E7,* which was minimal in the Cidofovir treated M08 cells at 12 hours, however, at 36 hours it was significantly 2 fold down-regulated. *E7* was significantly down-regulated in all other treatment conditions in the M08 samples at 36 hours. Similar to *E6* transcription in A09 cells, *E7* transcription was significantly down-regulated in the Cidofovir combined with 2 Gy radiation treated A09 cells 12 and 36 hours post treatment.

Figure 5.9 (C) and Table 5.4 show differential regulation of *TP53* in the M08 and A09 cell lines 12 and 36 hours post treatment. Significant change in transcription was found in the 20 Gy treated M08 cells 12 and 36 hour post treatment; and in A09 cells 12 hours post treatment with Cidofovir combined with 2 Gy radiation, 2 Gy radiation and 20 Gy radiation and 36 hours post treatment with 2 and 20 Gy radiation.

CDKN1A was significantly down-regulated in M08 cells 12 hours post treatment with Cidofovir and 20 Gy radiation. *CDKN1A* in M08 cells treated with all conditions was significantly differentially transcribed 36 hours post treatment. *CDKN1A* was significantly up-regulated in A09 cells 12 hours post treatment with Cidofovir combined with 2 Gy radiation and 20 Gy radiation. *CDKN1A* was significantly up-regulated in Cidofovir combined with 2 Gy radiation, 2 Gy radiation and 20 Gy radiation treated A09 cells 36 hours post treatment. This can be seen in Figure 5.9 (D) and Table 5.4.

5.5. RT3VIN RT-qPCR

Hypothesis

Differential expression of genes involved in apoptosis is evident in VIN tissue from patients undergoing topical Cidofovir treatment in the RT3VIN clinical trial

The data derived from the RT-qPCR apoptosis arrays in cell lines suggested that Cidofovir produced a transcriptional response specific to HPV positive cells (Section 5.2). However, *in vivo* molecular processes can differ to those observed in cell culture. Therefore, the molecular effects of Cidofovir were examined in RNA samples from 10 VIN patients who had biopsies taken before treatment and six weeks into topical treatment with Cidofovir. The same genes that were examined in the individual RT-qPCR assays of the cell line studies were examined in the clinical material to compare the effects of treatment between *in vitro* and *in vivo* states. It was also important to examine the molecular effects of Cidofovir in the clinical samples, as when used topically, Cidofovir shows macroscopic specificity to VIN as opposed to healthy tissue (Tristram and Fiander, 2005). The RT3VIN RT-qPCR study was carried out blind in that only the baseline HPV status of the patients was known throughout the experimental and data analysis processes. After the data was analysed the HPV status of the patients during and after treatment was revealed.

Sadie Jones of the HPV Research Group at Cardiff University carried out type specific PCR to determine the HPV16 status of the baseline, during treatment and post-treatment samples, the results of which are outlined in Table 5.5. The RT-qPCR results of *TP53, CDKN1A, BCL2A1, BIRC3* and *HRK* transcription in patients treated topically with Cidofovir for six weeks are outlined in Figure 5.10.

Table 5.5. HPV Status of VIN3 Patients Before, During and Post Cidofovir Treatment

Case Number	HPV16 Status		
	Before Treatment	During treatment	After Treatment
1	Negative	Negative	Negative
2	Negative	Negative	Negative
3	Negative	Negative	Positive
4	Positive	Negative	Negative
5	Positive	Positive	Negative
6	Positive	Positive	Positive
7	Positive	Positive	Positive
8	Positive	Positive	Positive
9	Positive	Negative	Positive
10	Positive	Negative	Positive

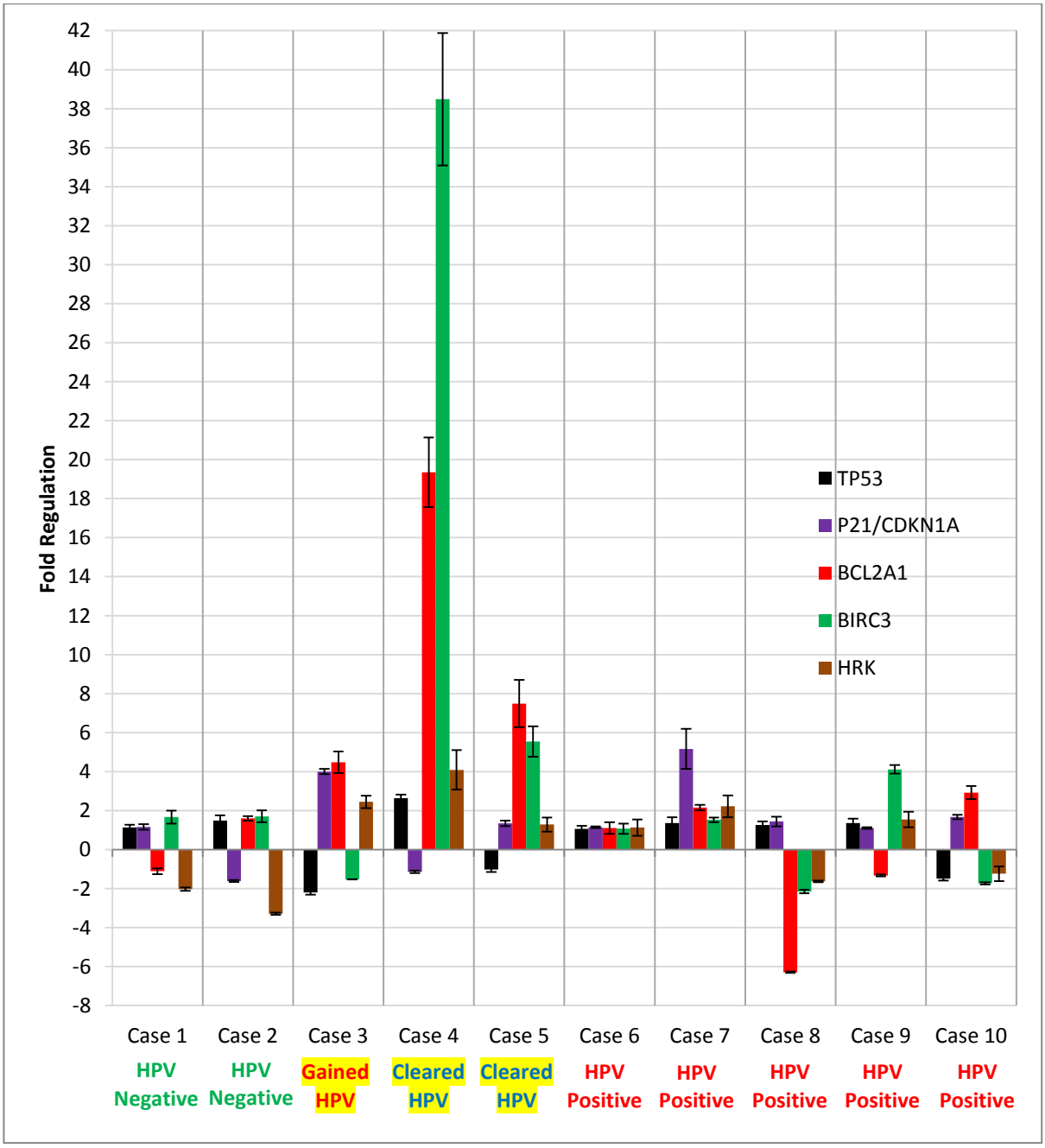

Figure 5.10. Transcription of *TP53, CDKN1A, BCL2A1, BIRC3* and *HRK* in VIN3 Patients Treated for 6 weeks with Topical Cidofovir

Fold regulation of TP53, CDKN1A, BCL2A1, BIRC3 and HRK in VIN3 patients treated for six weeks with topical Cidofovir. Fold regulation was derived from Relative Quantification, which was calculated manually using the ΔΔCt equation. Change in transcription was measured between the baseline samples and the six week (during treatment) samples for the each patient. RT-qPCR reactions were carried out in triplicate for each sample and error bars represent SEM of triplicate values.

There was no consistent response to treatment with Cidofovir for any of the genes examined. Equally, there was no obvious correlation between HPV status and response to treatment. Expression of *BCL2A1* and *BIRC3* were highly up-regulated six weeks into treatment in the cases that cleared HPV by the end of the trial. Expression of *BCL2A1* increased nearly 20 fold in Case 4 and nearly 8 fold in Case 5. Expression of *BIRC3* was up-regulated 38 fold in Case 4 and nearly 6 fold in Case 5.

Case 4 displayed the greatest fold change in *BCL2A1* and *BIRC3* transcription however, the Case 4 raw data showed a disproportional increase in Ct values for the two reference genes, *GAPDH* and *HPRT*, between the baseline and the six week/during treatment samples. Such a disproportional increase in reference gene Ct values was also seen in the Case 2 baseline sample. For the eight other cases, the Ct values were typically more consistent over the course of the study. The differences between reference gene Ct values for all cases, along with repeat values for Case 4, are presented in Figure 5.11. The purpose of the reference genes was to normalise expression differences that may have occurred due to sample loading errors, variation in RNA concentration, differences in RNA integrity and varying RT efficiencies. If a lower amount of cDNA was used in these RT-qPCR reactions, or if a lower concentration of RNA was used in the initial reverse transcription reaction, there would be an expected proportional increase in Ct values for all genes so long as they have similar PCR efficiencies.

When the raw Ct values for the five target genes were plotted in a similar manner (Figure 5.12), *TP53* and its target *P21/CDKN1A* followed a similar pattern to that of *GAPDH* and *HPRT* for Case 4*,* but *BCL2A1* and *BIRC3* did not. This suggests that in spite of potential underlying divergences in the normalization process for Case 4, there are genuine changes in transcription of these genes from baseline to the during treatment samples.

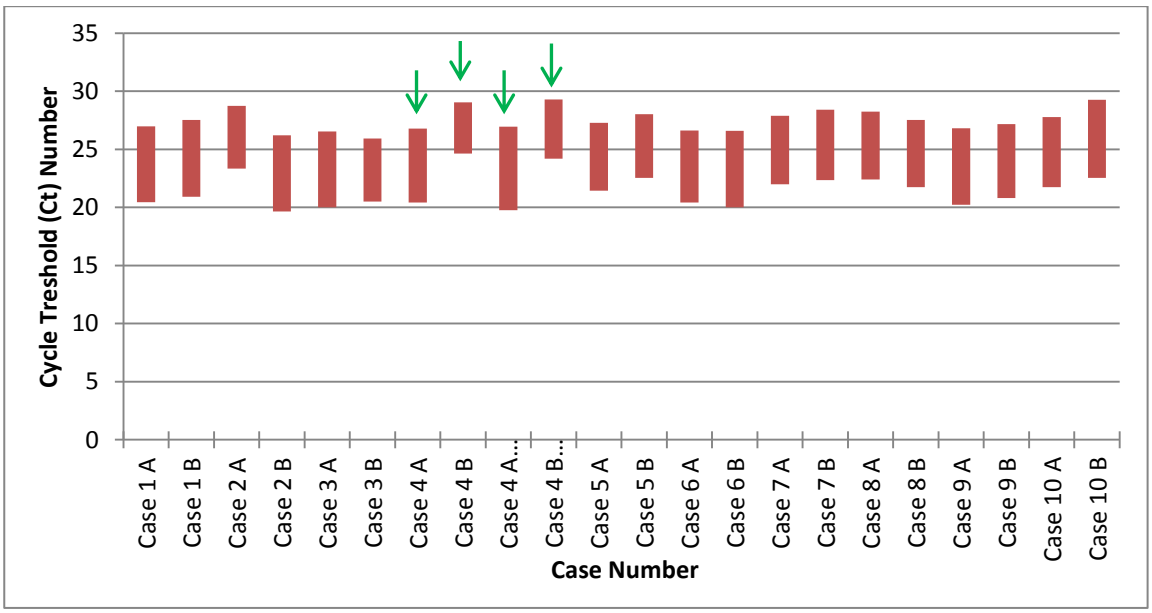

Figure 5.11. Difference in Ct Values between *GAPDH* and *HPRT1* for each RT3VIN Sample Analysed

Red bars illustrate the differences in Ct values between HPRT1 and GAPDH. HPRT1 had the higher Ct values; GAPDH had the lower Ct values. Ct values are the average of triplicate values for each sample. Case A denotes the baseline sample for each patient; Case B denotes the six week sample for each patient. Green arrows highlight Ct differences between housekeeping genes for Case 4.

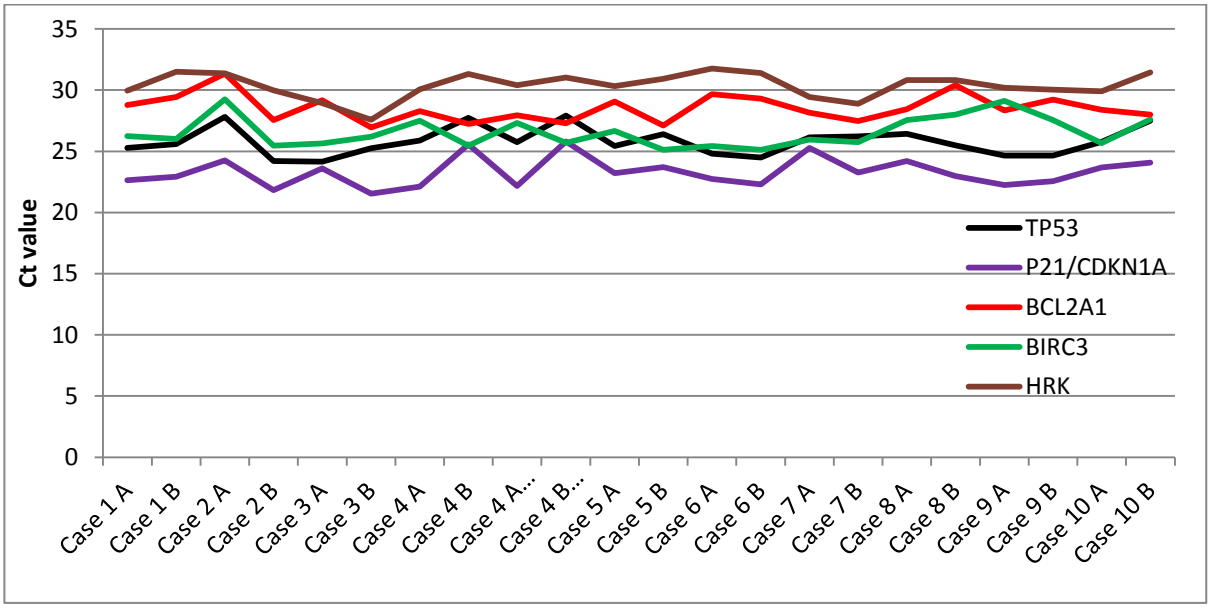

Figure 5.12. Raw Ct Values of *TP53, P21, BCL2A1, BIRC3* and *HRK* for each RT3VIN Sample Analysed

Ct values are the average of triplicate values for each sample. Case A denotes the baseline sample for each Case, Case B denotes the six week/during treatment sample for each Case.

TP53, P21, BCL2A1, BIRC3 and *HRK* expression in each of the patients before treatment is outlined in Figure 5.13. This analysis was carried out to determine differences, if any, in the baseline expression of these genes in the HPV positive and negative patients, as well as responders and non-responders. There appeared to be no difference in baseline expression of the target genes between HPV positive (Cases 1 – 3) and negative (Cases 4 – 10) patients, or between responders (Cases 4 and 5) and non-responders (Cases 6 -10). Additionally, Case 3, which appeared to have gained HPV16 DNA by the end of the trial, did not show any difference in baseline gene transcription similar to either the HPV positive or negative Cases.

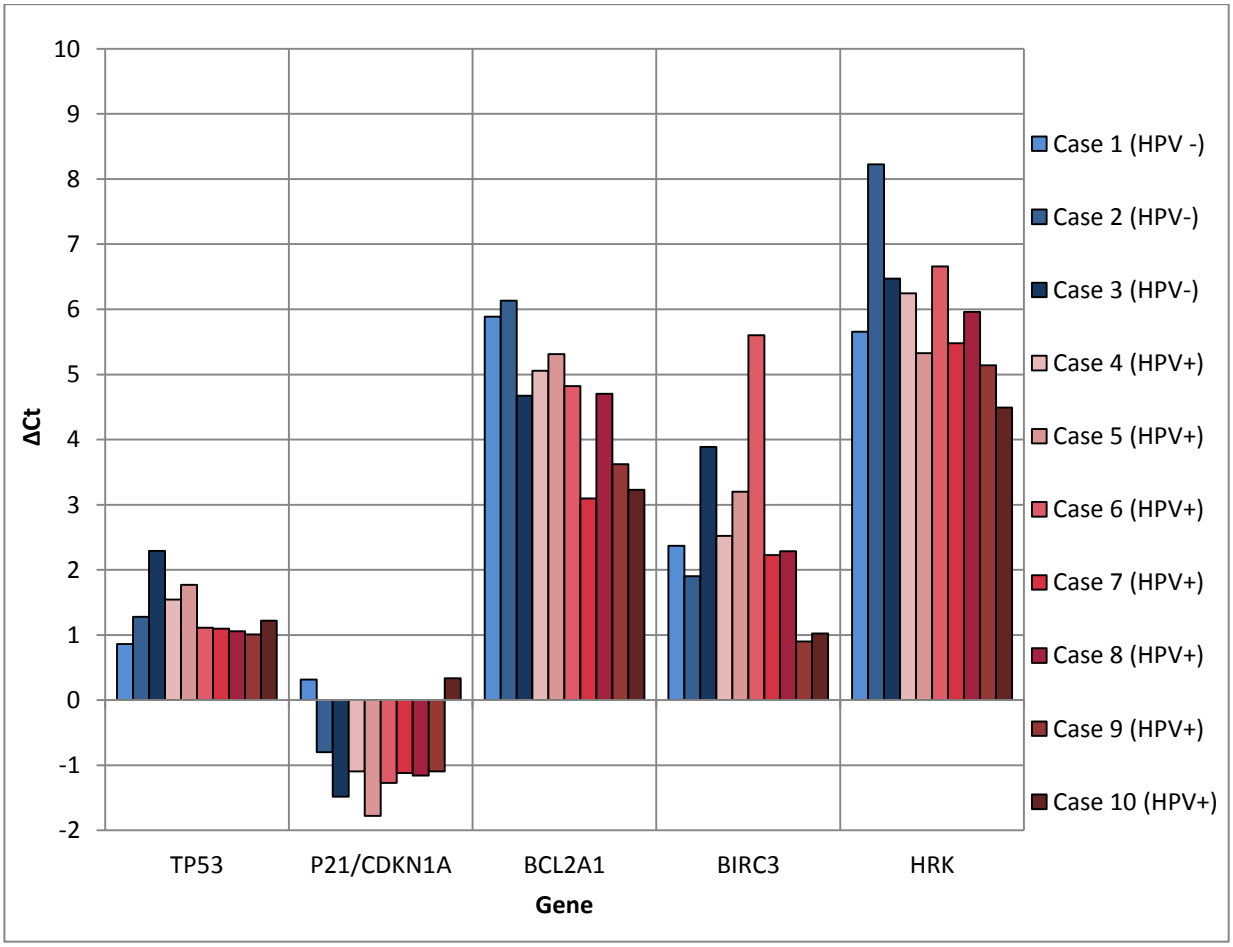

Figure 5.13. *TP53, P21, BCL2A1, BIRC3* and *HRK* ΔCt in HPV Positive and Negative RT3VIN Patients before Treatment

ΔCt values of baseline samples indicative of baseline transcription for each patient. A value of 0 indicates that the target gene is transcribed at the same level as the average of the housekeeping genes (GAPDH and HPRT1).

5.6. Discussion

Cidofovir Induction of Apoptosis and Effect of Combining Treatment with Radiation in NHIST Cell Lines

The caspase-3 data obtained for the A09 cell line was inconclusive. The western blot data suggested a possible caspase-3 response in Cidofovir treated A09 cells and possible synergistic effect when Cidofovir treatment was combined with radiation at 12 and 36 hours. However, this result was not observed in the caspase-3 activity assay.

Minimal caspase-3 responses were observed in the M08 cell line for all treatment conditions, with the exception of 20 Gy at 72 hours observed in the Western blotting data only. This would suggest Cidofovir, used individually or combined with a clinically relevant dose of radiation, does not produce an apoptotic response through caspase-3 activity in the M08 cell line. These findings suggest that apoptotic response pathways are defective in both lines, with the M08 line showing a greater defect.

In the untransformed HPV negative HEKs a sizable caspase-3 response was observed in the cells treated with Cidofovir and radiation together but not with either treatment individually; which suggests that this was a truly synergistic effect, rather than a merely additive one. Caspase activation in response to combined radiation and Cidofovir was not seen in the M08 and A09 cell line. This suggests that Cidofovir does not selectively radiosensitize HPV transformed cells to induce a caspase-3 response. This is important as it suggests that combining Cidofovir treatment with radiation in the clinic would produce a potently adverse effect on normal healthy tissue. The purpose of radiosensitizing compounds in cancer treatment is to selectively modify tumour cells and/or normal tissues so that therapeutic gain is achieved using conventional radiation (Coleman and Turrisi, 1990). These data oppose the results of Abdulkarim et al., 2002 , where they examined the radiosensitizing ability of Cidofovir using a clonogenic survival assay and found that exposure of HPV positive cells (Me180 and HEP2) to Cidofovir before irradiation was more efficient at inducing cell death than a relevant dose of radiation on its own. They concluded that this effect was more difficult to achieve in HPV negative C33A cells. As the C33A cell line was derived from a cervical carcinoma, the results presented in this study are more likely to represent a true clinical situation, as normal

untransformed HPV negative keratinocytes are genetically more comparable to healthy tissue.

The caspase-3 assays were used as opposed to other markers of apoptosis, such as annexin v staining, as cell membrane damage could occur during detachment of the adherent cells, which may interfere with the annexin v results, as this stain binds to phosphatidylserine on apoptosing cell membranes (Koopman et al., 1994). The caspase-3 assays were used instead of TUNEL assays as activated caspase-3 is responsible for nuclear fragmentation (Zheng et al., 1998), which is what the TUNEL assay ultimately detects (Gavrieli et al., 1992).

With regards to other studies, Andrei et al., 2001 , found that Cidofovir did induce caspase-3 activity in HPV33 transfected CK-1 cells using the ApoAlert CPP32/caspase-3 assay (Clontech, Saint-Germain-en-Laye, France). However, the cells they used for the assay were detached from the tissue culture surface prior to lysis, which may have altered the biochemical properties of the cells, possibly inducing caspase activity. Additionally, Andrei et al., 2001 , used higher concentrations of Cidofovir than used in the current study (20, 50 and 200 µg/mL, which equates to 64 µM, 159 µM and 635 µM respectively). They also found that the same concentrations of Cidofovir caused translocation of phosphatidylserine to the outer layer of the plasma membrane, disintegration of the nuclear matrix protein, DNA fragmentation and increased numbers of apoptotic cells following cell cycle analysis, all of which indicated that Cidofovir causes apoptosis in HPV 33 transfected CK-1s. However, these results were obtained 5 to 8 days post Cidofovir treatment, which was double the duration of treatment that was used in this study.

A strength of the caspase-3 study was that cleaved caspase-3 was measured by two separate methods in the same material. Appropriate controls were used, those being AMC and water as positive and negative controls respectively for the caspase-3 activity assay, and a MagicMark™ XP Western Protein Standard for Western blotting. The MagicMark™ XP Western Protein Standard and caspase-3 antibody specificity can be seen in Appendix 8.1. The 3 treatment options (IC50 Cidofovir, IC50 Cidofovir and 2 Gy and 2 Gy radiation

alone) made for a more comprehensive analysis of cellular caspase-3 response to various and combined treatment options. For the Western blots, the density of the individual bands was measured and normalized to those of a housekeeping gene in order to account for loading errors. Three cell lines were used; 2 HPV naturally immortalized and 1 untransformed cell line, which served as both a HPV negative control but also as a cell line whose stress/DNA damage response pathways were functionally intact.

A limitation of the study was the discordance between the caspase-3 activity assay and the cleaved caspase-3 Western blotting results, especially for the A09 cell line. Cleaved caspase-3 appeared to be higher in Cidofovir and Cidofovir plus 2 Gy irradiated cells at 12 hours in the Western blotting data compared with the caspase-3 activity assay data, and 2 Gy and 20 Gy treated cells appeared to be higher in the caspase-3 activity assay data compared to the Western blotting data at the same time point. The caspase-3 activity kit contains a fluorogenic substrate (N-Acetyl-Asp-Glu-Val-Asp-7-amino-4-methylcoumarin or Ac-DEVD-AMC) for activated caspase-3 enzyme and during the assay the activated enzyme cleaves the substrate between DEVD and AMC, generating highly fluorescent AMC, whereby fluorescence is proportional to apoptosing cells. The cleaved caspase-3 Western blotting on the other hand detects endogenous levels of the large fragment (17/19 kDa) of cleaved caspase-3. Technically both assays measure activated caspase-3, although in different ways. The caspase-3 activity assay was carried out using replicates of 3-4; however, only one run of Western blotting for cleaved caspase-3 was carried out due to protein quantity limitations. Furthermore, the dynamic range of densitometric analyses may be limited by signal saturation. Hence of the two assays, measurement of caspase-3 activity may give more reliable data.

Future work from the caspase-3 study would involve repeating the Western blotting with more lysate from the M08 and A09 cell lines to confirm the result obtained in this study. Additionally, as Western blotting was not performed on the HEK cell lysates due to low protein concentrations, future work would also include carrying out cleaved caspase-3 Western blotting on adequate lysates from this cell line.

Transcription of Apoptotic Response Pathway Genes post Cidofovir Treatment in NHIST Cell Lines

The data presented in the transcription of apoptotic response pathway genes section showed that Cidofovir appeared to affect transcription of pro- and anti-apoptotic genes in the M08 cell line, but this effect was not seen in the HEK cells. This data is consistent with the caspase-3 results for the HEKs, where caspase-3 activity was minimally, if not at all, induced by Cidofovir treatment; however, this data is less consistent for the M08 cell line where Cidofovir treatment did not induce a caspase-3 response. The results from this study also suggest that ADF Pro cf3475 did not cause transcription of apoptosis associated genes in both M08 and HEK cells when used at a concentration of 0.1 µM after 12 and 36 hours.

Clustergrams were used to display grouping of co-regulated genes and grouping of samples with similarly expressed genes. Clustergrams were constructed and displayed for the M08 line only as the genes in these cells showed greatest change in expression in response to treatment. Cidofovir treated M08 cells showed different profiles of gene expression when compared to those of the untreated as well as ADF Pro cf3475 treated cells.

Individual RT-qPCR assays were performed to validate the results obtained for genes differentially expressed at both time points in the RT-qPCR arrays. In the repeat individual RT-qPCR assays *BCL2A1* gene (BCL2-related protein A1) was 2 fold up-regulated in Cidofovir treated M08 cells at both time points. This gene is a direct transcriptional target of NF-kappa B in response to inflammatory mediators and is thought to have cell survival and cytoprotective functions. It can be up-regulated by different extracellular signals, such as CD40, inflammatory cytokine TNF and IL-1 among others. The protein encoded by *BCL2A1* can reduce the release of pro-apoptotic cytochrome C from mitochondria and block caspase activation (NCBI, September 2013c).

BCL2L10 (BCL2-like 10) was slightly more than 1 fold up-regulated at 12 hours but noticeably down-regulated at 36 hours after Cidofovir treatment in the M08 cell line in the RT-qPCR assay data. The protein encoded by this gene can interact with other members of BCL-2 protein family including BCL2, BCL2L1/BCL-X(L), and BAX. Similarly to *BCL2A1,*

BCL2L10 can inhibit apoptosis possibly through the prevention of cytochrome C release from the mitochondria and block caspase-3 activation (NCBI, September 2013s).

BIRC3 was down-regulated at both time points in the initial qPCR arrays and individual qPCR assays in the Cidofovir treated M08 cells. BIRC3 is a member of the IAP family of proteins that inhibit apoptosis by binding to tumour necrosis factor receptor-associated factors TRAF1 and TRAF2 and protects cells from formation of the ripoptosome, a multi-protein complex that can kill cancer cells in both a caspase-dependent and caspase-independent manner by ubiquitination. *BIRC3* also regulates inflammatory signalling and immunity. It modulates NF-kappa-B signalling through E3 ubiquitin-protein ligase activity. It regulates innate immune signalling via regulation of Toll-like receptors, NOD-like receptors and RIG-I like receptors. Additionally *BIRC3* helps control mitogenic kinase signalling and cell proliferation, cell invasion and metastasis (NCBI, September 2013a).

HRK was down-regulated at both time points after Cidofovir treatment in the M08 cell line in both the qPCR apoptosis array and individual qPCR assays. Similar to *BCL2A1* and *BCL2L10*, this gene encodes a member of the BCL-2 protein family. The translated protein localizes to intracellular membranes and promotes apoptosis by interacting with the apoptotic inhibitors BCL-2 and BCL-X(L) (NCBI, September 2013q).

TP53 was also down-regulated at both time points after treatment with Cidofovir in the M08 cell line, observed in both qPCR assays. *TP53* encodes tumour suppressor protein p53. The protein contains transcriptional activation, DNA binding, and oligomerization domains and responds to a range of cellular stresses by modulating expression of target genes, ultimately inducing apoptosis, cell cycle arrest, DNA repair or senescence (NCBI, September 2013p).

CDKN1A/p21 was slightly up-regulated at 12 hours and down-regulated at 36 hours in the M08 cell line post treatment with Cidofovir, as determined by the individual qPCR assay. *CDKN1A* encodes a cyclin-dependent kinase inhibitor, p21, which binds to and inhibits the activity of cyclin-CDK2 or -CDK4 complexes, modulating cell cycle progression at the G_1 phase. Its expression is stringently controlled by p53 in response to a variety of stress

stimuli. p21 can interact with the DNA polymerase accessory factor, PCNA, and helps regulate S phase DNA damage repair and replication (NCBI, September 2013g).

The results obtained for the Cidofovir treated M08 cell line showed no clear pro- or anti-apoptotic trends. *BCL2A1*, an anti-apoptotic gene, appeared to be up-regulated at both time points, whereas two other anti-apoptotic genes, *BCL2L10* and *BIRC3*, appeared to be down-regulated. *HRK*, a pro-apoptotic gene was also down-regulated. *TP53* was down-regulated at both time points, as was its transcriptional target, *CDKN1A*/*p21*, at 36 hours. Although down-regulation of *CDKN1A/p21* may coincide with down-regulation of *TP53* (if such a decrease in expression results in a decrease in p53 protein levels), the reason for a decrease in the expression of *TP53* is difficult to explain in this model. Regulation of transcription of *TP53* is not as well documented as regulation of p53 at a post translational level. One study found that p53 is able to induce its own transcription by binding to its promoter (Wang and El-Deiry, 2006). Another study found that exposure to genotoxic agents such as mitomycin and 5-fluorouracil also up-regulates *TP53* expression (Sun et al., 1995). The latter contrasts what was found in this study. The connection, if any, between the 6 genes appears to be complex in nature. These data do not suggest Cidofovir induces apoptosis at a transcriptional level, which can be linked to the results of the caspase-3 study, where apoptosis was absent at a protein level. However, these results may indicate that a process other than apoptosis is occurring specifically in the HPV positive cell line. Further work, ideally entailing full microarray analysis is required to determine this transcriptional relationship.

In relation to published literature, a study by De Schutter et al., 2013 , examined SiHa (HPV16 positive), HeLa (HPV18 positive) and HaCaT (HPV negative) transformed cell lines and primary human keratinocytes 24, 48 and 72 hours after treatment with 50 µg/mL (159 µM) Cidofovir in whole genome gene expression microarrays. They also validated microarray data by separate individual RT-qPCR assays. In SiHa cells 2 genes were differentially expressed after 24 hours (*DHRS2* and *HIST1H2A*, both down-regulated). At 48 hours 27 genes were differentially expressed and at 72 hours 140 genes were differentially expressed, with the majority being up-regulated. Twenty genes showed similar changes in expression between 48 and 72 hours. Expression was also examined in

HeLa, HaCaT and normal keratinocytes at 72 hours. The majority of differentially expressed genes in HeLa, HaCaT and the normal keratinocyte were up-regulated and the number of genes that were differentially expressed was higher in HPV negative HaCaT cells than in the HPV positive cell lines. Only 2 genes (*AOX1* and *CLIC3*) were differentially expressed (both up-regulated) in all 4 cell lines. Upon functional analysis of differential gene expression with Cidofovir treatment, they found 'immune response' and 'inflammatory response' to be the only functional groupings up-regulated in the four different cell types. With further functional analysis, the authors found that HPV positive cells showed differential regulation in genes linked to "cell death of tumour cells" following Cidofovir treatment. This response was not observed in the HPV negative primary keratinocytes. For example, *MDM4* was down-regulated and *BIK* and *CYLD* were up-regulated in SiHa cells, all of which are associated with cell death. Comparisons with the current study are limited as the De Schutter study examined 38,500 genes via microarray analysis, whereas this study examined 84 apoptosis pathway specific genes. A slight parallel between the studies was that Cidofovir was found to produce immune/inflammatory pathway responses in all cell lines post treatment in the De Schutter study, which may relate to the study presented here, where *BIRC3* and *BCL2A1*, both anti-apoptotic genes and genes involved in inflammation, were differentially regulated at 12 and 36 hours post treatment in the M08 cell line. Additionally, De Schutter et al., 2013, found a "cell death of tumour cell" pathway response specifically in HPV positive cells, while in the study presented here, differential regulation of several apoptosis pathway specific genes was observed specifically in the HPV positive M08 cells.

A strength of the current study was the examination of numerous apoptosis pathway specific genes (n = 84) in the RT-qPCR apoptosis arrays. Although a genome wide analysis would undoubtedly prove more informative, this study was designed to specifically assess the transcription of apoptosis linked genes in response to Cidofovir treatment. The RT-qPCR apoptosis arrays were commercially validated to a high standard and used with optimised reagents and analysed on a well maintained and calibrated ABI 7900HT RT-PCR instrument. Both HPV positive and negative cell lines were used to determine differences in expression of the genes analysed between virally transformed and untransformed

keratinocytes. The RNA used was of high quality and Agilent Bioanalyser checked. Two drugs, Cidofovir and ADF Pro cf3475, and a negative control were used to compare and contrast the expression of the genes between different treatment options. As samples/conditions could only be analysed once on a RT-qPCR apoptosis array due to cost, the genes that were flagged as greater than two fold up/down-regulated at both time points in the Cidofovir treated M08 cell line were examined further in triplicate using individual RT-qPCR assays, which contained identical primer sets to those in the RT-qPCR apoptosis arrays.

A weakness of the study was that the genes that did not display any differential regulation in the qPCR apoptosis array were not examined further to exclude false negative results. A second weakness may perhaps be that the HPV negative untransformed HEK cell line was derived from neonatal foreskin and the M08 line was derived from a vulval biopsy, thus a degree of heterogeneity was present between the two models, which should be highlighted when comparing these data. A final limitation of the study was that no true positive control was used in the RT-qPCR array experiments. In retrospect an apoptosis positive control, such as staurosporine, would have been useful.

To conclude, from the analysis of transcription patterns of M08 and HEK cells treated with both Cidofovir and ADF Pro cf3475 it would appear Cidofovir induced a transcriptional response specific to NHIST cells. However, from the transcription data obtained, the actual functional response is difficult to explain. Further work was conducted using Western blotting for p53 and p21 proteins to examine if the down-regulation of *TP53* and *p21* was carried to a translational level.

Total and Phospho-p53 Re-Accumulation in Cidofovir and Radiation Treated NHIST Cell Lines

From the total p53, phosphorylated-p53 and p21 Western blot data it would appear that Cidofovir treatment combined with radiation produced an increase in total and phosphorylated-p53 in the A09 cell line and, to a lesser extent, in the M08 cell line. These cells were pre-treated with Cidofovir before being subjected to a clinically relevant dose of 2 Gy radiation (Abdulkarim et al., 2002). The more prominent increases of these proteins in the A09 cell line compared with the M08 cell line may be due to the genotypic

differences between both. Both cell lines are *TP53* wild-type, however, M08 contains integrated HPV DNA, whereas, A09 contains episomal HPV16 DNA. As a result of the integration event in the M08 cell line the *E6* and *E7* transcriptional repressor, *E2*, is disrupted, which in theory should lead to unlimited expression of these oncogenes, and as a result, increased degradation of p53 protein. However, the transcriptional profiles of M08 and A09, outlined in section 3.1.4; Figure 3.8., suggest that oncogene transcription in both of the cell lines, in the absence of treatment, is similar. Interestingly however, *TP53* in the A09 cell line contains the SNV Arg72Pro, which translates to a p53 protein that some reports suggest has a higher affinity to *E6* oncoprotein, which therefore results in its increased *E6* mediated degradation (previously reviewed in section 3.8). However, from the results presented here it would appear the Arg72Pro SNV does not negatively affect the re-accumulation of total and phospho-p53 in Cidofovir combined with 2 Gy radiation treated A09 cells. Nevertheless, the reason why the p53 response in the A09 cell line was greater than in the M08 cell line, in the combination treated samples, is yet to be determined. A minimal increase in total and phospho-p53 was also noted in the HPV negative Cidofovir treated HEKs. This response appeared to be most evident 36 hours post treatment.

With regards to other studies, Johnson and Gangemi, 1999 , treated HPV16 transfected keratinocytes with 1 µM Cidofovir and examined p53 protein levels 2 days post treatment. Western blotting suggested that p53 levels were not affected by 1 µM Cidofovir. This result is similar to the one presented here where Cidofovir on its own did not produce an increase in total or phosphorylated p53. In contrast Abdulkarim et al., 2002 , found p53 protein levels to be increased three days post treatment with 10 µg/mL (32 µM) Cidofovir in HPV 18 positive HEP2 cells and HPV 39 positive Me180 cells. They also combined 10 µg/mL (32 µM) Cidofovir and 3 Gy radiation treatment in the same HPV positive HEP2 and Me180 cell lines and noted a prominent increase in p53 protein levels. Sirianni et al., 2005 , found that the growth of both SCC90 cells (HPV16 positive) and CaSki cells (HPV16/18 positive) was inhibited in the presence of 40 µg/mL (127 µM) Cidofovir after 30 Gy radiation. They further examined the effect of Cidofovir treatment on the expression of p53 protein through Western blotting and found that p53 expression was stabilized in the

presence of 20 µg/mL (64 µM) Cidofovir from two to four days. This result differed to the one presented here, where p53 protein levels only notably increased when Cidofovir treatment was combined with radiation.

Minimal if no effect was seen on p21 protein levels in each of the three cell lines, with the exception of small increases in the 20 Gy positive control samples for M08 and A09 cells. Unlike the data presented here, Abdulkarim et al., 2002 , did note an induction of p21 protein levels three days post treatment with 10 µg/mL (32 µM) Cidofovir in HPV positive Me180 and HEP2 cells. They did not report induction of p21 protein levels in the HPV negative C33A cell lines in response to Cidofovir treatment, nor was an induction observed in the HPV negative HEKs used in this study. Contrastingly, Johnson and Gangemi, 1999 , treated HPV 16 transfected keratinocytes with 1 µM Cidofovir and found via western blot analysis that p21 protein levels decreased by 82% two days post treatment.

These contrasting results could be explained by several reasons, in particular by the regulation of p21 expression and the differences between the HPV positive cell lines used in the three studies. Transcription of p21 can be induced by both p53-dependant and -independent mechanisms (Gartel and Tyner, 1999). The p21 promoter contains two p53-response elements, at least one of which is needed for p53-dependent transcription of p21 (el-Deiry et al., 1993). Transcription of p21 can be controlled independent of p53 through six SP1 binding sites located within the p21 promoter in response to a variety of intrinsic and extrinsic signals such as transforming growth factor-β (TGF-β), butyrate, lovastatin, phorbal ester, okadaic acid and Ca^{2+} (all reviewed in Gartel and Tyner, 1999). Additionally transactivation of p21 transcription can also occur by transcription factors such as E2F proteins via cis-acting regulatory elements within the p21 promoter (Hiyama et al., 1998).

In theory, the increase in phospho-p53 observed in the M08 and A09 cell lines in the Cidofovir combined with radiation treated samples should result in an increase in p21 expression at an mRNA and protein level. These data suggest activated p53 does not result in an up-regulation of p21 at a post-translational level. However, p21 expression is also regulated at a post-transcriptional pre-translational level. Ivanovska et al., 2008 ,

found that miR-106b reduced p21 mRNA levels by 38% and p21 protein levels by 46% through RT-qPCR and immunohistochemistry analysis of treated human mammary epithelial cells. They also found that replicas of several members of the miR-106b family down-regulated a luciferase reporter carrying the entire p21 mRNA 3' UTR (untranslated region), as this region of p21 mRNA contains two hexamers complementary to the miR-106b family seed region (Ivanovska et al., 2008). The study concluded that miR-106b regulation of p21 promotes cell cycle progression. To complement this, a different study by McBee W.C. et al., 2011 , examined miRNA expression in four normal HPV negative cervical tissue samples, three HPV16 positive CIN2/3 samples and six HPV16 positive invasive squamous cell carcinoma cervical samples using human MicroRNA Arrays. They found 18 miRNAs were up-regulated and 2 miRNAs were down-regulated in cervical cancer tissue compared to normal cervical tissue. Further to this, through individual micro-RNA assays they found 8 miRNAs, including miR-106b, to be significantly overexpressed in the cervical cancer tissue. miR-106b is located less than 1 Mb from the common fragile site FRA7F on chromosome 7q22 (Calin et al., 2004). HPV integration has been shown to occur around this common fragile site (reviewed by Wentzensen et al., 2004). It is thought that HPV integration causes changes in transcription patterns of adjacent DNA, therefore, it may be speculated that integration of HPV at this common fragile site causes overexpression of miR-106b. In addition to this, Petrocca et al., 2008 , found that transcription of the miR-106b-25 cluster, containing miR-106b, is transactivated by E2F1 by transcription of its target gene, MCM7. Therefore if HPV E7 mediates degradation of pRb, releasing E2F, this could be another mechanism whereby HPV can promote up-regulation of miR-106b and possible inhibition of p21 at a post-transcriptional level.

Therefore, HPV associated up-regulation of miR-106b, by integration dependant and independent mechanisms could be a reason for the apparent non-differential effect on p21 protein levels for all treatment options in both the M08 and A09 HPV positive cells. Perhaps differences in the miRNA expression capacities of the HEP2 and Me180 cells used by Abdulkarim et al., 2002 , the HPV16 transfected keratinocytes used by Johnson and Gangemi, 1999 and the VIN and VaIN M08 and A09 cell lines used in this study, were a

reason for these contradicting results. Future work will therefore examine p21 transcription at an mRNA level in response to Cidofovir and Cidofovir combined with radiation treatment in the NHIST cell lines and HEKs, as well as possible miRNA expression status of the NHIST cell lines.

Strengths of the total p53, phospho-p53 and p21 western blotting study include the variety of treatment options examined in two genetically different HPV naturally immortalized cell lines. Untreated cells were used as a negative control, and 20 Gy treated cells as a positive control. Twenty Grey was chosen at it has been shown to induce a p53 response in cultured cells (Cmielova et al., 2012). Combination treatment of Cidofovir plus 2 Gy radiation treatment was also evaluated as 2 Gy radiation in cell lines was equivalent to a clinically relevant dose (Abdulkarim et al., 2002). Membranes were visually inspected and also evaluated using densitometry software which enabled normalization to the house-keeping protein, β-Actin. Also, a MagicMark™ XP Western blot protein standard was also used to ensure the identification of the correct sized protein. The MagicMark™ XP Western blot protein standard and specificity of the antibodies used can be seen in appendix 8. Protein levels were examined 12, 36 and 72 hours post treatment in order to capture any variation in protein levels over a 3.5 day period post treatment.

A weakness of the study was that sufficient HEK cell lysate was unobtainable for Western blotting in the irradiated HEK cells. Thus the effect of combination treatment on total and phosphorylated-p53 levels cannot be compared between the HPV positive and HPV negative cell lines. However it was shown that Cidofovir combined with radiation could produce an augmented apoptotic response through cleaved caspase-3 activation in HEK cells. Upon examination of previously published studies (Abdulkarim et al., 2002, Sirianni et al., 2005), it may have been useful to have carried out a clonogenic survival assay to attain exact viable cell numbers post Cidofovir combined with radiation treatment to examine if the increase in total and phosphorylated-p53 in these samples resulted in a greater growth inhibitory effect in comparison to Cidofovir treatment on its own. Viable cell counting was carried out on all Cidofovir treated cells to calculate IC50 values for each cell type. However, cell counting was not performed to an accurate standard in this study as cells were lysed directly on tissue culture surfaces to avoid metabolic changes in the

cells caused by trypisization. From this, future work would involve clonogenic survival assays on irradiated NHIST cells and HPV negative untransformed HEKs to determine radiosensitizing ability, if any, of Cidofovir.

To conclude on the total p53, phospho-p53 and p21 western blotting data Cidofovir treatment combined with a clinically relevant dose of radiation induced re-accumulation of total and phosphorylated p53 at 12, 36 and 72 hours in the NHIST cell lines. Overall, this effect was most prominent at 36 hours and was more pronounced in the A09 cell line. This effect was not seen in individual Cidofovir or individual 2 Gy radiation treated NHIST cell lines, suggesting the effect was synergistic rather than simply additive. In addition to clonogenic survival assays, further work stemming from this data set would also involve examination of miRNA expression levels in the NHIST cell lines to establish a link if any with p21 expression levels.

E6, E7, TP53 and p21/CDKN1A Transcription Levels in Cidofovir and Cidofovir Combined with Radiation Treated NHIST Cell Lines

From the *E6, E7, TP53* and *p21/CDKNA1* transcription study the most notable change in *E6* and *E7* transcription for both the M08 and A09 cells at both time points appeared to be in the Cidofovir combined with 2 Gy radiation treated samples. *E6* was down-regulated in M08 cells in response to all treatments conditions at both time points. With the exception of the individual 2 Gy treated sample at 36 hours, an *E6* response similar to that of the M08 cell line was found in the A09 cell line. *E7* transcription showed a similar pattern to that of *E6* for both the M08 and A09 cell lines, with the only difference being that there was no change in *E7* transcription in the Cidofovir treated samples 12 hours post treatment. A similar pattern of expression of both oncogenes would be expected as *E6* and *E7* are transcribed as a single bicistronic pre-mRNA (Baker C and C., 1995, Tang et al., 2006). Therefore, a significant down-regulation of *E6*, with no accompanied down-regulation of *E7* in the 12 hour Cidofovir treated samples is intriguing.

Three exons and two introns form the HPV 16 and HPV 18 bicistronic E6E7 pre-mRNAs (Tang et al., 2006). Intron 1 is positioned in the *E6* ORF, consequently removal of this intron by RNA splicing would disrupt the *E6* ORF and prevent the expression of full length E6 (Tang et al., 2006). If intron 1 remains unspliced, the resulting E6E7 mRNA can be

translated into oncogenic E6 (Zheng et al., 2004). Intron 1 of HPV 16 E6E7 pre-mRNA contains one 5' splice site and three different 3' splice sites (Tang et al., 2006). Several different studies have found that splicing of intron 1 in the HPV 16 E6E7 pre-mRNA is extremely competent, where many transcripts in cervical cancer cell lines and cancer tissues are a spliced product without intron 1, denoted E6*I (Doorbar et al., 1990, Sherman et al., 1992). It is thought that splicing of intron 1 in this pre-mRNA transcript is necessary for E7 production, as there are only two nucleotides between the termination of E6 translation and the re-initiation of E7 translation in HPV 16 E6E7 pre-mRNA containing this intron (Tang et al., 2006). Zheng et al., 2004 , found that splicing of the E6E7 pre-mRNA provided more E7 RNA templates and increased the production of E7 oncoprotein, whereas absence of RNA splicing produced low levels of E7 oncoprotein. Therefore, mutation in intron 1 splice sites or inhibition of splicing may result in decreased levels of E7 oncoprotein, without a similar effect on levels of E6 oncoprotein. However, this does not explain why a decrease in *E6* transcript levels occurred in the absence of a corresponding decrease in E7 transcript levels 12 hours post Cidofovir treatment. As this difference occurred in each cell line, where all other conditions followed a similar pattern of oncogene regulation, it appears unlikely to be due to an assay fault.

In terms of molecule half-lives, if E7 mRNA had a longer half-life than *E6* mRNA perhaps this difference in transcript levels could be explained, but as *E7* transcript levels were the same as *E6* in all other conditions this is presumably not the case. Jeon and Lambert, 1995 , found E6/E7 mRNA molecules to have half-lives of three hours in cell lines that contain episomal HPV DNA and half-lives of 6 to greater than 12 hours in cell lines that contain integrated HPV DNA using an actinomycin-D mRNA decay assay. However, they did not differentiate between E6 and E7 mRNA molecules. In this study, where HPV DNA in the M08 cell line was hypothesized integrated and hypothesized episomal in the A09 cell line, differences in E6 and E7 transcript levels by differential half-lives depending on HPV DNA type were not noted.

The decrease in oncogene transcription in the other conditions may be due to DNA damage caused by Cidofovir and radiation, treated both individually and combined. If DNA damage, in the form of strand breaks occurred in the *E6* and *E7* ORFs, transcript levels of

these genes would decrease. However, this presumably would also happen in other genes including housekeeping genes, therefore, ΔCt between *E6/E7* and the housekeeping genes would remain similar. This does not explain why *E7* transcript levels in both M08 and A09 cells treated with Cidofovir remain the same as the corresponding untreated control cells, when in the same samples E6 levels decrease. Further work is warranted to elucidate this phenomenon.

There was no pattern in *TP53* transcription found between the M08 and A09 cell lines at both time points with all treatment conditions. However, *CDKN1A/p21* showed distinct up-regulation in both cell lines at both time points in the Cidofovir combined with 2 Gy treated cells. These data complement the p53 Western blot results outlined in section 5.3, where the prominent decrease in *E6* transcription may be linked to the large increases in total and phosphorylated-p53 protein levels in M08 and A09 cells treated with a combination of Cidofovir and 2 Gy radiation, which in turn may be linked to the corresponding increase in *CDKN1A/p21* transcription in the same samples. As *TP53* showed minimal changes in transcription in the Cidofovir combined with 2 Gy treated samples, and because there was a prominent increase in corresponding p53 protein levels, it would suggest that the increase in p53 in this treatment condition occurs via a post-translation mechanism.

The transcription results presented in this section contrast those in the initial individual RT-qPCR arrays and individual assays in results section 5.2, where *TP53* was 3 to 4 fold down-regulated and *P21/CDKN1A* was 1 to 3 fold down-regulated in Cidofovir treated M08 cells. In the data presented here both genes were just over 1 fold down-regulated in the Cidofovir treated M08 cells. The reasons for this discrepancy are unknown but may possibly have something to do with the different concentrations of Cidofovir used in the two experiments. The results obtained from the RT-qPCR apoptosis arrays and individual assays were from an earlier experiment where the IC50 value of Cidofovir in M08 cells was determined as 10 µM. However, following further experimentation the IC50 estimate was later revised to 5 µM Cidofovir. Therefore, 5 µM Cidofovir was used in all further experiments involving the M08 cell line. Perhaps the higher concentration of Cidofovir used in in the initial RT-qPCR apoptosis arrays and individual assays caused a greater

effect on the down-regulation of *TP53* and *p21/CDKN1A,* which may occur in a dose dependent manner.

E6 and *E7* transcript levels were measured using a different method to that for *TP53* and *p21/CDKN1A. TP53* and *p21/CDKN1A* cDNA levels were measured using commercially available RT-qPCR assays, where relative quantification was calculated using the standard ΔΔCt equation as target genes and reference genes (*GAPDH* and *HPRT1*) were designed to have similar PCR efficiencies as the individual RT-qPCR assays. However, *E6* and *E7* transcript levels were quantified using the Vandesompele equation (Vandesompele et al., 2002) as the *E6*, *E7* and reference gene (*TBP2* and *HPRT1*) primer sets had different PCR efficiencies. The qBase+ software (Biogazelle, Gent, Belgium) uses the Vandesompele equation to calculate relative gene quantification and corrects for differences in PCR efficiencies between the various target and reference genes. Additionally corresponding reverse transcription negative RNA samples were also subjected to RT-qPCR analysis for the HPV *E6* and *E7* genes to rule out contamination with genomic DNA, as the *E6* and E7 primer sets were not intron spanning.

In relation to published literature, one study examined *E6* expression after Cidofovir treatment (without radiation) at the protein level by Western blotting. They found 6 days of Cidofovir treatment inhibited *E6* expression more effectively than 3 days of treatment and they also found that *E6* inhibition in HeLa cells was associated with p53 restoration (Amine et al., 2009). In the study presented here, *E6* transcription was found to be down-regulated as early as 12 hours post Cidofovir treatment. However, in this study p53 restoration was only associated with E6 down-regulation in the Cidofovir combined with 2 Gy treated NHIST cells, not Cidofovir treatment on its own. However, it may be possible that Cidofovir treatment for a longer period of time (6 days) may have eventually resulted in p53 restoration.

A different study examined *E6* expression in Cidofovir treated SCC90 cells derived from a HPV naturally transformed SCC of the oropharynx and found that 2 doses of the drug were needed to produce a decrease in *E6* transcription by 4 days (Sirianni et al., 2005). This

again contrasted what was found in this study, where a decrease in *E6* transcription was observed as early as 12 hours post Cidofovir treatment.

Abdulkarim et al., 2002 , used Western blot analysis to examine E6 and E7 protein levels after 1 - 10 mg/ml Cidofovir exposure in Me180 and HEP2 cell lines. They found the amount of E6 protein in Me180 and HEP2 cells decreased by 30% and 25% respectively after 3 days of treatment, and by 60% and 80% after 6 days. They found 40% and 60% decreases in E7 protein levels in Me180 and HEP2 cells at 3 days, and 65% and 85% reductions at 6 days. They also examined E6/E7 mRNA levels by RT-qPCR in HEP2 cells after 1 to 10 mg/mL Cidofovir, 3 Gy, 6 Gy and 9 Gy ionizing radiation and combined treatment of both. Compared to the untreated cells, *E6/E7* mRNA levels in the Cidofovir treated cells decreased by 50% and 70% at 3 and 6 days respectively. Contrastingly, *E6/E7* mRNA levels were 2 fold increased 24 hours post 9 Gy ionizing radiation, however, this radiation-induced rise in *E6/E7* mRNA levels was eradicated when cells were pre-treated with Cidofovir. Similar to the Abdulkarim study, a decrease in *E6* and *E7* mRNA levels was observed post treatment with Cidofovir in this study. However, contrasting to what Abdulkarim et al., 2002 found*, E6/E7* transcript levels were also decreased 12 and 36 hours post 2 and 20 Gy gamma radiation in the NHIST cell lines. Santin et al., 1998 , also noted an increase in *E6/E7* expression by northern blot analysis of 12.5 - 100 Gy gamma irradiated CaSki and SiHa cervical carcinoma cell lines and suggested that irradiation could confer a significant growth advantage to radiation-resistant tumour cells. As other HPV positive cell lines have been found to be more radiosensitive than HPV negative cell lines (listed and described by Kimple et al., 2013, Rieckmann et al., 2013), perhaps the effect of radiation on HPV positive cells is cell line specific.

A strength of this RT-qPCR study was that the individual RT-qPCR assays used for *TP53* and *p21/CDKN1A* were commercially optimised, well validated assays used on a routinely calibrated ABI 7900HT RT-PCR analyser. To add to this *E6* and *E7* transcription was quantified by correcting for differences in PCR efficiencies and possible genomic DNA contamination. Furthermore, the variety of treatment conditions, as well as the combination treatment condition, examined in the two NHIST cell lines made for a more comprehensive evaluation of gene expression in response to a range of treatment

options. Similarly, the two time points used to examine the differential regulation of the genes allowed for the inspection of transcription patterns over time.

To conclude, examining the data from this section altogether, Cidofovir combined with 2 Gy radiation proved to be the most effective treatment condition at producing differential expression of *E6, E7* and *P21/CDKN1A,* when compared to the individual treatment conditions in M08 and A09 cell lines. Minimal effect on *TP53* transcription was observed in both cell lines with all treatment conditions, suggesting that increases in p53 protein levels in the combination treated samples (observed in results section 5.3), were a result of post-translational mechanisms.

Summary of in vitro Mechanism of Action of Cidofovir Data

A summary of the cell line data acquired from the mechanism of action of Cidofovir studies is outlined in Table 5.6.

Table 5.6. Summary of Mechanism of Action of Cidofovir and Combined Treatment with Radiation Findings

Assay	M08 (HPV 16)		A09 (HPV 16)		HEKs (HPV negative)	
	Cidofovir IC50 ‡ 5 µM	5 µM Cidofovir & 2 Gy radiation	Cidofovir IC50 ‡ 21 µM	21 µM Cidofovir & 2 Gy radiation	Cidofovir IC50 ‡ 6.6 µM	6.6 µM Cidofovir & 2 Gy radiation
Effect on cell morphology †	Increase in size with increase in concentration	Not Recorded	Difficult to interpret on photo-micrographs	Not Recorded	Increase in size with increase in concentration	Not Recorded
Caspase-3 Activity Assay	Decrease	Decrease	Decrease at 72 hours	Decrease at 72 hours	Slight Increase	Prominent Increase
Cleaved Caspase-3 protein levels	No Effect	No Effect	Slight Increase	Slight Increase	Not assayed	Not assayed
Apoptosis pathway specific gene arrays (mRNA levels)	Differential regulation of pro- and anti-apoptotic genes	Not assayed	Not assayed	Not assayed	No Effect	Not assayed
Total p53 protein levels	No Effect	Slight Increase	Slight Increase	Prominent Increase	Slight Increase	Not assayed
Phospho-p53 protein levels	No Effect	Slight Increase	No effect	Prominent Increase	Slight Increase	Not assayed
p21 protein levels	No Effect	No Effect	No Effect	No Effect	No Effect	Not assayed
***E6* mRNA levels**	Decrease	Prominent Decrease	Effect not significant	Prominent Decrease	Not assayed	Not assayed
***E7* mRNA levels**	No Effect at 12 hours Decrease at 36 hours	Prominent Decrease	Effect not significant	Prominent Decrease	Not assayed	Not assayed
***TP53* mRNA levels**	Effect not significant	Effect not significant	Effect not significant	Decrease	Not assayed	Not assayed
***CDKN1A* mRNA levels**	Decrease	Prominent Increase	Effect not significant	Prominent Increase	Not assayed	Not assayed

† Data taken from results section 4.1. Morphology measured 96 hours post treated with 0, 1, 5, 10 and 100 µM Cidofovir for M08 and A09 Cells; 0, 1, 10 and 100 µM Cidofovir for HEK cells.

‡ IC50 values were those calculated 96 hours post Cidofovir Treatment.

** M08 and HEK cells were treated with 10 µM Cidofovir for the apoptotic pathway specific gene arrays.*

To summarise the *in vitro* findings:

- Cleaved caspase-3 was assessed as an indicator of apoptosis and was examined by two different methods. Caspase-3 activity was not increased in the M08 or A09 cell lines by Cidofovir or Cidofovir plus gamma radiation at any of the time points examined. HEKs displayed the greatest induction of cleaved caspase-3, especially in the combination treated samples. The caspase data for the HEK cell line was obtained from the caspase-3 activity assay only.
- The RT-qPCR apoptosis arrays examined the transcriptional response of apoptosis related genes to treatment with Cidofovir in the M08 and HEK cell lines. This assay also examined the transcriptional response of these cell types to treatment with ADF Pro cf3475, the most potent ProTide ANP analogue (described in results section 4.3). Minimal transcriptional responses were observed in M08 and HEK cells treated with ADF Pro cf3475. However, Cidofovir induced a transcriptional response specific to the NHIST cell line, M08. Genes in the RT-qPCR apoptosis array, which were flagged as differentially regulated in the M08 cell line at 12 and 36 hours post Cidofovir treatment were examined further in individual RT-qPCR assays. The relationship between the genes that were differentially expressed at both time points appeared complex as both pro- and anti-apoptotic genes were similarly up-regulated or similarly down-regulated.
- The third section of this chapter examined levels of total and phosphorylated-p53 protein in the M08 and A09 cell lines in response to treatment with Cidofovir and Cidofovir combined with gamma radiation. In the M08 cell line, total and phosphorylated-p53 protein levels were slightly elevated compared to the untreated control samples in the Cidofovir combined with radiation treatment only. In the A09 cell line there was a substantial increase in both total and phosphorylated-p53 in the combination treated samples at each time point. There was also a slight increase in total p53 in the Cidofovir only treated A09 cells. Total and phosphorylated-p53 levels were additionally examined in HEKs treated with Cidofovir only and very slight increases in both proteins were observed in these samples. Finally, p21 protein levels were examined in the same cell lysates, however, no notable difference in p21 levels

was found in any of the cell lines with the exception of the positive control (20 Gy) samples in the M08 cell line.

- The data presented in the fourth section of this chapter was carried out in response to the p53 Western blotting results. RT-qPCR of *E6, E7, TP53* and *p21/CDKN1A* was undertaken on RNA from the same samples that were subjected to Western blotting. A reduction in *E6* mRNA levels was observed in M08 and A09 cells for all treatment conditions, with the exception of 2 Gy 12 hours post treatment in the A09 cell line. For both M08 and A09 cell lines, the most prominent reduction in *E6* was generally observed in the Cidofovir combined with radiation treated samples. *E7* mRNA levels followed the same pattern to those of *E6* for both cell lines, with the exception of the Cidofovir only treated cells at 12 hours for both cell lines. Changes in *TP53* mRNA levels in both the M08 and A09 cell lines were inconsistent. However, *p21/CDKN1A* mRNA levels were up-regulated in the Cidofovir combined with radiation treated samples in both cell lines.

Examining the previous findings simultaneously several deductions as to the mechanism of action of Cidofovir can be made. Firstly, the decrease in number of HPV positive cells post treatment with Cidofovir (as described in results section 4.1) does not appear to occur via induction of cleaved caspase-3. Secondly, differential transcription of apoptosis pathway specific genes in HPV positive cells post treatment with Cidofovir suggested a specific response when compared to HPV negative untransformed cells also treated with Cidofovir. However, as no patterns in regulation of pro- or anti-apoptotic genes were observed it may be suggested that a process other than apoptosis is inhibiting proliferation of HPV positive cell lines at the concentration examined. The 2-fold reduction in *E6* mRNA levels in Cidofovir treated HPV positive cell lines could be an important contributing factor to the inhibition of proliferation of these cells. Down-regulation of *E7* was also observed in Cidofovir treated cells, but not until 36 hours post treatment. This down-regulation of oncogene mRNA levels may have resulted in a reduction in the *E6* mediated ubiquitination of p53. However, minimal changes in levels of total and phosphorylated-p53 were found in the Cidofovir treated M08 and A09 cells at the

concentrations used. Similarly, there was little effect observed on *p21* transcription or p21 protein levels post treatment with IC50 concentrations of Cidofovir. Perhaps at higher concentrations or for longer periods of treatment with Cidofovir such a response may be induced. For example, Abdulkarim et al., 2002 , found increases in p53 and p21 protein levels 3 and 6 days post 32 μM Cidofovir treatment. Therefore, future work to further examine these data would involve the use of higher concentrations of Cidofovir and examination of its effect for more than 72 hours.

It was clear that combining Cidofovir treatment with a clinically relevant dose of radiation resulted in an augmented molecular response in HPV positive cell lines. Both total and phosphorylated-p53 levels in A09 cell lines were noticeably increased as early as 12 hours post irradiation and continued to be elevated for the remainder of the 72 hour experiment. This effect was also observed to a lesser extent in the M08 cell line. The induction of both forms of p53 protein in the combined treated samples may have been associated with the observed decrease in *E6* and *E7* mRNA in the same sample. Additionally, an increase in *p21/CDKN1A* mRNA levels was also observed in the same samples. However, the increase in *p21/CDKN1A* mRNA levels did not result in an increase in p21 protein in either cell line.

With the exception of the total and phospho-p53 Western blot data for the A09 cells, where the effect of Cidofovir combined with radiation appeared to be synergistic, the effect appeared to be additive in the *E6* and *CDKN1A* transcription data (36 hour). The large caspase-3 response observed in the HEK cells further indicated that Cidofovir does not specifically radiosensitize HPV positive/transformed cells. It may be speculated that the augmented molecular response in the Cidofovir combined with radiation treated cells may be due to the susceptibility of HPV positive cells to radiation induced DSBs (Bresler et al., 1984); and the possibility that Cidofovir can also induce DSBs.

Rieckmann et al., 2013, have shown that 10 Gy radiation alone did not induce apoptosis or G_1 cell cycle arrest in HPV positive HNSCC cell lines, in spite of these cell lines displaying increased radiosensitivity compared to HPV negative HNSCC. However, 6 Gy irradiated HPV positive HNSCC cell lines did show cell cycle arrest in G_2 proportional to the

radiosensitivity of the respective cell lines. They further examined whether the G_2 cell cycle arrest was a result of a persistent G_2/M-checkpoint activation triggered by unrepaired DSBs. Cells were subjected to 2 Gy radiation and incubated for 24 hours at 37°C before the examination of residual DSBs via cH2AX/53BP1-positive repair foci. The results indicated that the numbers of foci in the HPV positive HNSCC cell lines matched the extent of G_2 cell cycle arrest and that the numbers of foci found in these cell lines negatively correlated with survival post irradiation as established in a colony formation assay. As this result was not observed in the HPV negative HNSCC cell lines examined, a central role for DSB repair capacity in survival of HPV positive cell lines post irradiation was indicated.

Similarly, De Schutter et al., 2013, concluded that growth inhibitory selectivity of Cidofovir is due to the difference in responses of normal and cancer cells to DNA damage. Using an assay designed to examine Cidofovir incorporation into genomic DNA, they found that higher levels of Cidofovir were incorporated into tumour cell DNA in comparison to normal untransformed keratinocyte DNA. After 72 hours incubation, 4-fold, 6-fold and 9-fold higher levels of Cidofovir were found in HaCaT (HPV negative), HeLa (HPV positive) and SiHa (HPV positive) transformed cells respectively, when compared to Cidofovir levels found for HPV negative primary human keratinocytes. They complemented the data by genome wide expression profiling of the four cell types treated with Cidofovir. The gene expression data suggested that that Cidofovir induced DSBs in DNA and that HPV positive cells were more susceptible to the growth inhibitory effects of Cidofovir as they are incapable of responding to this induced genotoxic stress due to defective DNA repair pathways.

Complimentary to the findings of De Schutter et al., 2013, a study by Shin et al., 2006 , demonstrated that HPV16 E6 instigated abnormal DNA end joining activities, such as reduced error-free DNA end joining ability and increased DNA end joining errors. Additionally, their results indicated that high-risk HPV E6's capability to bind, degrade and/or modify p53 was a primary feature in inducing abnormal DNA DSB repair in HPV positive cells. Another study by Deberne et al., 2013 , examined combination treatment

of Cidofovir and cetuximab and also found that Cidofovir treatment on its own induced DSBs.

De Schutter et al., 2013, suggest that Cidofovir was incorporated to a greater degree into HPV positive and transformed cells due to their higher rate of cell division. Additionally, inhibition of chain elongation by Cidofovir may cause stalling of replication forks; which in some instances can lead to induction of DSBs (Unno et al., 2013) via nuclease activity (Hanada et al., 2007).

As DSBs can induce a p53 response, where p53 can cause inhibition of cell proliferation by mechanisms other than apoptosis (such as cell cycle arrest and senescence), future work derived from the *in vitro* mechanism of action data presented here could involve evaluation of cell cycle inhibition in response to Cidofovir treatment. Cell cycle inhibition could be assessed through propidium iodide staining and analysis by flow cytometry, examination of cell cycle regulators other than *p21/CDKN1A*, which are also linked to p53 but function later in the cell cycle, examination of DSBs and possible examination of DSB response protein and DNA damage pathways.

Various individual strengths and limitations of the *in vitro* work outlined in this chapter have been previously discussed. An important limitation of the entire study is perhaps the cell model used. As previously described the M08 and A09 cell lines are NHIST cell lines derived from intraepithelial neoplasia biopsies. When these cells are used in 2D/monolayer culture the experimental model lacks physiological attributes such as barrier and immune system responses. Raft culture of these keratinocytes or animal models of disease would provide a more accurate disease representation. Additionally, due to the less robust nature of the HPV negative HEK cells, a true disease free HPV negative control model was not available for examination of the effects of radiation in such cells.

To conclude on the *in vitro* mechanism of action studies it would appear that Cidofovir does not induce a molecular response specific to HPV positive cell lines. At the concentrations used and in the time frames examined, Cidofovir did not induce apoptosis in HPV positive cells. By comparing the data presented in this chapter to recently

published literature it may be suggested that Cidofovir induces DSBs by stalling of replication forks. As apoptosis was not observed in Cidofovir treated cells, it may be speculated that the compound inhibits the growth of HPV positive cells by causing cell senescence or cell cycle arrest, perhaps at the G_2/M phase of the cell cycle. Cidofovir combined with a clinically relevant dose of radiation produced a prominent down-regulation of *E6/E7* mRNA levels and increased accumulation of total and phosphorylated-p53, with an accompanying increase in *p21/CDKN1A* transcription; however, an increase in p21 protein level was not observed. In spite of this augmented molecular response in the Cidofovir combined with radiation treated HPV positive cells, this treatment option produced a profound cell death effect on HPV negative untransformed HEK cells, indicating such a treatment option may be difficult to develop for use *in vivo*.

RT3VIN RT-qPCR

The preliminary RT-qPCR study on the RT3VIN clinical material was the first of its kind in examining expression of apoptosis related genes in a small cohort of woman with VIN treated topically with Cidofovir. The results showed no consistent differential regulation of *TP53, P21, BCL2A1, BIRC3* and *HRK* across all samples. However, they did suggest a possible link between clearance of HPV and expression of genes involved in anti-apoptotic/inflammation in Cidofovir treated VIN. *BCL2A1* and *BIRC3* are anti-apoptotic as well as inflammatory genes (gene function outlined in section 5.2). The data for Cases 4 and 5 on face value might suggest that the affected tissue is responding to Cidofovir by inducing an anti-apoptotic and/or an inflammatory response. However, because these cases are the only two cases in the study that clear HPV by the end of treatment, and because only 5 genes were examined, the exact mechanism of action of Cidofovir in the RT3VIN samples cannot be determined.

BCL2A1 and *BIRC3* displayed notable up-regulation specific to the two RT3VIN Cases that cleared HPV16 by the end of the trial. *BCL2A1* is a direct transcriptional target of NF-kappa B, expressed in response to inflammatory mediators, and is up-regulated by different extracellular signals (NCBI, September 2013c). *BIRC3 i*s regulated in a G_2/M phase cell cycle dependant manner and is augmented by NF-kappa B activation. When expressed,

BIRC3 contributes to the survival of mitotically arrested cells (Jin and Lee, 2006). Not only is NF-kappa B a multi-functional transcription factor involved in cell survival (Baetz et al., 2005), inflammation (Tak and Firestein, 2001), regulation of an immune and anti-viral response (Hayden et al., 2006, Eickhoff and Cotten, 2005), it has also been implicated in cancer progression (Dolcet et al., 2005). Additionally, there has been a link proposed between HPV immortalization of cell lines and NF-kappa B. Some studies indicate that HPV represses NF-kappa B (Spitkovsky et al., 2002), whereas some studies indicate that HPV activates NF-kappa B (James et al., 2006). As NF-kappa B plays a role in both *BCL2A1* and *BIRC3* activation, further investigation of its application to HPV clearance in Cidofovir treated VIN may be warranted.

There is limited published literature linking HPV and Cidofovir to *BCL2A1* and *BIRC3.* However, a study examining DNA methylation patterns in HPV-Associated anal squamous neoplasia proposed a link between methylation of anti-apoptotic *BCL2A1* and HPV-related carcinogenesis (Hernandez et al., 2012). Using methylation arrays, bisulfite-converted DNA was examined for methylation at 1,505 CpG loci representing 807 genes in 29 formalin-fixed paraffin embedded samples from 24 patients, where 3 were neoplasia free, 11 had squamous cell carcinoma *in situ* and 15 had invasive squamous cell carcinoma. A range of different genes were found to be differentially methylated in pre-invasive and invasive HPV associated anal disease. Among others, *BCL2A1* was found to be highly methylated in invasive disease compared with pre-invasive disease. The authors concluded that *BCL2A1* gene (among 18 others), occupied a “methylation prone” area. Additionally, *BCL2A1* is located at chromosome position 15q25.3 (NCBI, September 2013c), which is adjacent to a hotspot site of HPV integration at 15q23 (Wentzensen et al., 2004). In light of this, Hernandez et al., 2012, suggested that HPV-associated methylation events appear to occur in a non-random fashion and that genes like *BCL2A1* may have potential as therapeutic targets. In terms of the data presented here, if DNA methylation in HPV associated disease resulted in silencing of *BCL2A1* and treatment with Cidofovir produced increased *BCL2A1* transcription in patients who cleared their HPV infection, it would be interesting to evaluate if this connection is purely coincidental or if Cidofovir

could possibly produce a de-methylating effect in HPV positive neoplasias. Such a link, although highly speculative, may warrant further investigation.

Not all HPV positivity test results were consistent across the three samples taken for each patient. For example, Case 3 was HPV positive at the end of the study but not at baseline or during the treatment. This may be related to the biopsy sampling process as Cases 9 and 10 were HPV positive before and after treatment but tested HPV negative during treatment. The RT3VIN Study Protocol required biopsies to be taken from the same location, which should be a representative area of the lesion. For Case 3, in which HPV was not detected at baseline or during treatment, it could be suggested that either the patient acquired the virus after the six week biopsy was taken or the virus was present all along but gave false negative results at baseline and six weeks possibly due to sampling of uninfected epithelium or low sensitivity of the HPV detection assay.

A link between HPV status at baseline and gene expression was not found. As HPV E6 oncoprotein promotes the degradation of p53 protein, greater *CDKN1A/p21* transcript levels may have been expected in the HPV negative patients. However for this study, mean baseline transcript levels were typically higher for *CDKN1A/p21* than for the other genes assessed. Conversely, *HRK* typically had the lowest transcript levels.

The reasons for the noticeable down-regulation of *BCL2A1* and *BIRC3* 36 hours post treatment in the Cidofovir treated M08 cell line (results section 5.2) and the reasons for the prominent up-regulation of the same genes in the two patients who cleared their infection six weeks into treatment may be complicated. Firstly, in the cell line model, the cells were subjected to a single exact measured dose of Cidofovir and expression of genes was examined at exactly 12 and 36 hours post treatment. At this early time point it was likely that the M08 cells were responding to Cidofovir treatment for the first time. However, in the clinical material, patients were self-applying topical Cidofovir gel three times a week for six weeks, where amount of Cidofovir compound could vary between applications. In contrast to the M08 cells used in the *in vitro* study, the cells in the RT3VIN biopsy material at the six week interval were likely to be those that survived Cidofovir treatment. Therefore, duration and concentrations of treatment varied greatly between

the cell line work and the clinical material. In addition to this, *BIRC3* and *BCL2A1* are thought to be involved in immune regulation as well as anti-apoptotic and cell survival processes. Therefore, the availability of an active immune system would be an important factor to signal to and modulate the expression of these genes.

A strength of the RT3VIN RT-qPCR study was that the experiment was conducted on histologically validated material from an ethically approved phase 2 clinical trial. RT3VIN had a robust methodology and strict inclusion criteria with access to a range of clinical information. HPV testing was well controlled, with CaSki DNA used as a positive control and water used as a negative control. Strengths of the gene expression data also include the use of negative controls and the production of reproducible Ct values. The individual RT-qPCR assays and the SYBR green master mixes were commercially validated as was the ABI 7900HT RT-PCR analyser.

A weakness of the RT3VIN RT-qPCR study was the limited number of genes assessed. The five target genes analysed in this study showed differential response in the cell line studies, but are only a very small subset of genes linked to apoptosis. More genes would make for a more informative data set. Additionally, differential transcription patterns of the genes were analysed in only a small number of Cases (n = 10). The small sample size was a result of the limited and irreplaceable nature of the clinical material and was deemed acceptable for use as a pilot study. Limitations of the data itself include the normalisation required for the six week sample for Case 4. It is clear from the raw Ct values outlined in Figure 5.11 that there was less cDNA in the six week sample for Case 4. As the Ct values of *GAPDH* increased a maximum of two cycles more than *HPRT1* (compared to the baseline Ct values for Case 4) there would appear to be a divergence in the efficiency of the RT-qPCR reaction for this primer set. All genes were examined in triplicate twice for Case 4 and equivalent results were observed for both experiments indicating that these increases in Ct values were not erroneous. The reason for this divergence cannot be deduced with confidence from the data set obtained. The primer assays are marketed as having equivalent efficiencies by the manufacturer (Qiagen, Hilden, Germany) and the recommended SYBR green RT-qPCR master mixes and thermocycler programs were used, such that the generation of significant differences in

PCR efficiencies between the two primer sets was unlikely. An alternative explanation might be that tissue or cell specific expression differences occur for these reference genes, which is plausible due to the fact that biopsies sample a cross section of epithelial layers. However, the *GAPDH* and *HPRT1* reference genes were selected as they appeared most stable in the initial RT-qPCR apoptosis arrays on the cell line material.

To conclude on the RT3VIN RT-qPCR study, extensive up-regulation of two anti-apoptotic/inflammatory related genes, *BCL2A1* and *BIRC3*, was found in the two patients who cleared HPV by the end of the trial. Future work should include a wider range of genes (apoptotic, inflammatory and anti-viral) in a larger cohort of women to gain a better understanding of the transcriptional processes taking place. Future work derived from this study would also examine the potential role of *BCL2A1*, *BIRC3* and NF-kappa B in Cidofovir treated VIN and HPV clearance.

6. General Discussion and Conclusions

This project investigated the treatment of HPV associated anogenital neoplasia using an *in vitro* cell based model derived from HPV16 positive vulval and vaginal intraepithelial neoplasia biopsies. It addressed two main questions. The first sought to determine the efficacy and specificity of nucleoside analogue compounds in a range of HPV positive and negative cell models. The second analysed the molecular mechanism by which Cidofovir inhibited cell growth in NHIST cell lines. As an extension of the second question, a pilot study was conducted to investigate the transcription of several apoptosis pathway specific genes that were differentially regulated in Cidofovir treated HPV positive cell in clinical material from the RT3VIN clinical trial.

Validation of the dosing procedure and experimental models was necessary before evaluation of the compounds could be performed. In terms of growth characteristics of the M08 and A09 NHIST cell models, the M08 cell line displayed greater seeding efficiency and shorter mean DT compared to the A09 cell line. Both cell lines exhibited similar polygonal morphologies with “cobblestone” effect post initial isolation; however, with continuous passage A09 cells displayed an elongated morphology. The results of *E2* PCR, DIPS and APOT indicated that A09 cells contained episomal HPV16 DNA and M08 cells contained integrated HPV16 DNA; however, these results were not confirmed by Southern blotting at the time of submission of this thesis. The final key difference observed between M08 and A09 cells was that M08 cells did not express *E2, E4* and *E5* HPV mRNA at any passage post initial isolation (passage 5 to 9); whereas, A09 cells did express *E2, E4* and *E5* HPV mRNA at stable levels at each passage examined post initial isolation (passage 5 to 10). Both *E6* and *E7* were transcribed at stable levels in M08 and A09 cells.

As *TP53* was a central component in the Cidofovir mechanism of action hypotheses, its mutational status in the NHIST cell lines was assessed. This study proved beneficial as in addition to showing that both the M08 and A09 cell lines were *TP53* wild-type it also identified the SNV Arg72Pro, where it has been suggested that the arginine variant of this polymorphism renders p53 protein more susceptible to degradation by HPV E6 (Storey et al., 1998).

Further characterisation of the NHIST cell models found a significant increase in HPV oncogene expression between 50 and 100% cell confluence in M08 cells. This result highlighted the need to maintain cell confluence at a constant level between all treatment conditions in mechanism of action studies, where oncogene transcripts of treated cells are normalized to those of the untreated control cells. In addition, through examination of growth rates, morphology and oncogene expression of M08 cells grown in the presence and absence of 3T3 feeder cells over an 8 day period it was concluded that the NHIST cell lines could be cultured in the absence of feeder cells for the mechanism of action studies.

Three different methods of assessing cell viability were examined to determine the most accurate for use in the compound dosing studies. Methods examined included: the CellTiter 96® AQueous One MTS Solution Reagent (Promega, Southampton, UK); manual cell counting using Trypan Blue dye exclusion staining; and automated cell counting using 7-AAD staining and flow cytometry. The results suggested that both forms of cell counting were more accurate at assessing cell viability than the MTS method.

In terms of nucleotide analogue dosing, initial experiments demonstrated dose response relationships for Cidofovir in the NHIST cell lines and HEKs using manual cell counting with Trypan blue staining. All cell lines were sensitive to Cidofovir at micromolar concentrations, which indicated lack of specificity of the compound to HPV immortalized cells. IC50 values were obtained for Cidofovir in M08, A09 and HEK cells for use in the mechanism of action studies. In clinical use, Cidofovir shows selectivity for VIN lesions; however the lack of specificity of Cidofovir for HPV immortalized cells *in vitro* may suggest that Cidofovir shows non-specific cytotoxicity but is specific in clinical use due to greater incorporation in rapidly proliferating cells. An alternative possibility would be that the presence of a stratified, partially keratinized epithelium over normal vulval tissue inhibits uptake of Cidofovir by proliferating cells adjacent to the basal layer, whereas in high grade VIN, proliferating cells are present at the surface of the epithelium and may receive a higher dose of Cidofovir, leading to their gradual erosion.

IC50 values were obtained for Cidofovir and its cyclic analogues in HeLa (HPV18 positive) and C33A (HPV negative) transformed cell lines to determine differences in efficacy

between parent and daughter compounds. Inconsistencies in growth inhibition were observed between Cidofovir and its daughter compounds in these cell types and upon structural analysis it was found that the cyclic ProTide analogue of Cidofovir had reverted to its acyclic form.

Unfortunately, the acyclic structure of Cidofovir was not responsive to ProTide modification; however, the Cidofovir sister compounds, Adefovir and Tenofovir, were amenable to this type of modification. Two ProTide analogues of Adefovir and three ProTide analogues of Tenofovir as well as their corresponding parent compounds were evaluated in terms of growth inhibition and effect on cell size and morphology in HeLa (HPV18 positive), SiHa (HPV16 positive) and C33A (HPV negative) transformed cell lines. The ProTide analogues proved to be extremely effective at inhibiting cell growth in HPV positive and negative cell lines at sub-micromolar concentrations, where the Adefovir ProTide analogues appeared more effective than the Tenofovir derivatives. While this potent effect successfully demonstrated the power of the ProTide technology, the compounds showed no specificity for transformed, or HPV positive cells.

From the data obtained in Chapter 5 the exact mechanism of action of Cidofovir remains unclear, but several relevant observations were made. Firstly, at its IC50 concentration, Cidofovir did not induce an increase in caspase-3 activity, indicative of apoptosis, at 12, 36 and 72 hours post treatment in HPV positive and negative cell lines. Consistent with this, both HPV positive and negative cells treated with Cidofovir became swollen and increased in size, rather than shrinking and undergoing blebbing. Cell swelling is indicative of permanent cell cycle arrest/senescence or necrosis, and the decrease in cell number and increase in cell size may suggest that Cidofovir treatment caused one of these two processes in HPV positive cell lines. The slight increase in total p53 observed in the Cidofovir treated A09 cell line may suggest that senescence is the inhibitory process occurring as opposed to necrosis, as the connection between p53 and cell senescence is better documented than its association with necrosis (Itahana et al., 2001, Leontieva et al., 2010, Santoro and Blandino, 2010, Wesierska-Gadek et al., 2005, Zhang et al., 2005).

The Cidofovir mechanism of action studies were carried out using IC50 values individual to each cell line. Other studies that found Cidofovir did induce apoptosis in HPV positive cell lines used higher standard concentrations of the compound and examined its effects for longer periods of time (Andrei et al., 2001, De Schutter et al., 2013, Abdulkarim et al., 2002). The experimental period for the mechanism of action of Cidofovir studies carried out for this project lasted a maximum of 4.5 days (including a 24 hour cell attachment period). This maximum time point was chosen as significant differences in cell number were not generally observed until four days post Cidofovir treatment. Therefore, the molecular processes leading to the growth inhibitory effect would have occurred prior to day four. Differences in time frames may also have contributed to the lack of correlation between the transcriptional responses observed in the NHIST cell lines and those in clinical material from the RT3VIN trial.

Pre-treating HPV positive cells with Cidofovir before radiation treatment was found to augment the molecular response. This response appeared to be more pronounced in the A09 cell line compared to the M08 cell line, which could be due to genetic differences, both host and viral, between the lines. Both M08 and A09 cell lines were found to be *TP53* wild-type, but the A09 cell line contained the arginine variant of Arg72Pro, which has been suggested to increase ubiquitination of p53 protein by E6. However, A09 showed greater induction of p53 following treatment with Cidofovir and radiation. Other host genetic differences may relate to nucleotide metabolizing pathways and DNA damage repair pathways. With regards to viral genetic differences, the two lines differ in the integration state of HPV, where *E2* PCR, DIPS and APOT indicate that A09 cells contain episomal HPV DNA and M08 cells contain integrated HPV DNA. It could be speculated that episomal HPV DNA could be lost due to genotoxic stress induced by Cidofovir and radiation treatment; this would manifest as a decrease in *E6/E7* expression and an increase in total and phosphorylated p53. However, as a decrease in *E6* expression was observed in the M08 cell line as well as the A09 cell line, episome loss may not be relevant. Another difference between the M08 and the A09 cell line was the absence of *E4* and *E5* expression in the M08 cell line. *E4* has been shown to be involved in virus maturation (Doorbar et al., 1986) and cytokeratin disruption (Doorbar et al., 1991, Roberts et al., 1993), while *E5* is thought

to promote cellular proliferation through interfering with intracellular signalling cascades, such as EGF signalling (Leechanachai et al., 1992) (Tomakidi et al., 2000, Straight et al., 1993). With these functions in mind, it is unclear how expression of *E4* and *E5* in the A09 cell line could contribute to p53 induction post Cidofovir and radiation treatment.

The combination of Cidofovir pre-treatment and radiation produced a large increase in cleaved caspase-3 activity in HPV negative untransformed HEK cells but not in the NHIST lines. This is consistent with abrogation of the apoptotic response in HPV infected cells due to the combined effects of E6 and E7 and suggests Cidofovir does not selectively radiosensitize HPV positive cells. Such a large increase in cleaved caspase-3 activity in HPV negative untransformed HEK cells suggests that to combine Cidofovir treatment with radiation could produce considerable cell death in healthy tissue, something that would be highly disadvantageous in the clinic.

The findings of the cell line work were applied to the patient material from the RT3VIN clinical trial to investigate whether the same trends were present in both the NHIST cell models and the *in vivo* disease from which they were derived. Five apoptosis pathway specific genes that were examined previously and shown to be differentially expressed in the M08 cell line were further examined in 20 biopsies taken before or during Cidofovir treatment (10 patient cases in total). In the cell line work the most notable change in expression of the genes examined was down-regulation; however the most prominent change in gene expression between the before and during treatment samples was up-regulation in the clinical material.

As the results of the Cidofovir mechanism of action studies in M08, A09 and HEK cells tentatively suggest Cidofovir induces cell cycle arrest/senescence, future experiments to confirm such mechanisms would involve cell cycle evaluation using Propidium iodide staining with flow cytometry or β-Galactosidase staining for cell senescence. Additional future work stemming from the results presented in this project could involve evaluation of Cidofovir uptake and metabolism in M08 and A09 cells. This may determine if the molecular effect produced by Cidofovir, which was more prominent in A09 cells when compared to M08 cells, was due to differences in nucleotide metabolising enzymes

including hENT, cENT, OCTs, OATs and nucleoside phosphorylating enzymes. Furthermore, Cidofovir dosing of M08 and A09 cells in raft culture could be performed to provide further insight into the potential mechanism of action of Cidofovir and its ability to permeate different epithelial layers, which would be more representative of an *in vivo* state when compared to monolayer culture.

To conclude, despite showing specificity to VIN lesions in clinical use, no specificity of Cidofovir for HPV immortalized cells was demonstrated *in vitro*. The ProTide analogues of Adefovir and Tenofovir displayed an extensive increase in efficacy when compared to their parent compounds; however, specificity to HPV positive or transformed cells was not observed. At the doses investigated, Cidofovir did not appear to cause apoptosis of HPV positive or negative cells. The inhibitory effect of Cidofovir on cell growth appears more likely to be associated with cell cycle arrest/senescence. In HPV negative HEK cells, combined treatment with Cidofovir and gamma radiation appeared to cause a significant apoptotic response. In HPV positive cells combined treatment with Cidofovir and gamma radiation was associated with accumulation and phosphorylation of p53, and with increased transcription of *p21/CDKN1A*, but not with increased p21 protein or apoptosis.

7. Bibliography

Cidofovir (Vistide®) Pack insert. *Gilead Sciences Inc,* 333 Lakeside Dr, Foster City, CA, USA.

ISRCTN34420460. *A Randomised phase II multi-centre Trial of topical treatment in women with Vulval Intraepithelial Neoplasia*.

1000GENOMES 2008 - 2012. A Deep Catalog of Human Genetic Variation. http://www.1000genomes.org/.

ABDULKARIM, B., SABRI, S., DEUTSCH, E., CHAGRAOUI, H., MAGGIORELLA, L., THIERRY, J., ESCHWEGE, F., VAINCHENKER, W., CHOUAIB, S. & BOURHIS, J. 2002. Antiviral agent Cidofovir restores p53 function and enhances the radiosensitivity in HPV-associated cancers. *Oncogene,* 21**,** 2334-46.

ADAMS, J. M. & CORY, S. 2002. Apoptosomes: engines for caspase activation. *Curr Opin Cell Biol,* 14**,** 715-20.

ADIMOOLAM, S. & FORD, J. M. 2003. p53 and regulation of DNA damage recognition during nucleotide excision repair. *DNA Repair (Amst),* 2**,** 947-54.

ADOLPHE, M. & THENET, S. 1990. [The concept of cellular immortality, a myth or a reality. Example of "immortalized" articular chondrocytes]. *Bull Acad Natl Med,* 174**,** 139-44; discussion 144-6.

AGUILERA, A. & GOMEZ-GONZALEZ, B. 2008. Genome instability: a mechanistic view of its causes and consequences. *Nat Rev Genet,* 9**,** 204-17.

AKIL, N., YASMEEN, A., KASSAB, A., GHABREAU, L., DARNEL, A. D. & AL MOUSTAFA, A. E. 2008. High-risk human papillomavirus infections in breast cancer in Syrian women and their association with Id-1 expression: a tissue microarray study. *Br J Cancer,* 99**,** 404-7.

AKYUZ, N., BOEHDEN, G. S., SUSSE, S., RIMEK, A., PREUSS, U., SCHEIDTMANN, K. H. & WIESMULLER, L. 2002. DNA substrate dependence of p53-mediated regulation of double-strand break repair. *Mol Cell Biol,* 22**,** 6306-17.

ALT, W. & DEMBO, M. 1999. Cytoplasm dynamics and cell motion: two-phase flow models. *Math Biosci,* 156**,** 207-28.

AMINE, A., RIVERA, S., OPOLON, P., DEKKAL, M., BIARD, D. S., BOUAMAR, H., LOUACHE, F., MCKAY, M. J., BOURHIS, J., DEUTSCH, E. & VOZENIN-BROTONS, M. C. 2009. Novel anti-metastatic action of cidofovir mediated by inhibition of E6/E7, CXCR4 and Rho/ROCK signaling in HPV tumor cells. *PLoS One,* 4**,** e5018.

ANDREI, G., SNOECK, R., PIETTE, J., DELVENNE, P. & DE CLERCQ, E. 1998. Antiproliferative effects of acyclic nucleoside phosphonates on human papillomavirus (HPV)-harboring cell lines compared with HPV-negative cell lines. *Oncol Res,* 10**,** 523-31.

ANDREI, G., SNOECK, R., SCHOLS, D. & DE CLERCQ, E. 2001. Induction of apoptosis by cidofovir in human papillomavirus (HPV)-positive cells. *Oncol Res,* 12**,** 397-408.

ANTINORE, M. J., BIRRER, M. J., PATEL, D., NADER, L. & MCCANCE, D. J. 1996. The human papillomavirus type 16 E7 gene product interacts with and trans-activates the AP1 family of transcription factors. *EMBO J,* 15**,** 1950-60.

BACKES, D. M., KURMAN, R. J., PIMENTA, J. M. & SMITH, J. S. 2009. Systematic review of human papillomavirus prevalence in invasive penile cancer. *Cancer Causes Control,* 20**,** 449-57.

BAETZ, D., REGULA, K. M., ENS, K., SHAW, J., KOTHARI, S., YURKOVA, N. & KIRSHENBAUM, L. A. 2005. Nuclear factor-kappaB-mediated cell survival involves transcriptional silencing of the mitochondrial death gene BNIP3 in ventricular myocytes. *Circulation,* 112**,** 3777-85.

BAKER C & C., C. 1995. Maps of papillomavirus mRNA transcripts. *The human papillomaviruses compendium***,** III 3 - III 20.

BALDWIN, S. A., MACKEY, J. R., CASS, C. E. & YOUNG, J. D. 1999. Nucleoside transporters: molecular biology and implications for therapeutic development. *Mol Med Today,* 5**,** 216-24.

BALLATORE, C., MCGUIGAN, C., DE CLERCQ, E. & BALZARINI, J. 2001. Synthesis and evaluation of novel amidate prodrugs of PMEA and PMPA. *Bioorganic & medicinal chemistry letters,* 11**,** 1053-6.

BALZARINI, J., HERDEWIJN, P. & DE CLERCQ, E. 1989. Differential patterns of intracellular metabolism of 2',3'-didehydro-2',3'-dideoxythymidine and 3'-azido-2',3'-dideoxythymidine, two potent anti-human immunodeficiency virus compounds. *J Biol Chem,* 264**,** 6127-33.

BANIN, S., MOYAL, L., SHIEH, S., TAYA, Y., ANDERSON, C. W., CHESSA, L., SMORODINSKY, N. I., PRIVES, C., REISS, Y., SHILOH, Y. & ZIV, Y. 1998. Enhanced phosphorylation of p53 by ATM in response to DNA damage. *Science,* 281**,** 1674-7.

BEADLE, J. R., HARTLINE, C., ALDERN, K. A., RODRIGUEZ, N., HARDEN, E., KERN, E. R. & HOSTETLER, K. Y. 2002. Alkoxyalkyl esters of cidofovir and cyclic cidofovir exhibit multiple-log enhancement of antiviral activity against cytomegalovirus and herpesvirus replication in vitro. *Antimicrob Agents Chemother,* 46**,** 2381-6.

BECKMAN, G., BIRGANDER, R., SJALANDER, A., SAHA, N., HOLMBERG, P. A., KIVELA, A. & BECKMAN, L. 1994. Is p53 polymorphism maintained by natural selection? *Hum Hered,* 44**,** 266-70.

BEDWELL, J., MACROBERT, A. J., PHILLIPS, D. & BOWN, S. G. 1992. Fluorescence distribution and photodynamic effect of ALA-induced PP IX in the DMH rat colonic tumour model. *Br J Cancer,* 65**,** 818-24.

BEN-PORATH, I. & WEINBERG, R. A. 2004. When cells get stressed: an integrative view of cellular senescence. *J Clin Invest,* 113**,** 8-13.

BERNARD, H. U. 2005. The clinical importance of the nomenclature, evolution and taxonomy of human papillomaviruses. *J Clin Virol,* 32 Suppl 1**,** S1-6.

BODILY, J. M. & MEYERS, C. 2005. Genetic analysis of the human papillomavirus type 31 differentiation-dependent late promoter. *J Virol,* 79**,** 3309-21.

BOJESEN, S. E. & NORDESTGAARD, B. G. 2008. The common germline Arg72Pro polymorphism of p53 and increased longevity in humans. *Cell Cycle,* 7**,** 158-63.

BOSCH, F. X. & DE SANJOSE, S. 2003. Chapter 1: Human papillomavirus and cervical cancer--burden and assessment of causality. *J Natl Cancer Inst Monogr*, 3-13.

BOUSARGHIN, L., TOUZE, A., SIZARET, P. Y. & COURSAGET, P. 2003. Human papillomavirus types 16, 31, and 58 use different endocytosis pathways to enter cells. *Journal of virology,* 77, 3846-50.

BRANDSMA, I. & GENT, D. C. 2012. Pathway choice in DNA double strand break repair: observations of a balancing act. *Genome Integr,* 3, 9.

BRESLER, S. E., NOSKIN, L. A. & SUSLOV, A. V. 1984. Induction by gamma irradiation of double-strand breaks of Escherichia coli chromosomes and their role in cell lethality. *Biophys J,* 45, 749-54.

BRONCKAERS, A., BALZARINI, J. & LIEKENS, S. 2008. The cytostatic activity of pyrimidine nucleosides is strongly modulated by Mycoplasma hyorhinis infection: Implications for cancer therapy. *Biochem Pharmacol,* 76, 188-97.

BRUCHIM, I., GOTLIEB, W. H., MAHMUD, S., TUNITSKY, E., GRZYWACZ, K. & FERENCZY, A. 2007. HPV-related vulvar intraepithelial neoplasia: outcome of different management modalities. *Int J Gynaecol Obstet,* 99, 23-7.

BRYAN, T. M. & CECH, T. R. 1999. Telomerase and the maintenance of chromosome ends. *Curr Opin Cell Biol,* 11, 318-24.

BUCK, C. B., CHENG, N., THOMPSON, C. D., LOWY, D. R., STEVEN, A. C., SCHILLER, J. T. & TRUS, B. L. 2008. Arrangement of L2 within the papillomavirus capsid. *J Virol,* 82, 5190-7.

BURD, E. M. 2003. Human papillomavirus and cervical cancer. *Clin Microbiol Rev,* 16, 1-17.

BURDALL, S. E., HANBY, A. M., LANSDOWN, M. R. & SPEIRS, V. 2003. Breast cancer cell lines: friend or foe? *Breast Cancer Res,* 5, 89-95.

BURMA, S., CHEN, B. P., MURPHY, M., KURIMASA, A. & CHEN, D. J. 2001. ATM phosphorylates histone H2AX in response to DNA double-strand breaks. *J Biol Chem,* 276, 42462-7.

CAHARD, D., MCGUIGAN, C. & BALZARINI, J. 2004. Aryloxy phosphoramidate triesters as pro-tides. *Mini Rev Med Chem,* 4, 371-81.

CALIN, G. A., SEVIGNANI, C., DUMITRU, C. D., HYSLOP, T., NOCH, E., YENDAMURI, S., SHIMIZU, M., RATTAN, S., BULLRICH, F., NEGRINI, M. & CROCE, C. M. 2004. Human microRNA genes are frequently located at fragile sites and genomic regions involved in cancers. *Proc Natl Acad Sci U S A,* 101, 2999-3004.

CAMPION, M. J. & SINGER, A. 1987. Vulval intraepithelial neoplasia: clinical review. *Genitourin Med,* 63, 147-52.

CESARE, A. J. & REDDEL, R. R. 2010. Alternative lengthening of telomeres: models, mechanisms and implications. *Nat Rev Genet,* 11, 319-30.

CHIANG, C. M., USTAV, M., STENLUND, A., HO, T. F., BROKER, T. R. & CHOW, L. T. 1992. Viral E1 and E2 proteins support replication of homologous and heterologous papillomaviral origins. *Proc Natl Acad Sci U S A,* 89, 5799-803.

CHOW, L. T., BROKER, T. R. & STEINBERG, B. M. 2010. The natural history of human papillomavirus infections of the mucosal epithelia. *APMIS,* 118**,** 422-49.

CHRISTENSEN, N. D., PICKEL, M. D., BUDGEON, L. R. & KREIDER, J. W. 2000. In vivo anti-papillomavirus activity of nucleoside analogues including cidofovir on CRPV-induced rabbit papillomas. *Antiviral Res,* 48**,** 131-42.

CHRISTOFORI, G. & SEMB, H. 1999. The role of the cell-adhesion molecule E-cadherin as a tumour-suppressor gene. *Trends Biochem Sci,* 24**,** 73-6.

CIHLAR, T. & CHEN, M. S. 1996. Identification of enzymes catalyzing two-step phosphorylation of cidofovir and the effect of cytomegalovirus infection on their activities in host cells. *Mol Pharmacol,* 50**,** 1502-10.

CIHLAR, T., LIN, D. C., PRITCHARD, J. B., FULLER, M. D., MENDEL, D. B. & SWEET, D. H. 1999. The antiviral nucleotide analogs cidofovir and adefovir are novel substrates for human and rat renal organic anion transporter 1. *Mol Pharmacol,* 56**,** 570-80.

CMIELOVA, J., HAVELEK, R., SOUKUP, T., JIROUTOVA, A., VISEK, B., SUCHANEK, J., VAVROVA, J., MOKRY, J., MUTHNA, D., BRUCKOVA, L., FILIP, S., ENGLISH, D. & REZACOVA, M. 2012. Gamma radiation induces senescence in human adult mesenchymal stem cells from bone marrow and periodontal ligaments. *Int J Radiat Biol,* 88**,** 393-404.

COHEN, G. M. 1997. Caspases: the executioners of apoptosis. *Biochem J,* 326 (Pt 1)**,** 1-16.

COLEMAN, C. N. & TURRISI, A. T. 1990. Radiation and chemotherapy sensitizers and protectors. *Crit Rev Oncol Hematol,* 10**,** 225-52.

COLLINS, K., JACKS, T. & PAVLETICH, N. P. 1997. The cell cycle and cancer. *Proc Natl Acad Sci U S A,* 94**,** 2776-8.

COLLINS, S. I., CONSTANDINOU-WILLIAMS, C., WEN, K., YOUNG, L. S., ROBERTS, S., MURRAY, P. G. & WOODMAN, C. B. 2009. Disruption of the E2 gene is a common and early event in the natural history of cervical human papillomavirus infection: a longitudinal cohort study. *Cancer Res,* 69**,** 3828-32.

CONGER, K. L., LIU, J. S., KUO, S. R., CHOW, L. T. & WANG, T. S. 1999. Human papillomavirus DNA replication. Interactions between the viral E1 protein and two subunits of human dna polymerase alpha/primase. *J Biol Chem,* 274**,** 2696-705.

COWDEN, R. R. & CURTIS, S. K. 1981. Microfluorometric investigations of chromatin structure. I. Evaluation of nine DNA-specific fluorochromes as probes of chromatin organization. *Histochemistry,* 72**,** 11-23.

CRIGHTON, D., WILKINSON, S., O'PREY, J., SYED, N., SMITH, P., HARRISON, P. R., GASCO, M., GARRONE, O., CROOK, T. & RYAN, K. M. 2006. DRAM, a p53-induced modulator of autophagy, is critical for apoptosis. *Cell,* 126**,** 121-34.

CROSS, S. M., SANCHEZ, C. A., MORGAN, C. A., SCHIMKE, M. K., RAMEL, S., IDZERDA, R. L., RASKIND, W. H. & REID, B. J. 1995. A p53-dependent mouse spindle checkpoint. *Science,* 267**,** 1353-6.

CRUSIUS, K., RODRIGUEZ, I. & ALONSO, A. 2000. The human papillomavirus type 16 E5 protein modulates ERK1/2 and p38 MAP kinase activation by an EGFR-independent process in stressed human keratinocytes. *Virus Genes,* 20**,** 65-9.

DALING, J. R., MADELEINE, M. M., SCHWARTZ, S. M., SHERA, K. A., CARTER, J. J., MCKNIGHT, B., PORTER, P. L., GALLOWAY, D. A., MCDOUGALL, J. K. & TAMIMI, H. 2002. A population-based study of squamous cell vaginal cancer: HPV and cofactors. *Gynecol Oncol,* 84**,** 263-70.

DALL, K. L., SCARPINI, C. G., ROBERTS, I., WINDER, D. M., STANLEY, M. A., MURALIDHAR, B., HERDMAN, M. T., PETT, M. R. & COLEMAN, N. 2008. Characterization of naturally occurring HPV16 integration sites isolated from cervical keratinocytes under noncompetitive conditions. *Cancer Res,* 68**,** 8249-59.

DAMARAJU, V. L., DAMARAJU, S., YOUNG, J. D., BALDWIN, S. A., MACKEY, J., SAWYER, M. B. & CASS, C. E. 2003. Nucleoside anticancer drugs: the role of nucleoside transporters in resistance to cancer chemotherapy. *Oncogene,* 22**,** 7524-36.

DAY, P. M., LOWY, D. R. & SCHILLER, J. T. 2003. Papillomaviruses infect cells via a clathrin-dependent pathway. *Virology,* 307**,** 1-11.

DE CLERCQ, E. 1996. Therapeutic potential of Cidofovir (HPMPC, Vistide) for the treatment of DNA virus (i.e. herpes-, papova-, pox- and adenovirus) infections. *Verhandelingen - Koninklijke Academie voor Geneeskunde van België,* 58**,** 19-47.

DE CLERCQ, E. 2003. Clinical potential of the acyclic nucleoside phosphonates cidofovir, adefovir, and tenofovir in treatment of DNA virus and retrovirus infections. *Clin Microbiol Rev,* 16**,** 569-96.

DE CLERCQ, E. 2011a. The clinical potential of the acyclic (and cyclic) nucleoside phosphonates. The magic of the phosphonate bond. *Biochemical pharmacology,* 82**,** 99-109.

DE CLERCQ, E. 2011b. The clinical potential of the acyclic (and cyclic) nucleoside phosphonates. The magic of the phosphonate bond. *Biochem Pharmacol,* 82**,** 99 - 109.

DE CLERCQ, E. & HOLY, A. 2005. Acyclic nucleoside phosphonates: a key class of antiviral drugs. *Nat Rev Drug Discov,* 4**,** 928-40.

DE LAAT, W. L., JASPERS, N. G. & HOEIJMAKERS, J. H. 1999. Molecular mechanism of nucleotide excision repair. *Genes Dev,* 13**,** 768-85.

DE SANJOSE, S., ALEMANY, L., ORDI, J., TOUS, S., ALEJO, M., BIGBY, S. M., JOURA, E. A., MALDONADO, P., LACO, J., BRAVO, I. G., VIDAL, A., GUIMERA, N., CROSS, P., WAIN, G. V., PETRY, K. U., MARIANI, L., BERGERON, C., MANDYS, V., SICA, A. R., FELIX, A., USUBUTUN, A., SEOUD, M., HERNANDEZ-SUAREZ, G., NOWAKOWSKI, A. M., WILSON, G., DALSTEIN, V., HAMPL, M., KASAMATSU, E. S., LOMBARDI, L. E., TINOCO, L., ALVARADO-CABRERO, I., PERROTTA, M., BHATLA, N., AGORASTOS, T., LYNCH, C. F., GOODMAN, M. T., SHIN, H. R., VIARHEICHYK, H., JACH, R., CRUZ, M. O., VELASCO, J., MOLINA, C., BORNSTEIN, J., FERRERA, A., DOMINGO, E. J., CHOU, C. Y., BANJO, A. F., CASTELLSAGUE, X., PAWLITA, M., LLOVERAS, B., QUINT, W. G., MUNOZ, N., BOSCH, F. X. & GROUP, H. V. S. 2013. Worldwide human

papillomavirus genotype attribution in over 2000 cases of intraepithelial and invasive lesions of the vulva. *Eur J Cancer,* 49**,** 3450-3461.

DE SANJOSE, S., QUINT, W. G., ALEMANY, L., GERAETS, D. T., KLAUSTERMEIER, J. E., LLOVERAS, B., TOUS, S., FELIX, A., BRAVO, L. E., SHIN, H. R., VALLEJOS, C. S., DE RUIZ, P. A., LIMA, M. A., GUIMERA, N., CLAVERO, O., ALEJO, M., LLOMBART-BOSCH, A., CHENG-YANG, C., TATTI, S. A., KASAMATSU, E., ILJAZOVIC, E., ODIDA, M., PRADO, R., SEOUD, M., GRCE, M., USUBUTUN, A., JAIN, A., SUAREZ, G. A., LOMBARDI, L. E., BANJO, A., MENENDEZ, C., DOMINGO, E. J., VELASCO, J., NESSA, A., CHICHAREON, S. C., QIAO, Y. L., LERMA, E., GARLAND, S. M., SASAGAWA, T., FERRERA, A., HAMMOUDA, D., MARIANI, L., PELAYO, A., STEINER, I., OLIVA, E., MEIJER, C. J., AL-JASSAR, W. F., CRUZ, E., WRIGHT, T. C., PURAS, A., LLAVE, C. L., TZARDI, M., AGORASTOS, T., GARCIA-BARRIOLA, V., CLAVEL, C., ORDI, J., ANDUJAR, M., CASTELLSAGUE, X., SANCHEZ, G. I., NOWAKOWSKI, A. M., BORNSTEIN, J., MUNOZ, N., BOSCH, F. X., RETROSPECTIVE INTERNATIONAL, S. & GROUP, H. P. V. T. T. S. 2010. Human papillomavirus genotype attribution in invasive cervical cancer: a retrospective cross-sectional worldwide study. *Lancet Oncol,* 11**,** 1048-56.

DE SCHUTTER, T., ANDREI, G., TOPALIS, D., NAESENS, L. & SNOECK, R. 2013. Cidofovir selectivity is based on the different response of normal and cancer cells to DNA damage. *BMC Med Genomics,* 6**,** 18.

DE VILLIERS, E. M., FAUQUET, C., BROKER, T. R., BERNARD, H. U. & ZUR HAUSEN, H. 2004. Classification of papillomaviruses. *Virology,* 324**,** 17-27.

DE VUYST, H., CLIFFORD, G. M., NASCIMENTO, M. C., MADELEINE, M. M. & FRANCESCHI, S. 2009. Prevalence and type distribution of human papillomavirus in carcinoma and intraepithelial neoplasia of the vulva, vagina and anus: a meta-analysis. *Int J Cancer,* 124**,** 1626-36.

DEBERNE, M., LEVY, A., MONDINI, M., DESSEN, P., VIVET, S., SUPIRAMANIAM, A., VOZENIN, M. C. & DEUTSCH, E. 2013. The combination of the antiviral agent cidofovir and anti-EGFR antibody cetuximab exerts an antiproliferative effect on HPV-positive cervical cancer cell lines' in-vitro and in-vivo xenografts. *Anticancer Drugs,* 24**,** 599-608.

DEHAY, C. & KENNEDY, H. 2007. Cell-cycle control and cortical development. *Nat Rev Neurosci,* 8**,** 438-50.

DELL, G., WILKINSON, K. W., TRANTER, R., PARISH, J., LEO BRADY, R. & GASTON, K. 2003. Comparison of the structure and DNA-binding properties of the E2 proteins from an oncogenic and a non-oncogenic human papillomavirus. *J Mol Biol,* 334**,** 979-91.

DI LEONARDO, A., LINKE, S. P., CLARKIN, K. & WAHL, G. M. 1994. DNA damage triggers a prolonged p53-dependent G1 arrest and long-term induction of Cip1 in normal human fibroblasts. *Genes Dev,* 8**,** 2540-51.

DOLCET, X., LLOBET, D., PALLARES, J. & MATIAS-GUIU, X. 2005. NF-kB in development and progression of human cancer. *Virchows Arch,* 446**,** 475-82.

DONNE, A. J., HAMPSON, L., HE, X. T., ROTHERA, M. P., HOMER, J. J. & HAMPSON, I. N. 2007. Effects of cidofovir on a novel cell-based test system for recurrent respiratory papillomatosis. *Head Neck,* 29**,** 741-50.

DOORBAR, J. 2005. The papillomavirus life cycle. *J Clin Virol,* 32 Suppl 1**,** S7-15.

DOORBAR, J. 2006. Molecular biology of human papillomavirus infection and cervical cancer. *Clin Sci (Lond),* 110**,** 525-41.

DOORBAR, J., CAMPBELL, D., GRAND, R. J. & GALLIMORE, P. H. 1986. Identification of the human papilloma virus-1a E4 gene products. *EMBO J,* 5**,** 355-62.

DOORBAR, J., ELY, S., STERLING, J., MCLEAN, C. & CRAWFORD, L. 1991. Specific interaction between HPV-16 E1-E4 and cytokeratins results in collapse of the epithelial cell intermediate filament network. *Nature,* 352**,** 824-7.

DOORBAR, J., PARTON, A., HARTLEY, K., BANKS, L., CROOK, T., STANLEY, M. & CRAWFORD, L. 1990. Detection of novel splicing patterns in a HPV16-containing keratinocyte cell line. *Virology,* 178**,** 254-62.

DRAVIAM, V. M., XIE, S. & SORGER, P. K. 2004. Chromosome segregation and genomic stability. *Curr Opin Genet Dev,* 14**,** 120-5.

DUMONT, P., LEU, J. I., DELLA PIETRA, A. C., 3RD, GEORGE, D. L. & MURPHY, M. 2003. The codon 72 polymorphic variants of p53 have markedly different apoptotic potential. *Nat Genet,* 33**,** 357-65.

EDINGER, A. L. & THOMPSON, C. B. 2004. Death by design: apoptosis, necrosis and autophagy. *Curr Opin Cell Biol,* 16**,** 663-9.

EICKHOFF, J. E. & COTTEN, M. 2005. NF-kappaB activation can mediate inhibition of human cytomegalovirus replication. *J Gen Virol,* 86**,** 285-95.

EISENHAUER, E. A., THERASSE, P., BOGAERTS, J., SCHWARTZ, L. H., SARGENT, D., FORD, R., DANCEY, J., ARBUCK, S., GWYTHER, S., MOONEY, M., RUBINSTEIN, L., SHANKAR, L., DODD, L., KAPLAN, R., LACOMBE, D. & VERWEIJ, J. 2009. New response evaluation criteria in solid tumours: revised RECIST guideline (version 1.1). *Eur J Cancer,* 45**,** 228-47.

EL-DEIRY, W. S., TOKINO, T., VELCULESCU, V. E., LEVY, D. B., PARSONS, R., TRENT, J. M., LIN, D., MERCER, W. E., KINZLER, K. W. & VOGELSTEIN, B. 1993. WAF1, a potential mediator of p53 tumor suppression. *Cell,* 75**,** 817-25.

FALCK, J., COATES, J. & JACKSON, S. P. 2005. Conserved modes of recruitment of ATM, ATR and DNA-PKcs to sites of DNA damage. *Nature,* 434**,** 605-11.

FEI, P. & EL-DEIRY, W. S. 2003. P53 and radiation responses. *Oncogene,* 22**,** 5774-83.

FEI, Y., YANG, J., HSIEH, W. C., WU, J. Y., WU, T. C., GOAN, Y. G., LEE, H. & CHENG, Y. W. 2006. Different human papillomavirus 16/18 infection in Chinese non-small cell lung cancer patients living in Wuhan, China. *Jpn J Clin Oncol,* 36**,** 274-9.

FIELD, A. K. & BIRON, K. K. 1994. "The end of innocence" revisited: resistance of herpesviruses to antiviral drugs. *Clin Microbiol Rev,* 7**,** 1-13.

FINNEN, R. L., ERICKSON, K. D., CHEN, X. S. & GARCEA, R. L. 2003. Interactions between papillomavirus L1 and L2 capsid proteins. *J Virol,* 77**,** 4818-26.

FLORIN, L., SAPP, C., STREECK, R. E. & SAPP, M. 2002. Assembly and translocation of papillomavirus capsid proteins. *Journal of virology,* 76**,** 10009-14.

FOIJER, F. & TE RIELE, H. 2006. Restriction beyond the restriction point: mitogen requirement for G2 passage. *Cell Div,* 1**,** 8.

FRANCH, H. A., SHAY, J. W., ALPERN, R. J. & PREISIG, P. A. 1995. Involvement of pRB family in TGF beta-dependent epithelial cell hypertrophy. *J Cell Biol,* 129**,** 245-54.

FRIEND, S. H., BERNARDS, R., ROGELJ, S., WEINBERG, R. A., RAPAPORT, J. M., ALBERT, D. M. & DRYJA, T. P. 1986. A human DNA segment with properties of the gene that predisposes to retinoblastoma and osteosarcoma. *Nature,* 323**,** 643-6.

FUNK, J. O., WAGA, S., HARRY, J. B., ESPLING, E., STILLMAN, B. & GALLOWAY, D. A. 1997. Inhibition of CDK activity and PCNA-dependent DNA replication by p21 is blocked by interaction with the HPV-16 E7 oncoprotein. *Genes Dev,* 11**,** 2090-100.

GARDIOL, D., KUHNE, C., GLAUNSINGER, B., LEE, S. S., JAVIER, R. & BANKS, L. 1999. Oncogenic human papillomavirus E6 proteins target the discs large tumour suppressor for proteasome-mediated degradation. *Oncogene,* 18**,** 5487-96.

GARTEL, A. L. & TYNER, A. L. 1999. Transcriptional regulation of the p21((WAF1/CIP1)) gene. *Exp Cell Res,* 246**,** 280-9.

GAVRIELI, Y., SHERMAN, Y. & BEN-SASSON, S. A. 1992. Identification of programmed cell death in situ via specific labeling of nuclear DNA fragmentation. *J Cell Biol,* 119**,** 493-501.

GENECARDS® 2013. NCBI Gene ID: 12177. . *http://www.genecards.org/cgi-bin/carddisp.pl?gene=BNIP3L*.

GENOVESE, N. J., BANERJEE, N. S., BROKER, T. R. & CHOW, L. T. 2008. Casein kinase II motif-dependent phosphorylation of human papillomavirus E7 protein promotes p130 degradation and S-phase induction in differentiated human keratinocytes. *J Virol,* 82**,** 4862-73.

GILLISON, M. L., KOCH, W. M., CAPONE, R. B., SPAFFORD, M., WESTRA, W. H., WU, L., ZAHURAK, M. L., DANIEL, R. W., VIGLIONE, M., SYMER, D. E., SHAH, K. V. & SIDRANSKY, D. 2000. Evidence for a causal association between human papillomavirus and a subset of head and neck cancers. *J Natl Cancer Inst,* 92**,** 709-20.

GLAXOSMITHKLINE 2012. CERVARIX Pack Insert. *GlaxoSmithKline Biologicals,* Rixensart, Belgium.

GLOBOCAN 2008. Cervical Cancer Incidence and Mortality Worldwide in 2008 Summary. *Cancer Fact Sheet (IARC)*.

GOLDMAN, I. D. 2002. Membrane transport of chemotherapeutics and drug resistance: beyond the ABC family of exporters to the role of carrier-mediated processes. *Clin Cancer Res,* 8**,** 4-6.

GOLSTEIN, P. & KROEMER, G. 2007. Cell death by necrosis: towards a molecular definition. *Trends Biochem Sci,* 32**,** 37-43.

GRAY, J. V., PETSKO, G. A., JOHNSTON, G. C., RINGE, D., SINGER, R. A. & WERNER-WASHBURNE, M. 2004. "Sleeping beauty": quiescence in Saccharomyces cerevisiae. *Microbiol Mol Biol Rev,* 68**,** 187-206.

GUO, L., LIEW, H. P., CAMUS, S., GOH, A. M., CHEE, L. L., LUNNY, D. P., LANE, E. B. & LANE, D. P. 2013. Ionizing radiation induces a dramatic persistence of p53 protein accumulation and DNA damage signaling in mutant p53 zebrafish. *Oncogene,* 32**,** 4009-16.

HA, H. C. & SNYDER, S. H. 1999. Poly(ADP-ribose) polymerase is a mediator of necrotic cell death by ATP depletion. *Proc Natl Acad Sci U S A,* 96**,** 13978-82.

HANADA, K., BUDZOWSKA, M., DAVIES, S. L., VAN DRUNEN, E., ONIZAWA, H., BEVERLOO, H. B., MAAS, A., ESSERS, J., HICKSON, I. D. & KANAAR, R. 2007. The structure-specific endonuclease Mus81 contributes to replication restart by generating double-strand DNA breaks. *Nat Struct Mol Biol,* 14**,** 1096-104.

HANAHAN, D. & FOLKMAN, J. 1996. Patterns and emerging mechanisms of the angiogenic switch during tumorigenesis. *Cell,* 86**,** 353-64.

HANAHAN, D. & WEINBERG, R. A. 2000. The hallmarks of cancer. *Cell,* 100**,** 57-70.

HANAHAN, D. & WEINBERG, R. A. 2011. Hallmarks of cancer: the next generation. *Cell,* 144**,** 646-74.

HARBOUR, J. W. & DEAN, D. C. 2000. Rb function in cell-cycle regulation and apoptosis. *Nat Cell Biol,* 2**,** E65-7.

HARRIS, S. A., MCGUIGAN, C., ANDREI, G., SNOECK, R., DE CLERCQ, E. & BALZARINI, J. 2001. Synthesis and antiviral evaluation of phosphoramidate derivatives of (E)-5-(2-bromovinyl)-2'-deoxyuridine. *Antivir Chem Chemother,* 12**,** 293-300.

HARWOOD, C. A. & PROBY, C. M. 2002. Human papillomaviruses and non-melanoma skin cancer. *Curr Opin Infect Dis,* 15**,** 101-14.

HAUPT, Y., MAYA, R., KAZAZ, A. & OREN, M. 1997. Mdm2 promotes the rapid degradation of p53. *Nature,* 387**,** 296-9.

HAYDEN, M. S., WEST, A. P. & GHOSH, S. 2006. NF-kappaB and the immune response. *Oncogene,* 25**,** 6758-80.

HAYFLICK, L. 1997. Mortality and immortality at the cellular level. A review. *Biochemistry (Mosc),* 62**,** 1180-90.

HE, G., SIDDIK, Z. H., HUANG, Z., WANG, R., KOOMEN, J., KOBAYASHI, R., KHOKHAR, A. R. & KUANG, J. 2005. Induction of p21 by p53 following DNA damage inhibits both Cdk4 and Cdk2 activities. *Oncogene,* 24**,** 2929-43.

HECKER, S. J. & ERION, M. D. 2008. Prodrugs of phosphates and phosphonates. *J Med Chem,* 51**,** 2328-45.

HELLEMANS, J., MORTIER, G., DE PAEPE, A., SPELEMAN, F. & VANDESOMPELE, J. 2007. qBase relative quantification framework and software for management and automated analysis of real-time quantitative PCR data. *Genome Biol,* 8**,** R19.

HENDERSON, L., CLEMENTS, A., DAMERY, S., WILKINSON, C., AUSTOKER, J., WILSON, S. & GROUP, H. P. V. C. M. W. 2011. 'A false sense of security'? Understanding the role of the HPV vaccine on future cervical screening behaviour: a qualitative study of UK parents and girls of vaccination age. *J Med Screen,* 18**,** 41-5.

HERFS, M., YAMAMOTO, Y., LAURY, A., WANG, X., NUCCI, M. R., MCLAUGHLIN-DRUBIN, M. E., MUNGER, K., FELDMAN, S., MCKEON, F. D., XIAN, W. & CRUM, C. P. 2012. A discrete population of squamocolumnar junction cells implicated in the pathogenesis of cervical cancer. *Proc Natl Acad Sci U S A,* 109**,** 10516-21.

HERNANDEZ, J. M., SIEGEL, E. M., RIGGS, B., ESCHRICH, S., ELAHI, A., QU, X., AJIDAHUN, A., BERGLUND, A., COPPOLA, D., GRADY, W. M., GIULIANO, A. R. & SHIBATA, D. 2012. DNA methylation profiling across the spectrum of HPV-associated anal squamous neoplasia. *PLoS One,* 7**,** e50533.

HERRERA, R. E., MAKELA, T. P. & WEINBERG, R. A. 1996. TGF beta-induced growth inhibition in primary fibroblasts requires the retinoblastoma protein. *Mol Biol Cell,* 7**,** 1335-42.

HILDESHEIM, A., HERRERO, R., CASTLE, P. E., WACHOLDER, S., BRATTI, M. C., SHERMAN, M. E., LORINCZ, A. T., BURK, R. D., MORALES, J., RODRIGUEZ, A. C., HELGESEN, K., ALFARO, M., HUTCHINSON, M., BALMACEDA, I., GREENBERG, M. & SCHIFFMAN, M. 2001. HPV co-factors related to the development of cervical cancer: results from a population-based study in Costa Rica. *Br J Cancer,* 84**,** 1219-26.

HIYAMA, H., IAVARONE, A. & REEVES, S. A. 1998. Regulation of the cdk inhibitor p21 gene during cell cycle progression is under the control of the transcription factor E2F. *Oncogene,* 16**,** 1513-23.

HOFSETH, L. J., HUSSAIN, S. P. & HARRIS, C. C. 2004. p53: 25 years after its discovery. *Trends Pharmacol Sci,* 25**,** 177-81.

HOLOWATY, P., MILLER, A. B., ROHAN, T. & TO, T. 1999. Natural history of dysplasia of the uterine cervix. *J Natl Cancer Inst,* 91**,** 252-8.

HOSTETLER, K. Y., ROUGHT, S., ALDERN, K. A., TRAHAN, J., BEADLE, J. R. & CORBEIL, J. 2006. Enhanced antiproliferative effects of alkoxyalkyl esters of cidofovir in human cervical cancer cells in vitro. *Mol Cancer Ther,* 5**,** 156-9.

HUH, K., ZHOU, X., HAYAKAWA, H., CHO, J. Y., LIBERMANN, T. A., JIN, J., HARPER, J. W. & MUNGER, K. 2007. Human papillomavirus type 16 E7 oncoprotein associates with the cullin 2 ubiquitin ligase complex, which contributes to degradation of the retinoblastoma tumor suppressor. *J Virol,* 81**,** 9737-47.

HUTTUNEN, K. M., RAUNIO, H. & RAUTIO, J. 2011. Prodrugs--from serendipity to rational design. *Pharmacol Rev,* 63**,** 750-71.

IARC 2007. HUMAN PAPILLOMAVIRUSES. *Monographs,* 90.

IARC 2010 Update. Detection of TP53 mutations by direct sequencing. *IARC Protocol*.

IARC 2012. Biological Agents. *Monographs,* 100B.

IARC November 2012. IARC *TP53* Database. http://p53.iarc.fr/.

IKIC, D., KRUSIC, J., KIRHMAJER, V., KNEZEVIC, M., MARICIC, Z., RODE, B., JUSIC, D. & SOOS, E. 1981. Application of human leucocyte interferon in patients with carcinoma of the uterine cervix. *Lancet,* 1**,** 1027-30.

ISAACSON WECHSLER, E., WANG, Q., ROBERTS, I., PAGLIARULO, E., JACKSON, D., UNTERSPERGER, C., COLEMAN, N., GRIFFIN, H. & DOORBAR, J. 2012. Reconstruction of human papillomavirus type 16-mediated early-stage neoplasia implicates E6/E7 deregulation and the loss of contact inhibition in neoplastic progression. *J Virol,* 86**,** 6358-64.

ITAHANA, K., DIMRI, G. & CAMPISI, J. 2001. Regulation of cellular senescence by p53. *Eur J Biochem,* 268**,** 2784-91.

IVANOVSKA, I., BALL, A. S., DIAZ, R. L., MAGNUS, J. F., KIBUKAWA, M., SCHELTER, J. M., KOBAYASHI, S. V., LIM, L., BURCHARD, J., JACKSON, A. L., LINSLEY, P. S. & CLEARY, M. A. 2008. MicroRNAs in the miR-106b family regulate p21/CDKN1A and promote cell cycle progression. *Mol Cell Biol,* 28**,** 2167-74.

JACKSON, S. P. 2002. Sensing and repairing DNA double-strand breaks. *Carcinogenesis,* 23**,** 687-96.

JAMES, M. A., LEE, J. H. & KLINGELHUTZ, A. J. 2006. Human papillomavirus type 16 E6 activates NF-kappaB, induces cIAP-2 expression, and protects against apoptosis in a PDZ binding motif-dependent manner. *J Virol,* 80**,** 5301-7.

JEON, S. & LAMBERT, P. F. 1995. Integration of human papillomavirus type 16 DNA into the human genome leads to increased stability of E6 and E7 mRNAs: implications for cervical carcinogenesis. *Proc Natl Acad Sci U S A,* 92**,** 1654-8.

JIN, H. S. & LEE, T. H. 2006. Cell cycle-dependent expression of cIAP2 at G2/M phase contributes to survival during mitotic cell cycle arrest. *Biochem J,* 399**,** 335-42.

JIN, S., ANTINORE, M. J., LUNG, F. D., DONG, X., ZHAO, H., FAN, F., COLCHAGIE, A. B., BLANCK, P., ROLLER, P. P., FORNACE, A. J., JR. & ZHAN, Q. 2000. The GADD45 inhibition of Cdc2 kinase correlates with GADD45-mediated growth suppression. *J Biol Chem,* 275**,** 16602-8.

JOHNSON, J. A. & GANGEMI, J. D. 1999. Selective inhibition of human papillomavirus-induced cell proliferation by (S)-1-[3-hydroxy-2-(phosphonylmethoxy)propyl]cytosine. *Antimicrob Agents Chemother,* 43**,** 1198-205.

JORDAN, J. & SINGER, A. 1976. *The Cervix,* London, The Whitefriars Press Limited

JUDSON, P. L., HABERMANN, E. B., BAXTER, N. N., DURHAM, S. B. & VIRNIG, B. A. 2006. Trends in the incidence of invasive and in situ vulvar carcinoma. *Obstet Gynecol,* 107**,** 1018-22.

KALANTARI, M., CHASE, D. M., TEWARI, K. S. & BERNARD, H. U. 2010. Recombination of human papillomavirus-16 and host DNA in exfoliated cervical cells: a pilot study of

L1 gene methylation and chromosomal integration as biomarkers of carcinogenic progression. *J Med Virol,* 82**,** 311-20.

KANAAR, R., HOEIJMAKERS, J. H. & VAN GENT, D. C. 1998. Molecular mechanisms of DNA double strand break repair. *Trends Cell Biol,* 8**,** 483-9.

KANNAN, K., KAMINSKI, N., RECHAVI, G., JAKOB-HIRSCH, J., AMARIGLIO, N. & GIVOL, D. 2001. DNA microarray analysis of genes involved in p53 mediated apoptosis: activation of Apaf-1. *Oncogene,* 20**,** 3449-55.

KARNOUB, A. E. & WEINBERG, R. A. 2006. Chemokine networks and breast cancer metastasis. *Breast Dis,* 26**,** 75-85.

KAUFMAN, R. H. 1995. Intraepithelial neoplasia of the vulva. *Gynecologic oncology,* 56**,** 8-21.

KERN, E. R., HARTLINE, C., HARDEN, E., KEITH, K., RODRIGUEZ, N., BEADLE, J. R. & HOSTETLER, K. Y. 2002. Enhanced inhibition of orthopoxvirus replication in vitro by alkoxyalkyl esters of cidofovir and cyclic cidofovir. *Antimicrob Agents Chemother,* 46**,** 991-5.

KERR, J. F., WYLLIE, A. H. & CURRIE, A. R. 1972. Apoptosis: a basic biological phenomenon with wide-ranging implications in tissue kinetics. *Br J Cancer,* 26**,** 239-57.

KIM, S. K. 1997. Polarized signaling: basolateral receptor localization in epithelial cells by PDZ-containing proteins. *Curr Opin Cell Biol,* 9**,** 853-9.

KIMPLE, R. J., SMITH, M. A., BLITZER, G. C., TORRES, A. D., MARTIN, J. A., YANG, R. Z., PEET, C. R., LORENZ, L. D., NICKEL, K. P., KLINGELHUTZ, A. J., LAMBERT, P. F. & HARARI, P. M. 2013. Enhanced Radiation Sensitivity in HPV-Positive Head and Neck Cancer. *Cancer Res,* 73**,** 4791-800.

KIYONO, T., HIRAIWA, A., FUJITA, M., HAYASHI, Y., AKIYAMA, T. & ISHIBASHI, M. 1997. Binding of high-risk human papillomavirus E6 oncoproteins to the human homologue of the Drosophila discs large tumor suppressor protein. *Proc Natl Acad Sci U S A,* 94**,** 11612-6.

KLAES, R., WOERNER, S. M., RIDDER, R., WENTZENSEN, N., DUERST, M., SCHNEIDER, A., LOTZ, B., MELSHEIMER, P. & VON KNEBEL DOEBERITZ, M. 1999. Detection of high-risk cervical intraepithelial neoplasia and cervical cancer by amplification of transcripts derived from integrated papillomavirus oncogenes. *Cancer Res,* 59**,** 6132-6.

KLINGELHUTZ, A. J., FOSTER, S. A. & MCDOUGALL, J. K. 1996. Telomerase activation by the E6 gene product of human papillomavirus type 16. *Nature,* 380**,** 79-82.

KLUG, S. J., RESSING, M., KOENIG, J., ABBA, M. C., AGORASTOS, T., BRENNA, S. M., CIOTTI, M., DAS, B. R., DEL MISTRO, A., DYBIKOWSKA, A., GIULIANO, A. R., GUDLEVICIENE, Z., GYLLENSTEN, U., HAWS, A. L., HELLAND, A., HERRINGTON, C. S., HILDESHEIM, A., HUMBEY, O., JEE, S. H., KIM, J. W., MADELEINE, M. M., MENCZER, J., NGAN, H. Y., NISHIKAWA, A., NIWA, Y., PEGORARO, R., PILLAI, M. R., RANZANI, G., REZZA, G., ROSENTHAL, A. N., ROYCHOUDHURY, S., SARANATH, D., SCHMITT, V. M., SENGUPTA, S., SETTHEETHAM-ISHIDA, W., SHIRASAWA, H., SNIJDERS, P. J., STOLER,

M. H., SUAREZ-RINCON, A. E., SZARKA, K., TACHEZY, R., UEDA, M., VAN DER ZEE, A. G., VON KNEBEL DOEBERITZ, M., WU, M. T., YAMASHITA, T., ZEHBE, I. & BLETTNER, M. 2009. TP53 codon 72 polymorphism and cervical cancer: a pooled analysis of individual data from 49 studies. *Lancet Oncol,* 10**,** 772-84.

KNIGHT, G. L., PUGH, A. G., YATES, E., BELL, I., WILSON, R., MOODY, C. A., LAIMINS, L. A. & ROBERTS, S. 2011. A cyclin-binding motif in human papillomavirus type 18 (HPV18) E1^E4 is necessary for association with CDK-cyclin complexes and G2/M cell cycle arrest of keratinocytes, but is not required for differentiation-dependent viral genome amplification or L1 capsid protein expression. *Virology,* 412**,** 196-210.

KOOPMAN, G., REUTELINGSPERGER, C. P., KUIJTEN, G. A., KEEHNEN, R. M., PALS, S. T. & VAN OERS, M. H. 1994. Annexin V for flow cytometric detection of phosphatidylserine expression on B cells undergoing apoptosis. *Blood,* 84**,** 1415-20.

KRAMATA, P., VOTRUBA, I., OTOVA, B. & HOLY, A. 1996. Different inhibitory potencies of acyclic phosphonomethoxyalkyl nucleotide analogs toward DNA polymerases alpha, delta and epsilon. *Molecular Pharmacology,* 49**,** 1005 - 1011.

KREIMER, A. R., CLIFFORD, G. M., BOYLE, P. & FRANCESCHI, S. 2005. Human papillomavirus types in head and neck squamous cell carcinomas worldwide: a systematic review. *Cancer Epidemiol Biomarkers Prev,* 14**,** 467-75.

KREJCI, L., ALTMANNOVA, V., SPIREK, M. & ZHAO, X. 2012. Homologous recombination and its regulation. *Nucleic Acids Res,* 40**,** 5795-818.

KRZESLAK, A., WOJCIK-KROWIRANDA, K., FORMA, E., JOZWIAK, P., ROMANOWICZ, H., BIENKIEWICZ, A. & BRYS, M. 2012. Expression of GLUT1 and GLUT3 glucose transporters in endometrial and breast cancers. *Pathol Oncol Res,* 18**,** 721-8.

LAI, K. W. & MERCURIO, M. G. 2010. Medical and surgical approaches to vulvar intraepithelial neoplasia. *Dermatol Ther,* 23**,** 477-84.

LAURSON, J. & RAJ, K. 2011. Localisation of human papillomavirus 16 E7 oncoprotein changes with cell confluence. *PLoS One,* 6**,** e21501.

LEE, J. H. & PAULL, T. T. 2005. ATM activation by DNA double-strand breaks through the Mre11-Rad50-Nbs1 complex. *Science,* 308**,** 551-4.

LEECHANACHAI, P., BANKS, L., MOREAU, F. & MATLASHEWSKI, G. 1992. The E5 gene from human papillomavirus type 16 is an oncogene which enhances growth factor-mediated signal transduction to the nucleus. *Oncogene,* 7**,** 19-25.

LEIROS, G. J., GALLIANO, S. R., SEMBER, M. E., KAHN, T., SCHWARZ, E. & EIGUCHI, K. 2005. Detection of human papillomavirus DNA and p53 codon 72 polymorphism in prostate carcinomas of patients from Argentina. *BMC Urol,* 5**,** 15.

LEONTIEVA, O. V., GUDKOV, A. V. & BLAGOSKLONNY, M. V. 2010. Weak p53 permits senescence during cell cycle arrest. *Cell Cycle,* 9**,** 4323-7.

LEVINE, A. J. & OREN, M. 2009. The first 30 years of p53: growing ever more complex. *Nat Rev Cancer,* 9**,** 749-58.

LI, G. M. 2008. Mechanisms and functions of DNA mismatch repair. *Cell Res,* 18**,** 85-98.

LIEBER, M. R., MA, Y., PANNICKE, U. & SCHWARZ, K. 2003. Mechanism and regulation of human non-homologous DNA end-joining. *Nat Rev Mol Cell Biol,* 4**,** 712-20.

LINDEL, K., BEER, K. T., LAISSUE, J., GREINER, R. H. & AEBERSOLD, D. M. 2001. Human papillomavirus positive squamous cell carcinoma of the oropharynx: a radiosensitive subgroup of head and neck carcinoma. *Cancer,* 92**,** 805-13.

LONGWORTH, M. S. & LAIMINS, L. A. 2004. The binding of histone deacetylases and the integrity of zinc finger-like motifs of the E7 protein are essential for the life cycle of human papillomavirus type 31. *J Virol,* 78**,** 3533-41.

LOO, Y. M. & MELENDY, T. 2004. Recruitment of replication protein A by the papillomavirus E1 protein and modulation by single-stranded DNA. *J Virol,* 78**,** 1605-15.

LUE, R. A., MARFATIA, S. M., BRANTON, D. & CHISHTI, A. H. 1994. Cloning and characterization of hdlg: the human homologue of the Drosophila discs large tumor suppressor binds to protein 4.1. *Proc Natl Acad Sci U S A,* 91**,** 9818-22.

LUFT, F., KLAES, R., NEES, M., DURST, M., HEILMANN, V., MELSHEIMER, P. & VON KNEBEL DOEBERITZ, M. 2001. Detection of integrated papillomavirus sequences by ligation-mediated PCR (DIPS-PCR) and molecular characterization in cervical cancer cells. *Int J Cancer,* 92**,** 9-17.

LUKAS, J., PARRY, D., AAGAARD, L., MANN, D. J., BARTKOVA, J., STRAUSS, M., PETERS, G. & BARTEK, J. 1995. Retinoblastoma-protein-dependent cell-cycle inhibition by the tumour suppressor p16. *Nature,* 375**,** 503-6.

LUKASHEV, M. E. & WERB, Z. 1998. ECM signalling: orchestrating cell behaviour and misbehaviour. *Trends Cell Biol,* 8**,** 437-41.

MARKOWITZ, S., WANG, J., MYEROFF, L., PARSONS, R., SUN, L., LUTTERBAUGH, J., FAN, R. S., ZBOROWSKA, E., KINZLER, K. W., VOGELSTEIN, B. & ET AL. 1995. Inactivation of the type II TGF-beta receptor in colon cancer cells with microsatellite instability. *Science,* 268**,** 1336-8.

MARTIN, G. S. 1970. Rous sarcoma virus: a function required for the maintenance of the transformed state. *Nature,* 227**,** 1021-3.

MCBEE W.C., GARDINER A.S., EDWARDS R.P., LESNOCK J.L., BHARGAVA R., AUSTIN R.M., GUIDO R.S. & S.A., K. 2011. MicroRNA Analysis in Human Papillomavirus (HPV)-Associated Cervical Neoplasia and Cancer. *Carcinogenesis & Mutagenesis,* 2**,** 2157-2518.

MCCLUGGAGE, W. G. 2009. Recent developments in vulvovaginal pathology. *Histopathology***,** 156-173.

MCGUIGAN, C., KELLEHER, M. R., PERRONE, P., MULREADY, S., LUONI, G., DAVERIO, F., RAJYAGURU, S., LE POGAM, S., NAJERA, I., MARTIN, J. A., KLUMPP, K. & SMITH, D. B. 2009. The application of phosphoramidate ProTide technology to the potent anti-HCV compound 4'-azidocytidine (R1479). *Bioorg Med Chem Lett,* 19**,** 4250-4.

MCGUIGAN, C., THIERY, J. C., DAVERIO, F., JIANG, W. G., DAVIES, G. & MASON, M. 2005. Anti-cancer ProTides: tuning the activity of BVDU phosphoramidates related to thymectacin. *Bioorg Med Chem,* 13**,** 3219-27.

MCKENNA, C., KASHEMIROV, B., ERIKSSON , U., AMIDON, G., KISH, P., MITCHELL, S., KIM, J. & HILFINGER, J. 2005. Cidofovir peptide conjugates as prodrugs. *Journal of Organometallic Chemistry,* 690**,** 2673–2678.

MCMILLAN, N. A., PAYNE, E., FRAZER, I. H. & EVANDER, M. 1999. Expression of the alpha6 integrin confers papillomavirus binding upon receptor-negative B-cells. *Virology,* 261**,** 271-9.

MCMURRAY, H. R. & MCCANCE, D. J. 2003. Human papillomavirus type 16 E6 activates TERT gene transcription through induction of c-Myc and release of USF-mediated repression. *J Virol,* 77**,** 9852-61.

MCMURRAY, H. R. & MCCANCE, D. J. 2004. Degradation of p53, not telomerase activation, by E6 is required for bypass of crisis and immortalization by human papillomavirus type 16 E6/E7. *J Virol,* 78**,** 5698-706.

MCVEY, M. & LEE, S. E. 2008. MMEJ repair of double-strand breaks (director's cut): deleted sequences and alternative endings. *Trends Genet,* 24**,** 529-38.

MEDEMA, R. H. & BOS, J. L. 1993. The role of p21ras in receptor tyrosine kinase signaling. *Crit Rev Oncog,* 4**,** 615-61.

MEHELLOU, Y., BALZARINI, J. & MCGUIGAN, C. 2009. Aryloxy phosphoramidate triesters: a technology for delivering monophosphorylated nucleosides and sugars into cells. *ChemMedChem,* 4**,** 1779-91.

MERCK 2011. GARDASIL Pack Insert. *Merck & Co., Inc.,* Whitehouse Station, NJ08889, USA.

MIDDLETON, K., PEH, W., SOUTHERN, S., GRIFFIN, H., SOTLAR, K., NAKAHARA, T., EL-SHERIF, A., MORRIS, L., SETH, R., HIBMA, M., JENKINS, D., LAMBERT, P., COLEMAN, N. & DOORBAR, J. 2003. Organization of human papillomavirus productive cycle during neoplastic progression provides a basis for selection of diagnostic markers. *J Virol,* 77**,** 10186-201.

MODIS, Y., TRUS, B. L. & HARRISON, S. C. 2002. Atomic model of the papillomavirus capsid. *EMBO J,* 21**,** 4754-62.

MONSONEGO, J., CORTES, J., GREPPE, C., HAMPL, M., JOURA, E. & SINGER, A. 2010. Benefits of vaccinating young adult women with a prophylactic quadrivalent human papillomavirus (types 6, 11, 16 and 18) vaccine. *Vaccine,* 28**,** 8065-72.

MOONEN, P. M., BAKKERS, J. M., KIEMENEY, L. A., SCHALKEN, J. A., MELCHERS, W. J. & WITJES, J. A. 2007. Human papilloma virus DNA and p53 mutation analysis on bladder washes in relation to clinical outcome of bladder cancer. *Eur Urol,* 52**,** 464-8.

MOORE, J. K. & HABER, J. E. 1996. Cell cycle and genetic requirements of two pathways of nonhomologous end-joining repair of double-strand breaks in Saccharomyces cerevisiae. *Mol Cell Biol,* 16**,** 2164-73.

MUNGER, K., PHELPS, W. C., BUBB, V., HOWLEY, P. M. & SCHLEGEL, R. 1989. The E6 and E7 genes of the human papillomavirus type 16 together are necessary and sufficient for transformation of primary human keratinocytes. *J Virol,* 63**,** 4417-21.

MUNOZ, N., CASTELLSAGUE, X., DE GONZALEZ, A. B. & GISSMANN, L. 2006. Chapter 1: HPV in the etiology of human cancer. *Vaccine,* 24 Suppl 3**,** S3/1-10.

MURRAY, A. 1994. Cell cycle checkpoints. *Curr Opin Cell Biol,* 6**,** 872-6.

NAKAHARA, T., NISHIMURA, A., TANAKA, M., UENO, T., ISHIMOTO, A. & SAKAI, H. 2002. Modulation of the cell division cycle by human papillomavirus type 18 E4. *Journal of virology,* 76**,** 10914-20.

NARISAWA-SAITO, M. & KIYONO, T. 2007. Basic mechanisms of high-risk human papillomavirus-induced carcinogenesis: roles of E6 and E7 proteins. *Cancer Sci,* 98**,** 1505-11.

NCBI Basic Local Alignment Search Tool. *http://blast.ncbi.nlm.nih.gov/Blast.cgi?CMD=Web&PAGE_TYPE=BlastHome*.

NCBI October 2013. Gene ID: 596. BCL2 B-cell CLL/lymphoma 2 [Homo sapiens (human)]. *http://www.ncbi.nlm.nih.gov/gene/596*.

NCBI September 2013a. Gene ID: 330. BIRC3 baculoviral IAP repeat containing 3 [Homo sapiens (human)]. *http://www.ncbi.nlm.nih.gov/gene/330*.

NCBI September 2013b. Gene ID: 356. FASLG Fas ligand (TNF superfamily, member 6) [Homo sapiens (human)]. *http://www.ncbi.nlm.nih.gov/gene/356*.

NCBI September 2013c. Gene ID: 597. BCL2A1 BCL2-related protein A1 [Homo sapiens (human)]. *http://www.ncbi.nlm.nih.gov/gene/597*.

NCBI September 2013d. Gene ID: 939. CD27 CD27 molecule [Homo sapiens (human)]. *http://www.ncbi.nlm.nih.gov/gene/939*.

NCBI September 2013e. Gene ID: 944. TNFSF8 tumor necrosis factor (ligand) superfamily, member 8 [Homo sapiens (human)]. *http://www.ncbi.nlm.nih.gov/gene/944*.

NCBI September 2013f. Gene ID: 970. CD70 CD70 molecule [Homo sapiens (human)]. *http://www.ncbi.nlm.nih.gov/gene/970*.

NCBI September 2013g. Gene ID: 1026. CDKN1A cyclin-dependent kinase inhibitor 1A (p21, Cip1) [Homo sapiens (human)]. *http://www.ncbi.nlm.nih.gov/gene/1026*.

NCBI September 2013h. Gene ID: 1149. CIDEA cell death-inducing DFFA-like effector a [Homo sapiens (human)]. *http://www.ncbi.nlm.nih.gov/gene/1149*.

NCBI September 2013i. Gene ID: 1612. DAPK1 death-associated protein kinase 1 [Homo sapiens (human)]. *http://www.ncbi.nlm.nih.gov/gene/1612*.

NCBI September 2013j. Gene ID: 3586. IL10 interleukin 10 [Homo sapiens (human)]. *http://www.ncbi.nlm.nih.gov/gene/3586*.

NCBI September 2013k. Gene ID: 3604. TNFRSF9 tumor necrosis factor receptor superfamily, member 9 [Homo sapiens (human)]. *http://www.ncbi.nlm.nih.gov/gene/3604*.

NCBI September 2013l. Gene ID: 4049. LTA lymphotoxin alpha [Homo sapiens (human)]. http://www.ncbi.nlm.nih.gov/gene/4049.

NCBI September 2013m. Gene ID: 4671. NAIP NLR family, apoptosis inhibitory protein [Homo sapiens (human)]. http://www.ncbi.nlm.nih.gov/gene/4671.

NCBI September 2013n. Gene ID: 4982. TNFRSF11B tumor necrosis factor receptor superfamily, member 11b [Homo sapiens (human)]. http://www.ncbi.nlm.nih.gov/gene/4982.

NCBI September 2013o. Gene ID: 7124. TNF tumor necrosis factor [Homo sapiens (human)]. http://www.ncbi.nlm.nih.gov/gene/7124.

NCBI September 2013p. Gene ID: 7157. TP53 tumor protein p53 [Homo sapiens (human)]. http://www.ncbi.nlm.nih.gov/gene/7157.

NCBI September 2013q. Gene ID: 8739. HRK harakiri, BCL2 interacting protein (contains only BH3 domain) [Homo sapiens (human)]. http://www.ncbi.nlm.nih.gov/gene/8739.

NCBI September 2013r. Gene ID: 8743. TNFSF10 tumor necrosis factor (ligand) superfamily, member 10 [Homo sapiens (human)]. http://www.ncbi.nlm.nih.gov/gene/8743.

NCBI September 2013s. Gene ID: 10017. BCL2L10 BCL2-like 10 (apoptosis facilitator) [Homo sapiens (human)]. http://www.ncbi.nlm.nih.gov/gene/10017.

NCBI September 2013t. Gene ID: 23581. CASP14 caspase 14, apoptosis-related cysteine peptidase [Homo sapiens (human)]. http://www.ncbi.nlm.nih.gov/gene/23581.

NCBI September 2013u. Gene ID: 27242. TNFRSF21 tumor necrosis factor receptor superfamily, member 21 [Homo sapiens (human)]. http://www.ncbi.nlm.nih.gov/gene/27242.

NELSON, D. L. & COX, M. M. 2005. *Lehninger Principles of Biochemistry,* New York, Sara Tenney.

NIP, J., STROM, D. K., EISCHEN, C. M., CLEVELAND, J. L., ZAMBETTI, G. P. & HIEBERT, S. W. 2001. E2F-1 induces the stabilization of p53 but blocks p53-mediated transactivation. *Oncogene,* 20**,** 910-20.

OFFER, H., WOLKOWICZ, R., MATAS, D., BLUMENSTEIN, S., LIVNEH, Z. & ROTTER, V. 1999. Direct involvement of p53 in the base excision repair pathway of the DNA repair machinery. *FEBS Lett,* 450**,** 197-204.

OHTA, T., HORI, H., OGAWA, M., MIYAHARA, M., KAWASAKI, H., TANIGUCHI, N. & KOMADA, Y. 2004. Impact of cytidine deaminase activity on intrinsic resistance to cytarabine in carcinoma cells. *Oncol Rep,* 12**,** 1115-20.

OLIYAI, R., SHAW, J. P., SUEOKA-LENNEN, C. M., CUNDY, K. C., ARIMILLI, M. N., JONES, R. J. & LEE, W. A. 1999. Aryl ester prodrugs of cyclic HPMPC. I: Physicochemical characterization and in vitro biological stability. *Pharm Res,* 16**,** 1687-93.

OSBORNE, C., WILSON, P. & TRIPATHY, D. 2004. Oncogenes and tumor suppressor genes in breast cancer: potential diagnostic and therapeutic applications. *Oncologist,* 9**,** 361-77.

PANDE, P., MATHUR, M., SHUKLA, N. K. & RALHAN, R. 1998. pRb and p16 protein alterations in human oral tumorigenesis. *Oral Oncol,* 34**,** 396-403.

PARDEE, A. B. 1989. G1 events and regulation of cell proliferation. *Science,* 246**,** 603-8.

PARK, P., COPELAND, W., YANG, L., WANG, T., BOTCHAN, M. R. & MOHR, I. J. 1994. The cellular DNA polymerase alpha-primase is required for papillomavirus DNA replication and associates with the viral E1 helicase. *Proc Natl Acad Sci U S A,* 91**,** 8700-4.

PASTOR-ANGLADA, M., CANO-SOLDADO, P., ERRASTI-MURUGARREN, E. & CASADO, F. J. 2008. SLC28 genes and concentrative nucleoside transporter (CNT) proteins. *Xenobiotica,* 38**,** 972-94.

PECORINO, L. 2008. *Molecular Biology Of Cancer,* New York

Oxford University Press Inc.

PECORINO, L. 2012. *Molecular Biology of Cancer: Mechanisms, Targets, and Therapeutics*, Oxford University Press.

PERRONE, P., LUONI, G. M., KELLEHER, M. R., DAVERIO, F., ANGELL, A., MULREADY, S., CONGIATU, C., RAJYAGURU, S., MARTIN, J. A., LEVEQUE, V., LE POGAM, S., NAJERA, I., KLUMPP, K., SMITH, D. B. & MCGUIGAN, C. 2007. Application of the phosphoramidate ProTide approach to 4'-azidouridine confers sub-micromolar potency versus hepatitis C virus on an inactive nucleoside. *J Med Chem,* 50**,** 1840-9.

PERTUSATI, F., HINSINGER, K., FLYNN, A., POWELL, N., TRISTRAM, A., BALZARINI, J. & MCGUIGAN, C. Submitted for publication PMPA and PMEA Prodrugs for the Treatment of HIV Infections and Human Papillomavirus (HPV) Associated Neoplasia and Cancer. *Journal of Medicinal Chemistry*.

PETIT-FRERE, C., CAPULAS, E., LYON, D. A., NORBURY, C. J., LOWE, J. E., CLINGEN, P. H., RIBALLO, E., GREEN, M. H. & ARLETT, C. F. 2000. Apoptosis and cytokine release induced by ionizing or ultraviolet B radiation in primary and immortalized human keratinocytes. *Carcinogenesis,* 21**,** 1087-95.

PETROCCA, F., VISONE, R., ONELLI, M. R., SHAH, M. H., NICOLOSO, M. S., DE MARTINO, I., ILIOPOULOS, D., PILOZZI, E., LIU, C. G., NEGRINI, M., CAVAZZINI, L., VOLINIA, S., ALDER, H., RUCO, L. P., BALDASSARRE, G., CROCE, C. M. & VECCHIONE, A. 2008. E2F1-regulated microRNAs impair TGFbeta-dependent cell-cycle arrest and apoptosis in gastric cancer. *Cancer Cell,* 13**,** 272-86.

PFAFFL, M. W. 2001. A new mathematical model for relative quantification in real-time RT-PCR. *Nucleic Acids Res,* 29**,** e45.

PIRAMI, L., GIACHE, V. & BECCIOLINI, A. 1997. Analysis of HPV16, 18, 31, and 35 DNA in pre-invasive and invasive lesions of the uterine cervix. *J Clin Pathol,* 50**,** 600-4.

PONTING, C. P. & PHILLIPS, C. 1995. DHR domains in syntrophins, neuronal NO synthases and other intracellular proteins. *Trends Biochem Sci,* 20**,** 102-3.

REIMERS, N., KASPER, H. U., WEISSENBORN, S. J., STUTZER, H., PREUSS, S. F., HOFFMANN, T. K., SPEEL, E. J., DIENES, H. P., PFISTER, H. J., GUNTINAS-LICHIUS, O. & KLUSSMANN, J. P. 2007. Combined analysis of HPV-DNA, p16 and EGFR expression to predict prognosis in oropharyngeal cancer. *Int J Cancer,* 120**,** 1731-8.

RIECKMANN, T., TRIBIUS, S., GROB, T. J., MEYER, F., BUSCH, C. J., PETERSEN, C., DIKOMEY, E. & KRIEGS, M. 2013. HNSCC cell lines positive for HPV and p16 possess higher cellular radiosensitivity due to an impaired DSB repair capacity. *Radiother Oncol,* 107**,** 242-6.

RISTRIANI, T., MASSON, M., NOMINE, Y., LAURENT, C., LEFEVRE, J. F., WEISS, E. & TRAVE, G. 2000. HPV oncoprotein E6 is a structure-dependent DNA-binding protein that recognizes four-way junctions. *J Mol Biol,* 296**,** 1189-203.

ROBERTS, S., ASHMOLE, I., JOHNSON, G. D., KREIDER, J. W. & GALLIMORE, P. H. 1993. Cutaneous and mucosal human papillomavirus E4 proteins form intermediate filament-like structures in epithelial cells. *Virology,* 197**,** 176-87.

ROBERTS, S., KINGSBURY, S. R., STOEBER, K., KNIGHT, G. L., GALLIMORE, P. H. & WILLIAMS, G. H. 2008. Identification of an arginine-rich motif in human papillomavirus type 1 E1;E4 protein necessary for E4-mediated inhibition of cellular DNA synthesis in vitro and in cells. *J Virol,* 82**,** 9056-64.

RODEN, R. & VISCIDI, R. 2006. *Papillomavirus-like Particles and Their Applications in Molecular Virology, Human Serology and Vaccines,* Norfolk, England, Caister Academic Press.

ROSENTHAL, A. N., RYAN, A., HOPSTER, D. & JACOBS, I. J. 2000. p53 codon 72 polymorphism in vulval cancer and vulval intraepithelial neoplasia. *Br J Cancer,* 83**,** 1287-90.

ROTH, M., OBAIDAT, A. & HAGENBUCH, B. 2012. OATPs, OATs and OCTs: the organic anion and cation transporters of the SLCO and SLC22A gene superfamilies. *Br J Pharmacol,* 165**,** 1260-87.

ROTHKAMM, K., KRUGER, I., THOMPSON, L. H. & LOBRICH, M. 2003. Pathways of DNA double-strand break repair during the mammalian cell cycle. *Mol Cell Biol,* 23**,** 5706-15.

ROUS, P. 1911. A Sarcoma of the Fowl Transmissible by an Agent Separable from the Tumor Cells. *J Exp Med,* 13**,** 397-411.

SALEH-GOHARI, N. & HELLEDAY, T. 2004. Conservative homologous recombination preferentially repairs DNA double-strand breaks in the S phase of the cell cycle in human cells. *Nucleic Acids Res,* 32**,** 3683-8.

SANDERS, C. M. & STENLUND, A. 1998. Recruitment and loading of the E1 initiator protein: an ATP-dependent process catalysed by a transcription factor. *EMBO J,* 17**,** 7044-55.

SANTIN, A. D., HERMONAT, P. L., RAVAGGI, A., CHIRIVA-INTERNATI, M., PECORELLI, S. & PARHAM, G. P. 1998. Radiation-enhanced expression of E6/E7 transforming oncogenes of human papillomavirus-16 in human cervical carcinoma. *Cancer,* 83**,** 2346-52.

SANTORO, R. & BLANDINO, G. 2010. p53: The pivot between cell cycle arrest and senescence. *Cell Cycle,* 9**,** 4262-3.

SCHEFFNER, M., HUIBREGTSE, J. M., VIERSTRA, R. D. & HOWLEY, P. M. 1993. The HPV-16 E6 and E6-AP complex functions as a ubiquitin-protein ligase in the ubiquitination of p53. *Cell,* 75**,** 495-505.

SCHREIBER, M., KOLBUS, A., PIU, F., SZABOWSKI, A., MOHLE-STEINLEIN, U., TIAN, J., KARIN, M., ANGEL, P. & WAGNER, E. F. 1999. Control of cell cycle progression by c-Jun is p53 dependent. *Genes Dev,* 13**,** 607-19.

SCHWABE, R. F., BRADHAM, C. A., UEHARA, T., HATANO, E., BENNETT, B. L., SCHOONHOVEN, R. & BRENNER, D. A. 2003. c-Jun-N-terminal kinase drives cyclin D1 expression and proliferation during liver regeneration. *Hepatology,* 37**,** 824-32.

SCUDIERO, D. A., SHOEMAKER, R. H., PAULL, K. D., MONKS, A., TIERNEY, S., NOFZIGER, T. H., CURRENS, M. J., SENIFF, D. & BOYD, M. R. 1988. Evaluation of a soluble tetrazolium/formazan assay for cell growth and drug sensitivity in culture using human and other tumor cell lines. *Cancer Res,* 48**,** 4827-33.

SEAVEY, S. E., HOLUBAR, M., SAUCEDO, L. J. & PERRY, M. E. 1999. The E7 oncoprotein of human papillomavirus type 16 stabilizes p53 through a mechanism independent of p19(ARF). *J Virol,* 73**,** 7590-8.

SEDMAN, J. & STENLUND, A. 1998. The papillomavirus E1 protein forms a DNA-dependent hexameric complex with ATPase and DNA helicase activities. *J Virol,* 72**,** 6893-7.

SEEBERG, E., EIDE, L. & BJORAS, M. 1995. The base excision repair pathway. *Trends Biochem Sci,* 20**,** 391-7.

SERPI, M., MADELA, K., PERTUSATI, F. & SLUSARCZYK, M. 2013. Synthesis of phosphoramidate prodrugs: ProTide approach. *Curr Protoc Nucleic Acid Chem,* Chapter 15**,** Unit15 5.

SHAFTI-KERAMAT, S., HANDISURYA, A., KRIEHUBER, E., MENEGUZZI, G., SLUPETZKY, K. & KIRNBAUER, R. 2003. Different heparan sulfate proteoglycans serve as cellular receptors for human papillomaviruses. *J Virol,* 77**,** 13125-35.

SHAY, J. W. & BACCHETTI, S. 1997. A survey of telomerase activity in human cancer. *Eur J Cancer,* 33**,** 787-91.

SHERMAN, L., ALLOUL, N., GOLAN, I., DURST, M. & BARAM, A. 1992. Expression and splicing patterns of human papillomavirus type-16 mRNAs in pre-cancerous lesions and carcinomas of the cervix, in human keratinocytes immortalized by HPV 16, and in cell lines established from cervical cancers. *Int J Cancer,* 50**,** 356-64.

SHIEH, S. Y., IKEDA, M., TAYA, Y. & PRIVES, C. 1997. DNA damage-induced phosphorylation of p53 alleviates inhibition by MDM2. *Cell,* 91**,** 325-34.

SHIELDS, J. D., KOURTIS, I. C., TOMEI, A. A., ROBERTS, J. M. & SWARTZ, M. A. 2010. Induction of lymphoidlike stroma and immune escape by tumors that express the chemokine CCL21. *Science,* 328**,** 749-52.

SHIN, K. H., AHN, J. H., KANG, M. K., LIM, P. K., YIP, F. K., BALUDA, M. A. & PARK, N. H. 2006. HPV-16 E6 oncoprotein impairs the fidelity of DNA end-joining via p53-dependent and -independent pathways. *Int J Oncol,* 28**,** 209-15.

SHYLASREE, T. S., KARANJGAOKAR, V., TRISTRAM, A., WILKES, A. R., MACLEAN, A. B. & FIANDER, A. N. 2008. Contribution of demographic, psychological and disease-related factors to quality of life in women with high-grade vulval intraepithelial neoplasia. *Gynecologic oncology,* 110**,** 185-9.

SIDDIQUE, M. & SABAPATHY, K. 2006. Trp53-dependent DNA-repair is affected by the codon 72 polymorphism. *Oncogene,* 25**,** 3489-500.

SIDDIQUI, A. Q., MCGUIGAN, C., BALLATORE, C., ZUCCOTTO, F., GILBERT, I. H., DE CLERCQ, E. & BALZARINI, J. 1999. Design and synthesis of lipophilic phosphoramidate d4T-MP prodrugs expressing high potency against HIV in cell culture: structural determinants for in vitro activity and QSAR. *J Med Chem,* 42**,** 4122-8.

SINGH, B., REDDY, P. G., GOBERDHAN, A., WALSH, C., DAO, S., NGAI, I., CHOU, T. C., P, O. C., LEVINE, A. J., RAO, P. H. & STOFFEL, A. 2002. p53 regulates cell survival by inhibiting PIK3CA in squamous cell carcinomas. *Genes Dev,* 16**,** 984-93.

SINGH, L., GAO, Q., KUMAR, A., GOTOH, T., WAZER, D. E., BAND, H., FEIG, L. A. & BAND, V. 2003. The high-risk human papillomavirus type 16 E6 counters the GAP function of E6TP1 toward small Rap G proteins. *J Virol,* 77**,** 1614-20.

SINGH, R. K., GUTMAN, M., BUCANA, C. D., SANCHEZ, R., LLANSA, N. & FIDLER, I. J. 1995. Interferons alpha and beta down-regulate the expression of basic fibroblast growth factor in human carcinomas. *Proceedings of the National Academy of Sciences of the United States of America,* 92**,** 4562-6.

SIRIANNI, N., WANG, J. & FERRIS, R. L. 2005. Antiviral activity of Cidofovir on a naturally human papillomavirus-16 infected squamous cell carcinoma of the head and neck (SCCHN) cell line improves radiation sensitivity. *Oral Oncol,* 41**,** 423-8.

SMITH, J. S., HERRERO, R., BOSETTI, C., MUNOZ, N., BOSCH, F. X., ELUF-NETO, J., CASTELLSAGUE, X., MEIJER, C. J., VAN DEN BRULE, A. J., FRANCESCHI, S., ASHLEY, R. & INTERNATIONAL AGENCY FOR RESEARCH ON CANCER MULTICENTRIC CERVICAL CANCER STUDY, G. 2002. Herpes simplex virus-2 as a human papillomavirus cofactor in the etiology of invasive cervical cancer. *J Natl Cancer Inst,* 94**,** 1604-13.

SNOECK, R., ANDREI, G. & DE CLERCQ, E. 2001a. Cidofovir in the treatment of HPV-associated lesions. *Verh K Acad Geneeskd Belg,* 63**,** 93-120, discussion 120-2.

SNOECK, R., BOSSENS, M., PARENT, D., DELAERE, B., DEGREEF, H., VAN RANST, M., NOEL, J. C., WULFSOHN, M. S., ROONEY, J. F., JAFFE, H. S. & DE CLERCQ, E. 2001b. Phase II double-blind, placebo-controlled study of the safety and efficacy of cidofovir topical gel for the treatment of patients with human papillomavirus infection. *Clin Infect Dis,* 33**,** 597-602.

SNOECK, R., NOEL, J. C., MULLER, C., DE CLERCQ, E. & BOSSENS, M. 2000. Cidofovir, a new approach for the treatment of cervix intraepithelial neoplasia grade III (CIN III). *J Med Virol,* 60**,** 205-9.

SPIRTOS, N. M., SMITH, L. H. & TENG, N. N. 1990. Prospective randomized trial of topical alpha-interferon (alpha-interferon gels) for the treatment of vulvar intraepithelial neoplasia III. *Gynecol Oncol,* 37**,** 34-8.

SPITKOVSKY, D., HEHNER, S. P., HOFMANN, T. G., MOLLER, A. & SCHMITZ, M. L. 2002. The human papillomavirus oncoprotein E7 attenuates NF-kappa B activation by targeting the Ikappa B kinase complex. *J Biol Chem,* 277**,** 25576-82.

STANLEY, M. A. & PARKINSON, E. K. 1979. Growth requirements of human cervical epithelial cells in culture. *Int J Cancer,* 24**,** 407-14.

STEHELIN, D., VARMUS, H. E., BISHOP, J. M. & VOGT, P. K. 1976. DNA related to the transforming gene(s) of avian sarcoma viruses is present in normal avian DNA. *Nature,* 260**,** 170-3.

STEIN, G. H., DRULLINGER, L. F., SOULARD, A. & DULIC, V. 1999. Differential roles for cyclin-dependent kinase inhibitors p21 and p16 in the mechanisms of senescence and differentiation in human fibroblasts. *Mol Cell Biol,* 19**,** 2109-17.

STOLER, M. H., SCHIFFMAN, M. & ATYPICAL SQUAMOUS CELLS OF UNDETERMINED SIGNIFICANCE-LOW-GRADE SQUAMOUS INTRAEPITHELIAL LESION TRIAGE STUDY, G. 2001. Interobserver reproducibility of cervical cytologic and histologic interpretations: realistic estimates from the ASCUS-LSIL Triage Study. *JAMA,* 285**,** 1500-5.

STOREY, A., THOMAS, M., KALITA, A., HARWOOD, C., GARDIOL, D., MANTOVANI, F., BREUER, J., LEIGH, I. M., MATLASHEWSKI, G. & BANKS, L. 1998. Role of a p53 polymorphism in the development of human papillomavirus-associated cancer. *Nature,* 393**,** 229-34.

STRAIGHT, S. W., HINKLE, P. M., JEWERS, R. J. & MCCANCE, D. J. 1993. The E5 oncoprotein of human papillomavirus type 16 transforms fibroblasts and effects the downregulation of the epidermal growth factor receptor in keratinocytes. *J Virol,* 67**,** 4521-32.

SUN, X., SHIMIZU, H. & YAMAMOTO, K. 1995. Identification of a novel p53 promoter element involved in genotoxic stress-inducible p53 gene expression. *Mol Cell Biol,* 15**,** 4489-96.

SUN, Y., TRAN, B. N., WORLEY, L. A., DELSTON, R. B. & HARBOUR, J. W. 2005. Functional analysis of the p53 pathway in response to ionizing radiation in uveal melanoma. *Invest Ophthalmol Vis Sci,* 46**,** 1561-4.

SYMONDS, H., KRALL, L., REMINGTON, L., SAENZ-ROBLES, M., LOWE, S., JACKS, T. & VAN DYKE, T. 1994. p53-dependent apoptosis suppresses tumor growth and progression in vivo. *Cell,* 78**,** 703-11.

TAK, P. P. & FIRESTEIN, G. S. 2001. NF-kappaB: a key role in inflammatory diseases. *J Clin Invest,* 107**,** 7-11.

TANG, S., TAO, M., MCCOY, J. P., JR. & ZHENG, Z. M. 2006. The E7 oncoprotein is translated from spliced E6*I transcripts in high-risk human papillomavirus type 16- or type 18-positive cervical cancer cell lines via translation reinitiation. *J Virol,* 80**,** 4249-63.

TANG, W., WILLERS, H. & POWELL, S. N. 1999. p53 directly enhances rejoining of DNA double-strand breaks with cohesive ends in gamma-irradiated mouse fibroblasts. *Cancer Res,* 59**,** 2562-5.

TASDEMIR, E., MAIURI, M. C., GALLUZZI, L., VITALE, I., DJAVAHERI-MERGNY, M., D'AMELIO, M., CRIOLLO, A., MORSELLI, E., ZHU, C., HARPER, F., NANNMARK, U., SAMARA, C., PINTON, P., VICENCIO, J. M., CARNUCCIO, R., MOLL, U. M., MADEO, F., PATERLINI-BRECHOT, P., RIZZUTO, R., SZABADKAI, G., PIERRON, G., BLOMGREN, K., TAVERNARAKIS, N., CODOGNO, P., CECCONI, F. & KROEMER, G. 2008. Regulation of autophagy by cytoplasmic p53. *Nat Cell Biol,* 10**,** 676-87.

TAYLOR-ROBINSON, D. & BEBEAR, C. 1997. Antibiotic susceptibilities of mycoplasmas and treatment of mycoplasmal infections. *J Antimicrob Chemother,* 40**,** 622-30.

TEMMINK, O. H., BIJNSDORP, I. V., PRINS, H. J., LOSEKOOT, N., ADEMA, A. D., SMID, K., HONEYWELL, R. J., YLSTRA, B., EIJK, P. P., FUKUSHIMA, M. & PETERS, G. J. 2010. Trifluorothymidine resistance is associated with decreased thymidine kinase and equilibrative nucleoside transporter expression or increased secretory phospholipase A2. *Mol Cancer Ther,* 9**,** 1047-57.

THOMAS, M. & BANKS, L. 1998. Inhibition of Bak-induced apoptosis by HPV-18 E6. *Oncogene,* 17**,** 2943-54.

TINDLE, R. W. 2002. Immune evasion in human papillomavirus-associated cervical cancer. *Nat Rev Cancer,* 2**,** 59-65.

TOMAKIDI, P., CHENG, H., KOHL, A., KOMPOSCH, G. & ALONSO, A. 2000. Modulation of the epidermal growth factor receptor by the human papillomavirus type 16 E5 protein in raft cultures of human keratinocytes. *Eur J Cell Biol,* 79**,** 407-12.

TOMMASINO, M. 2013. The human papillomavirus family and its role in carcinogenesis. *Semin Cancer Biol*.

TRISTRAM, A. & FIANDER, A. 2005. Clinical responses to Cidofovir applied topically to women with high grade vulval intraepithelial neoplasia. *Gynecol Oncol,* 99**,** 652-5.

UNNO, J., TAKAGI, M., PIAO, J., SUGIMOTO, M., HONDA, F., MAEDA, D., MASUTANI, M., KIYONO, T., WATANABE, F., MORIO, T., TERAOKA, H. & MIZUTANI, S. 2013. Artemis-dependent DNA double-strand break formation at stalled replication forks. *Cancer Sci,* 104**,** 703-10.

VAN DE NIEUWENHOF, H. P., VAN DER AVOORT, I. A. & DE HULLU, J. A. 2008. Review of squamous premalignant vulvar lesions. *Crit Rev Oncol Hematol,* 68**,** 131-56.

VAN SETERS, M., VAN BEURDEN, M., TEN KATE, F. J., BECKMANN, I., EWING, P. C., EIJKEMANS, M. J., KAGIE, M. J., MEIJER, C. J., AARONSON, N. K., KLEINJAN, A., HEIJMANS-ANTONISSEN, C., ZIJLSTRA, F. J., BURGER, M. P. & HELMERHORST, T. J.

2008. Treatment of vulvar intraepithelial neoplasia with topical imiquimod. *The New England journal of medicine,* 358**,** 1465-73.

VANDER HEIDEN, M. G., CANTLEY, L. C. & THOMPSON, C. B. 2009. Understanding the Warburg effect: the metabolic requirements of cell proliferation. *Science,* 324**,** 1029-33.

VANDESOMPELE, J., DE PRETER, K., PATTYN, F., POPPE, B., VAN ROY, N., DE PAEPE, A. & SPELEMAN, F. 2002. Accurate normalization of real-time quantitative RT-PCR data by geometric averaging of multiple internal control genes. *Genome Biol,* 3**,** RESEARCH0034.

VARNAI, A. D., BOLLMANN, M., GRIEFINGHOLT, H., SPEICH, N., SCHMITT, C., BOLLMANN, R. & DECKER, D. 2006. HPV in anal squamous cell carcinoma and anal intraepithelial neoplasia (AIN). Impact of HPV analysis of anal lesions on diagnosis and prognosis. *Int J Colorectal Dis,* 21**,** 135-42.

VELDMAN, T., HORIKAWA, I., BARRETT, J. C. & SCHLEGEL, R. 2001. Transcriptional activation of the telomerase hTERT gene by human papillomavirus type 16 E6 oncoprotein. *J Virol,* 75**,** 4467-72.

VOUSDEN, K. H. & LU, X. 2002. Live or let die: the cell's response to p53. *Nat Rev Cancer,* 2**,** 594-604.

VU, H. L., SIKORA, A. G., FU, S. & KAO, J. 2010. HPV-induced oropharyngeal cancer, immune response and response to therapy. *Cancer Lett,* 288**,** 149-55.

WAGNER, C. R., IYER, V. V. & MCINTEE, E. J. 2000. Pronucleotides: toward the in vivo delivery of antiviral and anticancer nucleotides. *Med Res Rev,* 20**,** 417-51.

WALBOOMERS, J. M., JACOBS, M. V., MANOS, M. M., BOSCH, F. X., KUMMER, J. A., SHAH, K. V., SNIJDERS, P. J., PETO, J., MEIJER, C. J. & MUNOZ, N. 1999. Human papillomavirus is a necessary cause of invasive cervical cancer worldwide. *J Pathol,* 189**,** 12-9.

WANG, J., ZHOU, D., PRABHU, A., SCHLEGEL, R. & YUAN, H. 2010. The canine papillomavirus and gamma HPV E7 proteins use an alternative domain to bind and destabilize the retinoblastoma protein. *PLoS Pathog,* 6**,** e1001089.

WANG, S. & EL-DEIRY, W. S. 2006. p73 or p53 directly regulates human p53 transcription to maintain cell cycle checkpoints. *Cancer Res,* 66**,** 6982-9.

WANG, S. S., ZUNA, R. E., WENTZENSEN, N., DUNN, S. T., SHERMAN, M. E., GOLD, M. A., SCHIFFMAN, M., WACHOLDER, S., ALLEN, R. A., BLOCK, I., DOWNING, K., JERONIMO, J., CARREON, J. D., SAFAEIAN, M., BROWN, D. & WALKER, J. L. 2009. Human papillomavirus cofactors by disease progression and human papillomavirus types in the study to understand cervical cancer early endpoints and determinants. *Cancer Epidemiol Biomarkers Prev,* 18**,** 113-20.

WATSON, R. A., THOMAS, M., BANKS, L. & ROBERTS, S. 2003. Activity of the human papillomavirus E6 PDZ-binding motif correlates with an enhanced morphological transformation of immortalized human keratinocytes. *J Cell Sci,* 116**,** 4925-34.

WEINBERG, R. A. 2013. *The Biology of Cancer*, Garland Science.

WEINBERGER, P. M., YU, Z., HAFFTY, B. G., KOWALSKI, D., HARIGOPAL, M., BRANDSMA, J., SASAKI, C., JOE, J., CAMP, R. L., RIMM, D. L. & PSYRRI, A. 2006. Molecular classification identifies a subset of human papillomavirus--associated oropharyngeal cancers with favorable prognosis. *J Clin Oncol,* 24**,** 736-47.

WENTZENSEN, N., VINOKUROVA, S. & VON KNEBEL DOEBERITZ, M. 2004. Systematic review of genomic integration sites of human papillomavirus genomes in epithelial dysplasia and invasive cancer of the female lower genital tract. *Cancer Res,* 64**,** 3878-84.

WESIERSKA-GADEK, J., WOJCIECHOWSKI, J., RANFTLER, C. & SCHMID, G. 2005. Role of p53 tumor suppressor in ageing: regulation of transient cell cycle arrest and terminal senescence. *J Physiol Pharmacol,* 56**,** 15-28.

WIJNHOLDS, J., MOL, C. A., VAN DEEMTER, L., DE HAAS, M., SCHEFFER, G. L., BAAS, F., BEIJNEN, J. H., SCHEPER, R. J., HATSE, S., DE CLERCQ, E., BALZARINI, J. & BORST, P. 2000. Multidrug-resistance protein 5 is a multispecific organic anion transporter able to transport nucleotide analogs. *Proc Natl Acad Sci U S A,* 97**,** 7476-81.

WILSON, R., RYAN, G. B., KNIGHT, G. L., LAIMINS, L. A. & ROBERTS, S. 2007. The full-length E1E4 protein of human papillomavirus type 18 modulates differentiation-dependent viral DNA amplification and late gene expression. *Virology,* 362**,** 453-60.

WOODMAN, C. B., COLLINS, S. I. & YOUNG, L. S. 2007. The natural history of cervical HPV infection: unresolved issues. *Nat Rev Cancer,* 7**,** 11-22.

WOODS, D. F., HOUGH, C., PEEL, D., CALLAINI, G. & BRYANT, P. J. 1996. Dlg protein is required for junction structure, cell polarity, and proliferation control in Drosophila epithelia. *J Cell Biol,* 134**,** 1469-82.

WRIGHT, T. C. 2006. Pathology of HPV infection at the cytologic and histologic levels: Basis for a 2-tiered morphologic classification system. *International Journal of Gynecology and Obstetrics* 94**,** S22 - S31.

WU, X. & LEVINE, A. J. 1994. p53 and E2F-1 cooperate to mediate apoptosis. *Proc Natl Acad Sci U S A,* 91**,** 3602-6.

XIONG, X., SMITH, J. L. & CHEN, M. S. 1997. Effect of incorporation of cidofovir into DNA by human cytomegalovirus DNA polymerase on DNA elongation. *Antimicrob Agents Chemother,* 41**,** 594-9.

YLISKOSKI, M., CANTELL, K., SYRJANEN, K. & SYRJANEN, S. 1990. Topical treatment with human leukocyte interferon of HPV 16 infections associated with cervical and vaginal intraepithelial neoplasias. *Gynecol Oncol,* 36**,** 353-7.

YOU, J., CROYLE, J. L., NISHIMURA, A., OZATO, K. & HOWLEY, P. M. 2004. Interaction of the bovine papillomavirus E2 protein with Brd4 tethers the viral DNA to host mitotic chromosomes. *Cell,* 117**,** 349-60.

YOUNG, J. D., YAO, S. Y., SUN, L., CASS, C. E. & BALDWIN, S. A. 2008. Human equilibrative nucleoside transporter (ENT) family of nucleoside and nucleobase transporter proteins. *Xenobiotica,* 38**,** 995-1021.

YU, T., FERBER, M. J., CHEUNG, T. H., CHUNG, T. K., WONG, Y. F. & SMITH, D. I. 2005. The role of viral integration in the development of cervical cancer. *Cancer Genet Cytogenet,* 158**,** 27-34.

ZHANG, X., LI, J., SEJAS, D. P. & PANG, Q. 2005. The ATM/p53/p21 pathway influences cell fate decision between apoptosis and senescence in reoxygenated hematopoietic progenitor cells. *J Biol Chem,* 280**,** 19635-40.

ZHAO, K. N., HENGST, K., LIU, W. J., LIU, Y. H., LIU, X. S., MCMILLAN, N. A. & FRAZER, I. H. 2000. BPV1 E2 protein enhances packaging of full-length plasmid DNA in BPV1 pseudovirions. *Virology,* 272**,** 382-93.

ZHENG, T. S., SCHLOSSER, S. F., DAO, T., HINGORANI, R., CRISPE, I. N., BOYER, J. L. & FLAVELL, R. A. 1998. Caspase-3 controls both cytoplasmic and nuclear events associated with Fas-mediated apoptosis in vivo. *Proc Natl Acad Sci U S A,* 95**,** 13618-23.

ZHENG, Z. M., TAO, M., YAMANEGI, K., BODAGHI, S. & XIAO, W. 2004. Splicing of a cap-proximal human Papillomavirus 16 E6E7 intron promotes E7 expression, but can be restrained by distance of the intron from its RNA 5' cap. *J Mol Biol,* 337**,** 1091-108.

ZHOU, J., AHN, J., WILSON, S. H. & PRIVES, C. 2001. A role for p53 in base excision repair. *EMBO J,* 20**,** 914-23.

ZUR HAUSEN, H. 1999. Immortalization of human cells and their malignant conversion by high risk human papillomavirus genotypes. *Semin Cancer Biol,* 9**,** 405-11.

8. Appendix

8.1. MagicMark™ XP Western blot Protein Standard and Western blot Antibody Specificity

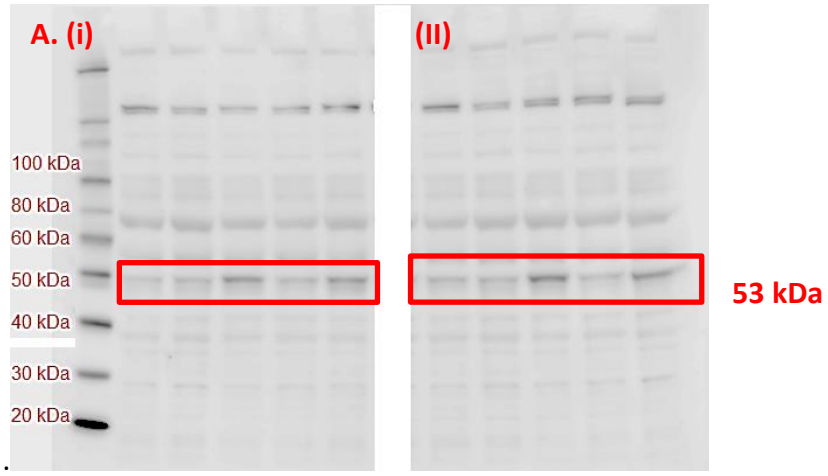

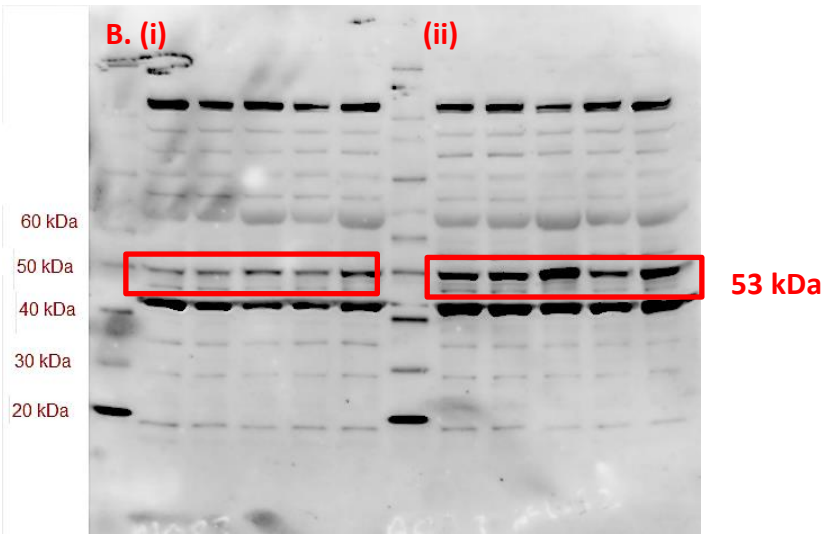

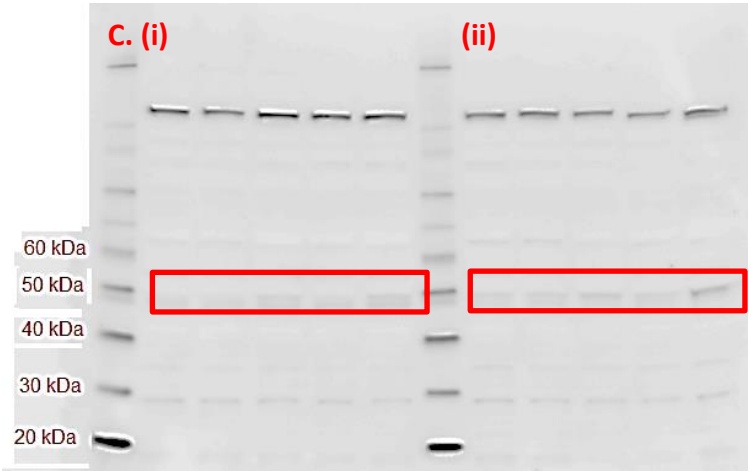

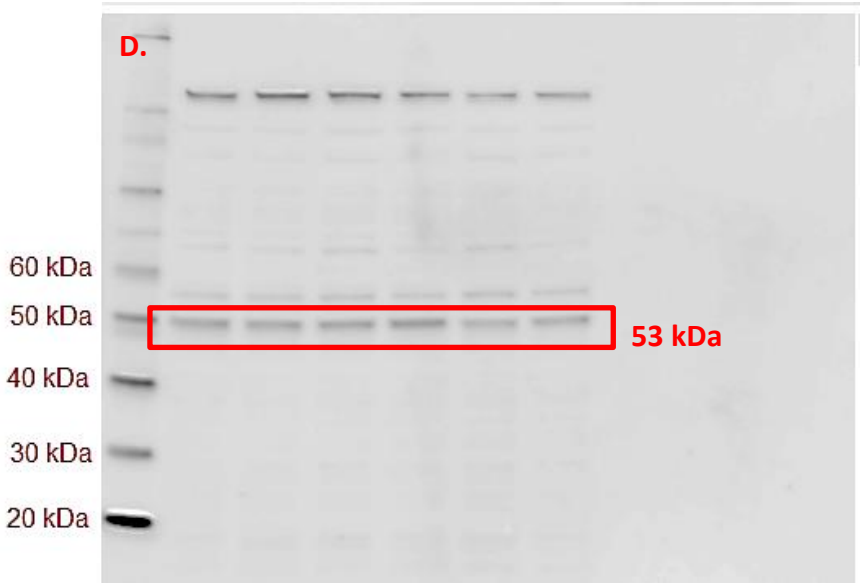

Figure 8.1. Total p53 Antibody Specificity and MagicMark™ XP Western blot Protein Standard

Western blot images for total p53 antibody, which can be seen at 53 kDa on each blot. The MagicMark™ XP Western blot Protein Standard can be seen running down the left hand side of each blot as well as running through the middle of the blots in B. and C.. Treatment conditions in lanes from left to right are [untreated control], [IC50 Cidofovir], [IC50 Cidofovir + 2 Gy XRT], [2 Gy XRT], [20 Gy XRT] for A (i) A09 cells 12 hours post treatment; A (ii) A09 cells 36 hours post treatment; B (i) M08 cells 72 hours post treatment; B (ii) A09 cells 72 hours post treatment; C (i) M08 cells 12 hours post treatment; C (ii) M08 cells 36 hours post treatment. The blot in D is of HEKs and lanes running from left to right contain [12 hour untreated control], [12 hour IC50 Cidofovir], [36 hour untreated control], [36 hour IC50 Cidofovir], [72 hour untreated control], [72 hour IC50 Cidofovir]. Blots A, C and D were imaged using a 1 minute exposure time. Blot B was imaged using a 30 minute exposure time to overcome the β-Actin signal for which it was previously imaged.

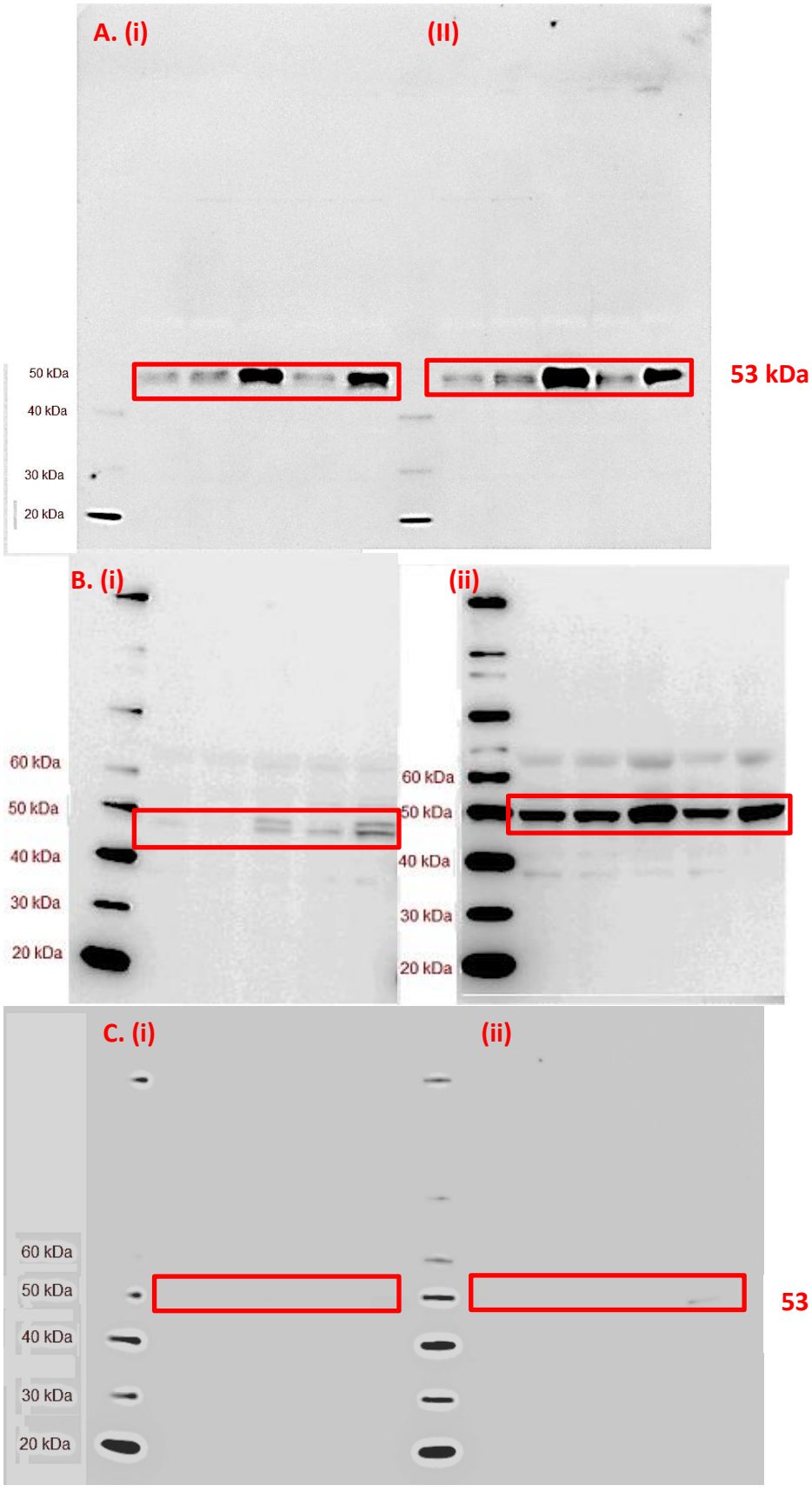
A. (i)
(II)
50 kDa
40 kDa
30 kDa
20 kDa
53 kDa
B. (i)
(ii)
60 kDa
50 kDa
40 kDa
30 kDa
20 kDa
60 kDa
50 kDa
40 kDa
30 kDa
20 kDa
53 kDa
C. (i)
(ii)
60 kDa
50 kDa
40 kDa
30 kDa
20 kDa
53 kDa

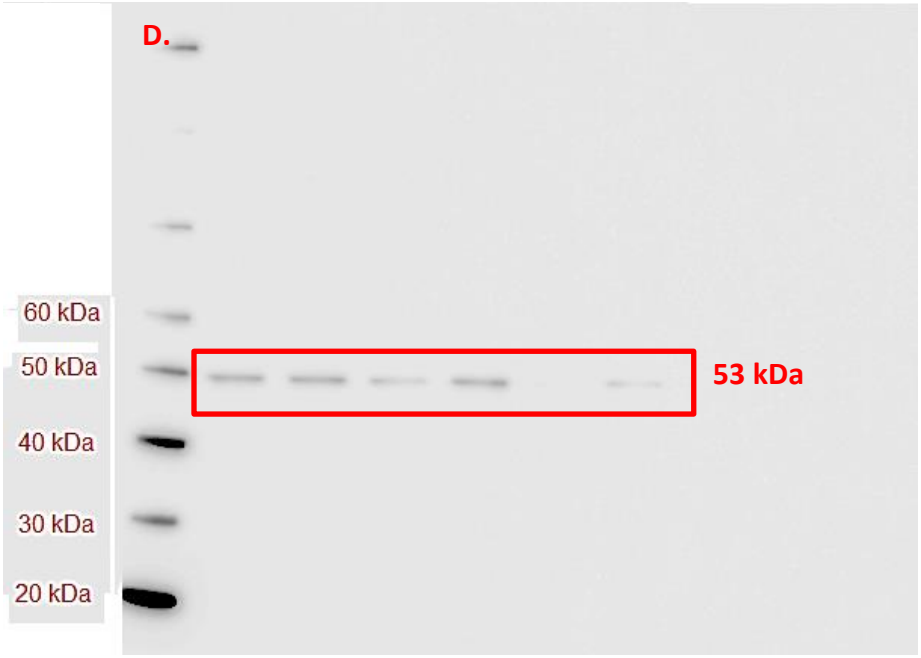

Figure 8.2. Phospho-p53 Antibody Specificity and MagicMark™ XP Western blot Protein Standard

Western blot images for phospho p53 antibody, which can be seen at 53 kDa on each blot. The MagicMark™ XP Western blot Protein Standard can be seen running down the left hand side of each blot as well as running through the middle of the blots in B. and C.. Treatment conditions in lanes from left to right are [untreated control], [IC50 Cidofovir], [IC50 Cidofovir + 2 Gy XRT], [2 Gy XRT], [20 Gy XRT] for A (i) A09 cells 12 hours post treatment; A (ii) A09 cells 36 hours post treatment; B (i) M08 cells 72 hours post treatment; B (ii) A09 cells 72 hours post treatment; C (i) M08 cells 12 hours post treatment; C (ii) M08 cells 36 hours post treatment. The blot in D is of HEKs and lanes running from left to right contain [12 hour untreated control], [12 hour IC50 Cidofovir], [36 hour untreated control], [36 hour IC50 Cidofovir], [72 hour untreated control], [72 hour IC50 Cidofovir]. All blots were imaged using a 30 minute exposure time.

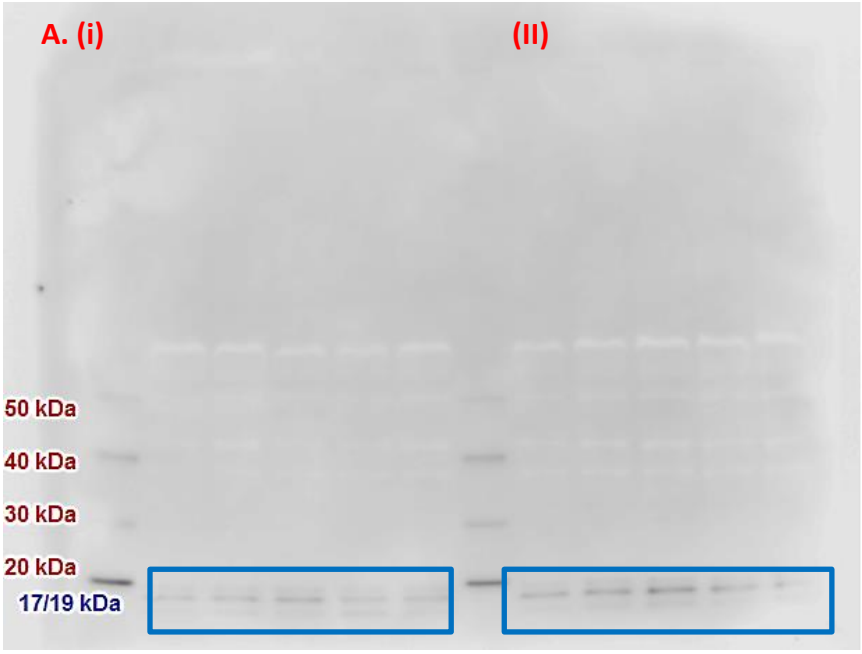
A. (i)
(II)
50 kDa
40 kDa
30 kDa
20 kDa
17/19 kDa

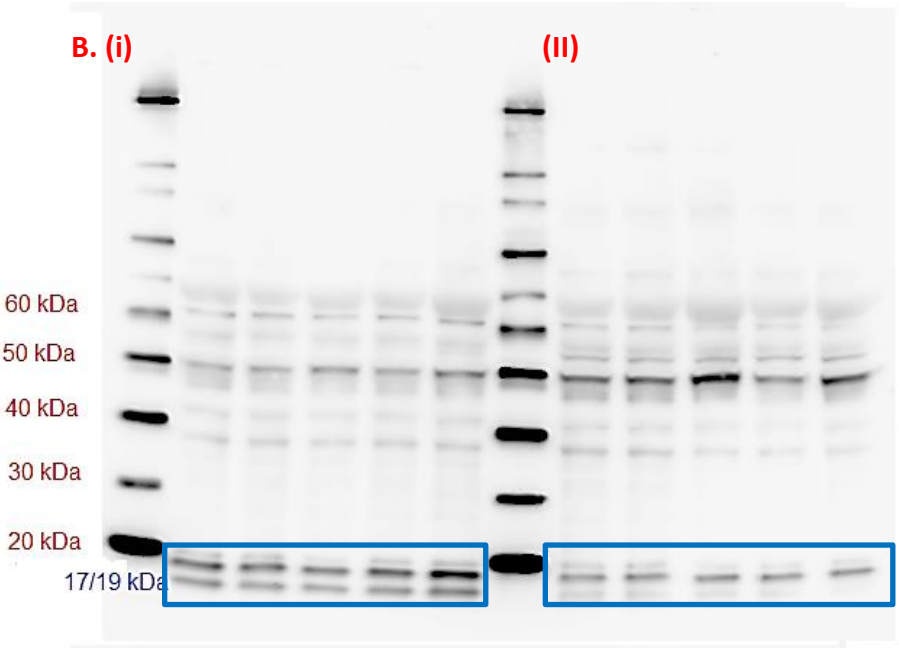
B. (i)
(II)
60 kDa
50 kDa
40 kDa
30 kDa
20 kDa
17/19 kDa

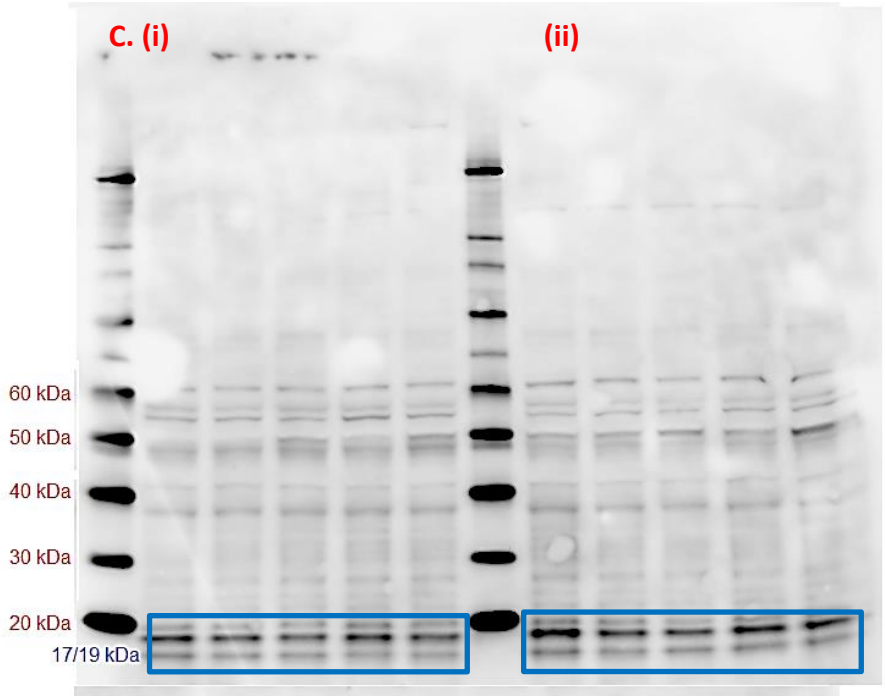

Figure 8.3. Cleaved Caspase-3 Antibody Specificity and MagicMark™ XP Western blot Protein Standard

Western blot images for cleaved caspase-3 antibody, which can be seen at 17/19 kDa on each blot. The MagicMark™ XP Western blot Protein Standard can be seen running down the left hand side of each blot as well as running through the middle of the blots in B. and C.. Treatment conditions in lanes from left to right are [untreated control], [IC50 Cidofovir], [IC50 Cidofovir + 2 Gy XRT], [2 Gy XRT], [20 Gy XRT] for A (i) A09 cells 12 hours post treatment; A (ii) A09 cells 36 hours post treatment; B (i) M08 cells 72 hours post treatment; B (ii) A09 cells 72 hours post treatment; C (i) M08 cells 12 hours post treatment; C (ii) M08 cells 36 hours post treatment. All blots were imaged using a 30 minute exposure time.

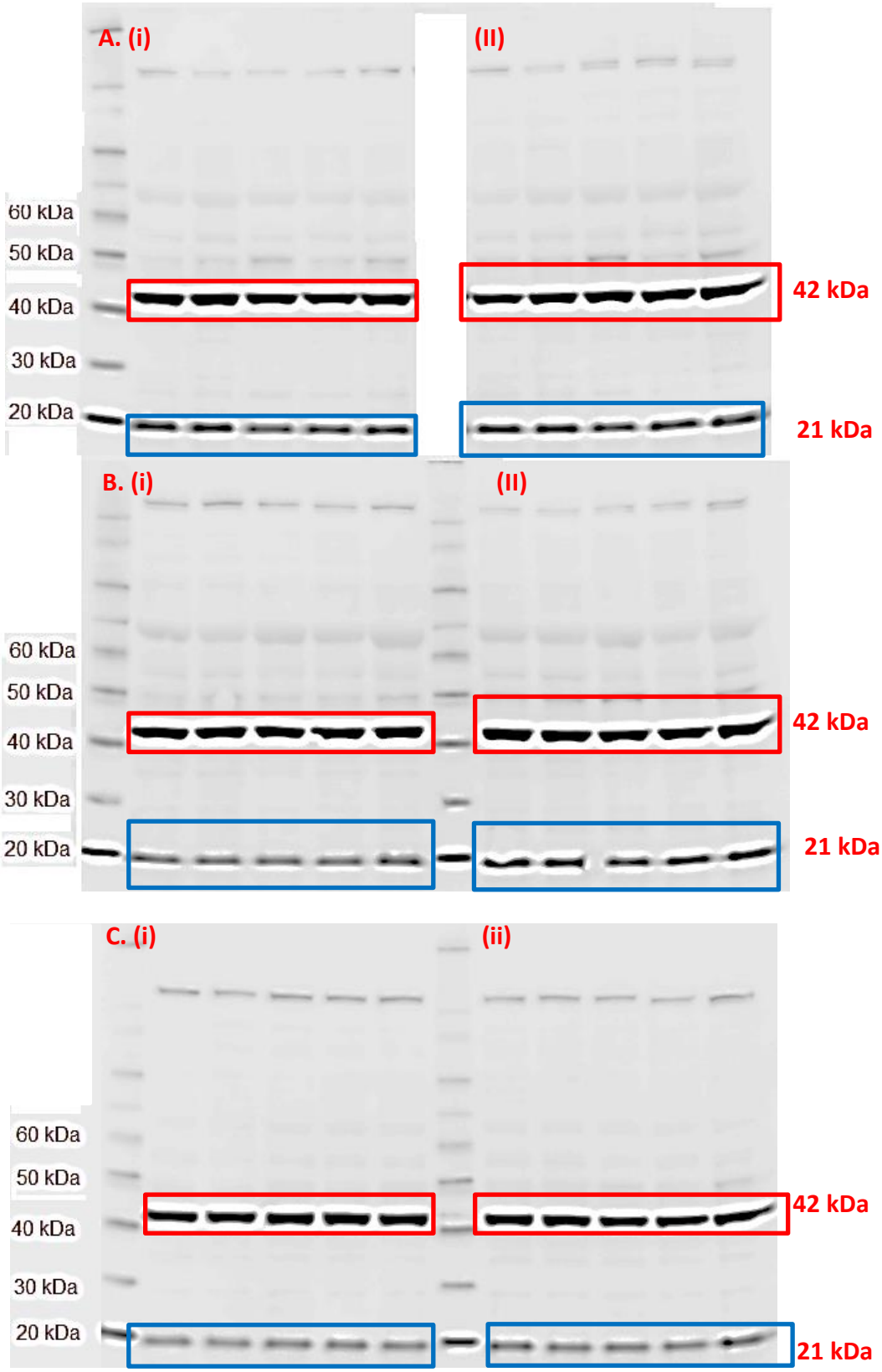
A. (i)
(II)
60 kDa
50 kDa
40 kDa
30 kDa
20 kDa
42 kDa
21 kDa
B. (i)
(II)
60 kDa
50 kDa
40 kDa
30 kDa
20 kDa
42 kDa
21 kDa
C. (i)
(ii)
60 kDa
50 kDa
40 kDa
30 kDa
20 kDa
42 kDa
21 kDa

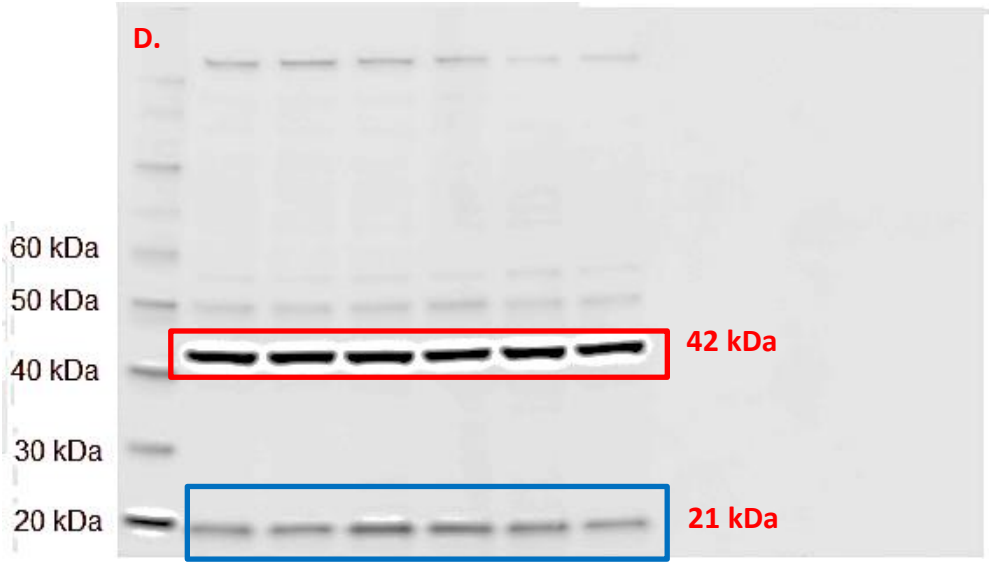

Figure 8.4. p21 and β-Actin Antibody Specificity and MagicMark™ XP Western blot Protein Standard

Western blot images for p21 and β-Actin antibodies, which can be seen at 21 and 42 kDa respectively on each blot. The MagicMark™ XP Western blot Protein Standard can be seen running down the left hand side of each blot as well as running through the middle of the blots in B. and C.. Treatment conditions in lanes from left to right are [untreated control], [IC50 Cidofovir], [IC50 Cidofovir + 2 Gy XRT], [2 Gy XRT], [20 Gy XRT] for A (i) A09 cells 12 hours post treatment; A (ii) A09 cells 36 hours post treatment; B (i) M08 cells 72 hours post treatment; B (ii) A09 cells 72 hours post treatment; C (i) M08 cells 12 hours post treatment; C (ii) M08 cells 36 hours post treatment. All blots were imaged using a 30 minute exposure time. The blot in D is of HEK cell lysates, where lanes running from left to right contain [12 hour untreated control], [12 hour IC50 Cidofovir], [36 hour untreated control], [36 hour IC50 Cidofovir], [72 hour untreated control], [72 hour IC50 Cidofovir]. All blots were imaged using a 1 minute exposure time. The blots in this figure correspond to those in Figure 8.1. Total p53.

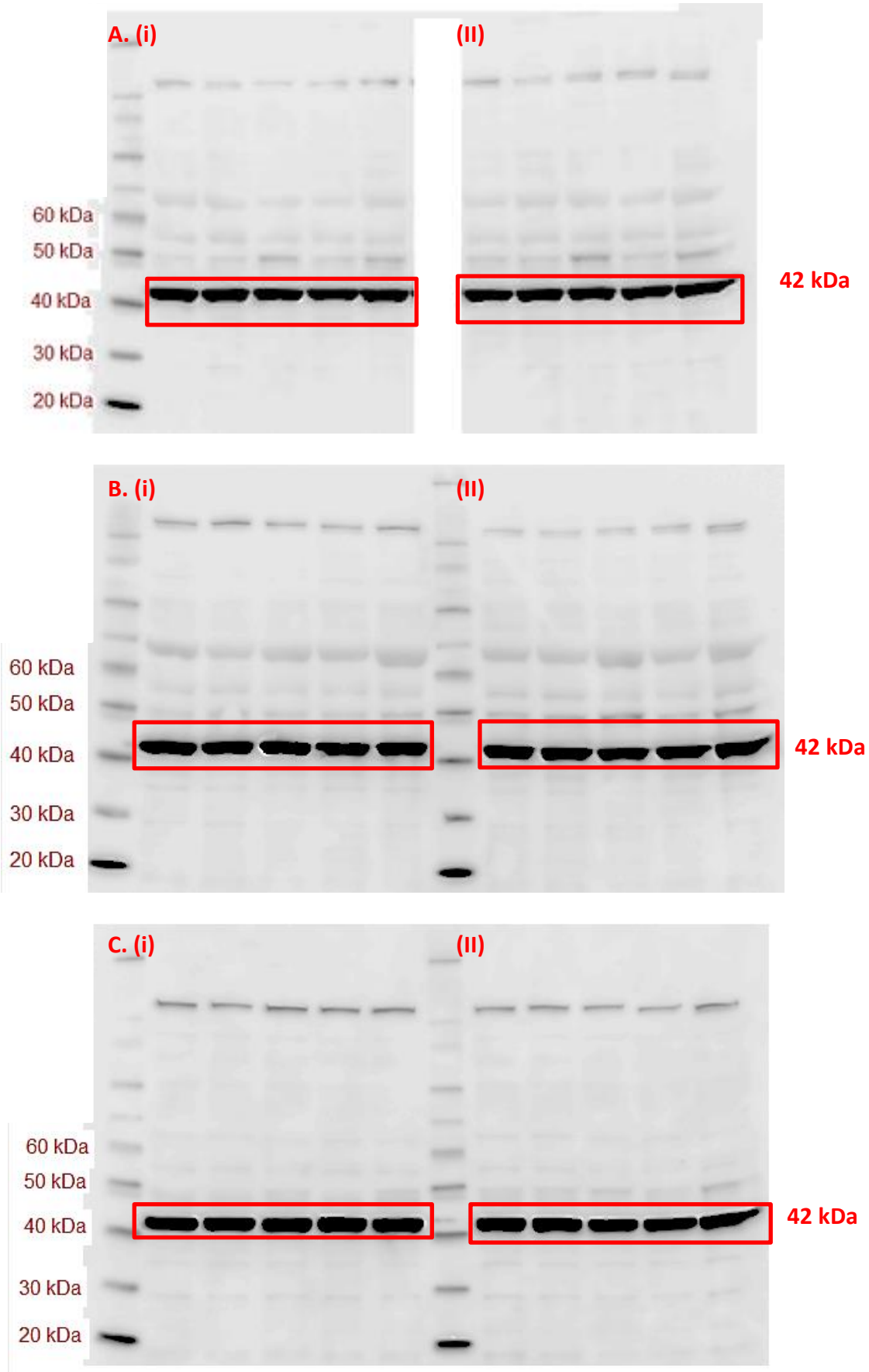
A. (i)
(II)
60 kDa
50 kDa
40 kDa
30 kDa
20 kDa
42 kDa
B. (i)
(II)
60 kDa
50 kDa
40 kDa
30 kDa
20 kDa
42 kDa
C. (i)
(II)
60 kDa
50 kDa
40 kDa
30 kDa
20 kDa
42 kDa

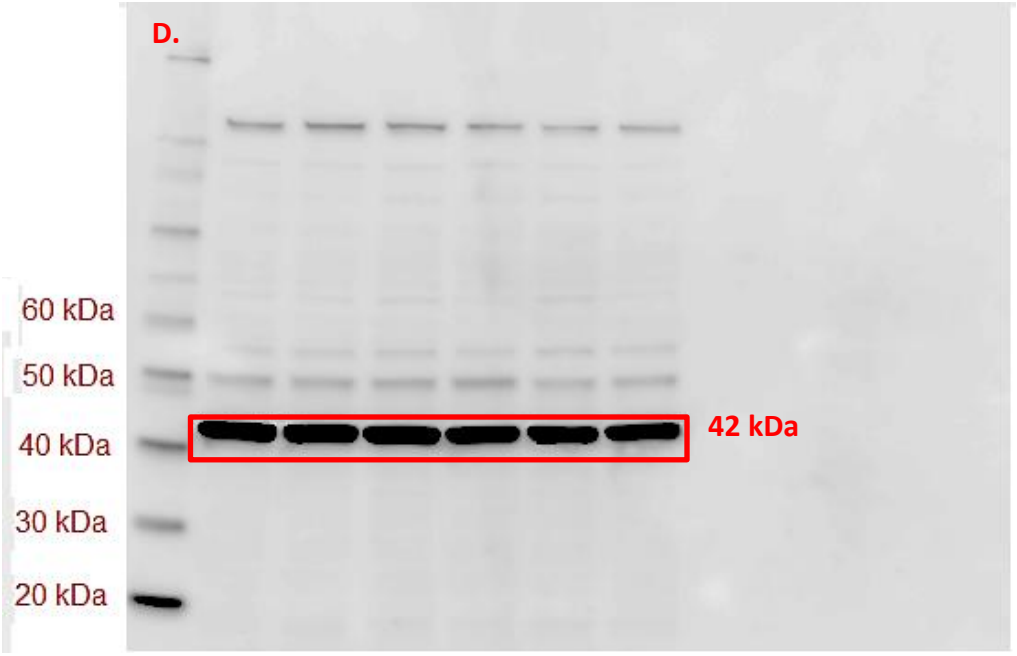

Figure 8.5. β-Actin Antibody Specificity and MagicMark™ XP Western blot Protein Standard

Western blot images for β-Actin antibodies, which can be seen at 42 kDa on each blot. The MagicMark™ XP Western blot Protein Standard can be seen running down the left hand side of each blot as well as running through the middle of the blots in B. and C.. Treatment conditions in lanes from left to right are [untreated control], [IC50 Cidofovir], [IC50 Cidofovir + 2 Gy XRT], [2 Gy XRT], [20 Gy XRT] for A (i) A09 cells 12 hours post treatment; A (ii) A09 cells 36 hours post treatment; B (i) M08 cells 72 hours post treatment; B (ii) A09 cells 72 hours post treatment; C (i) M08 cells 12 hours post treatment; C (ii) M08 cells 36 hours post treatment. All blots were imaged using a 30 minute exposure time. The blot in D is of HEK cell lysates, where lanes running from left to right contain [12 hour untreated control], [12 hour IC50 Cidofovir], [36 hour untreated control], [36 hour IC50 Cidofovir], [72 hour untreated control], [72 hour IC50 Cidofovir]. All blots were imaged using a 1 minute exposure time. The blots in this figure correspond to those in Figure 8.2 and 8.3; phospho-p53 and cleaved caspase-3 respectively.